MSCC3

3rd MINERAL SCIENCES IN THE CARPATHIANS
INTERNATIONAL CONFERENCE

Miskolc, Hungary, 9–10 March 2006

ABSTRACTS

Edited by

Gábor Papp, Béla Fehér and Ferenc Kristály

Sponsored by

International
Visegrad Fund

International Visegrad Fund
Koch Sándor Foundation (Miskolc)
Foundation for Hungarian Minerals (Miskolc)
Socrates/Erasmus Curriculum Development Programme (CDA) on
a Co-ordinated European Curriculum in Mineral Sciences

Szeged, Hungary

2006

Organizers

University of Miskolc
Herman Ottó Museum, Miskolc
Mineralogical and Geochemical Branch of the Hungarian Geological Society

Co-organizers

Austrian Mineralogical Society
Mineralogical Society of Poland
Mineralogical Society of Romania
Slovak Geological Society
Ukrainian Mineralogical Society
CBGA Commission on Mineralogy and Geochemistry
Nanomineralogy Working Group of the Committee for Geochemistry, Mineralogy and Petrology of HAS

International Scientific Board

Martin Chovan
Comenius University, Bratislava, Slovakia

Aleksandra Gawęda
University of Silesia, Sosnowiec, Poland

Corina Ionescu
Babeş-Bolyai University, Cluj-Napoca, Romania

Victor M. Kvasnytsya
Institute of Geochemistry, Mineralogy and Ore Formation, National Academy of Sciences, Kyiv, Ukraine

Milan Novák
Masaryk University, Brno, Czech Republic

Gábor Papp
Hungarian Natural History Museum, Budapest, Hungary

Mihály Pósfai
University of Veszprém, Veszprém, Hungary

Ekkehart Tillmanns
University of Vienna, Vienna, Austria

Gheorghe Udubaşa
Geological Institute of Romania, Bucharest, Romania

Local Organizing Committee

Sándor Szakáll (Chairman)
University of Miskolc, Miskolc, Hungary

Béla Fehér
Herman Ottó Museum, Miskolc, Hungary

Ferenc Kristály
University of Miskolc, Miskolc, Hungary

Ferenc Mádai
University of Miskolc, Miskolc, Hungary

MACALC: A PROGRAM FOR SUPPORTING MODAL ANALYSIS OF ROCKS

ALMÁSI, B.[1], CSÁMER, Á.[2], FARKAS, J.[3] & RÓZSA, P.[2]
[1] Department of Informatics Systems and Networks, University of Debrecen, Egyetem tér 1, Debrecen, H-4032 Hungary
[2] Department of Mineralogy and Geology, University of Debrecen, Egyetem tér 1., Debrecen, H-4032 Hungary
E-mail: csamera@delfin.unideb.hu
[3] Department of Information Technology, University of Debrecen, Egyetem tér 1, Debrecen, H-4032 Hungary

Modal analysis is one of the most common microscopic methods in the igneous, metamorphic, and sedimentary petrographic practice. Using this method two types of data series can be obtained: (1) relative quantity or frequency of rock-forming minerals, and (2) microscopic grain size distribution of rocks. Moreover, grain size distribution of certain minerals of the rocks may be also determined. By these data series further petrographic-petrologic conclusions, such as type of the texture, distinction of varieties and facies, cooling history, *etc.* can be drawn. In accordance with JÁRAI *et al*. (1997) we regard the modified Rosiwal's method, *i.e.* method of measuring along lines as the most favourable one. Its application requires no expensive or complex measuring and recording apparatus: the minimal requirement is only a scaled cross-line eyepiece. Moreover, relative quantity of the rock forming minerals as well as grain-size distribution can be simultaneously determined by the same measuring process. Due to its simplicity and acceptable accuracy the classic Rosiwal's method is widely used in analysis of rocks (see for example SAROCCHI & MACÍAS, 2004; SAROCCHI *et al*., 2005) and of some building materials (see for example ELSEN, 2000).

To eliminate the "huge" amount of paperwork, which has been regarded as the main disadvantage of this method, a computational data record and evaluation seems to be the most plausible solution. The Modal Analysis Calculator (MACALC) program introduced by this paper makes possible to evaluate the computational record, and creates tables on the basis of the measured data. The program selects and arranges the data by the optional grain-size intervals and mineralogical components. As a final result the program creates three tables listing the grain-size distribution and mineral composition data as well as statistical parameters. Calculations can be directly controlled by changing some parameters, *e.g.*, it determines the actual required length of the measuring line according to the fixed acceptable accuracy.

The Modal Analysis Calculator (MACALC) software performs all the computing that one needs to gain information about a modal analysis measurement. MACALC is a web-based program available through the Internet by using a web-browser (*e.g.* Internet Explorer 5.0, Netscape Navigator 4.8, Konqueror 3.0, *etc.*). No special requirements and no software installation are required from the client side. The address of the MACALC homepage is http://irh.inf.unideb.hu/macalc. To access the Modal Analysis Calculator the user must perform a free registration process by giving his/her name and e-mail address. The e-mail address is required only to contact the user, sending the necessary information to him. After the successful registration the user will get an e-mail containing his personal modal analysis calculator web-page data (address, login name and password) so he will be ready to use the MACALC software to perform modal analysis calculation.

Acknowledgements

This work has been supported by the Hungarian National Science Research Foundation (OTKA) under Research Contract No. T046579.

References

ELSEN, J. (2000): Cement and Concrete Research, 31: 1027–1031.

JÁRAI, A., KOZÁK, M. & RÓZSA, P. (1997): Mathematical Geology, 29/8: 977–991.

SAROCCHI, D. & MACÍAS, J. L. (2004): In: Abstracts of 32nd IGC Florence 2004, 1: 602–603.

SAROCCHI, D., BORSELLI, L. & MACIAS, J.L. (2005): Revista Mexicana de Ciencias Geológicas, 22/3: 371–382.

HEAVY METALS IN ANIMAL TISSUES FROM THE DUMPS AT ŠTIAVNICKÉ BANE DEPOSIT

ANDRÁŠ, P. & KRIŽÁNI, I.
Geological Institute, Slovak Academy of Sciences, Severná 5, 97401 Banská Bystrica, Slovakia
E-mail: andras@savbb.sk

The locality Štiavnické Bane – Lúky nad Tonádom represents a mining country influenced by historical exploitation of Au-Ag polymetallic ores from the 14th until the 19th century. The mines were closed in 1903.

The possibility of the utilization of the higher animals as indicator of contamination depends on their stressor sensibility and on the extent of their reaction in time and area. The group of small mammals is a suitable model group for monitoring of environment toxicity (TALMAGE & WALTON, 1991) in respect of their short-living (several months). Their living space is small (maximum 1–2 hectares), so they give chance to monitor a particular locality. At all investigated localities the dominant species were *Apodemus flavicollis* (53.9%, *AFLA*), *Microtus arvalis* (24.5%, *MARV*) and *Clethrionomys glareolus* (18.2%, *CGLA*) and subordinately also *Microtus subterraneus* (*PSUB*) and the only representative of insectivorous animals, *Crocidura suaveolens*.

The graphic representation in differences of tissue contamination of livers, kidney and spleens of *AFLA* species at localities between the summer and autumn set of analyzed samples (Fig. 1) shows, that there is an obvious similarity between the contamination degree of the studied organs from localities I and IV. Localities at the older (II) and younger (III) dumps differ by proportional contamination of the analyzed organs. The contents of individual elements at younger dumps from the summer and autumn set intersect and at the older dumps there is a differentiation between the summer and autumn set. It is similar to the differentiation at localities I and IV.

The exposure time – the period while the animal is exposed to the activity of stressors – plays an important role. If the organs of short-living organisms are markedly contaminated, it is very probable, that in animals with longer lifetime the contamination of internal organs will rise proportionally. Among herbivorous animals those species are present that mainly feed on the vegetal organs of plants and seeds. Higher contamination by heavy metals and toxic elements of analyzed tissues of internal organs was determined at animals having a preference for consuming vegetal organs of plants. Animals consuming predominantly the seeds show lower contamination by heavy metals. Different contamination of internal tissues was found at individual monitored elements from the summer and autumn sets of the studied rodents within the individual localities and between the localities.

Reference

TALMAGE, S.S. & WALTON, B.T. (1991): Reviews of Environmental Contamination and Toxicology. 119: 48–99.

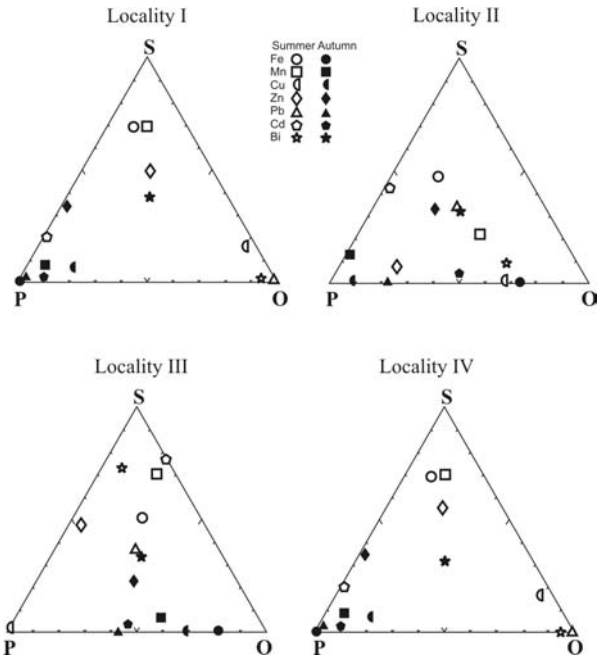

Fig. 1: Triangular plots of rate concentrations of selected elements in tissues of livers (P), kidneys (O) and spleens (S) of *Apodemus flavicolis* species from localities I – reference area; II – dump from the 17th century, III – dump Babčo (17th–18th centuries); IV – dump Wolf (18th century).

Pb ISOTOPE STUDY OF STIBNITE MINERALIZATION FROM THE WESTERN CARPATHIANS

ANDRÁŠ, P.[1], LUPTÁKOVÁ, J.[1] & CHOVAN, M.[2]
[1] Geological Institute, Slovak Academy of Sciences, Severná 5, 974 01 Banská Bystrica, Slovakia
E-mail: andras@savbb.sk
[2] Deparment of Mineralogy and Petrology, Comenius University, Mlynská dolina G, 842 15 Bratislava, Slovakia

The most important Sb mineralization of the Western Carpathian region are located in four structural and metallogenic zones: 1) Tatric unit, 2) Veporic unit, 3) Gemeric unit and 4) neovolcanic complexes. The stibnite mineralization in Western Carpathians are genetically related both to the Variscan and Alpine orogenic cycles.

The original source of the lead from the stibnite deposits is not homogeneous. The μ_2 values are close to the evolution curves of orogenic lead (Fig. 1). Lead was predominantly derived from crustal granitic and metasedimentary rocks or from related material. It is possible to distinguish three individual crustal orogenic lead sources: 1) for the Tatric unit, 2) for the Gemeric unit and 3) for stibnite mineralization in neovolcanites. The samples from Gemeric unit shows different mixture of crustal and mantle materials and a later enrichment in μ and W, *i.e.* during younger events, *e.g.* metamorphosis, mobilization of metals, recrystallization *etc*. Stibnite samples from Nízke Tatry Mts. and those from the Gemeric unit contain more radiogenic lead than that in galena (Fig. 1). The most radiogenic lead was found in samples from the Gemeric unit and Malé Karpaty Mts. These results correspond to those of the paleotectonic study published by CHOVAN *et al.* (1999). According to this study the Gemeric unit and Malé Karpaty Mts. represent Late Variscan accretionary prisms.

The presented data are comparable with those of KANTOR & RYBÁR (1964) and ČERNYŠEV *et al.* (1984). They show identical patterns of metamorphic processes and correspond to the paleotectonic scheme of Sb-Au mineralization presented by CHOVAN *et al*. (1999) and indicate that the most radiogenic lead is in stibnite samples from mineralization formed in paleotectonic accretionary prisms (Malé Karpaty Mts. and the Gemeric unit).

References

AMOV, B. G. (1993): Earth and Planetary Science Letters, 65: 61–74, 311–321.

ČERNYŠEV, I., CAMBEL, B. & KODĚRA, M. (1984): Geologický Zborník – Geologica Carpathica, 35: 307–327.

CHOVAN, M., PUTIŠ, M., NÉMETH, Z., MAŤO, Ľ., ANDRÁŠ, P. & JELEŇ, S. (1999): Mineralia Slovaca, 31: 175–178.

KANTOR, J. & RYBÁR, M. (1964): Geologický Zborník – Geologica Carpathica, 15: 285–297.

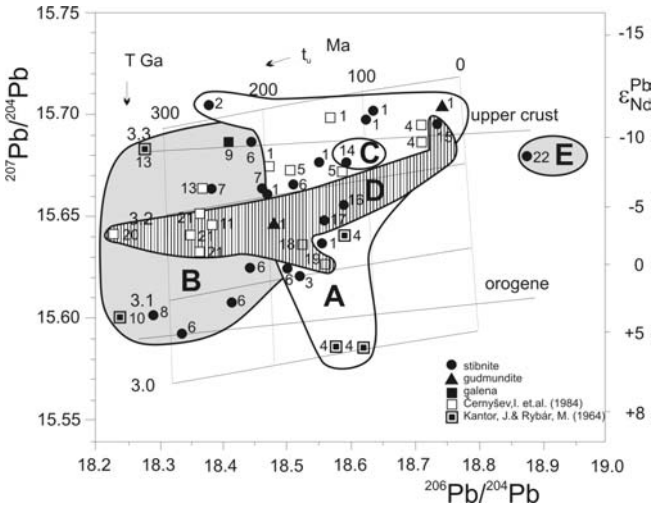

Fig. 1: Evolution diagram of $^{206}Pb/^{204}Pb$ *vs*. $^{207}Pb/^{204}Pb$ – isotopic composition in Sb minerals and galena (according to AMOV, 1993) from the Western Carpathians. **A – Malé Karpaty Mts.:** 1–Pezinok, 2–Kuchyňa, 3–Pernek-Pod Krížnicou, 4–Pod Babou, 5–Častá; **B – Nízke Tatry Mts.:** 6–Dúbrava, 7–Magurka, 8–Mlynná Dolina Valley, 9–Malužiná, 10–Lom, 11–Jasenie-Soviansko, 12–Dve Vody, 13–Trangoška; **C – Tatry Mts.:** 14–Kriváň; **D – Spiš-Gemer Mts. (Gemeric unit):** 15–Poproč, 16–Grexa, 17–Helcmanovce, 18–Hnúšťa-Ostrá, 19–Rochovce, 20–Nižná Slaná, 21–Rákoš; **E – Eastern Slovakian Neovolcanites:** 22–Zlatá Baňa.

WIDESPREAD OCCURRENCE OF GREIGITE IN THE FINE-GRAINED SEDIMENTS OF LAKE PANNON: IMPLICATIONS FOR ENVIRONMENT AND MAGNETOSTRATIGRAPHY

BABINSZKI, E.[1], MÁRTON, E.[2], MÁRTON, P.[3] & KISS, L. F.[4]
[1] Geological Institute of Hungary; Stefánia út 14, H-1143 Budapest, Hungary
E-mail: babinszki@mafi.hu
[2] Eötvös Loránd Geophysical Institute of Hungary, Palaeomagnetic Laboratory, Columbus u. 17-23, H-1145 Budapest, Hungary
[3] Department of Geophysics, Eötvös Loránd University, Pázmány Péter sétány 1/C, H-1117 Budapest, Hungary
[4] Research Institute for Solid State Physics and Optics HAS, POB 49, H-1525 Budapest, Hungary

Lake Pannon was a large, brackish water lake that occupied the Pannonian Basin during the Late Miocene. Its sedimentary sequence was studied from several aspects, among others for magnetostratigraphy. However magnetic mineralogy experiments were rarely carried out in these studies, magnetite alone was supposed to be the carrier of the natural remanent magnetization (NRM); while mineralogical studies only described framboidal pyrite from the fine-grained sediments.

More recently, magnetic mineralogical experiments carried out in connection with tectonically oriented palaeomagnetic investigations revealed that the principal magnetic mineral was greigite (Fe_3S_4) in these sediments. To follow up this finding, we started a systematic study on the magnetic minerals of fully oriented samples from 34 outcrops and of several specimens from three cores.

First, we measured the NRMs, all samples using stepwise thermal demagnetizations accompanied by susceptibility monitoring during heating to detect phase changes and investigated the consistency of the NRM. Then we identified the magnetic minerals by magnetic methods (acquisition of isothermal remanent magnetization (IRM), stepwise thermal demagnetization of a three-component IRM, hysteresis measurements and tests for distinguishing between greigite and pyrrhotite). The use of classical mineralogical methods were prevented by the extremely low content of magnetic minerals (0.004 to 0.2 mass% for greigite).

The main result of the present experiments is that in the sampled fine-grained sediments the most common magnetic mineral is greigite as was expected from the earlier studies. The localities with greigite (as the magnetic carrier) give consistent palaeomagnetic results both of normal and reversed polarities, as well as a declination deviation from the present north characteristic of the studied area. These together can be taken as proof of the pristine nature of the NRM, which means that the NRM is contemporaneous with the formation of greigite during (preferably early) diagenesis. On the other hand, localities with magnetite often failed to yield palaeomagnetic results. This suggests that the magnetite here is more often a secondary mineral than the original one.

This widespread occurrence of greigite in the fine-grained sediments of Lake Pannon points to oxygen depleted conditions of deposition and early diagenesis, even in the absence of lamination or palaeontological evidence for anoxic-suboxic conditions.

While our results are relevant to the environment of deposition and early diagenesis, the very presence of greigite raises questions as to its usefulness for magnetostratigraphy. In the best case, greigite forms during early diagenesis, i. e. the magnetization is not much younger than the time of deposition. But to demonstrate it, fully oriented samples were needed. The earlier studies from the sediments of the lake, however, were based on cores without azimuthal orientation. Another difficulty is that when greigite and magnetite occur together, their polarities may be opposite. Then either the greigite or the magnetite (or both?) must be of later formation, but it is difficult to decide which.

The results of present study as well as the possibility of neoformation of greigite and other magnetic minerals suggest that the magnetostratigraphic investigations in sediments formed under oxygen depleted conditions must be carried out on fully oriented samples (or at least on samples which are oriented with respect to one another) and should be accompanied by detailed mineral magnetic studies in order to avoid pitfalls in the interpretation.

SECONDARY CARBONATE FORMS IN THE BASAHARC DOUBLE PALEOSOIL (BASAHARC, HUNGARY)

BAJNÓCZI, B.[1] & HORVÁTH, E.[2]
[1] Institute for Geochemical Research, Hungarian Academy of Sciences, Budaörsi út 45, H-1112 Budapest, Hungary
E-mail: bajnoczi@geochem.hu
[2] Department of Physical Geography, Eötvös Loránd University, Pázmány Péter sétány 1/C, H-1117 Budapest, Hungary

Pedogenic (or secondary) carbonate as indicator of pedogenesis and paleoenvironment was examined in a Pleistocene paleosoil complex. The studied Basaharc Double (BD) paleosoil, a reference horizon in the Young Loess Series in Hungary, is a forest-steppe-like soil of OIS 7 age. BD paleosoil was sampled at its type locality: the former Basaharc brickyard located in the valley of the Danube at the northern end of the Transdanubian Range (PÉCSI & HAHN, 1987). In the 20 to 25 m thick loess-paleosoil sequence several paleosoil pedocomplexes occur, one of them is the Basaharc Double composed of upper BD1 and lower BD2 soil horizons with intercalating loess.

Various types of pedogenic carbonates (*e.g.* diffuse carbonate, nodules and concretions as "loess dolls") are present, but in this study only forms and distribution of discrete, small scale precipitates were investigated in detail due to their environmental significance. The discrete small scale carbonate (less than a few millimetres in size) appears as

- calcified root cells ("corn-ear"-like aggregates consisting of sparry crystals) in root channels,
- hypocoatings (micritic impregnations of matrix) around root channels,
- bundles of calcite needles in pores and cavities,
- earthworms spheroids (nodules composed of drusy calcite crystals).

These small scale carbonate accumulations are also known from other loess-paleosoil sequences and their formation is related directly or indirectly to biological activity during pedogenesis (BECZE-DEÁK *et al*., 1997).

Earthworm spheroids and hypocoatings distribute uniformly in the sequence, while higher amount of calcified root cells was detected in the paleosoil layers than in the host loess suggesting longer stability of soil surface. Enrichment of needle-fiber calcite is typical for the upper BD1 horizon, but this carbonate form is practically absent in the lower BD2 horizon and in the loess. Calcite needles formed by biomineralization of fungal filaments (VERRECCHIA & VERRECCHIA, 1994) indicate the presence of former fresh organic matter in BD1 decomposed by fungi (BECZE-DEÁK *et al*., 1997). Since needle-fiber calcite is rarely preserved in fossil soils, more investigations are needed to determine whether it was later leached out from the lower paleosoil or it precipitated primarily in a very small amount in BD2.

This study was supported by the Hungarian Research Fund (OTKA D 048631).

References

BECZE-DEÁK, J., LANGOHR, R. & VERRECCHIA, E. P. (1997): Geoderma, 76: 221–252.

PÉCSI, M. & HAHN, G. (1987): Catena Supplement, 9: 95–102.

VERRECCHIA, E. P. & VERRECCHIA, K. E. (1994): Journal of Sedimentary Research, A64: 650–664.

SULPHOSALTS FROM CHYŽNÉ-HERICHOVÁ IN THE WESTERN CARPATHIANS (SLOVAKIA)

BÁLINTOVÁ, T. & OZDÍN, D.
Department of Mineralogy and Petrology, Faculty of Natural Sciences, Comenius University, Mlynská dolina G, 842 15 Bratislava, Slovak Republic
E-mail: ozdin@fns.uniba.sk

Herichová occurrence is found ~ 3 km NNE from the village of Chyžné (County Revúca) in Central Slovakia. The locality is situated in the western part of the Spišsko-gemerské rudohorie Mts. near the contact zone of two significant tectonic units of the Western Carpathians – Gemericum and Veporicum Unit. The host rocks of the hydrothermal mineralization is granite of Rimavica type and Carboniferous metamorphosed fine-grained sandstones cyclically alternating with phyllite schists of the Slatvina formation.

We described the following mineral assemblages: 1) arsenopyrite–pyrite (with arsenopyrite, pyrite, sphalerite, hübnerite, quartz); 2) stibnite (stibnite, jamesonite, zinkenite, berthierite, chalcostibite, tetrahedrite, kermesite, andorite I, robinsonite, chalcopyrite, sphalerite, quartz); 3) carbonate (rhodochrosite, calcite, kutnohorite); 4) Galena (galena, bismuthinite, native bismuth, heyrovskýite, lillianite, gustavite, joséite-A, joséite-B, baksanite, andorite II, quartz). The hypergene stage is represented by secondary minerals: cerussite, anglesite, gypsum, senarmontite, stibiconite (?), valentinite (?), scorodite and oxides of Mn, Fe and Sb.

Sulphosalts are mainly represented by Pb-Sb, Ag-Pb-Sb and Ag-Pb-Bi phases (groups).

From the group of Pb-Sb sulphosalts jamesonite is most common. Jamesonite show a stable chemical composition, sometimes with increased content of Cu (up to 0.16 *apfu*), Ag (up to 0.04 *apfu*) and Bi (up to 0.03 *apfu*). Zinkenite frequently forms euhedral needle crystals enclosed by tetrahedrite, antimonite and jamesonite or by idiomorphic crystals of sphalerite. Zinkenite has sometimes an increased content of Zn (0.68 wt%, 0.62 *apfu*) and/or Bi (0.88 wt%, 0.25 *apfu*). Robinsonite sporadically contains up to 0.02 *apfu* Bi. All the Pb-Sb sulphosalts contain 0.01–0.05 *apfu* Cd and 0.01–0.09 *apfu* Cl.

Ag-Pb-Bi sulphosalts are represented by lillianite homologues $N = 4$ (gustavite and lillianite) and $N = 7$ (heyrovskýite). According to their chemical composition all the Ag-Pb-Bi sulphosalts are markedly enriched the Ag-Bi end-member. Content of the Ag-Bi end-member in lillianite reaches 54.11–73.45 mol% range, in heyrovskýite 46.58–64.21 mol% range and in gustavite 79.57 to 93.86 mol% range, which is almost the Ag-Bi end-member of the lillianite–gustavite series. Lillianite and heyrovskýite have an increased content of Sb (up to 0.09 *apfu*) and Cd (up to 0.16 *apfu*). An increased concentration of Sb (up to 0.08 *apfu*) and Cd (up to 2.07 *apfu*) was detected in gustavite, too.

Ag-Pb-Sb sulphosalts are represented by the analogues of the lillianite homologous series ($N = 4$). Two types of andorite occur on the locality. The first type of andorite forms tiny needles and inclusions in stibnite together with robinsonite and jamesonite. It contains 97.76–101.38% molecule of andorite and according to MOËLO *et al*. (1989) it is senandorite (andorite VI). This andorite have an increased content of Cu (up to 0.22 *apfu*), Fe (up to 0.02 *apfu*), Cd (up to 0.02 *apfu*) and sometimes Bi (up to 0.01 *apfu*), too. The second type of Ag-Pb-Sb sulphosalts (andorite?) occurs associated with Bi-Pb-Ag sulphosalts, native bismuth, bismuthinite and Bi-Te minerals in galena. These sulphosalts contain 77.81–81.79% andorite molecule and can be grouped between ramdohrite and an unnamed member of the series "81.25", with the theoretical formula of $Pb_{22}Ag_{13}Sb_{45}S_{96}$. These sulphosalts have an increased content of Cd (up to 0.09 *apfu*) and especially Bi (up to 1.38 *apfu*).

Tetrahedrite frequently forms idiomorphic to allotriomorphic crystals in the quartz. We described two types of tetrahedrite. The first type forms isolate grains in quartz and it can be characterised by an increased content of Hg (up to 0.03 *apfu),* Cu (up to 9.77 *apfu*) and a decreased content of Ag (up to 1.38 *apfu*) as compared to the second type of tetrahedrite. The second type occurs together with zinkenite, jamesonite and sphalerite. Both types of tetrahedrite have an increased content of Cd (up to 0.03 *apfu*) and sometimes As (up to 0.32 *apfu*).

Bi-Te minerals occurs together with native bismuth, bismuthinite and Ag-Pb-Bi(-Sb) sulphosalts in galena. We identified joséite-A, joséite-B and baksanite. In these tellurides the content of Se is very low. On the average joséite-A and joséite-B contain about 0.16 *apfu* Pb and baksanite 0.34 *apfu* Pb. Content of tellurium varies at from 1.23 *apfu* to 1.36 *apfu* for joséite-A, from 1.49 *apfu* to 1.54 *apfu* for joséite-B and from 1.82 *apfu* to 2.02 *apfu* for baksanite. The average empirical crystal chemical formula of the tellurides is as follow: baksanite $(Bi_{5.66}Sb_{0.01})_{5.67}(Pb_{0.34}Cu_{0.01})_{0.35}Te_{1.92}Se_{0.01}S_{3.0}5$, joséite-A $(Bi_{4.11}Sb_{0.01})_{4.12}Pb_{0.16}Te_{1.29}S_{1.41}$ and joséite-B $(Bi_{3.97}Sb_{0.01})_{3.98}Pb_{0.16}Te_{1.55}Se_{0.02}S_{1.30}$.

Reference

MOËLO, Y., MAKOVICKY, E. & KARUP-MØLLER, S. (1989): Sulfures complexes plombo-argentifères: minéralogie et cristallochimie de la série andorite-fizelyite $(Pb,Mn,Fe,Cd,Sn)_{3-2x}(Ag,Cu)_x(Sb,Bi,As)_{2+x}(S,Se)_6$. Documents du BRGM, 167, Orléans: BRGM, 107 p.

MINERALOGY OF LAMPROPHYRES FROM THE DITRĂU ALKALINE MASSIF, ROMANIA

BATKI, A. & PÁL-MOLNÁR, E.
Department of Mineralogy, Geochemistry and Petrology, University of Szeged, P.O. Box 651, H-6701 Szeged, Hungary
E-mail: batki@geo.u-szeged.hu

Lamprophyres are a group of H_2O and/or CO_2-rich, alkaline rocks ranging from sodic to potassic and from ultrabasic to intermediate. They typically form subvolcanic dykes, sills, pipes and vents (ROCK, 1991).

The Ditrău Alkaline Massif (DAM) is one of the most diverse and compound geological formations of the Eastern Carpathians. The massif was formed by hornblendite, diorite (called Tarnica Complex, PÁL-MOLNÁR, 2000), syenite, nepheline syenite, alkali granite and monzonite which are cut by late-stage lamprophyre (camptonite and kersantite) dykes. This paper presents the results of mineralogical analyses investigated on lamprophyres from the northern part of the DAM.

Mineral compositions were measured with a Cameca SX50 electron microprobe at the Department of Earth Sciences, University of Uppsala, Sweden. Operating conditions: probe current 15 nA, acceleration voltage 20 kV.

Essential ferromagnesian phases in the studied lamprophyres are calcic and Ti-rich groundmass amphiboles (Fig. 1A, B) and phenocrystic pyroxenes (Fig. 1E), abundant biotites-phlogopites with mg# = 0.47-0.75 (Fig. 1D) and melanitic garnets with the composition of $Ca_{3.1}Fe_{1.4}Ti_{0.16}Al_{0.5}Si_3O_{12}$. Lamprophyres from the DAM also carry plagioclase feldspars (albite–andesine with $An_{0.1–34}$), some K-feldspars (Fig. 1F), feldspathoids and carbonates. Accessories are apatite, titanite, magnetite and zircon. Post-magmatic or secondary phases are tremolite–actinolite (Fig. 1C) chlorite (FeO 13 to 24 wt%), sericite, epidote and allanite-(Ce, La).

Acknowledgements

The financial background for this work was provided by the Hungarian National Science Found (OTKA, Grant No. T 046736) and the Department of Geology and Geochemistry, Stockholm University, Sweden.

References

PÁL-MOLNÁR, E. (2000): Hornblendites and diorites of the Ditró Syenite Massif. Szeged: University of Szeged, Department of Mineralogy, Geochemistry and Petrology, 172 pp.

ROCK, N.M.S. (1991): Lamprophyres. Glasgow: Blackie, 285 pp.

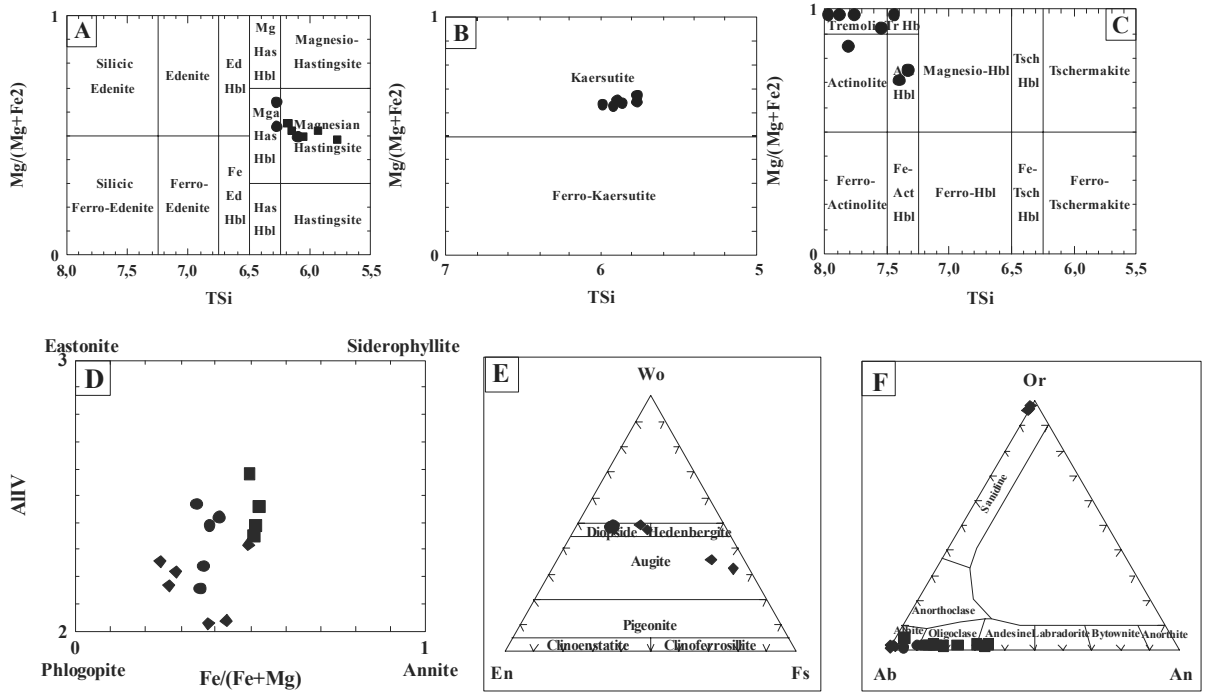

Fig. 1: Compositions of amphiboles (A, B, C), biotites (D), pyroxenes (E) and feldspars (F) in ● camptonites – Tarnica Complex, ■ camptonites – Török Creek and ◆ kersantites – Török and Nagyág Creek (DAM).

GEOCHEMICAL CHANGES IN SIDERITES FROM THE LUBLIN COAL BASIN – PRELIMINARY RESULTS

BAZARNIK, J.
Department of Mineralogy, Petrography and Geochemistry, AGH University of Science and Technology, al. Mickiewicza 30, Krakow, Poland
E-mail: JBazarnik@poczta.fm, jbazarnik@geolog.geol.agh.edu.pl

Siderite samples were collected from the Lublin Beds (Westphalian B) in the "Bogdanka" coal mine the Lublin Coal Basin (LCB). The LCB forms an elongated NW–SE depression split by the Kock Structure into two major regions – the asymmetric Radzyń–Bogdanka Syncline and the Stoczek–Dorohucza Syncline (ZDANOWSKI, 1999). Fresh-water and brackish environments are characteristic of the LCB sedimentation. The Westphalian B sediments enclose coal seams intercalated by sandstones, mudstones, claystones and occasionally limestones and siderites (CEBULAK, 1988).

Siderites occur in every type of sedimentary rocks and are differ in their size, shape and form of occurrence. Small siderite concretions, siderite ooids and siderite layers from the sandstones, mudstones and claystones were chosen to examination.

X-ray powder diffractometry (XRD) analyses were carried out at the Department of Mineralogy, Petrography and Geochemistry, AGH – University of Science and Technology (AGH-UST), Krakow, using a Philips X'Pert diffractometer with a graphite monochromator under the following operating conditions: CuK_{α} radiation, scanning speed 0.02°(2θ)/sec, range 3–73°2θ.

Distribution of Fe, Mg, Mn and Ca within siderites and the chemical composition of associated minerals were determined with a cold field emission scanning electron microscope (FESEM) Hitachi S-4700 coupled with an energy dispersive spectrometer (EDS) NORAN Vantage at the Institute of Geological Sciences of the Jagiellonian University, Kraków.

The results indicate the presence of clay minerals (mainly kaolinite and illite), quartz, sometimes feldspars and siderite in the samples studied. Siderite XRD peak positions are shifted in comparison to those of pure siderite. It might be a result of isomorphic substitution of Mg^{2+}, Mn^{2+} or Ca^{2+} in the siderite structure. SEM investigations point to the presence of sulphides (pyrite, sphalerite), quartz and carbonate minerals (ferroan dolomite, calcite and siderite). Sphalerite, pyrite, calcite and ferroan dolomite are present in septarian cracks, while siderite, pyrite, quartz and clay minerals are common in the concretion bodies themselves.

High variability of isomorphic substitutions of Mg, Mn and Ca for Fe was observed in the analysed siderite samples. The inner parts of siderites are relatively purer and have less isomorphic substitutions than the outer ones. The purest inner parts of siderites (oolites up to 98.61 wt%, concretions up to 94.17 wt%, siderite layers up to 96.27 wt% of $FeCO_3$) are characteristic of the early stage of siderite formation. The highest value of Mg is characteristic of the outer parts of siderite bodies and suggests the late diagenetic (or even epigenetic) origin of these parts of siderites. Higher content of Mg (up to 35.42 wt% of $MgCO_3$) than that of Mn (up to 10.85 wt% of $MnCO_3$) or Ca (up to 9.34 wt% of $CaCO_3$) was calculated. Compositions corresponding to sideroplesite or even pistomesite (in accordance with the peak shifts observed in the XRD patterns) were recorded. Despite the fact that oolites are purer than the other types of siderite (up to 98.61 wt% $FeCO_3$), the characteristic evolution from highest values of Fe in the inner parts of the oolites to highest values of Mg (up to 22.91 wt% of $MgCO_3$), Ca (up to 4.89 wt% of $CaCO_3$) and Mn (up to 2.81 wt% of $MnCO_3$) in the outer parts of the oolites is also observed. The chemical composition of siderite cements in the sandstones and mudstones is similar to that of the late type of siderite present in the outer parts of concretions (up to 37.28 wt% of $MgCO_3$; up to 5.94 wt% of $MnCO_3$; up to 6.95 wt% of $CaCO_3$).

Mg, Mn and Ca isomorphic substitutions for Fe and chemical evolution were observed in siderites from all types of sedimentary rocks of the Lublin Beds but there were only small quantitative differences among them.

Evolution of chemical compositions in the analysed siderite samples has been proven. Similar changes were indicated in sediments from other regions by previous authors (*e.g.* MIDDLETON & NELSON, 1996; MOZLEY, 1989).

Acknowledgements

The investigations were supported by AGH-UST research project no. 10.10.140.180. This manuscript greatly benefited from help of and discussions with Prof. Tadeusz Ratajczak, Dr. Lucjan Gazda, Adam Gaweł, M. Sc., and Bartosz Budzyń, M. Sc.

References

CEBULAK, S. (1988): Prace Instytutu Geologicznego, 72: 77–88.

MIDDLETON, H.A. & NELSON, C.S. (1996): Sedimentary Geology, 103: 93–115.

MOZLEY, P.S. (1989): Geology, 17: 704–706.

ZDANOWSKI, A. (1999): Geological atlas of the Lublin Coal Basin 1:50 000. Warszawa: Państwowy Instytut Geologiczny. (in Polish and in English)

APPLICATION OF K-Ar AGE DETERMINATION OF HYDROTHERMAL CLAY MINERALS FOR RECONSTRUCTION OF FLUID MOBILIZATION PROCESSES IN THE VARISCAN GRANITE INTRUSION OF THE VELENCE MTS. (TRANSDANUBIA, HUNGARY)

BENKÓ, ZS.[1], MOLNÁR, F.[1] & PÉCSKAY, Z.[2]
[1] Department of Mineralogy, Eötvös Loránd University, Pázmány Péter sétány 1/C, H-1117 Budapest, Hungary
E-mail: benkoo@elte.hu
[2] Institute of Nuclear Research, Hungarian Academy of Sciences (ATOMKI), Bem tér 18, H-4026 Debrecen, Hungary

The age of the biotitic monzogranite intrusion in the Velence Mts. is 280-300 Ma based on K-Ar age determinations on fresh biotite (BUDA, 1985). Granite hosts vein-type quartz-polymetallic and quartz-fluorite mineralization with argillic wall rock alteration. By the time of the Palaeogene age, several andesite veins intruded the granite and along the eastern border of the granite body a large intrusive-volcanic structure has formed in relation to the Alpine collision. The Palaeogene hydrothermal circulation resulted in intense alteration in the diorite intrusion and in the stratovolcanic sequence and also caused intense argillitization and brecciation around the andesite veins in the granite. For reconstruction of age relationships of magmatic and hydrothermal processes, systematic mineralogical studies and K-Ar age determination was carried out on the K-rich mineral phases of the argillic alteration zones in the granite and on rock forming K-feldspars. Oriented and ethylene-glycolated clay mineral fractions were analysed by X-ray power diffraction (XPD) method. Morphological analysis of the clay minerals was carried out by scanning electron microscope (SEM). Four different argillic alteration types of granite were detected: 1) Pure illite occurs along andesite veins intruding granite, along quartz-barite veins and in hydrothermal breccias. Illite is well crystallized (10 μm) based on the short sedimentation time during smoothing and the sharpness of the (001) peaks and SEM photographs. 2) Pure kaolinite was found in the matrix of some hydrothermal breccias. 3) Mixture of illite and kaolinite was found in hydrothermal alteration zones away from the andesite veins intruding granite and in the breccias. Both mineral phases are well crystallized based on the sedimentation time and XPD measurements. 4) Mixture of illite-kaolinite-smectite occurs in the altered granite along polymetallic veins. Based on the sedimentation time and the XPD measurements, illite is less crystallized and kaolinite is the dominant mineral.

The kaolinite-illite-smectite clay mineral mixtures and fresh K-feldspar along polymetallic veins of granite provided 209-232 Ma K-Ar ages, obviously not matching with the 280-300 Ma age of the granite. If this association did not undergo any overprint by younger hydrothermal events, then the age of the polymetallic mineralization is Triassic. Thus this type of mineralization could be related to a regional heat effect causing fluid mobilization. Regional fluid mobilization and mineralizing processes forming Pb-Zn deposits are widely known in relation to the early opening of the Tethys-ocean in the Alp-Carpathian-Dinaride region.

K-Ar ages for the illite-kaolinite association scatter between 55 and 125 Ma. The 55-125 Ma ages may reflect the fluid mobilization effect of the Alpine subduction-collision events. Theoretically, it also cannot be excluded that hydrothermal fluids of Palaeogene volcanic events penetrated the whole granite body and overprinted the radiometric clock of the Variscan minerals due to their heat effect, however, systematic fluid inclusion studies (MOLNÁR, 2004) do not confirm the regional character of the Palaeogene hydrothermal circulation within the granite body.

The K-Ar age of pure illite samples is between 40-29 Ma. The younger ages corresponds to the 29-31 Ma age of alunite from the hydrothermally altered stratovolcanic series and K-Ar ages for K-feldspar and illite from the diorite intrusion along the eastern boundary of granite (BAJNÓCZI, 2004). The 33-40 Ma K-Ar age range of some illite samples correspond to the K-Ar age of andesite veins intruding granite. The age of the quartz-barite vein mineralization in the granite is also Palaeogene based on the 30 Ma age of illite along those veins.

Results indicate that systematic analysis of K-rich clay minerals from argillic alteration zones and rock forming minerals in old granite intrusions provides new aspects to discrimination fluid circulation events. Determination of the radiometric age of those events contributes to the better understanding of the tectonic and geodynamic evolution of the area.

References

BAJNÓCZI B. (2005): Tertiary hydrothermal systems of the Velence Mountains. Unpublished PhD Thesis, Budapest: Eötvös L. University, 79–86. (in Hungarian)

BUDA, GY. (1985): Origin of collision-type Variscan granitoids in Hungary, West Carpathian and Central Bohemian Pluton. Unpublished CSc Thesis, Budapest: Hungarian Academy of Sciences, 95. (in Hungarian)

MOLNÁR F. (2004): Acta Mineralogica–Petrographica, 45: 39–48.

CLINOPYROXENE COMPOSITION: A POSSIBLE DISCRIMINATION BETWEEN MAGMATIC ROCKS WITH MOR AND SSZ AFFINITIES

BEQIRAJ, A.[1] & MASI, U.[2]
[1] Faculty of Geology and Mining, Rruga Elbasani, Tirana, Albania
E-mail: ae_beqiraj@yahoo.com
[2] Department of Earth Sciences, P.le Aldo Moro 5, I-00185 Rome, Italy

16 clinopyroxenes from magmatic rocks of the Bulqiza ophiolitic complex (Albania) have been analysed for major and minor elements (electron microprobe) and for the trace and subtrace elements (ionic microprobe). The magmatic rocks belong to two different cumulatic series: a) plagioclase series and b) clinopyroxene series with Ol + Sp – Pl – Cpx – Opx – Amf – Mt and Ol + Sp – Cpx – Opx – Pl crystallization order, respectively (TASHKO & MARTO, 1990). All the clinopyroxene analyses fall within the tholeiitic trend (LEBAS, 1962). In addition, in the framework of the general tholeiitic trend, two separated clinopyroxene composition sub trends can be seen. The smoother trend belongs to clinopyroxenes from the rocks of the plagioclase series (dunite–plagioclase dunite–troctolite–olivine gabbro–gabbro norite) which shows a MOR-type magmatic affinity. On the contrary, the cumulates from the clinopyroxene series yield clinopyroxene data arrays characterized by a trend slope greater than the first, which is characteristic for the subduction generated magmas (LOUKS, 1990).

References

LEBAS, M. J. (1962): American Journal of Science, 260: 267–288.

LOUKS, R. R. (1990): Geology, 18: 346–349.

TASHKO, A & MARTO, A. (1990): Transition between ultrabasic tectonites and cumulates in the Bulqiza massif (in Albanian), Buletini i shkencave gjeologjike, (2): 67–81.

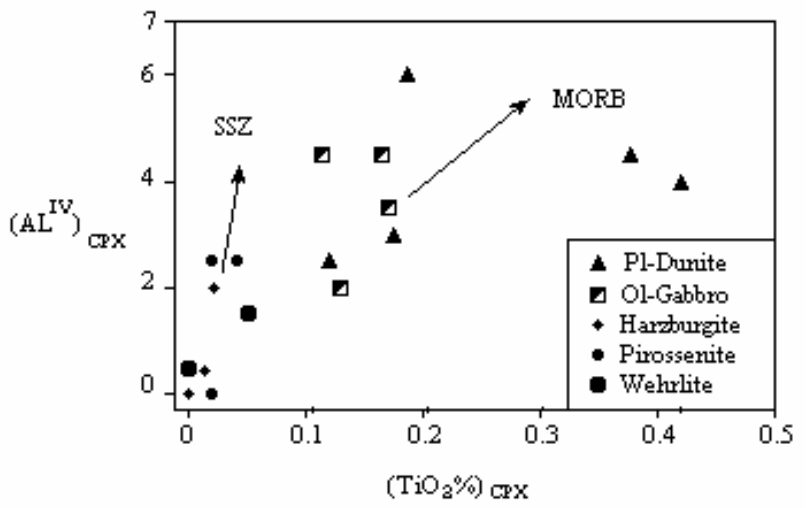

ZEOLITES OF MUNELLA (ALBANIA) – A STILBITE-STELLERITE SOLID SOLUTION

BEQIRAJ (GOGA), E.[1], MULLER, F.[2], TOURAY, J. C.[2] & JOZJA, N.[2]
[1] Faculty of Geology and Mining, Rruga Elbasani, Tirana, Albania
E-mail: ea_beqiraj@yahoo.com
[2] Institut des Sciences de la Terre d'Orléans, Rue de la Férollerie Orléans, Cedex 2, France

Zeolites of Munella are found between the SSZ-type volcanic rocks of the Mirdita zone (Jurassic Albanian ophiolitic complex). From the bottom to the top, the volcanic section consists of basalts, basaltic andesites, dacites and rhyolites. Zeolites crop out as separated up to 2-3 m thick layers, intercalated with rhyolites, dacites and andesites of the uppermost part of the volcanic sequence (SHALLO, 1994; BECCALUVA *et al.*, 1994).

Critical evaluation of other reported chemical analyses of stilbite phase from metabasalts indicates that most compositions lie along a binary solid solution between stilbite ($Ca_2NaAl_5Si_{13}O_{36}$ • $16H_2O$) and stellerite ($Ca_2Al_4Si_{14}O_{36}$ • $14H_2O$) (Fig.1) (FRIDRIKSSON *et al.*, 2001).

Microprobe data indicate that Munella zeolites fit the above stilbite–stellerite solid solution series (SS), showing a Ca-rich trend because of the domination of the stellerite end member (BEQIRAJ, 2004).

References

BECCALUVA, L., COLTORTI, M., PREMTI, I., SACCANI, E., SIENA, F. & ZEDA, O. (1994): Ofioliti, 19/1: 77–96.

BEQIRAJ (GOGA), E. (2004): PhD Thesis. Tirana: Polytechnic University of Tirana.

FRIDRIKSSON, TH., NEUHOFF, P.S., ARNORSSON, S. & BIRD, K.D. (2001): Geochimica et Cosmochimica Acta, 65: 3993–4008.

SHALLO, M. (1994): Ofioliti, 19: 25-37-96.

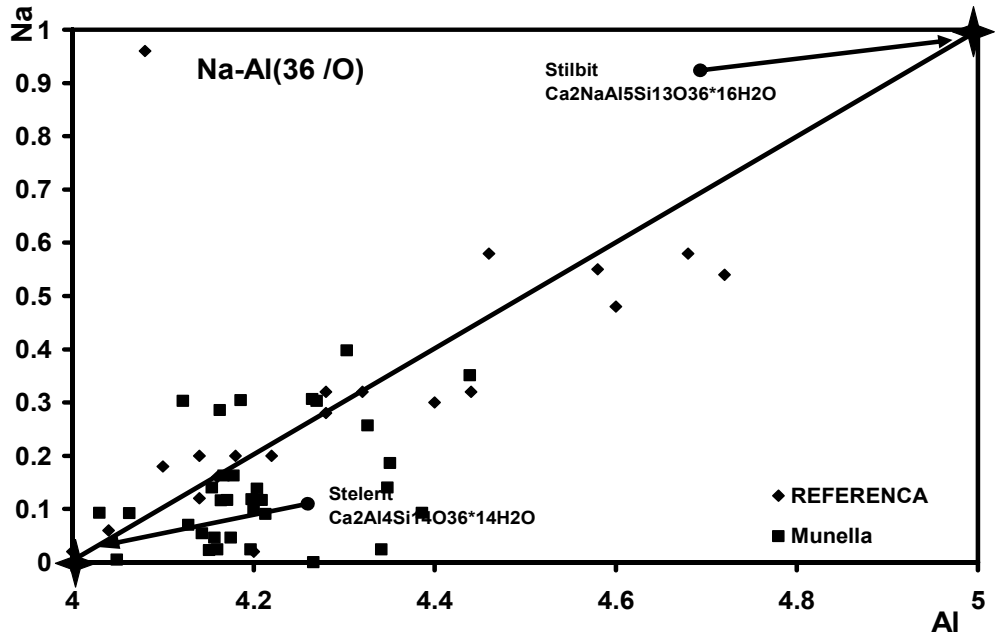

Fig. 1: Composition of natural stilbite SS minerals in metabasalts (solid squares represent the Munella zeolites).

GOLD IN PRE-ALPINE MINERALIZATIONS FROM ROMANIA

BERBELEAC, I.[1], JUDE, R.[1], UDUBAŞA, S. S.[1] & NUŢU, M. L.[2]
[1] Faculty of Geology and Geophysics, University of Bucharest, Bucharest, Romania
[2] Institute of Geodynamics of the Romanian Academy, Bucharest, Romania
E-mail: lmnutzu@geodin.ro

The territory of Romania is situated in Central-East Europe; it is dominated by the orogenic areas of the East (ECM) and South Carpathian Mountains (SCM) and the Apuseni Mountains (AM) (Fig. 1). It is a segment of the Alpine–Himalayan Orogen and the Tisza–Dacia block. Gold, with some exceptions, has been found in different fabrics and types of deposition in gold and gold-bearing mineralizations related to Precambrian to Palaeozoic schists from these orogenic area. Gold, gold-copper, gold-polymetallic, gold-arsenic and other occurrences and deposits were formed during the Baikalian and Hercynian metallogenetic events in areas that are included now in the Carpathian chain. It has been found in different proportions in two dominant types of ore deposits: 1) in shear-zone related gold and gold-bearing occurrences and deposits in the AM and SCM (Fig. 2) and 2) in volcanic-hosted massive sulphide (VHMS) deposits from EC (Fig. 3) and Dobrogea.

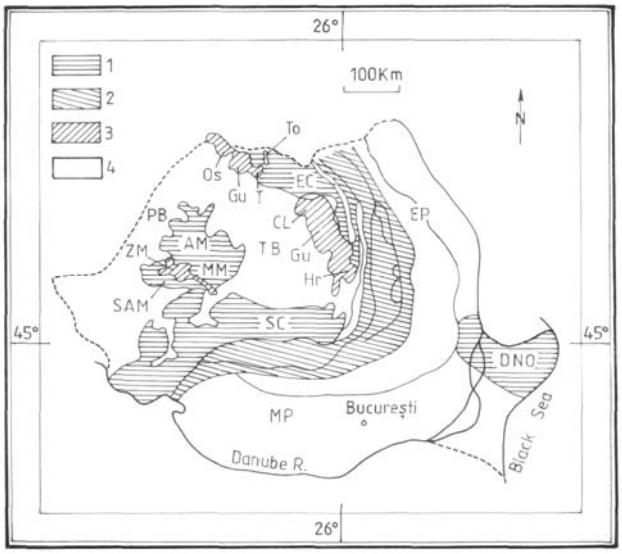

Fig. 1: Distribution of major tectonic units and Tertiary volcanic areas on the territory of Romania. 1: orogenic areas, 2: Carpathian flysch, 3: volcanic areas, 4: post-Precambrian–Palaeozoic cover. EC: East Carpathian Chain: Os: Oaş, Gu: Gutâi, T: Tibleş, Cl: Călimani, Gu: Gurghiu and Hr: Harghita Mts., AM: Apuseni Mts, SAM: South Apuseni Mts: ZM: Zarand Mts, MM: Metaliferi Mts., SC: South Carpathian Chain, PB: Pannonian Basin, TB: Transylvanian Basin, MP: Moesian Platform, EP: European Platform, DNO: North Dobrogea Orogen.

The first type of mineralization is controlled by interlayer ductile shear zones with reformation and probably superimposed mineralization from dip fluid sources. It is recognised by: 1) deep fracture; 2) brittle and brittle-ductile shear zones beside the deep fracture controlled the spatial locations of ore; 3) the intersections of secondary ductile shear zones with other tectonic elements are very favourable for the enrichment of gold; 4) the ore-controlling ductile shear zones show multistage features and a long period of evolution, the gold-bearing mylonites seem to be formed in the early stage and the gold-bearing quartz veins in the late stage. The most frequent mineral assemblages in which gold appears as common mineral are: quartz-Au; Au-Pb-Zn(Cu); quartz-pyrite-Au (Bi) and quartz-arsenopyrite. Further, we introduce some of the most representative occurrences in which gold is present.

1. Gold in auriferous quartz mineralizations

Mineralizations of this type are frequently located within Precambrian and Palaeozoic crystalline schists of medium or low grade of metamorphism, usually affected by migmatic and retrograde processes. Their close relation to shear zones is characteristic. They usually form lenticular veins and nests within the dilatation segments of the faults. The most representative occurrences are hosted in Precambrian schists of the Sebeş-Lotru Group (Căpăţânei, Lotru, Cibin and Semenic Mts.) in the South Carpathians (SC); Precambrian schists of the Someş Series (Gilău Massive) and Palaeozoic schists of the Padeş Series (Rapolt Crystalline Island) in the Apuseni Mts. (AM) The paragenesis is simple: native gold and gold associated with pyrite, arsenopyrite and chalcopyrite in quartz gangue with minor amounts of sphalerite and galena and occasionally Sb, Mo, Bi, Co and Ni minerals. Quartz, carbonates, sericite and chlorite represent the main gangue minerals. Hydrothermal-metamorphic genesis is considered for these mineralizations. As regards the source, gold is assumed to be originated both from Precambrian metabasite and/or the deep lithospheric crustal solutions as trace element mobilized in pre-Alpine (UDUBAŞA & HANN, 1988) and/or Alpine tectonogenesis (BERBELEAC, 1985, 1995, 1997).

In SC the main gold mineralizations are given in Fig. 2.

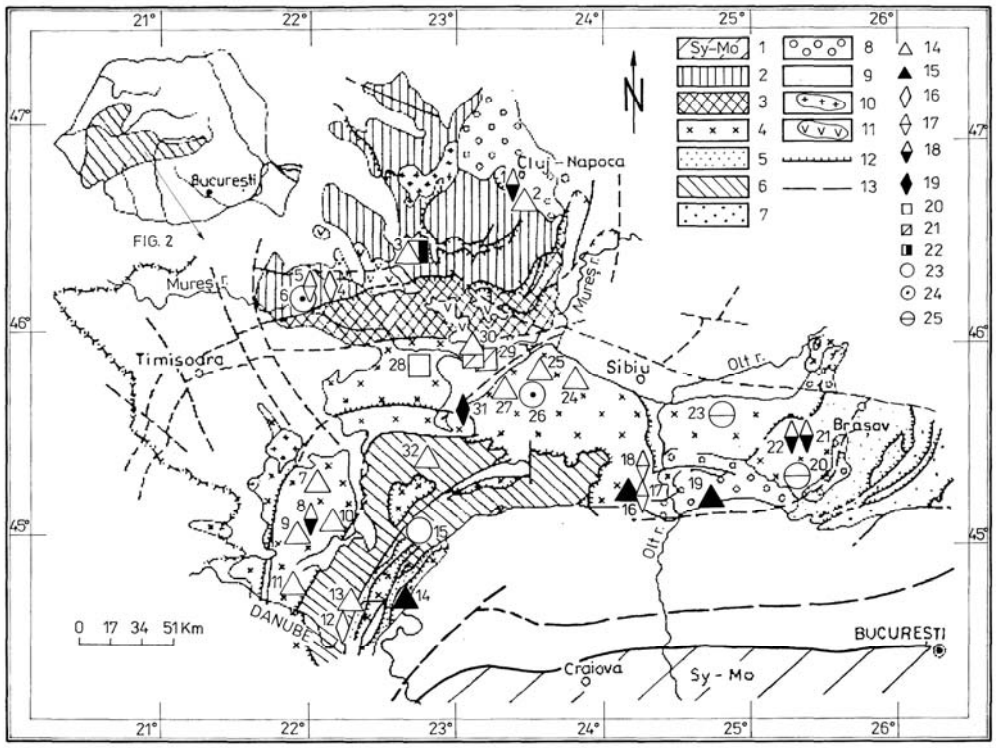

Fig.2: Tectonic sketch map of Southwestern Romania, with the distribution of pre-Alpine gold mineralizations related to shear zones (according to BERBELEAC, 1995, with amendments). 1: Scythian–Moesian Platform, 2: Inner Dacides, 3: Transylvanides, 4: Median Dacides, 5: Outer Dacides, 6: Marginal Dacides, 7: Moldavides, 8: post-tectonic cover, 9: Neogene molasses, depressions and foredeep, 10: Laramides, 11: Neogene magmatites, 12: nappe, 13: fault. Auriferous occurrences: 14: Qz, Fe (S) ± Au, Ag, 15: Qz, Fe (S) As, Au (Bi, Pb, Ag), 16: Qz, Fe (S + Ox), Zn, (Pb, Cu, As, Au), 17: Qz, Fe (S), Cu, Au (Zn, As), 18: Qz, Fe(S), Pb, Zn, Cu, Au, As, 19: Qz, Fe (S), Pb, Zn (Cu, Au), 20: Qz, Fe (S), Pb, Zn (Au), 21: Qz, Fe (S), Pb, Zn, Cu, Au, As, 22: Qz ± Fe (S), Au, 23: Qz, Fe (S), Au, Bi, 24: Qz, Fe (S), Au, Bi, Po, (Mo), 25: Qz, Fe (S), Zn, Pb, Au (Po): Occurrences: 1: Valea Băilor, 2: Ierții Valley-Valea Seacă, 3: Lazuri-Brusturi, 4: Ascutitu, 5: South Highiş, 6: Şoimuş Valley, 7: Buceava Valley, 8: Bogatu Bătrana (Văliug), 9: Liscovul inferior (Văliug), 10: Slătinic Brook (Bozovici), 11: Sichevița, 12–13: Mraconia, 14: Jidoştița, 15: Iepii Valley (Motru Sec River), 16: Netedu Brook (Costeşti), 17: Comârnici, 18 Valea lui Stan, 19: Băeşului Brook (Perişani), 20: Țâbra-Tâncava, 21: Ghimbav Valley, 22: Brusturi Brook, 23: Arpaş Valley, 24: Dobra Valley, 25: Pianu de Sus, 26: North Sebiş, 27: Cugir Valley, 28: Muncelul Mic, 29: Bobâlna, 30: Vărmaga, 31: Cioclovina, 32: Râul Mare Gallery.

1.1. Valea lui Stan

The gold mineralization is related to a regional N–S shear zone in Precambrian crystalline schists of the Sebeş-Lotru Group (Fig. 2). It is situated at 2 km southeast of Brezoi town, and is characterized by Au-As-Cu association. The rocks metamorphosed in amphibolite facies, underwent a greenschist retrograde metamorphism. The quartz-auriferous lenses are related to a broad (300 m) NNW–SSE and NNE–SSW fault zone. The mineral paragenesis consists of pyrite, arsenopyrite, chalcopyrite, subordinately sphalerite and galena as main minerals and of minor amounts of pyrrhotite and marcasite. Quartz and some carbonates are the gangue minerals. Gold as micron-size grains is frequently included in arsenopyrite and chalcopyrite, or associated with quartz (UDUBAŞA & HANN, 1988; UDUBAŞA, 2001). At the beginning of the last century the auriferous quartz vein of this deposit has been exploited at four levels, within 100 m depths. The ore grade is 11.7 g/t Au and 10.3 g/t Ag for the ore richer in chalcopyrite, and 2.6 g/t Au and 5.3 g/t Ag for the sort of ore richer in arsenopyrite. The fineness of the gold is 708–715 ‰.

1.2. Bozovici

In the southeastern side of the Semenic Mts. (South Carpathians), the metamorphic rocks of the Sebeş-Lotru Group host the auriferous-quartz mineralization (ÎNTORSUREANU *et al.*, 1985; BERBELEAC, 1985). It occurs along the Slătinic stream, a tributary of the Minis Valley, on the border zone of the Bozovici Miocene sedimentary basin (Fig.2). Lenses, lenticular veins and nests of auriferous quartz are hosted in a sequence of amphibolite and amphibole schists. A lenticular vein of 200 m length and 0.2–2 m thickness was exploited until the 1950s. Fragments of auriferous quartz may be found in the lower conglomerate horizon of the Miocene sedimentary formation.

The mineralization consists of native gold and pyrite in massive and fissured quartz; nests of carbonates and films of chlorite may be found occasionally. There are three varieties

of quartz: white-yellowish, grey-greenish and white-milky; the last two are auriferous. Macroscopically grains of gold up to 2-3 mm may be seen as disseminations in massive white quartz; under reflected light some grains of 0.072–0.120 mm have been observed. Mean gold content is around 5 g/t. The fineness of the gold is 840–860 ‰ (ÎNTORSUREANU *et al.*, 1985).

The Bozovici gold-quartz mineralization seems to be of pre-Alpine age, eventually reactivated by Alpine tectogenesis. Such type of mineralization in the Semenic Mts. represents probably the main source for the recent auriferous placers of the Nera River.

1.3. Someşul Rece

The gold mineralization occurs in the Gilău Mts. on both sides of the Someşul Rece River at the Băilor stream and Valea Seacă, up to the confluence with the Someşul Cald River, at about 20 km WSW of Cluj-Napoca town (Fig. 2). It appears as concordant and penecontemporaneous lenticular bodies within Precambrian retrograde mesometamorphic schists of the Someş Series. The ore bodies are 20-30 m in length and about 1 m in thickness and are related to N-S and NE-SW shear zones in quartz-chlorite and quartz-sericite schists (BERBELEAC, 1995).

The mineral assemblage consists of white, white-grey and pinkish quartz, chlorite, siderite, pyrite, chalcopyrite, gold, sphalerite, galena, arsenopyrite, tetrahedrite and rutile. Occasionally stibnite and molybdenite may be present. The distribution of gold in ores is in direct relationship with the frequency of chalcopyrite (2.4→20 g/t Au), while the lenses poor in chalcopyrite but with tetrahedrite are richer in Ag. The gold-rich lenses have been exploited in last centuries. From the Someşul Rece River, the shear zone, accompanied by similar but smaller occurrences of gold, continues up to 25 km, towards south, in the Ierţii and Vadului Valleys. In this deposit the gold appears as small grains of native gold in fissured and brecciated quartz and free gold in chalcopyrite appears as small grains.

The study of fluid inclusions in quartz from the Bozovici (Semenic Mts) and Someşul Rece (Gilău Mts) shows a range of temperature from 283 to 420°C, aqueous solutions with CO_2, and salinity of 2–14 wt% NaCl equivalent (POMARLEANU & MÂRZA, 2002)

2. Gold occurrences related to stratiform massive sulfides

The second type of mineralizations represents large hydrothermally metamorphosed stratiform and stratabound polymetallic deposits (like Kuroko type) related to acid volcanism to acid volcanism in the East Carpathians.

The Precambrian and Palaeozoic stratiform massive sulfide deposits usually contain native gold, visible under reflected light. Fine gold grains have been observed as example, in stratiform massive sulfide deposits hosted by Precambrian metamorphic schists at Altân Tepe (Central Dobrogea), associated with pyrite, chalcopyrite, magnetite, subordinated pyrrhotite, sphalerite and galena, and quartz, barite, sericite and chlorite as gangue minerals (BERBELEAC *et al.*, 1985). Gold is presents also in stratiform cupriferous-pyrite and Pb-Zn (+ Cu) deposits of Kuroko type in the EC (Fig. 3). The last one is associated with Cambrian (KRÄUTNER *et al.*, 1976, in BERBELEAC, 1998) or Ordovician (MUREŞAN, 2000) meta-eruptive felsic rocks of the Tulgheş Group. The mineralizations lie in pre-Alpine and Alpine overthrust nappes. The ore consists of pyrite, chalcopyrite, sphalerite, galena, pyrrhotite and arsenopyrite with minor amounts of tetrahedrite, bournonite, bismutite, galenobismutite, semseyite and gold, and quartz, chlorite, sericite, calcite and siderite as gangue minerals (ZINCENCO, 1999; BERBELEAC *et al.*, 1998). Gold in these deposits is usually invisible, rarely it appears as fine idiomorphic or anhedral grains. Gold is connected to sulfide minerals.

Similar gold occurrences associated with the metallogenesis of Lower Carboniferous meta-rhyolites are known at Muncel and Veţel as disseminations and massive base metal sulfide deposits in the Poiana Ruscă Mountains (South Carpathians). They are frequently sheared and remobilized (Fig. 1).

References

BERBELEAC, I. (1985): Gold deposits. (Zăcăminte metalifere; in Romanian). Bucureşti: Editura Tehnică, 336 p.

BERBELEAC, I. (1995): In: Mineral deposits: From the origin to their environmental impacts. Proceeding of the Third Biennial SGA Meeting, Prague. Rotterdam: Balkema, 93–96.

BERBELEAC, I. (1997): In: Mineral deposits, research and exploration. Where do they meet? Proceedings of the 4th Biennial SGA Meeting, Turku, Finland. Rotterdam: Balkema, 141–144.

BERBELEAC, I. (1998): Pb-Zn ore deposits. (Zăcăminte de plumb-zinc; in Romanian). Bucureşti: Editura Tehnică, 537 p.

ÎNTORSUREANU, I., POMÂRLEANU, V., NEGUŢ, G., SERAFIMOVICI, V., STREAMGA, V., ANASTASE, S., STEFĂNESCU, A. & VOICU, M. (1985): Dări de Seamă ale Şedinţelor Institutul de Geologie şi Geofizică, 69: 41–59

MUREŞAN, M. (2000): Romanian Journal of Mineral Deposits, 79, Suppl. 1: 66–68.

POMARLEANU, V. & MÂRZA, I. (2002): Studia Universitatis Babeş–Bolyai, Geologia, 47/1: 105–116.

UDUBAŞA, S. (2004): Romanian Journal of Mineral Deposits, 81, Special Issue (Fourth Symposium on Economic Geology, Bucharest): 195–199.

UDUBAŞA, G. & HANN, H. P. (1988): Dări de Seamă ale Şedinţelor Institutul de Geologie şi Geofizică, 72–73/2: 259–282.

ZINCENCO, D. (1999): Metalogenetic study of stratificated Py-Zn-Pb-Cu deposits in Maramureş Mountains (In Romanian). PhD Thesis. Unpublished manuscript, University of Bucharest.

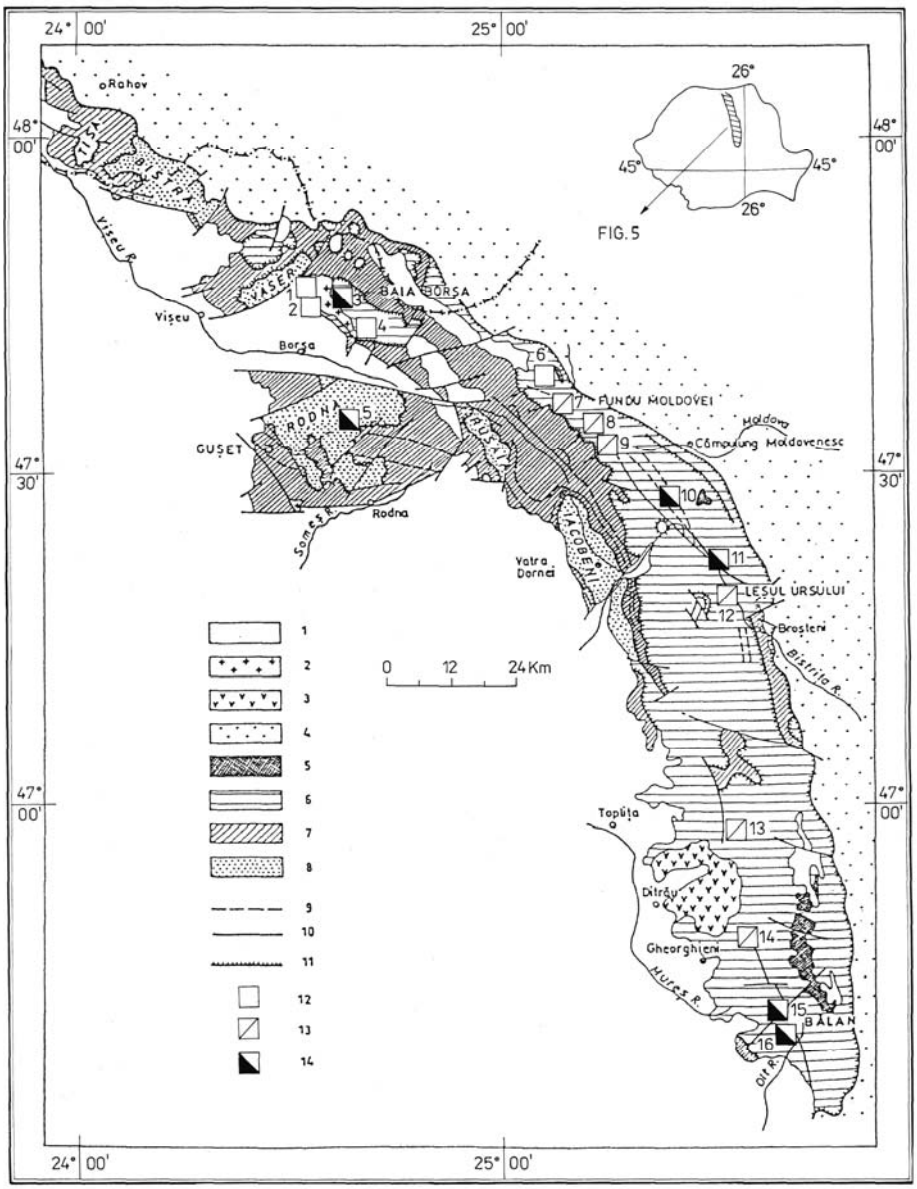

Fig. 3: East Carpathians: sketch map of Alpine geo-structural continental crust of Dacides with the distribution of metallogenic fields and some VHMS deposits in the pre-Alpine basement of the Bucovinian and Infra-Bucovinian nappes (according to BERBELEAC, 1998, modified).
1: post-Mesozoic sedimentary cover, 2: Neogene volcanites, 3: Lower Jurassic alkaline rocks, 4: Flysch Nappe, 5: Transylvanian nappes, 6: Bucovinian Nappe, 7: Sub-Bucovinian Nappe, 8: Infra-Bucovinian Nappe, 19: VHMS levels, 10: fault, 11: Alpine nappe plane. Type of deposits: 12: Py, Pb, Zn, Cu (± Au, Ag) or Py, Cu, Zn, Pb (± Au, Ag), 13: Py, Zn, Pb (Cu, Au, Ag), 14: Py, Cu, (Zn , Au, Ag). Metallogenic fields and some deposits (from North to South): Baia Borşa: 1: Novicior, 2: Novăţ-Capra, 3: Măcârlău, 4: Burloaia and Baia Borşa-Dealul Bucăţii; Izvorul Cepii: 5: Izvorul Cepii; Fundul Moldovei: 6: Arşiţa-Botoşel, 7: Fundul Moldovei, 8: Leuştean-Prasca, 9: Valea Putnei, 10: Colbu; Lesul Ursului: 11: Fagul, 12: Lesul Ursului, 13: Putna; Bălan: 14: Mediaş, 15: Bălan, 16: Fagul Cetăţii.

THE COLLECTION OF SERBIAN MINERALS FROM 1889

BLAGOJEVIĆ-BABIČ, S., BABIČ, D. & VASKOVIĆ, N.
Institute of Mineralogy, Crystallography, Petrology and Geochemistry, Faculty of Mining & Geology, University of Belgrade, Đušina 7, 11 000 Belgrade, Serbia and Montenegro
E-mail: danislav@mkpg.rgf.bg.ac.yu; nadavask@eunet.yu

The year 1880 has been taken as an official beginning of the Serbian Geology School. This is the time when the Chair of Mineralogy and Geology was split from the Department of Natural and Engineering Science at the High Education School (HES) in Belgrade. The well-respected scientist, JOVAN ŽUJOVIĆ (1856–1936) held professorship at this chair.

The roots of modern geology in Serbia can be traced a few decades before *i.e.* at the reign of Prince MILOŠ, who initiated prospecting of mineral resources in 1835 by calling HERDER to visit Serbia. Namely, the progression of geology in Serbia started with the opening of the Department of Natural and Technical Science (NTS) in 1853 at the Serbian Royal Lyceum. The first Professor of Mineralogy and Geology was the world famous botanist JOSIF PANČIĆ (1814–1888). The Mineralogical Cabinet was founded at the Lyceum in 1845. It comprised the first collection of minerals and rocks with basic equipment for mineralogical research. The lyceum was later transformed into the HES.

The HES owned a few collections of minerals and rocks. Among them the most unique was a collection of Serbian minerals established on the 1st January in 1889 by professor ŽUJOVIĆ. He arranged the specimens according to the districts of Serbian Kingdom and within them by localities. According to the original list written by ŽUJOVIĆ the collection involved specimens from 17 districts with 183 localities (Fig. 1). Each district contained several localities. Currently, the collection comprises 200 specimens from 120 localities. This is chiefly a collection of ore minerals. Careful examination of specimens within each district has shown that the collection represents a result of the contemporary ore prospecting of the Serbian Kingdom. The specimens from the collection were also used as a teaching means at the HES.

The available documents and literature data were carefully scrutinized. Despite all, it is not possible to find out how this collection arose. We can only suppose that foreign and later Serbian geologists collected specimens during their prospecting journeys through Serbia and stored them at the Mineralogical Cabinet, the NTS and the HES.

There is no doubt, according to the plentiful geological archive (1835–1889), that a lot of foreign geologists visited Serbia: BOUÉ (1836–37), HERDER (1835), RECKENDORF (1842), HOCHSTETTER (1869), TIETZE (1870), SZABÓ (1872–75), TOULA (1875, 1880). Among them only HERDER and RECKENDORF left a great number of mineral specimens in Serbia from their prospecting journeys. These specimens probably were the basis for creation of the first collection of Serbian minerals. Inspired by their example, the first Serbian geologists, educated abroad, had started to enrich this collection by new specimens.

The collection of Serbian minerals from 1889 is a part of the Museum of Minerals and Rocks at the Department of Mineralogy, Crystallography, Petrology and Geochemistry (Faculty of Mining and Geology, University of Belgrade) and represents one of the earliest ordered collections known in Serbia.

Fig. 1: Distribution of districts in Serbia in 1889.

TETRAD EFFECT IN THE WESTERN CARPATHIANS GRANITES AND THEIR PETROLOGICAL INTERPRETATION

BROSKA, I.[1], GAAB, A.[2] & KUBIŠ, M.[1]
[1] Geological Institute, Slovak Academy of Sciences, Dúbravská cesta 9, 840 05 Bratislava, Slovakia
E-mail: geolbros@savba.sk
[2] Max-Planck-Institut für Chemie, Abt. Geochemie, PF 3060, 55020 Mainz, Germany

Rare earth elements generally show similar geochemical behaviour controlled by their charge and ionic radii. Chondrite normalized rare earth element patterns are often used to estimate fractionation trends in comagmatic suites and they usually show smooth pattern, except the often observable Eu-anomaly. In contrast to these smooth patterns also strongly kinked patterns can occur in evolved granitoid systems and in sedimentary regimes. Such patterns are generated by the tetrad effect, when the geochemical behaviour is not determined only by charge and ionic radii.

Tetrad effect can be characterized as the division of Rare Earth Elements into four segments called tetrads (MASUDA *et al.*, 1987: first tetrad = La-Nd, second tetrad = (Pm)Sm-Gd, third tetrad = Gd-Ho, fourth tetrad = Er-Lu). According to BAU (1996) the tetrad effect is caused by complexation of the REE with ligands *e.g.* H_2O, CO_2, F^-, and Li. If such complexation occurs, the behaviour of the REE is no longer simply dependent on the ionic radii, which are comparable for all REE, but is dependent on the filling stages of the 4*f* orbitals (IRBER, 1999). Thus REEs with 0/4 (La), 1/4 (Nd, Pm), 2/4 (Gd), 3/4 (Ho, Er) and 4/4 (Lu) filled 4*f* orbitals can be fractionated from the other REEs. Tetrad effect occurs in highly evolved igneous rocks and it is often interpreted as an indicator of the transition between magmatic to high-temperature hydrothermal systems. The tetrad effect can not be modelled as fractional crystallization (*e.g.*, BAU, 1996; IRBER *et al.*, 1997). Tetrad effect can be expressed graphically or numerically as the $T_{1,3}$ parameter and it can be controlled by the presence of accessory mineral phases.

No tetrad effect can be observed for Variscan I-type granitic rocks and only very slight tetrad effects are revealed by differentiated S-type granites. Only A-type post-orogenic granites show sometimes tetrad effects, but the strongest is developed in the Permian-Triassic special S-type granites in the Gemeric unit. Tetrad effect is present almost in the all special S-type granites and the most prominent in the granite cupolas or in the most evolved samples. This indicates the strong synmagmatic hydrothermal activity during their magmatic intrusion. Taking into account that the tetrad effect is the result of complexation of the rare earth elements in hydrothermal systems, its presence indicates a strong influence of fluids in the granite evolution.

A very intense tetrad effect can be observed in the granites of the Dlhá dolina area, but also in the Hnilec area. Data presented in this study suggests that the tetrad effect observed in the Gemeric granites and especially in the Dlhá Dolina area is in correspondence with similar evolved granitoid suites (GAAB *et al.*, submitted).

References

BAU, M. (1996): Contributions to Mineralogy and Petrology, 123: 323–333.
GAAB, A., BROSKA, I., KUBIŠ, M., DIANIŠKA I., TODT, W. & POLLER, U.: Geologica Carpathica, submitted.
IRBER, W. (1999): Geochimica et Cosmochimica Acta, 63: 489–508.
MASUDA, A., KAWAKAMI, O., DOHMOTO, Y. & TAKENAKA, T. (1987): Geochemical Journal, 21: 119–124.

BERYLLOPHOSPHATE ASSEMBLAGES FROM THE ROŽNÁ PEGMATITE, CZECH REPUBLIC

CEMPÍREK, J.[1] & NOVÁK, M.[2]
[1] Department of Mineralogy and Petrography, Moravian Museum, Zelný trh 6, 659 37 Brno, Czech Republic
E-mail: jcempirek@mzm.cz
[2] Institute of Geological Sciences, Masaryk University, Kotlářská 2, 611 37 Brno, Czech Republic

SEKANINA (1950) described an unusual occurrence of herderite from lepidolite pegmatite at Rožná-Borovina. This uncommon mineral was originally found in euhedral crystals in cavities of miarolitic pegmatites at Ehrenfriedensdorf, Saxony (HAIDINGER, 1828). At Rožná, it forms pseudomorphs after an unknown mineral of cubic or pseudocubic shape and because the matrix of the pseudomorph is fine-grained and is commonly partially replaced by later fluorapatite, the original mineral remained unknown up to now. The origin of the hydroxylherderite pseudomorphs was discussed several times (SEKANINA, 1950; NĚMEC, 1993). Judging from the shape of the "crystals", SEKANINA (1950) mentioned garnet and tourmaline as a possible precursor, whereas NĚMEC (1993) suggested the cubic borate rhodizite, usually found in highly fractionated elbaite-subtype pegmatites (*e.g.* SIMMONS *et al*., 2001).

Recent study of this material (powder X-ray diffraction, electron microprobe, cathodoluminiscence study) revealed that several beryllium minerals occur within the pseudomorphs and two distinct assemblages involving hydroxylherderite as a dominant mineral. Assemblage I consists of beryllonite + hurlbutite + hydroxylherderite + fluorapatite, whereas assemblage II contains bertrandite + quartz + hydroxylherderite + fluorapatite. In both assemblages, small inclusions of unknown Ba or Sr phosphates occur; they best correspond to Ba and Sr equivalents of hurlbutite based on their stoichiometry. Beryllonite was very likely the original primary mineral in the pseudomorphs with assemblage I, in the case of assemblage II the primary mineral might be beryllonite or beryl. The herderite pseudomorphs from Rožná are a good example of complicated polyphase replacement of Be-dominant primary mineral (beryllonite and/or beryl) in highly variable activities of Ca, P, F and Si producing various beryllophosphates *versus* Be silicates (bertrandite).

This work was supported by the research projects MK9486201 to JC and MSM0021622412 to MN.

References

HAIDINGER, W. (1828): Philosophical Magazine, 2nd ser., 4: 1–3.
NĚMEC, D. (1993): Acta Musei Moraviae. Scientiae naturales, 78: 13–19.
NOVÁK, M., HOUZAR, S. & PFEIFEROVÁ, A. (1998): Acta Musei Moraviae. Scientiae geologicae, 83: 3–48.
SEKANINA, J. (1950): Práce Moravskoslezské akademie věd přírodních, 22 (6-7): 211–218.
SIMMONS, W.B., PEZZOTTA, F., FALSTER, A.U. & WEBBER, K.L. (2001): Canadian Mineralogist, 39: 747–755.

MINERALOGICAL STUDY OF UPPER CAMBRIAN GLAUCONITES FROM TEXAS, USA

CORA, I.[1], TÓTH, E.[1], WEISZBURG, T. G.[1] & ZAJZON, N.[2]
[1] Department of Mineralogy, Eötvös Loránd University, Pázmány Péter sétány 1/C, H-1117 Budapest, Hungary
E-mail: coraildiko@gmail.com
[2] Department of Mineralogy and Petrology, University of Miskolc, H-3515 Miskolc-Egyetemváros, Hungary

This work presents the first step of our study, the thorough mineralogical characterisation of two Palaeozoic glauconite populations. Palaeozoic glauconites are thought to have formed under different conditions than their Cenozoic counterparts (CHAFETZ & REID, 2000). To better understand the formation conditions of glauconites prevailing during the Palaeozoic era, we started to study glauconite-bearing Palaeozoic rocks. As such rock types are not typical for the Carpathian Region, we selected two glauconite-rich limestones from the Upper Cambrian of Texas, USA. The first sample originates from the Lion Mountain Member of the Riley Formation, while the other comes from the Morgan Creek Member of the Wilbern Formation, the latter being younger by a few million years. A detailed geological background of the studied samples is given by CHAFETZ & REID (2000).

Both samples were crushed and decarbonated by 5% acetic acid. The free grains were separated upon grain size (> 1000 μm, 1000–500 μm, 500–250 μm, 250–125 μm, 125–63 μm, 63–32 μm and < 32 μm), magnetic susceptibility (0.3, 0.4, 0.5, 0.6, 0.7, 0.8 and 0.9 A current) and density. For the density separation bromoform (tribromomethane) was diluted with ethyl alcohol, and density separation was carried out in the 2.83–2.48 g/cm^3 range with density steps of 0.05 g/cm^3.

The sample from the Lion Mountain Member is a limestone, cemented by white sparry calcite (67 wt% of the whole rock). Glauconite often forms dark green horizons within the rock. The total glauconite content of the rock is 8 wt% (for glauconite grains > 32 μm). The total amount of insoluble grains below 32 μm is 4.5 wt% of the whole rock, and this fraction contains glauconite grain fragments, too.

The grains insoluble in acetic acid were separated into 84 fractions. Glauconite proved to be very mature: 80% of the grains are of a density above 2.78 g/cm^3. The glauconite grains are usually rounded, cracked and some of them are bowl-shaped. The cracks in the glauconite grains are sometimes filled with "limonite". The surface of the glauconite grains is usually smooth. The glauconite population is characterised by a broader, symmetric 001, d_{001} = 10.16 Å, d_{060} = 1.517 Å. Beside glauconite the sample contains rounded quartz grains (17 wt%), some of them still preserving their original euhedral shape. Sphere-shaped "magnetite" (= strongly magnetic, opaque grains) appears as inclusions in quartz. Apatitic brachiopod test fragments (0.3 wt%) are also present. In the 63–32 μm grain size fraction elongated euhedral zircons are also abundant. The grains are often cemented into aggregates by "limonite".

WDX analyses on non-separated glauconite grains in thin section yielded the following average formula (Fe^{2+} estimated for 15% of the total Fe content):

$$K_{0.77}Na_{0.01}Ca_{0.02}(Fe^{3+}_{1.24}Mg_{0.40}Fe^{2+}_{0.22}Al_{0.18})[Si_{3.67}Al_{0.33}O_{10}(OH)_2].$$

The limestone sample from the Morgan Creek Member is cemented by yellowish sparry calcite, which is more coarsely crystalline than in the case of the other sample and composes 86 wt% of the whole rock. Glauconite grains are evenly dispersed within the rock, they do not accumulate into dark green horizons as in the other sample, and the total glauconite content is also lower (approx. 1.8 wt% in the grain size fractions > 32 μm). The density distribution curve of the glauconite grains is a bit more elongated towards the lower densities, but the population is still very mature: 65% of the glauconite population is denser than 2.78 g/cm^3. The glauconite grains are usually angular, elongated grains of biogenic origin are also frequent. The glauconite population is characterised by symmetric 001, d_{001} = 10.16 Å and d_{060} = 1.521 Å. Separated glauconite grains still contain apatite and calcite. Beside glauconite, the sample contains euhedral dolomite (0.43 wt%) of some iron substitution. The dolomite rhombohedra are originally transparent, but some of the grains are stained with "limonite" along the cleavage planes. Limonite pseudomorphs after dolomite rhombohedra are also frequent. Further detrital constituents are chlorite, biotite, muscovite, quartz and apatitic brachiopod test fragments.

Chemical and crystallographic data collection on the separated glauconite fractions is in progress.

The authors thank GRY BARFOD (University of California, Davis, USA) for providing the studied samples. This research was financially supported by the European Commission's Research Infrastructure Action via the SYNTHESYS Project and the Natural History Museum, London.

Reference

CHAFETZ, H.S. & REID, A. (2000): Sedimentary Geology, 136: 29–42.

THE FIRST OCCURRENCE OF BISMUTH SULPHOSALTS IN THE ŞUIOR ORE DEPOSIT, BAIA MARE DISTRICT, ROMANIA

DAMIAN, GH.[1], CIOBANU, C. L.[2], COOK, N. J. [3] & DAMIAN, F.[1]
[1] North University of Baia Mare, 430083 Baia Mare, Romania
E-mail: damgeo@ubm.ro
[2] Department of Earth Sciences, University of Adelaide, North Terrace, S. A. 5000, Australia
[3] Natural History Museum, University of Oslo, Postboks 1172 Blindern, N-0318 Oslo, Norway

The Baia Mare metallogenetic district, Romania, represents the NW part of the Neogene Volcanic Chain inside the Carpathian Mountains. The polymetallic Şuior-Cremenea deposit is one of the most economically important deposits within the Baia Mare district. Ag-Bi sulphosalts are reported from Cu-rich ores within base metal mineralization situated beneath Au ores below level 750-800m in the Cremenea vein of the Şuior epithermal vein deposit. The Cremenea 'vein' is an important ore body in the Baia Mare district due to its size at upper levels; the vein extends *ca*. 800m along strike, reaching a depth of 1,200m, with a width between 2 and 40 m. Beneath the Au-Ag ores at upper levels, base metal mineralization is predominant in middle and lower parts. Telescoping is recognised in the middle part of the vein, with Au-Ag mineralization overlapping the base metal ores. The Cremenea vein lies on the northern side of a subvolcanic intrusion of porphyritic microdiorite. The upper Au-Ag-rich part consists of pyrite, wurtzite, sphalerite, arsenopyrite, chalcopyrite, tetrahedrite, galena, boulangerite and marcasite. Below 800 m, sphalerite and galena are predominant, frequently associated with chalcopyrite. Inclusions of Sb sulphosalts (tetrahedrite, proustite and pyrargyrite) appear frequently within galena. Beneath the gold zone, Cu-rich ores (pyrite – chalcopyrite ± arsenopyrite) may be present at the northern boundary of the ore body. They may also include Bi-minerals.

Electron probe microanalytical data were collected using a Cameca SX-51 instrument at the University of Adelaide, Australia and a Hitachi scanning electron microscope equipped with an Oxford Instruments wavelength-dispersive spectrometer at the Natural History Museum, University of Oslo, Norway.

The Bi sulphosalts occur within a Cu-rich ore (pyrite-chalcopyrite assemblage). The Bi sulphosalts appear as clustered elongated patches placed mostly at contacts between quartz and sulphides. They may also be located at grain boundaries in the quartz aggregates especially when pyrite is the only sulphide adjacent to the cluster. Typically, however, they are found in close association with chalcopyrite. When in chalcopyrite, they occur instead as well-shaped lamellae. With the exception of wittichenite, the Bi sulphosalts correspond to compounds that plot along the matildite-galena join in the Ag(+Cu)-Bi(+Sb)-Pb system.

Only a small number of the lamellae and blebs are fully homogenous. Microanalytical data show the presence of a homogeneous unnamed phase with empirical composition $[(Ag_{0.81}Cu_{0.12})_{0.93}Pb_{0.91}\ (Bi_{1.11}Sb_{0.06})_{1.17}(S_{2.98}Se_{0.02})_3]$, showing light Bi-enrichment relative to ideal **$AgPbBiS_3$**. The compositional clusters of homogenous lamellae overlap with one another in an area of the (Ag + Cu)–(Bi + Sb)–Pb diagram between the ideal composition $PbAgBiS_3$ and half way towards the tie line corresponding to the lillianite homologue $N^L = 9$. Microanalysis profiles taken along and across the homogenous lamella confirm the compositional homogeneity.

The second group of lamellae within the samples display such lamellar intergrowths. Compositional plots for the parallel intergrowths show a spread between the phases $PbAgBiS_3$ and $PbAg_2Bi_2S_5$. Parallel lamellar intergrowths have bulk compositions approximating **$Pb_4Ag_{5.6}Bi_{5.6}S_{15.2}$**. These compositions represent natural equivalents of phases synthesized in the $PbS–AgBiS_2$ system.

The most abundant type of lamellae, however, is that display well-developed basket-weave intergrowths of galena and matildite. Needle-shaped matildite is generally coarser than the galena. The compositional plot for patches with basket weave intergrowths expands on both sides of the ideal phase $PbAgBiS_3$ along the $PbS–AgBiS_2$ join, between **$Pb_3Ag_2Bi_2S_7$** and **$Pb_4Ag_{5.6}Bi_{5.6}S_{15.2}$**. These intergrowths with a characteristic basket-weave texture are interpreted as decomposition products of $AgPbBiS_3$.

Close-to-galena compositions were measured from larger, homogeneous areas separated from the basket weave intergrowths (brighter areas in the BSE images); close-to-matildite compositions are determined for the needle-shaped lamellae in the same intergrowths (darker areas in the BSE images).

Although galena and matildite end- and decomposition-products may be formed at still lower temperatures, interpretation of observed textures and microanalytical data, in combination with published phase diagrams, indicate formation of the intermediate phases at temperatures as low as 144 °C. Similarly, we interpret minimum temperatures of initial precipitation as melts (in the range 40–70 % $AgBiS_2$) to be in the range 230–175 °C. The observed Bi excess may be a factor preventing decomposition of $AgPbBiS_3$ into galena and matildite.

FITTING THE BACKGROUND CURVE ON THE SPECTRA OF X-RAY MICROANALYSIS OF MINERALS

DATSYUK, YU. & FOURMAN, V.
Chair of Physics of Earth, Faculty of Geology, L'viv National University; Hrushevskogo str., 4, 79005 L'viv, Ukraine
E-mail: yudat@ukr.net

We present the results of the development of a computer based peak/background ratio technique for quantitative X-ray microanalysis.

The energy dispersive X-ray microanalysis is a successful method due to its rapidness and relative simplicity. The standard ZAF technique is a complicated procedure, requiring special preparation of the samples and usage of external standards. However, the peak/background technique is an outstanding one because it considers the spectra as a whole *i.e.* treats the peaks and the background as single complex formation. Moreover, the peak/background technique is less dependent on the effects of fluorescence and secondary absorption. This new technique is basically a computer simulation of the spectrum followed by successive cycles of iteration aiming to minimize the difference between the calculated and observed spectrum.

According to our approach the background curve consists of two parts i) a lognormal curve, which describes background emission free of absorption and ii) the components that are responsible for the absorption edge and described by staircase functions. The fitted spectrum consists of a convolution of Gaussians, lognormal functions and staircase functions. The parameters of both the background curves and Gaussian peaks are treated with the least-squares method, in order to minimize the difference between empirical and the calculated functions.

Experimental studies have been performed using a JEOL scanning electron microscope equipped with an energy dispersive spectrometer of the Oxford Instruments Analytical. Results by our iterative calculation method demonstrate reliable coincidence with the standard based EDAX methods.

The goals of the proposed technique is to extend the potential of X-ray microanalysis to samples that cannot be studied by standard EDAX methods and to those for which no reliable standard can be found (*e.g.* due to special chemistry). Our technique allows to increase both the accuracy and sensitivity of the X-ray microanalysis of such samples and more efficient in precise measurements and analysis of rough and/or not prepared samples.

References

GOLDSTEIN, J., NEWBURY, D.E., JOY, D.C., LYMAN, C.E., ECHLIN, P., LIFSHIN, E., SAWYER, L.C. & MICHAEL, J.R. (1981): Scanning electron microscopy and X-ray microanalysis. New York: Plenum Press.

STATHAM, P.J. (2002): In: Proceedings NIST-MAS Special Topics Workshop "Understanding the Accuracy Barrier in Quantitative Electron Probe Microanalysis and the Role of Standards" NIST, Gaithersburg, MD, USA, April 8–11.

CEC AND EGME RETENTION *VS.* TEXTURAL PROPERTIES OF Na-X (FAU) ZEOLITE

DERKOWSKI, A.[1], FRANUS, W.[2], WANIAK-NOWICKA, H.[2] & CZÍMEROVÁ, A.[3]
[1] Institute of Geological Sciences, Polish Academy of Sciences, Senacka 1, 31-002 Krakow, Poland
[2] Department of Geotechnics, Lublin University of Technology, Nadbystrzycka 40, 20-618 Lublin, Poland
E-mail: w.franus@pollub.pl
[3] Institute of Inorganic Chemistry, Slovak Academy of Sciences, Dúbravská cesta 9, 845-36 Bratislava, Slovakia

The retention of ethylene glycol monoethyl ether (EGME) is a useful technique for determination of the total surface area (TSA) of expandable clay minerals (CARTER *et al.*, 1965). Diameter of zeolite X micropores is probably wide enough for access of EGME molecules, thus EGME should fill pores in a capillary way and cover as monolayer the external surface of grains in the produced material (DERKOWSKI *et al.*, submitted). Cobalt (III) hexamine chloride (ORSINI & REMY, 1976) is commonly used for the determination of CEC of clay minerals, beside the conventional methodology.

The study focuses on EGME and cation exchange capacity of zeolitic materials containing various percent of Na-X zeolite (FAU structure), versus their textural characterization. Zeolite X was synthesized at room temperature directly from raw fly ash, without prior treatment.

Increase of the BET surface area clearly depends on the development of microporous texture (S_{BET} *vs.* V_{mic} and S_{mic}, $R^2 = 0.99$). Micropore volume and area strictly follow the Na-X content but mesopore volume and surface area calculated from the BJH adsorption algorithm are independent on the zeolite content.

The CEC values measured with $[Co(NH_3)_6]Cl_3$ increase with the perfect linearity according to the development of micropore texture (CEC *vs*. V_{mic} and S_{mic}, $R^2 = 0.99$). Due to the great share of S_{mic} in the total surface area, the linearity for CEC *vs*. S_{BET}, may seem to be derivative of CEC *vs*. S_{mic}. But $R^2 = 0.99$ for CEC *vs*. S_{BET} exists even for samples with distinctive S_{ext} values. Thus, it is clear that CEC depends on the total surface area, including external one. Total CEC value (including sodalite cages) of materials rich in Na-X zeolite, measured using $Ba^{2+}$and Mg^{2+} cations is ca. twice higher than CEC measured by $[Co(NH_3)_6]^{3+}$ cation. Exchange positions available for $[Co(NH_3)_6]^{3+}$ cation occur only inside 12-ring space and loops of FAU framework.

The temperature of pre-heating is a crucial factor for the amount of retained EGME. Insufficient dehydration at 250 ºC (as in conventional procedure for clays) does not allow EGME molecules to enter all micropores. Pre-heating at 400 ºC causes EGME adsorption on all available surfaces. Mass of retained EGME linearly correlates with micropore volume and surface area ($R^2 = 0.96$), as well as S_{BET} ($R^2 = 0.97$). The retention of EGME does not correlate with micropore volume, however the incomplete dehydration (preheating at 250 ºC) allows for the partial EGME-water substitution in micropores and depends more on available mesopore surface area. Potential dimension of cylindrical micropores of the Na-X phase is ca. 43 $Å^2$, thus EGME retention inside the structure may be considered as a capillary infilling as well as surface adsorption (QUIRK & MURRAY, 1999). EGME molecule occupation area is ca. 41 $Å^2$, using BET algorithm and ca. 52 $Å^2$ for Langmuir equation, or package ratio 16 $Å^3$/1 EGME molecule if calculating adsorption as mechanism of micropores infilling.

Simple procedure of EGME retention can be successfully used to determine microporous texture of X zeolite available to organic molecules. The adsorption of EGME probably does not depend on charge density inside 12-ring space of FAU framework.

This work was financially supported by the Polish Ministry of Education and Science grant No 4 T12B 042 29

References

CARTER, D.L., HEILMAN, M.D. & GONZALES, C.L. (1965): Soil Science, 100: 356–360.

DERKOWSKI, A., FRANUS W., BERAN, E. & CZÍMEROVÁ, A.: Powder Technology, submitted.

ORSINI, L. & REMY, J.C. (1976): Science du sol, 4: 269–275.

QUIRK, J.P. & MURRAY, R.S. (1999): Soil Science Society of America Journal, 63: 839–849.

STRUCTURAL VARIABILITIES IN SERPENTINE-GROUP MINERALS. AN HRTEM VIEW

DÓDONY, I.
Department of Mineralogy, Eötvös Loránd University; Pázmány Péter sétány 1/C, H-1117 Budapest, Hungary

The magnesian serpentine minerals are trioctahedral phyllosilicates with idealized composition $Mg_3[Si_2O_5(OH)_4]$. The most abundant serpentine minerals are antigorite, chrysotile, and lizardite.

High-resolution transmission electron microscopy (HRTEM) affords a close look at the complex structures and intergrowths of the serpentine minerals. All contain alternating sheets of cations in tetrahedral and octahedral coordination. Lizardite, the flat species, and it is the reference mineral for estimates of the structures of antigorite, chrysotile, 15-sectored, and 30-sectored polygonal serpentines. Here the lizardite structure is used as a reference for the other serpentine minerals. We provide examples of disordered stacking, coherent intergrowths of lizardite and chlorite, HRTEM images of different polygonal serpentines, and antigorites, as well as HRTEM images and simulated diffraction data of chrysotile structures both along and perpendicular to the fibre axis.

References

DÓDONY, I. (1997): Physics and Chemistry of Minerals, 24: 39–49.

DÓDONY, I. & BUSECK, P.R. (2004a): International Geology Review, 46: 507–527.

DÓDONY, I. & BUSECK, P.R. (2004b): American Mineralogist, 89: 1631–1639.

DÓDONY, I., PÓSFAI, M. & BUSECK, P.R. (2002): American Mineralogist, 87, 1443–1457.

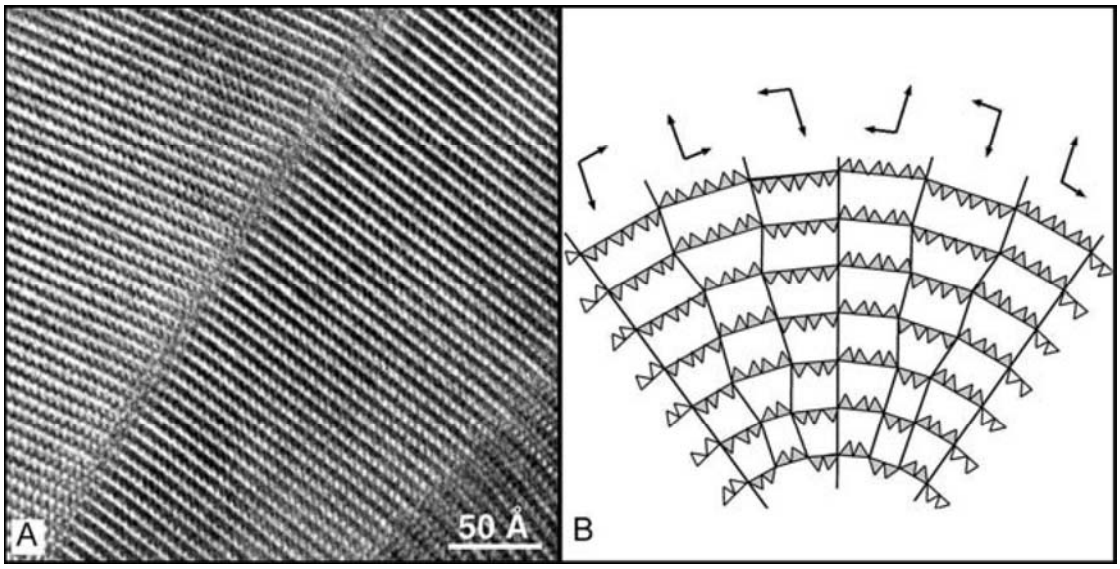

Fig. 1: (A) A part of an experimental HRTEM image on 30-sectored polygonal serpentine (30PS). Discontinuity in (001) lizardite planes at sector boundaries indicates reversals in tetrahedral sheets. (B) A schematic sketch of tetrahedral sheet structure in 30PS. The arrows show **b**/2 and **c** axes for the illustrated sectors.

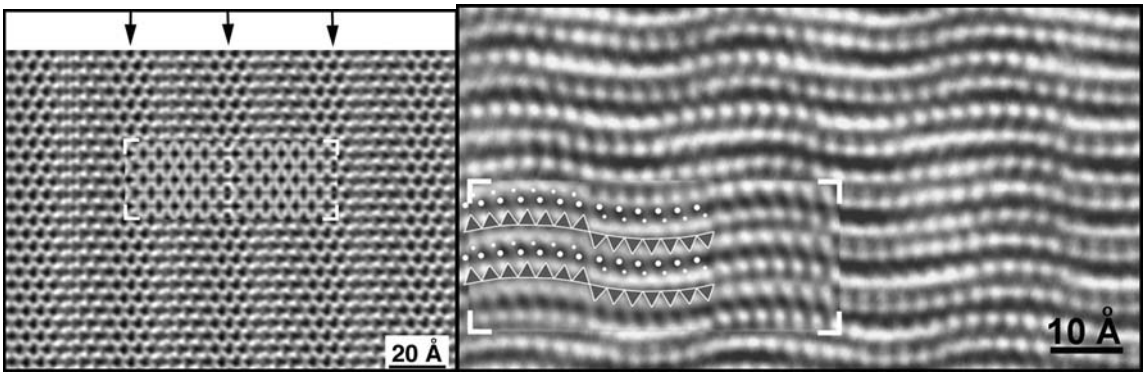

Fig. 2: Experimental [001] HRTEM image of antigorite (m = 14) and the corresponding simulated HRTEM image (inserted). The arrows show the places of inversion in the tetrahedral sheet. The lack of 4- and 8-membered silicate rings is evident.

Fig. 3: Experimental and simulated (inserted) [010] HRTEM images of antigorite (m = 14). A sketch indicates the tetrahedral sheets (triangles) and Mg positions (larger white spots), hydroxyls are small white dots.

DIOCTAHEDRAL VERMICULITE IN THE BODA SILTSTONE FORMATION (BODA, MECSEK MTS., SW-HUNGARY)

DÓDONY, I. & LOVAS, GY. A.
Department of Mineralogy, School of Geology and Environmental Physics, Institute of Geography and Earth Sciences, Faculty of Sciences, Eötvös Loránd University, Pázmány Péter sétány 1/C, H-1117 Budapest, Hungary
E-mail: lovas@ludens.elte.hu

An interesting layer silicate assemblage containing smectite, vermiculite, chlorite and illite will be shown from a borehole of the title area. The XRD phase analysis of average samples showed that the main constituents are albitic claystone, alternating with siltstone, sandstone and dolomite. A detailed clay mineral analysis was performed on the >2 μ fraction of the samples. From the lowest depth downwards the following trend was observed for the clay minerals; smectite (swelling to ~ 16 Å by EG [ethylene glycol] and to ~ 17 Å by GLY [glycerine]), vermiculite (swelling to ~ 16 Å by EG and no swelling by GLY), illite (slight decrease in *d* value from 10 Å).

Going down some 10 m the swelling by GLY vanished indicating that no more vermiculite is present beside the smectite and illite. Another 10 m lower no more swelling by EG was found and a diffuse peak at 7 Å appeared indicating the presence of chlorite. Going further down diffuse peak at 14-15 Å, peak at l0 Å and another diffuse peak at 7 Å was only observed that showed no swelling effect except for the 10 Å illite peak that continued showing slight decrease in *d* value from 10 Å. Thus the XRD results indicated a peculiar layer silicate assemblage. To discover some more details ATEM and TEM investigation were undertaken. The crystallites showed morphological variety from platy, to lathy and fibrous habit. Each type was investigated by ATEM and chemical formula as well as layer charge was calculated based on the ATEM results. Except two out of some tens of crystallites the chemical composition was unambiguously interpreted as ***smectite***. The calculated layer-charge showed the expected increasing trend downwards but in a depth rage of some 40 m-s as compared to the similar trend in deep (several 1000s of m) basins. In some cases the layer charge calculation showed anomaly and therefore the formula calculation was reiterated. In these cases the feasible interpretation of the calculated formula is the presence of the fairly rare ***dioctahedral vermiculite.*** The peculiar XRD behaviour as well as the unexpected ATEM based chemical compositions suggest the presence of a peculiar structural interaction within the above phase assemblage and gives strong initiation for its further investigation on the unit cell level by SAED and HRTEM.

This research was undertaken within the T 32450 OTKA project whose financial support is greatly acknowledged.

References

ÁRKAI, P., BALOGH, K., DEMÉNY, A. FÓRIZS, I., NAGY, G. & MÁTHÉ, Z. (2000): Acta Geologica Hungarica, 43: 351–378.

BARABÁS, A. & BARABÁS-STUHL, Á. (1998): In: BÉRCZI, I. & JÁMBOR, Á. (ed.): Magyarország geológiai képződményeinek rétegtana (Stratigraphy of the geological formations of Hungary. In Hung.). Budapest: MOL Rt. & MÁFI, 187–215.

MÁTHÉ, Z. (ed.) (1998): Summary report of the site characterization program of the Boda Siltstone Formation Manuscript (in Hung.) Mecsekérc Plc., Pécs. Vol. 4., p. 76.

MOORE, D.M. & REYNOLDS, R.C., Jr. (1997): X-ray diffraction and the identification and analysis of clay minerals. Oxford: Oxford University Press.

VARGA, A.R., SZAMÁNY, GY., RAUCSIK, B. & MÁTHÉ, Z. (2005): Acta Geologica Hungarica, 48: 49–68.

VELDE, B. (1995): Origin and mineralogy of clays, clays and the environment. Berlin: Springer-Verlag.

HYDROXYLAPATITE CRUSTS ON THE CARBONATE FLOOR FROM PEŞTERA MARE DE LA BALTA (MEHEDINŢI PLATEAU, ROMANIA)

DUMITRAŞ, D.-G.[1], MARINCEA, Ş.[1], DIACONU, G.[2] & MOUTTE, J.[3]
[1] Geological Institute of Romania, Bucharest, Romania
E-mail: delia@igr.ro
[2] "Emil Racoviţă" Institute of Speleology, Bucharest, Romania
[3] École Nationale Supérieure des Mines, Saint Etienne, France

A recent investigation carried out in one of the most attractive caves from the Mehedinţi Plateau (South Carpathians, Romania), namely Peştera Mare de la Balta ("the Big Cave" of Balta, hereafter referred to as the cave of Balta), allowed us to identify massive deposits of hydroxylapatite on the carbonate floor of the cave. These deposits, partly extended to the walls of the cave, are the result of the influence of the phosphoric solutions derived from the bat droppings on the carbonate background (limestone or moonmilk flows). The aim of this note is to give new morphologic, optical, crystallographic, chemical and infrared absorption data on hydroxylapatite from the cave. The analytical methods used in investigation were scanning electron microscopy (SEM), inductively coupled plasma-atomic emission spectrometry (ICP-AES), Fourier-transfom infrared spectrometry (FTIR) and X-ray powder diffraction (XRD).

The cave of Balta is located on the administrative territory of the homonymous village (Mehedinţi county), on the so-called "Cave Hill" (Dealul Peşterii), part of the Mehedinţi Plateau. It is a medium-sized cave (1075 m in length) consisting of two active galleries: the Passage Gallery (eastward) and the Rimstone Pools Gallery (westward). The draining water in both galleries has low levels. The cave is developed in massive limestones of Upper Jurassic – Neocomian age. The hydroxylapatite crusts investigated by us were taken off from the floor and the walls of a room located at approximately 150 m from the southern entrance of the Rimstone Pools Gallery. Restricted to these crusts, the mineral association consists of hydroxylapatite with minor quartz, illite 2*M*1 and X-ray amorphous iron sesquioxides.

Hydroxylapatite occurs as ochre to dull white aggregates composing multilayered, centimeter-sized crusts or mounds that are directly overgrown on the carbonate support. The SEM examination shows that both the crusts and the mounds are composed by thick beds of crystalline aggregates whose morphology varies from randomly disposed hexagonal laths to post-colloidal, rosette-like, deposits. Crystals are typically smaller than 10 μm and rarely attain 20 μm across.

The crystallinity indices (C.I.) calculated for many samples using the method proposed by SIMPSON (1964) are given in the following table. All but three samples in the table show very good crystallinity. The cell parameters obtained for these samples, after *n* cycles of least-squares refinement of *N* X-ray powder reflections in the 2θ range between 10 and 86° (Fe K_α, λ = 1.93735 Å) are also given in the Table 1.

The chemical composition of a selected sample (PB 45A), determined by ICP-AES, is (in wt% oxides): K_2O = 0.01, Na_2O = 0.01, CaO = 55.66, MnO = 0.01, MgO = 0.01, FeO = 0.01, P_2O_5 = 42.25, SO_3 = 0.21, H_2O (calculated) = 1.83. The resulting chemical-structural formula, calculated on the basis of basis of 6 (S+P) and 26 (O,OH) per formula unit (*pfu*), is: $[K_{0.002}Na_{0.003}Ca_{9.961}Mn_{0.001}Mg_{0.002}Fe^{2+}_{0.001}](P_{5.974}S_{0.026})O_{23.961}(OH)_{2.039}$. CO_2 was not checked for, but, as shown by the IR spectrum, is present in the sample. In fact, the FTIR spectrum of the sample PB 45 A gave a pattern typical for a hydrated carbonate-bearing hydroxylapatite, characterized by OH stretching (3570 cm^{-1}) and librational (635 cm^{-1}) bands, stretching (3414 cm^{-1}) and bending (1647 cm^{-1}) bands of molecular water, CO_3 (ν_3 1451 cm^{-1}, ν_3' 1426 cm^{-1}, ν_2 873 cm^{-1}) and PO_4 (ν_3 1082 cm^{-1}, ν_3' 1033 cm^{-1}, ν_1 962cm^{-1}, ν_4 602 cm^{-1}, ν_4' 563 cm^{-1}, ν_2 472 cm^{-1}) bands.

Reference

SIMPSON, D.R. (1964): American Mineralogist, 49: 363–376.

Table 1

Sample	*a* (Å)	*c* (Å)	*V* (Å^3)	*n*	*N*	C. I.
PB 17 A	9.413(2)	6.883(3)	528.2(2)	4	32	0.038
PB 18 A	9.418(2)	6.885(3)	528.9(3)	3	29	0.038
PB 18 B	9.408(6)	6.869(4)	526.6(6)	3	18	0.157
PB 20 A	9.414(3)	6.871(3)	527.4(3)	3	31	0.037
PB 22 C	9.416(4)	6.867(5)	527.3(4)	3	22	0.103
PB 23 B	9.412(3)	6.871(3)	527.1(3)	3	28	0.037
PB 26 A	9.414(3)	6.876(3)	527.8(4)	3	21	0.059
PB 27 A	9.417(5)	6.884(6)	528.8(6)	3	22	0.059
PB 45 A	9.432(9)	6.883(5)	530.3(9)	3	17	0.097

MICRO- AND MESOPOROUS MINERALS PHASES

FERRARIS, G.
Dipartimento di Scienze Mineralogiche e Petrologiche, Università di Torino, and Istituto di Geoscienze e Georisorse, CNR, Via Valperga Caluso, 35, I-10125, Torino, Italy
E-mail: giovanni.ferraris@unito.it

The crystal structure of porous materials (minerals) is characterized by the presence of a framework (host structure) which is crossed by channels (pores) wide enough to allow exchange of guest chemical species. Conventionally the effective width of a channel must be larger than 3.2 Å, *i.e.* the size of a N_2 molecule. Micro- and mesoporous materials have effective channel widths in the range 3.2–20 Å and 20–500 Å, respectively; for sizes larger than 500 Å a material is classified as macroporous.

The exchange and catalytic properties connected with zeolites, also known as molecular sieves, are well known. Less known is instead that other minerals show, at least in principle, the same porous features and are thus zeolite-like mineral phases. Following an international meeting (Accademia dei Lincei, Roma, December 2004; FERRARIS, 2005) dedicated to porous mineral phases other than zeolites, a volume has been published (FERRARIS & MERLINO, 2005) which reports twelve invited contributions there presented. It turns out that porous features are shown by the crystal structures of mineral and mineral-like phases belonging, among others, to the following groups: heterophyllosilicates, palysepioles, rhodesite-related structures, labuntsovite, several titano-, niobo-, zircono-, vanado-, stanno-, and indo-silicates, sodalite, cancrinite, davyne, tobermorite, gyrolite, manganese oxides (tunnel oxides), apatite, sulfides, selenides, chrysotile, carbon forms, and clathrates.

In several cases porous properties of the mentioned phases have been observed in Nature, but their technological exploitation is still in its infancy. A promising feature is that their framework is not only tetrahedral as in zeolites, but includes also other polyhedra: the terms heteropolyhedral and mixed octahedral-pentahedral-tetrahedral frameworks are in use. In other cases completely non-silicate frameworks occurs as in sulfides and oxides. The presence of coordination polyhedra other than tetrahedral ones opens the possibility of inserting a wide variety of cations in the framework thus allowing the synthesis of porous compounds showing, *e.g.*, interesting optical and magnetic properties. Tunability of these properties can be achieved by inserting the most appropriate cation (*e.g.*, rare earth elements) and/or by using intermediate members of solid solutions. Examples of the mentioned types of porous structures will be presented at the meeting.

Of particular interest is the possibility, based on analogy with clays, of obtaining from heretophyllosilicates (*cf.* FERRARIS & GULA, 2005) mesoporous pillared materials (FERRARIS, 2006). According to the IUPAC nomenclature, "pillaring is the process by which a layered compound is transformed into a thermally stable micro- and/or mesoporous material with retention of the layer structure." The structural parallelism between phyllosilicates, like micas and smectites, and heterophyllosilicates leads to speculate on the possible use of some of the latter compounds as starting material to produce structures analogous to the pillared clays. Observations in the field (KHOMYAKOV, 1995; CHUKANOV & PEKOV, 2005) and few laboratory experiments (CHELISHCHEV, 1972) suggest that research work aiming to obtain pillared heterophyllosilicates could be rewarding. In particular, there are several evidences of solid-state transformations from one to another member of the bafertisite series via leaching/substitution of the interlayer composition (*i.e.*, the *HOH* layer is preserved). In some cases, swelling becomes evident by comparing the structures of the parent and daughter phases. As summarized by KHOMYAKOV (1995), an active interaction with water, at epithermal and hypergene or even atmospheric conditions, is characteristic of many highly alkaline titanosilicates in the bafertisite-like series. For example, the following transformations lead to phases that show a (more) hydrated and, to some extent, swelled interlayer relative to the parent phases: vuonnemite → epistolite; lomonosovite → murmanite.

References

CHELISHCHEV, N.F. (1972): Geokhimiya, 7: 856–860.
CHUKANOV, N.V. & PEKOV, I.V. (2005): Reviews in Mineralogy & Geochemistry, 57: 105–144.
FERRARIS, G. (2005): Episodes, 28: 218–219.
FERRARIS, G. (2006): Solid State Phenomena, in press.
FERRARIS, G. & GULA, A. (2005): Reviews in Mineralogy & Geochemistry, 57: 69–104.
FERRARIS, G. & MERLINO, S. (eds.) (2005): Micro and mesoporous mineral phases. (Reviews in Mineralogy & Geochemistry, 57). Washington (DC): Mineralogical Society of America.
FERRARIS, G., MAKOVICKY, E. & MERLINO, S. (2004): Crystallography of modular materials. Oxford: IUCr/Oxford University Press.
KHOMYAKOV, A.P. (1995): Mineralogy of hyperagpaitic alkaline rocks. Oxford: Clarendon Press.

GLAUCONITE-QUARTZ COMPOUNDS APPLIED FOR THE REMOVAL OF HEAVY METALS FROM AQUEOUS SOLUTION – COLUMN STUDY

FRANUS, M.
Department of Geotechnics, Lublin University of Technology, Nadbystrzycka 40, 20-618 Lublin, Poland
E-mail: m.franus@pollub.pl

Glauconite concentrate was separated by sieving (>63 μm) and magnetic fractionation from sandy deposits of the Lubartow Lowland (Eastern Poland, GAZDA *et al.*, 2002). Glauconite belongs to polytype 1M which characteristic for high ordering of the structure (FRANUS *et al.*, 2004). The aim of the present study is to determine the sorption properties of filtration mixtures, composed of variable contents of glauconite (5 wt% – G5, 10 wt% – G10, 50 wt% – G50, 100% – G100) and quartz. Sorption properties were measured on standard solutions of the following heavy metals: Pb(II), Zn(II), Cd(II), Cu(II)

Four filtration mixtures were placed into glass columns. The mass of each mixture was 12 g, giving the thickness of deposit 0.08 m. After all tests, the runs of planar isotherms were plotted. On the basis of breakpoint, the total adsorption capacity (TAC) and the efficient sorption capacity (EAC) were calculated for each mixture.

During running off the filtrates G5 and G10, the increase of Zn and Cu ions content was observed while even only 50 ccm of solution was eluted from the column. Full saturation took place at volume in range from 280 to 480 ccm of effluent. During removal of Zn and Cu from solution by the sample G50, the breakpoint was detected at 470 ccm of effluent and the saturation of the sorptive complex appeared at 1050 ccm. The concentration of Cu ion in solution passing through the bed G100 increase at volume 910 ccm, and the bed is exploited at 150 ccm of effluent.

Beds G5 and G10 adsorb Cd ion in a way similar to Zn and Cu. For the G5 bed the breakpoint was observed at 50 ccm and for G10 – at 150 ccm of effluent. Saturation of Cd ion takes place at 450 and 560 ccm, respectively. The highest efficiency of Cd adsorption occurs while using filtrates G50 and G100, showing breakpoints at 790 and 1430 ccm and full saturation at 1430 and 2190 ccm of effluent, respectively.

Tested filtration mixtures showed the best efficiency for lead adsorption, in relation to the applied heavy metals. For beds G5 and G10, the breakpoint occurs at 200 and 2500 ccm of effluent volume, and the saturation takes place at 700 and 850 ccm, respectively. Saturation of bed G50 was found at 2040 ccm and the breakpoint – at 1520 ccm. The bed G100 turned to be the best adsorbent. The breakpoint was observed at 2910 ccm and saturation takes place at 3510 ccm.

The total and efficient adsorption capacities rise following the content of glauconite in filtration mixtures. Test of adsorption on beds G5 and G10 showed equal EAC values yielding 215 mg/kg for Zn and 212 mg/kg for Cu. Their TAC values are generally twice higher than EAC values. The highest TAC and EAC values were calculated for Pb adsorption by all tested samples.

Concluding: the TAC is higher than EAC for all tested mixtures. The highest TAC value is characteristic for G100 sample and the lowest TAC occurs for G5 sample.

This work was financially supported by the Polish Ministry of Education and Science, grant No 3 T09D 007 28.

References

FRANUS, W., KLINIK, J. & FRANUS, M. (2004): Mineralogia Polonica, 35: 53–62.

GAZDA, L., FRANUS, M., FRANUS, W. & KRZOWSKI, Z. (2002): In: PAWŁOWSKI L. (ed.): Monografie Komitetu Inżynierii Środowiska PAN, 11: 715–719.

HYDROTHERMAL MINERALIZATION IN THE HÁRSHEGY SANDSTONE FORMATION OF MIDDLE OLIGOCENE AGE IN THE BUDA HILLS, HUNGARY

GÁL, B., POROS, ZS. & MOLNÁR, F.
Department of Mineralogy, Eötvös Loránd University, Pázmány Péter sétány 1/C, H-1117 Budapest, Hungary
E-mail: galbenedek@mail.yahoo.com

The distribution of the Hárshegy Sandstone Formation, which is a transgressive, coastal formation of Middle Oligocene age is strongly defined by the NE–SW striking Buda Line that forms the eastern boundary of its extension. The Buda Line was a paleogeographic boundary in the Late Palaeogene and location of an intensive post-volcanic activity as well (FODOR, 1995). The sandstone is strongly silicified in what is called the Buda Zone, a 5–20 km wide belt along the western side of the Buda Line (BÁLDI & NAGYMAROSY, 1976). Stratigraphic and tectonic evidences suggest a Late Oligocene age for silicification (BÁLDI & NAGYMAROSY, 1976). A particular interest in this silicified zone is related to the elevated As and Au concentrations (KORPÁS & HOFSTRA, 1999)

Hydrothermal formations in the typical facies of Hárshegy Sandstone were studied in two reference areas: in the surroundings of Pilisborosjenő village (Köves-bérc [hereinafter Köves Hill] and Ezüst Hill) and in the vicinity of Csobánka village (Majdán-nyereg [hereinafter Majdán Saddle]). In both areas, hydrothermal mineralization consists of chalcedony and barite veins. Most of these veins are usually rather thin (1–5 cm in thickness) and appear to be simple extensional fractures, however, occasional displacement can also be observed along the veins. The density of veins is uneven. In the vicinity of Pilisborosjenő and especially on the Köves Hill, siliceous veinlets form dense stockwork, whereas barite veins are more common on the Majdán Saddle where chalcedony veins are subordinate. The orientation of the chalcedony veins is dominantly WNW–ESE, and that of the barite veins is NNW–SSE (Fig. 1). Barite veins always cut through chalcedony veins, clearly indicating their younger age. Considering the mostly simple extensional nature of veins and their relative age relationships, their orientation fits with the model of stress-field variation during the Late Oligocene–Miocene (MÁRTON & FODOR, 2003; BADA *et al.*, 1996).

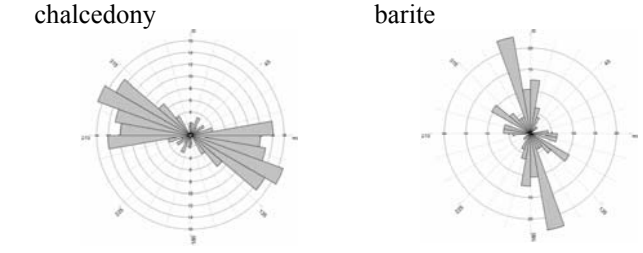

Fig. 1: Strike orientation of veins.

Chalcedony veins often have argillic alteration selvage mainly consisting of kaolinite with a small amount of illite. Hematite and limonite are also present in the alteration zone, which is usually not wider than a few centimetres. Veins with barite do not contain other minerals and have sharp contact with the sandstone without an alteration halo. Barite veins have open spaces therefore the crystals are usually euhedral. Barite crystals most commonly have simple orthorhombic-tabular morphology in most of the thin veins, however, a definite zoning in distribution of various habits of barite was observed in the major and thickest vein (approx. 2 m in thickness) on the Majdán Saddle. There the first phase of the crystallization of barite was related to the brecciation of sandstone and the habit of crystals is determined by pyramidal and prism faces in addition to the {001} form (Fig. 2).

Fig. 2: Barite from breccia. Majdán Saddle, Csobánka.

Crystals formed in open fractures beside the breccia have more simple, orthorhombic-tabular habit with the dominant {001} form associated with smaller faces of the {100} and {010} prisms. Far away from the breccia zone, open fractures contain thin lamellae of barite with the dominant {001} form. Variation of crystal habit as a function of distance from the central hydrothermal zone probably reflects variation of temperature and saturation of solution for barium and sulphate. This observation can be used in prediction of occurrence of major fluid flow zones precipitating barite in the sandstone. Fluid inclusions in the barite crystals were subject of homogenization and cryoscopic investigations. Only the larger, rhombic-tabular crystals from the Majdán Saddle contained two-phase (aqueous liquid + vapour on room temperature) inclusions sufficient for study. After the investigations, it could be said, that these barite crystals precipitated from low-salinity solutions during a low-temperature (T = 50–70 ºC) hydrothermal process.

References

BADA, G., FODOR, L., SZÉKELY, B. & TIMÁR, G. (1996): Tectonophysics, 255: 269–289.
BÁLDI, T. & NAGYMAROSY, A. (1976): Földtani Közlöny, 106: 257–275.
FODOR, L. (1995): Földtani Közlöny, 124: 132–140.
MÁRTON, E. & FODOR, L. (2003): Tectonophysics, 363: 201-224.
KORPÁS, L. & HOFSTRA, A.H. (eds.) (1999): Carlin Gold in Hungary. Geologica Hungarica, 24: 131–331.

MINERALOGICAL AND PETROGRAPHIC CHARACTERISTICS OF THE XVIITH CENTURY CERAMIC WARE FOUND IN THE ORADEA FORTRESS (ROMANIA)

GHERGARI, L., LAZAR, C. & IONESCU, C.
Department of Mineralogy, Babeş-Bolyai University, 1 Kogălniceanu Str., RO-400084 Cluj-Napoca, Romania
E-mail: ghergari@bioge.ubbcluj.ro

In the Medieval fortress of Oradea (west Romania) a high number of Medieval archaeological objects were exhumed during the 2001 archaeological campaign. From these, the beautiful glazed ceramic ware, archaeologically dated at the XVIIth century, was studied from mineralogical, petrographic and technological point of view. Macroscopically, the recovered material represents either whole household pots or fragments, in general with the surface covered by coloured glaze. From macroscopical point of view, the ceramic fragments can be divided into two categories: type A ceramics, with zoned distribution of colours, i.e. a reddish external part and a more brownish-blackish internal part, reflecting the variable firing atmosphere, from reducing to oxidizing one and type B ceramics, of homogeneous creamy colour, mirroring a constant, oxidizing, firing atmosphere and Fe-poor raw materials.

Type A ceramics can be classified mainly as coarse one, with a significant contribution of inclusions larger than 0.05 mm. Some vessels show a fine to semifine character. Mineralogically, the composition of the ceramic fragments is quite similar, for all categories of fineness. In the mainly sintered, slightly vitrified matrix, with microcrystalline-amorphous texture, various clasts occur. The crystalloclasts are quartz, plagioclase and alkaline feldspars, micas, and heavy minerals fragments, the lithoclasts are quartzites, gneisses, micaschists, granites, granodiorites, andesites, volcanic glass, sandstones, limestones, and silicastones fragments. The potsherds (ceramoclasts) are rare. The porosity is relatively low, with irregular-shaped pores, often filled in with glass. The arrangement of the mica lamellae as well of the pores in rows parallel to the surface is ubiquitous. This oriented structure is mainly due to the modelling of the ware at the potter's wheel. The ceramic body is covered by glaze, a brown glassy mass, with a high refractive index, containing probably Pb-based pigments. Based on the alteration of both the microscopical features and some XRD lines compared with literature data (SHEPARD, 1976; VELDE & DRUC, 1999 *etc.*), we presumed a high firing temperature between 850 and 900 °C for type A ceramics. Most likely, illitic-kaolinitic clays with some calcite content were used as raw materials.

Type B ceramics has mainly semifine and only subordinately coarse character. The ceramic body is composed, microscopically, from a high amount (up to 70%) of transparent, slightly brownish microcrystalline-vitreous matrix and a lower amount of clasts (maximum 30%). The matrix contains high amounts of newly formed glass, as a result of the high temperature of firing. Quartz, feldspars, micas and heavy minerals fragments form the crystalloclasts, while quartzites, gneisses, quartzitic-biotitic schists, granodiorites, rhyolites, dacites, andesites, silicastones, sandstones and clays form the lithoclasts. The porosity is relatively high and is represented mainly by primary, elongated pores. The structure of the ceramic body is clearly oriented, with both lamellae and pores arranged in parallel rows to the surface of the ceramic wall, result of the potter's wheel modelling. The firing products are represented by the high amount of glass, the sintering of the clayish matrix, and the forming of mullite. Based on the thermal alteration processes noticed in thin sections and X-ray diffractograms, we inferred a high temperature of firing, in the range of 900 to 1000°C. For Type B ceramics most likely kaolinitic-illitic clay was used as raw material.

This study was financially supported by the Romanian Ministry of Education and Research (Grant 1762/2005).

References

SHEPARD, A.O. (1976): Ceramics for the archaeologist. 7th ed. Washington: Carnegie Institution of Washington, 414 p.

VELDE, B. & DRUC, I.C. (1999): Archaeological ceramic materials. Berlin: Springer, 299 p.

THE INFLUENCE OF VADU CRIŞULUI KAOLIN ON TECHNOLOGICAL CHARACTERISTICS AND MICROSTRUCTURE OF SILICA PORCELAIN

GOREA, M.[1], KRISTÁLY, F.[2] & ZAJZON, N.[2]
[1] Department of Chemical Engineering and Oxide Material Science, Babeş-Bolyai University, Arany János Str. no. 11, RO-400028 Cluj-Napoca, Romania
E-mail: mgorea@chem.ubbcluj.ro
[2] Department of Mineralogy and Petrology, University of Miskolc, H-3515 Mikolc-Egyetemváros, Hungary

Porcelain has been used as an electrical insulating material since a long time due to its specific properties (mechanical strength, high-power dielectric strength, and corrosion resistance). Two types of porcelain insulators are mostly used, the silica and alumina porcelain (classified as C-110 and C-120 sub-groups, respectively, according to the IEC 672-3 standard). In the silica porcelain body the solid quartz content is higher than in that of the alumina porcelain and, correspondingly, its mechanical strength is greater. The difference between thermal expansion of the quartz grains and the surrounding liquid phase causes mechanical stress that can produce, during thermal treatment, microcracks in the porcelain.

The main raw materials used for obtaining traditional porcelains are kaolins (about 50%), feldspar (25%) and quartz (25%). The clay acts as a binder for the other constituents in the raw materials mixture, and it confers plasticity to the body for shaping. Feldspar is a flux material that reacts with the other compounds, forms a liquid phase in the system and leads to densification of the body microstructure. Quartz is a refractory material, stable filler that reduces distortion and shrinkage of the ceramics during the thermal treatment.

The final microstructure of the fired porcelain consists of coarse aggregate particles held together by a finer matrix or bond system that is dense.

The goal of this paper is to study the influence of Vadu Crişului kaolin, used as a replacement for other clay materials, on the technological characteristics and microstructure of silica electrical porcelain. The experiments are focused on two aspects: characterization of Vadu Crişului kaolin and synthesis and characterization of three compositions of porcelain.

The chemical composition of Vadu Crişului kaolin is presented in Table 1.

Results of the semi-quantitative mineralogical analysis: quartz – 11%; kaolinite – 78%; illite/micas – 9%; iron oxides and hidroxides – 2%.

The main technological characteristics are: Pffeferkorn plasticity index – 41.10%; bending strength – 24 daN/cm^2; total shrinkage – 19%; whiteness – 45%.

The experimental compositions also include other clay raw materials: Bojidar, KDH and Zettlitz kaolin, as well as the nonplastic materials, AC-type feldspar and Miorcani quartz-rich sand. The first composition contains 43% clayey materials (no Vadu Crişului kaolin), with a feldspar/sand (F/S) ratio 1.28; the second composition includes 47.5% clayey materials (21% Vadu Crişului kaolin) with a F/S ratio of 1.28; the third composition consists of 46.5% clayey materials (10.75% Vadu Crişului kaolin) with a F/S ratio of 1.37. The main technological characteristics of the ceramic masses have similar values.

The microstructure of the porcelain bodies obtained from the three compositions was further investigated by EDS analyses combined with SEM observations. EDS analyses were carried out on the vitreous matrix of the bodies, delimited by the use of BSE images, in order to establish the Si/Al ratio and content of Na and K of the matrix, which is determined by the initial clay component and feldspar dispersion in the volume of ceramic body before firing. The porosity of porcelain strongly depends on the variation of Si/Al ratio and alkali content of the vitreous matrix. Thus, porosity deduced from SEM images, correlated with the composition of the matrix shows the influence of clay components on the microstructure of porcelain body.

Table 1: Chemical composition of Vadu Crişului kaolin.

SiO_2	Al_2O_3	Fe_2O_3	CaO	MgO	Na_2O	K_2O	L.O.I.
52.99	31.35	1.43	0.66	0.53	0.09	1.09	11.46

ARCHEOMETRY OF CELTIC REFRACTORY CRUCIBLES FROM BRATISLAVA'S OPPIDUM

GREGOR, M.[1] & VRTEĽ, A.[2]
[1] Geological Institute, Faculty of Natural Science, Comenius University, Mlynská dolina, 842 15 Bratislava, Slovakia
E-mail: geolgregor@yahoo.com
[2] Municipal Institute of Monument Preservation, Uršulínska 9, 811 01 Bratislava, Slovakia

During the younger La Tène period, the rise of Celtic fortified centre (oppidum) in Bratislava's surroundings was related to migration of Celtic tribes in central Danubian area. The position of the oppidum on the crossroads of trade channels crossing Alps and Carpathians was of great strategic and economic importance. This importance is documented by the discovery of numerous finds of artefacts and objects associated with craftwork. Except of pottery kilns and ceramics fragments also numerous fragments of metalworking (slags, refractory ceramics) and coinage industry (dosing plates) has been found (PIETA & ZACHAR, 1993; ČAMBAL, 2004).

In general for this research, six fragments of Celtic ceramic crucibles found on Ventúrska street in Bratislava, were studied by standard mineralogical analytical techniques, which included optical microscopy, powder X-ray diffraction analyses (PXRD), scanning electron microscopy (SEM) and thermal analysis. PXRD and optical microscopy show that crucibles consist of a mixture of quartz, plagioclase, potassium feldspars, micas, mullite as well as an amorphous phase, *e.g.* glass. A greenish layer covers the interior of some shards. This layer is composed of atacamite or brochantite and linarite, respectively. Formation of these minerals was considered in another paper (OZDÍN & GREGOR, in press). Based upon the mineralogical composition of the shards and the greenish cover, we presume that the ceramic vessels were used as refractory crucibles for melting copper-bearing ores. The primary firing temperature of the crucibles is difficult to establish because their subsequent use for ore-processing when the temperature reached at least 1000–1100 (± 50) °C. Based upon thermal analysis and optical microscopy, we presume that the melting of copper-bearing mineral took place in reducing atmosphere. Due to the intense thermal alteration, it is difficult to establish the geological source for the raw clays (which might come from the alluvial sediments of the Danube). Graphite added as a temper could be imported from south Bohemia (Czech Republic) as in Bratislava's oppidum numerous founds of graphitic ceramics with craftwork marks typical for Celtic inhabitation from that area has been found.

Acknowledgement

In this way we would like to thank to the Municipal Institute of Monument Preservation, Bratislava for providing the crucibles samples. Special thanks are due also to the Geological Institute of Natural Science Faculty and the Central Laboratories for the Electronic and Optic Methods, Comenius University, Bratislava for permission to use XRD, DTA and SEM facilities. Also we are very grateful to Dr. Corina Ionescu (Babeş–Bolyai University of Cluj-Napoca, Romania) for her help.

References

ČAMBAL, R. (2004): Zborník. SNM – Archeológia, Supplementum, 1: 204.

OZDÍN, D. & GREGOR, M. (in press): Mineralia Slovaca

PIETA, K. & ZACHAR, L. (1993): In: ŠTEFANOVIČOVÁ, T. (ed.): Najstaršie dejiny Bratislavy. Bratislava: Tatiana–ELÁN, 148–159.

ALTERATION PROCESSES IN THE MESOZOIC ISLAND ARC VOLCANICS FROM THE TRASCĂU MOUNTAINS (ROMANIA)

GROVU, P.
Department of Mineralogy, Babeş-Bolyai University, 1 Kogălniceanu Str., RO-400084 Cluj-Napoca, Romania
E-mail: pgrovu@bioge.ubbcluj.ro

In the eastern part of the Apuseni Mountains (Romania), Mesozoic island arc volcanics occur. Tectonically, they are part of the Bedeleu Nappe (BALINTONI & IANCU, 1986) and have on the top Oxfordian–Tithonian radiolarites and limestones and, in places, post-tectonic Miocene sediments. The volcanic sequence is Middle to Late Jurassic in age and is not genetically related with ophiolites from the southern parts of the Apuseni Mts. (SACCANI *et al.*, 2001). In the Buru–Borzeşti–Corneşti area (Trascău Mountains, north of Arieş Valley), the island arc volcanics show a wide range of rocks such as basalts, basaltic andesites, andesites, dacites and rhyolites. They form massive or pillowed lava flows, dykes or pyroclastic deposits, *e.g.* agglomerates, breccias and tuffs.

Basalts and basaltic andesites have a dark green, almost black colour and form massive or pillowed lavas. The porphyritic fabric is expressed by olivine, augite and plagioclase ($An_{50–90}$ and $An_{45–80}$, respectively) phenocrysts, in intergranular or pilotaxitic groundmass, sometimes containing small vacuoles filled in with calcite, quartz and/or chlorite. Andesites have greyish-greenish colour and form massive lava flows. The structure is glomeroporphyritic, with clusters of plagioclase ($An_{40–60}$) and isolated phenocrysts of augite, ferrohornblende and quartz. The groundmass has microcrystalline to pilotaxitic fabric. Dacites and rhyolites are rare and form small, isolated dykes with porphyritic or aphyric fabric.

The pyroclastites, represented by layers of andesitic agglomerates and breccias, andesitic lapilli tuffs and vitroclastic rhyolitic tuffs, interbedded with massive lava flows or pillow lavas levels, are the prevalent rocks in the studied area.

The above-described volcanic rocks exhibit different degrees of hydrothermal alteration, which affected mainly clinopyroxene and plagioclase phenocrysts and the glassy groundmass. Clinopyroxenes (augite) are partly or completely altered and transformed into clinochlore. Plagioclase occurs either in fresh crystals or is partly replaced by a mixture of albite, calcite and illite. The groundmass exhibits much more intense alteration processes, expressed by the presence of clinochlore, smectite, calcite, fibrous microquartz (chalcedony) and pyrite.

The andesitic agglomerates, breccias and lapilli tuffs exhibit advanced hydrothermal alteration, which affected less the clasts and mainly the matrix, in general almost completely transformed into clinochlore, smectites and calcite. The rhyolitic vitroclastic tuffs are completely replaced by smectites and form deposits of bentonites.

The hydrothermal alteration of the Mesozoic volcanics from the Trascău Mountains can be assigned to the activity of the postmagmatic fluids.

References

BALINTONI, I. & IANCU, V. (1986): Dări de Seamă ale Şedinţelor Institutul de Geologie şi Geofizică, 5. Tectonică şi geologie regională, 70–71: 45–56.

SACCANI, E., NICOLAE, I. & TASSINARI, R. (2001): Ofioliti, 26: 9–22.

INFRARED SPECTROSCOPY OF THE MUSCOVITE (SOPRON)–ILLITE (FÜZÉRRADVÁNY) SYSTEM

GUCSIK, A.[1], GASHAROVA, B.[2], BIDLÓ, A.[1], KOVÁCS, G.[1], HEIL, B.[1] & PATOCSKAI, Z.[1]
[1] Dept. of Soil Sciences, University of West Hungary, Bajcsy Zs. E. u. 4., H-9400 Sopron, Hungary
E-mail: ciklamensopron@yahoo.com
[2] Institute for Synchrotron Radiation, P.O. Box 36040, D-76021 Karlsruhe, Germany

Mid-infrared (MIR) spectral regions of muscovite (Sopron, Hungary) and illite (Füzérradvány, Hungary) samples were measured as KBr pellets with a Globar source and a MCT detector at ANKA, Institute for Synchrotron Radiation (ISS), Forschungszentrum Karlsruhe, Germany. The cut-off of this detector is about 530 cm^{-1}. Muscovite/illite exhibits MIR spectral features at 552/538 (bending vibration of SiO_4^{4-}), 1030/1038 (stretching vibrations of SiO_4^{4-}), 1661/1664 (bending vibrations of H_2O), 3475/3481 and 3634/3641 (stretching vibrations of OH group) (Figs. 1A,B). These spectral features mainly show similarities indicating that there is a very strong structural relationship between muscovite and illite. But, in the lower frequencies some differences occur, which might be due to more stretching Si modes involving weakly bonded cations in illite. FIR spectrum of Sopron muscovite as reference material for the muscovite-illite system contains ten peaks at 110, 137, 166, 189, 262, 351, 382, 407, 478, and 532 cm^{-1}. Füzérradvány illite shows eleven peaks at 94, 118, 193, 260, 334, 384, 419, 473, 505, 528, and 544 cm^{-1}. There are five peaks, which are dominant in both spectra at around 189, 262, 382, and 478 cm^{-1} (Figs. 1C,D). These peaks also belong to the bending and stretching vibrations (NAVROTSKY, 1994).

Reference

NAVROTSKY, A. (1994): Physics and chemistry of earth materials. Cambridge: Cambridge University Press, 116 p.

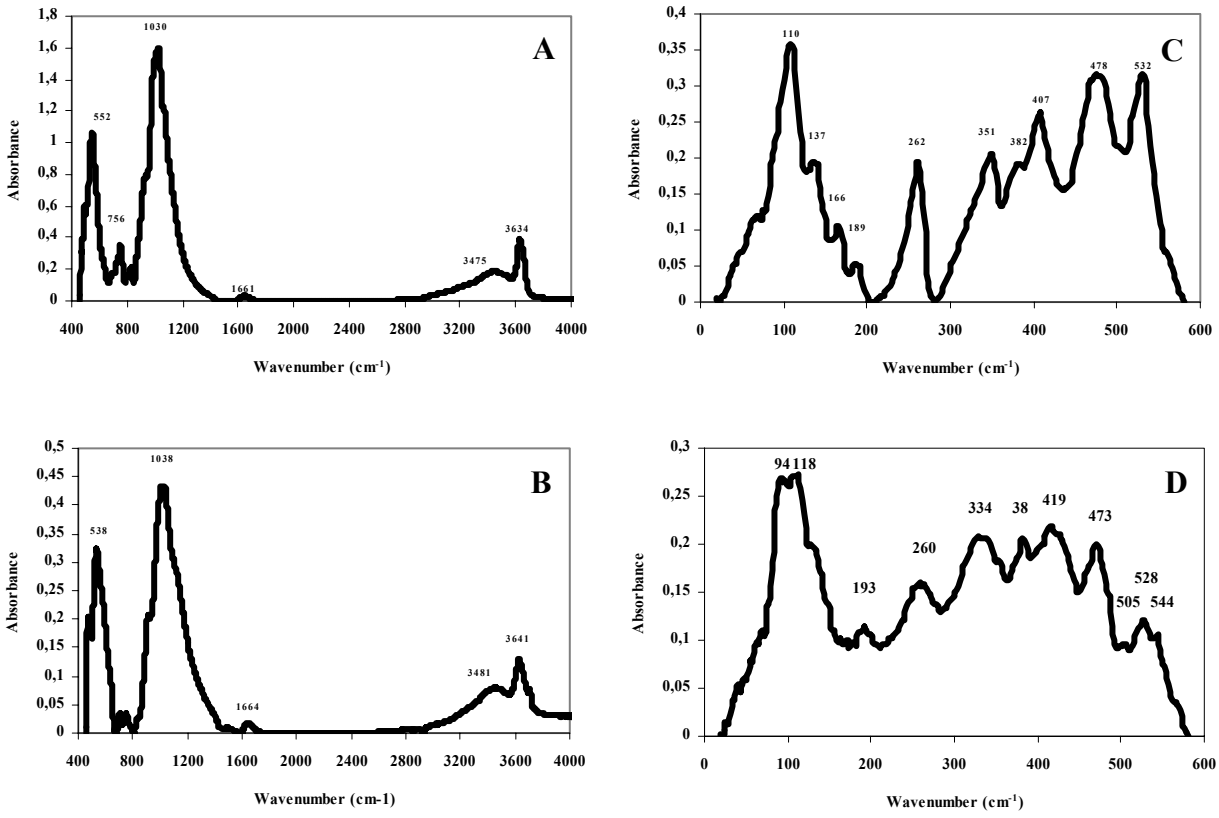

Fig. 1: Mid-infrared (MIR) and far-infrared (FIR) spectroscopic features of muscovite (Sopron: A, C) and illite (Füzérradvány: B, D).

CATHODOLUMINESCENCE MICROCHARACTERIZATION OF ILLITE FROM FÜZÉRRADVÁNY, NE HUNGARY

GUCSIK, A.[1], NINAGAWA, K.[2], NISHIDO, H.[2], OKUMURA, T.[2], BIDLÓ, A.[1], KOVÁCS, G.[1], HEIL, B.[1] & PATOCSKAI, Z.[1]
[1] Dept. of Soil Sciences, University of West Hungary, Bajcsy Zs. E. u. 4., H-9400 Sopron, Hungary
E-mail: ciklamensopron@yahoo.com
[2] Dept. of Applied Physics, Okayama University of Science, Ridai-cho 1-1, Okayama, 700-0005, Japan

The purpose of this study is to contribute to the structural characterization of illite by the application of the cathodoluminescence technique.

The operating conditions for all SEM-CL investigation as well as SEM and backscattered electron (BSE) microscopy were accelerating voltage: 15 kV, and 1.0 nA at room temperature (MARSHALL, 1988; IKENAGA *et al.*, 2000). CL spectra were recorded in the wavelength range of 300-800 nm, with 1 nm resolution by the photon counting method using a photomultiplier detector, Hamamatsu Photonics R2228.

The SEM images, especially secondary electron images, (SEI) of illite from Füzérradvány show individual grains with highly altered or damaged rim structures. The core of these grains does not contain any cracks or other mineral phases. The pore spaces are relatively low. In general, mostly hexagonal grains are separated by fractures, which occur in variable widths between 1 and 10 μm (Fig. 1A). CL image of illite shows relatively bright, crystallographically controlled bands and zones in the otherwise CL-dark background. The CL-bright patchy areas and spots in the CL images may be related to the quartz impurity. The presence of minor amounts of quartz was indicated by XRD analyses of the illitic raw material. The presence of quartz may also be expected from the extensive silification of the area as revealed by the geological exploration (CSONGRÁDI *et al*., 1996). The CL-dark background of these images is due to lack of the recombination centers or electron traps producing the non-luminescent nature of the CL emission in the illite samples. The low intensity might also be caused by quenchers such as Fe, however this particular illite practically does not contain iron (Fig. 1B).

CL spectrum of illite from Füzérradvány shows a broad band centered at 589 nm (2.1 eV), which contains a shoulder peak with a peak maximum at 456 nm (2.71 eV). A relatively weak narrow emission peak is centered at 428 nm (2.89 eV). The characteristic blue CL in the clay minerals is known as an intense emission band around 400 nm (double peak with two maxima at 375 and 410 nm) (3.3-3.0 eV) on kaolinite. Electron Paramagnetic Resonance (EPR) measurements indicate that this blue emission can be related to the radiation-induced defect centers (RID), which occur as electron holes trapped on apical oxygens (Si-O centre) or located at the Al-O-Al group (Al substituting Si in the tetrahedron) (Fig. 2.) (GÖTZE *et al*., 2002).

References

CSONGRÁDI, J., TUNGLI, GY. & ZELENKA, T. (1996): Földtani Közlöny, 126: 67–75.

GÖTZE, J., PLÖTZE, M., GÖTTE, TH., NEUSER, R.D. & RICHTER, D.K. (2002): Mineralogy and Petrology, 76: 195–212.

IKENAGA, M., NISHIDO, H. & NINAGAWA, K. (2000): Bulletin of Research Institute of Natural Sciences, Okayama University of Science, 26: 61–75.

MARSHALL, D.J. (1988): Cathodoluminescence of geological materials. Boston: Unwin Hyman, 146 p.

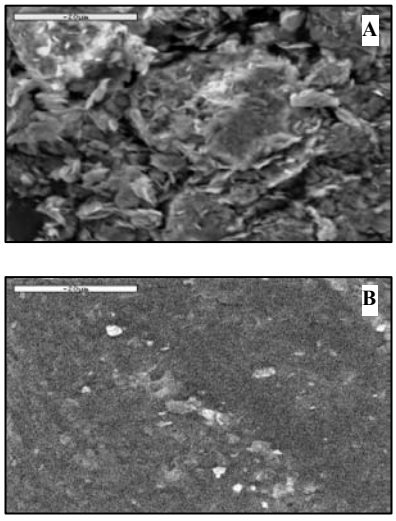

Fig. 1: SE (A) and CL (B) images of illite.

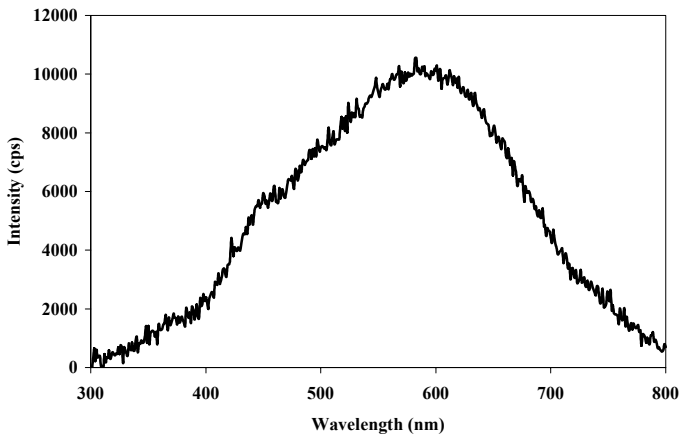

Fig. 2: CL spectrum of illite.

SILICATE MELT INCLUSION STUDY ON PLAGIOCLASE FROM OLIGOCENE DACITE, ZALA BASIN, WESTERN HUNGARY

HAVANCSÁK, I., TÖRÖK, K. & SZABÓ, CS.
Lithosphere Fluid Research Lab, Department of Petrology and Geochemistry, Eötvös University, Pázmány Péter sétány 1/C, H-1117 Budapest, Hungary
E-mail: hizabella@vipmail.hu

Silicate melt inclusions are small samples of magma drops that are trapped during crystal growth at magmatic temperature and pressure. They are very useful tools in petrologic research because they provide direct information about the composition of melt and physical parameters of crystallization at various stages in the evolution of magmatic systems.

In this paper we use silicate melt inclusions to study composition and crystallization history and temperature of dacitic melt from Zala Basin, western Hungary. The Zala Basin, situated in the ALCAPA block West to the Lake Balaton and North to the Balaton Line, is the north-eastern continuation of the Periadriatic Line and Igneous Belt. The basement of Zala Basin is made mostly up by Mesozoic sedimentary formations followed by Eocene sedimentary sequences. A thick effusive and explosive andesitic-dacitic volcanic sequence occurs in the northern part of the Zala Basin, in the Bak–Nova depression, where the youngest Eocene sediments (Padrag Marl) intercalate with the oldest products of the volcanic rocks. Age of the andesitic-dacitic rocks ranges from 34.9±1.4 to 26.0±1.2 Ma (BENEDEK *et al.*, 2004). The studied Söjtör dacite is only know in drill cores. The volcanic rock shows porphyritic texture with large amount of plagioclase and amphibole phenocrysts. Plagioclase is the dominant phenocryst; the size of the crystals is 0.5–5.0 mm. They are euhedral, zoned, mostly fresh, but some of them are slightly altered. The anorthite content varies between An81 and An51 and gradually decreases from cores towards rims. Plagioclase contains numerous silicate melt inclusions (Fig. 1). Amphibole phenocrysts, forming euhedral–subhedral grains, are significantly less abundant than plagioclases. The groundmass is made up fine-grained plagioclase, quartz, amphibole, oxides, and glass. The glass is partially altered to clay minerals.

Plenty of silicate melt inclusions are trapped in the plagioclases. Their distribution is sometimes randomly; sometimes follows zones of plagioclase (Fig. 1). The silicate melt inclusions, which sizes are between 20–50 μm, show negative crystal shape. They contain glass and a large bubble (Fig. 1). All of theses are characteristic of primary silicate inclusions (ROEDDER, 1984). Besides these constituents, accidentally trapped euhedral apatite crystals can also be observed associated with the silicate melt inclusions. Apatite also occurs as single inclusions in both phenocrysts.

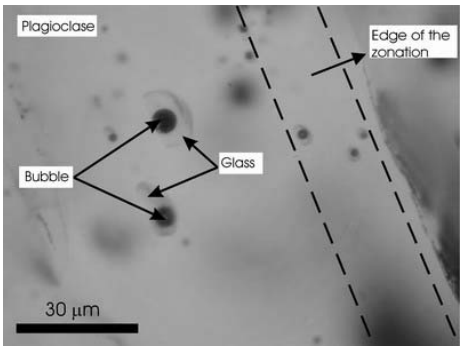

Fig. 1: Silicate melt inclusions in plagioclase next to zonation.

Chemical composition of glass in silicate melt inclusions shows high SiO_2 and K_2O content (up to 77.8 wt% and 5.51 wt%, respectively). The other major elements, particularly Al_2O_3, CaO, MgO and FeO are strongly depleted (down to 11.2 wt%, 2.13 wt%, 0.75 wt%, 1.08 wt%, respectively). This composition is extremely different from the dacitic composition of the bulk rock; the glass could not be in equilibrium with the crystallizing host plagioclase crystals. Therefore, significant post-entrapment crystallization can be considered within the silicate melt inclusion, which took away the majority of CaO and Al_2O_3 and formed plagioclase on the wall of inclusions with the same composition as the host.

This work is supported by the Papp Simon Foundation to I. Havancsák.

References

BENEDEK, K., PÉCSKAY, Z., SZABÓ, CS., JÓSVAI, J. & NÉMETH, T. (2004): Geologica Carpathica, 55: 43–50.

ROEDDER, E. (1984): Fluid inclusions. (Reviews in Mineralogy, 12). Washington (D.C.): Mineralogical Society of America.

ONE HUNDRED MINERALS FOR ONE HUNDRED YEARS (DEDICATED TO THE CENTENNIAL OF THE GEOLOGICAL INSTITUTE OF ROMANIA)

HÎRTOPANU, P.
Geological Institute of Romania, 1 Caransebeş Street, Bucharest, Romania
E-mail: paulinahirtopanu@hotmail.com

There were investigated mainly three types of mineral occurrences: **I**. The Mn-Fe occurrences in Romania, *i.e.* (A) the Răzoare Fe-Mn deposit, Preluca Mountains; (B) the Bistriţa Mn belt, Bistriţa Mountains; (C) the Delineşti Mn-Fe deposit, Semenic Mountains; (D) the Răscoala Fe-Mn deposit, Sebeş Mountains. **II**. The Ditrău carbonatite alkaline intrusive complex (DCAIC). **III**. There were also investigated the slags of Galaţi blastfurnace.

I. A. In the Răzoare Fe-Mn deposit, besides manganoan ferrosilite and fayalite, all the members of the manganoan humite series were detected; very rare minerals, wustite and pyroxferroite, good indicators of redox conditions, were also identified. B. In the Bistriţa Mn belt a suite of new minerals for the area was discovered, such as bannisterite, benstonite, barytocalcite, kozulite, brokenhillite, caryopilite, kellyite, manganpyrosmalite, nelenite, natronambulite, parsettensite, pennantite, pyrophanite, ribbeite, schallerite, nambulite, thorianite, mcgillite, minnesotaite, winchite, xonotlite, yoshimuraite, *etc.*, thus being one of the most complex Mn deposits of the world. The mineralogical richness of the Bistriţa Mn belt as well as their complex mineral equilibria, help us to reconstruct the P, T, X, f_{CO2}, f_{O2}, f_{Cl}, f_{H2O} conditions of the ore, thus completing the data on the country rock, strongly influenced by retromorphism and thus more difficult to decipher. The established metamorphic evolution of the Mn ore, achieved through repeated and superimposed metamorphic events, explains the complex mineralogy, each metamorphic events being a source of new minerals. C. In the Răscoala Fe-Mn deposit, among others, a rare Ba-Mn mica, kinoshitalite was identified. D. In the Delineşti Mn-Fe deposit pyrophanite, senaite, neltnerite were discovered, just to mention the more rare minerals.

II. The main mineral groups (halides, sulphides, oxides, carbonates, phosphates and silicates) of the DCAIC were investigated optically as well as by SEM, EPMA and XRD; our work was focussed on REE, Nb-Ta and (REE + Nb-Ta) minerals. Among the halides gagarinite (?) and cryolite (?) were identified. In addition to bastnäsite-(Ce), bastnäsite-(La), parisite-(Ce) and parisite-(La) other REE carbonate species were determined: ancylite-(Ce), calcioancylite-(Ce), cordylite-(Ce), synchysite-(Ce), synchysite-(Y), hydroxylbastnäsite-(Ce), hydroxylbastnäsite-(Nd), burbankite. Beside ceriopyrochlore, uranpyrochlore, bariopyrochlore and plumbopyrochlore other oxides were also determined: aeschynite, betafite, calciobetafite, fergusonite, loparite-(Ce), latrappite, microlite, strüverite, tapiolite, zirkelite. New sulphides for the area were identified as well: lautite, arsenosulvanite, tungstenite, kesterite, hemusite, geerite, gallite, briartite, renierite. Besides monazite-(Ce), monazite-(La), new phosphates were also found: REE apatite, crandallite, florencite-(Ce), carbonate-fluorapatite, goyazite, rhabdophane. Rare silicates, such as aenigmatite, lamprophyllite, pectolite, wairakite, zeophyllite or rare silicates with Zr, Zr-Ti or Nb-Ti such as catapleiite, eudialyte, kupletskite, rosenbuschite, hiortdahlite, götzenite, låvenite, fersmanite, lovozerite, and murmanite were identified. REE-silicates such as cerite, nordite (?), yttrialite were also determined.

III. Many artificial minerals, such as fayalite, metallic Fe, melilite, wüstite and oldhamite were determined in the blastfurnace slags at Galaţi.

References

HÎRTOPANU, P. (2004): Mineralogeneza centurii manganifere din Munţii Bistriţei. Bucureşti: Cartea Universitara, 352 p.

HÎRTOPANU, P. (2006): Mineralogical atlas. Bucureşti: Cartea Universitara, in press.

MESOZOIC OPHIOLITES IN THE DINARIDES AND THE CARPATHIANS: A REVIEW

HOECK, V.[1], IONESCU, C.[2] & KOLLER, F.[3]
[1] Department of Geography and Geology, University of Salzburg, Hellbrunnerstr. 34, A-5020 Salzburg, Austria
E-mail: volker.hoeck@sbg.ac.at
[2] Department of Mineralogy, Babeş-Bolyai University, 1 Kogălniceanu Str., RO-400084 Cluj-Napoca, Romania
[3] Institute of Geological Sciences, University of Vienna, Althan Str. 14, A-1090 Vienna, Austria

Ophiolites and related rocks are important indicators in deciphering paleogeography and tectonic evolution of crustal segments. Despite a large variability and overlap in their lithological appearance, petrology and geochemistry it is generally possible to assign individual ophiolite bodies and related rocks to certain geotectonic environments such as MOR, SSZ, a transition from subcontinental to suboceanic mantle or intraplate environments (DILEK, 2003). In Europe the most widespread and complete Mesozoic ophiolites are found in the Balkan Peninsula, south and south-east of the Alps (ROBERTSON, 2002). Three ophiolite belts can be traced:

(1) From the northern Dinarides through Albania to western Greece;

(2) From the Transylvanian Depression along the inner Dinarides to north-eastern Greece;

(3) From the Western Carpathians through the Eastern Carpathians to the Southern Carpathians.

The westernmost ophiolites can be called Dinaride–Mirdita–Hellenide Ophiolite Zone (DMHZ). It extends from the vicinity of Zagreb in Croatia via Serbia and Albania (Mirdita Ophiolite) to the Beothian ophiolites in Greece. Geologically it is situated between the Drina–Ivanjica–Pelagonia microcontinent in the east and the Adriatic continental margin in the west (KARAMATA & KRSTIĆ, 1996; CHANNELL & KOZUR, 1997). The opening of the DMH oceanic realm is often related to the Middle Triassic fragmentation of the northern margin of the Gondwana supercontinent. A line of evidence, based on metamorphic sole ages (e.g. LANPHERE *et al.*, 1975; DIMO-LAHITTE *et. al.*, 2001; SPRAY & RODDICK, 1980) and Early Cretaceous overstep sequences suggest that it was closed in the Late Jurassic.

The DMHZ has a complex structure. In its central part, in Albania and north-western Greece, it consists of two belts, different in composition and origin but still related to each other. Above a mélange and a metamorphic sole the western belt is dominated by lherzolites, harzburgites are less abundant (BORTOLOTTI *et al.*, 1996; BORTOLOTTI *et al.*, 2004). The tectonites are overlain by a mantle-crust transition zone consisting of plagioclase-bearing peridotites, followed by ultramafic and mafic cumulates and intrusive gabbros. An occasionally developed thin MOR basalt cover, sometimes with a transition to SSZ basalts represents the extrusive section. In the eastern belt, harzburgites prevail followed by a mantle-crust transition zone, with ultramafic and mafic cumulates and intrusive gabbros including diorites and plagiogranites. A locally thick developed sheeted dyke complex follows, leading to the volcanics ranging from tholeiitic basalts to andesites, dacites and rhyolites.

Within the Dinarides the ophiolite belt consists, similar to the western belt in Albania, of a number of ultramafic bodies associated with a melange and it is characterized by a far-reaching lack of oceanic crust rocks (LUGOVIĆ *et al.*, 1991). The mélange is composed of a shaly-silty matrix, embedding different blocks of oceanic (ultramafics, gabbro-dolerite, pillow-lava, chert) and continental fragments (greywacke, limestone and granite). Larger ultramafic massifs (100–1000 km^2) represent thrust sheets that overlay the mélange. They are predominately lherzolitic in composition and usually associated with metamorphic rocks that are typical metamorphic soles, with additional HP/HT mafic granulites. The latter have an unusual thickness of up to 1000 m and are characterized by high pressure (up to 10 kbars) mineralogy. The thickness of the former is much smaller (up to 250 m) and they exhibit a low-pressure metamorphic zoning. The association of granulite facies metamorphic rocks with ultramafic massifs and the absence of upper oceanic crust led LUGOVIĆ *et al.* (1991) to question the ophiolitic nature of the Dinaride ophiolite belt. These observations allow a hypothesis that a large part of DMH ophiolite zone may represent a continental margin sequence.

East of the Drina–Ivanjica–Pelagonia microcontinent, a second ophiolite zone known as Vardar Zone (VZ) occurs. One subzone (Eastern VZ) ranges from north-eastern Greece via Macedonia and Serbia (BÉBIEN, 1983; RESIMIĆ-ŠARIĆ *et al.*, 2000) to Romania, where it is found in the Apuseni Mtns. (NICOLAE; 1995; SACCANI *et al.*, 2001) and the basement of the Transylvanian Depression, (IONESCU & HOECK, 2004). A second subzone (western VZ) can be followed from southern Serbia to Croatia (KARAMATA *et al.*, 2000). The former ophiolites differ from those in the DMHZ in that they contain (1) only little mantle tectonites but a well developed crustal section, (2) the ophiolites are often overlain by an island arc sequence and (3) the crustal rocks are intruded by granites and granodiorites. Radiometric age determinations and palaeontological evidence of overlying sediments suggest Middle to Late Jurassic age for the ophiolites and the intruding granites and granodiorites. The most prominent examples are the Guevgueli ophiolites at the Greece – Macedonian border (BÉBIEN, 1983) and the Apuseni ophiolites in the Mureş Nappe (SACCANI *et al.*, 2001) in Romania. The latter is discussed here in some details as an example.

The ophiolites contain ultramafic and mafic cumulates, gabbros, sheeted dykes and basalts, but no mantle tectonites. Basalts, rarely basaltic andesites and even andesites, display mainly a MOR geochemistry with a high amount of Fe-Ti gabbros and Fe-Ti basalts (SACCANI *et al.*, 2001). Nevertheless, transitional compositions from MORB to SSZ and intraplate basalts occur. The ophiolites are overlain and intruded respectively by an island arc plutonic (?) and volcanic sequence (BORTOLOTTI *et al.*, 2002), which is widely distributed in the eastern part (Trascău Mts.). The volcanic

rocks range from basalts to rhyolites forming dykes, massive lava flows and pillow lavas. Volcaniclastics are common. By contrast to the ophiolites, they exhibit clear signs of a SSZ genesis with low content of HFSE, a negative Nb anomaly and enrichment of LREE over the HREE. They are in turn overlain by thin radiolarite beds and Upper Jurassic limestones. Palaeontological evidence and K-Ar as well as U-Pb data indicate Middle to Late Jurassic age of the formation of the ophiolites and the island arc sequence (PANA *et al*., 2002). To what extent granites, granodiorites and diorites represent the plutonic part of the island arc sequence or are alternatively independent Jurassic intrusions, remains a matter of debate.

The Transylvanian Depression was drilled by a large number of boreholes, from which some reached the pre-Cretaceous basement and consequently basaltic rocks. In particular the deep well Deleni-6042 and Zoreni-1 drilled each several hundred metres of basaltic and andesitic rocks. The Deleni borehole drill cores form approximately 10% of the whole length of the basalt drilling, *i.e.* approximately 40 m drill cores. Basalts and andesites from the drill cores can be grouped in three petrographic and geochemical entities. All of them, despite small geochemical differences, resemble strongly basalts and andesites on top of the ophiolites of the Apuseni Mtns. and the Trascău Mts. (IONESCU & HOECK, 2004). From the drill-hole Zoreni-1 a few core remnants are available for investigation. They show boninitic affinities with high SiO_2 and MgO, Cr and Ni but low to very low Ti, Zr, Y and Sm. The REE are depleted, the chondrite-normalised pattern is slightly U-shaped. All these features highlight the suprasubduction zone character of these rocks.

In the Eastern Carpathians (EC) basalts and ultramafics are found in the Transylvanian nappes (TN) in the tectonic highest position above the Bucovinian Nappe (SĂNDULESCU, 1984; RUSSO-SĂNDULESCU *et al*., 1983) closely associated with the Wildflysch. The major occurrences are from N to S: Rarău, Hăghimaş and Perşani. The ophiolites occur often as olistoliths, partly as tectonic slivers (?). Among the smaller blocks (hundred of meters) larger continuous occurrences of basalts or ultramafics are regarded as remnants of the Transylvanian nappes. How far these larger units can be interpreted as mega-olistoliths remains to be discussed. Such an interpretation would disregard the existence of a separate Transylvanian Nappe.

The age of the ophiolites from the Eastern Carpathians is debatable. At least a large part is Triassic in age, inferred from the close connection to Mid-Triassic sediments with well preserved original interfaces among basalts and sediments. The ophiolitic fragments consist mainly of lherzolitic ultramafics, serpentinites and various basalts. Gabbros and related rocks such as diorites and plagiogranites as well as fragments of sheeted dikes are rare. The most frequent rocks are basalts. In the northern parts (Rarău and Hăghimaş) lherzolites prevail, in the Perşani Mtns. harzburgites are more common. In the Rarău, MORB-type volcanics with a variable subduction component are common. They also show a certain variation towards andesitic (trachyandesitic) compositions. However, according to RUSSO-SĂNDULESCU *et al*. (1983) intraplate basalts are likely to occur. They seem to be more widely distributed in Hăghimaş and are common also in Perşani. It should be noted however, that except for one occurrence no remnants of an ophiolitic sequence could be detected so far. Trachytes are additionally common in the Perşani Mtns. Until now no similar rocks were found in Rarău or Hăghimaş.

Compared with other ophiolites, in particular with those in the Southern Apuseni Mtns. a number of differences can be noted:

(1) Intraplate compositions of basalts or their differentiation products are missing in the Apuseni Mtns.
(2) The Apuseni ophiolites have an almost complete ophiolite sequence ranging from ultramafic cumulates over gabbros and sheeted dykes to basaltic extrusives. Gabbros, dykes and basalts show often Fe-Ti enrichment trend. By contrast, the Eastern Carpathians MOR-type basalts have a slight subduction component, but no Fe-Ti enrichment. There are almost no ophiolite sections, but isolated ultramafic bodies. Gabbros are almost missing.
(3) The Apuseni ophiolites are overlain by island arc sequence. No such equivalents could be found so far in the Eastern Carpathians.
(4) Inferred from the depositionally overlying Late Jurassic limestones, the Apuseni ophiolites are regarded to be Late Jurassic in age. Contrary, Late Jurassic limestones are not reported to be spatially associated with the Eastern Carpathians basalts and ultramafics. Strong relations to Mid to Late Triassic sediments are more common.

Within the Southern Carpathians the Severin Nappe, sandwiched between the Danubian unit below, and the Getic nappes above, contains Mesozoic ophiolites. They are believed to be Jurassic in age and consist of serpentinized peridotites (mainly lherzolites), rare gabbros and basalts (SAVU, 1982). The latter display geochemically a MOR characteristic and are accompanied by enriched intraplate basalts. In this respect the Severin Nappe ophiolites resemble those from Rarău in the Transylvanian nappes, notwithstanding the different tectonic position. The ophiolites from the Severin Nappe are thought to have a continuation in the Ceahlău and Black Flysch nappes in the Eastern Carpathians. There, blocks of basic volcanic material are found embedded in coarse grained clastic sediments of Late Jurassic and Cretaceous age. Larger, mappable units occur in the north of Romania and in the Ukraine in the continuation of the Ceahlău–Black Flysch units. The Severin–Ceahlău ophiolites and basalts respectively are regarded as remnants of an intracontinental oceanic basin situated within the European continental margin.

The relation among the ophiolite belts and their according oceanic basins in south-eastern Europe remains enigmatic. The rhetoric question "How many oceans?" put forward by CHANNELL & KOZUR (1997) is not satisfactorily answered yet. To envisage their three "Meliata, Vardar and Pindos" oceans is most likely not enough. The Upper Cretaceous MOR-type basalts and sediments in the western Vardar Zone require a separate marginal or back-arc basin (*cf.* PAMIĆ *et al*., 2002). Additionally, the Severin ophiolites in the Southern Carpathians and their possible continuation (?) in the Eastern Carpathians, the mafic volcanic remnants in the Ceahlău and Black Flysch nappes are probably formed in a small intra-continental oceanic basin E of the Vardar Zone. Based on the lithological, petrological, geochemical and geochronological differences, we propose here that the ophio-

lites in the Transylvanian nappes of the Eastern Carpathians represent the continuation of the Triassic Meliata Ocean from the Western Carpathians (CHANNELL & KOZUR, 1997) rather than the north-eastern most continuation of the eastern Vardar Ocean (SĂNDULESCU, 1984), which we believe has terminated at the northern end of the Transylvanian Depression (HOECK *et al*., 2004).

This study was financially supported by the Land Salzburg Research Fellowships (Austria) Grant: "Karpatische Ophiolithe des Mesozoikums in Rumänien"/2005.

Selected references

BÉBIEN, J. (1983): Ofioliti, 8: 293–301.

BORTOLOTTI, V., KODRA, A., MARRONI, M., MUSTAFA, F., PANDOLFI, L., PRINCIPI, G. & SACCANI, E. (1996): Ofioliti, 21: 3–20.

BORTOLOTTI, V., MARRONI, M., NICOLAE, I., PANDOLFI, L., PRINCIPI, G. & SACCANI, E. (2002): International Geology Review, 44: 938–955.

BORTOLOTTI, V., CHIARI, M., MARCUCCI, M., MARRONI, M., PANDOLFI, L., PRINCIPI, G. & SACCANI, E.: (2004): Ofioliti, 29: 19–35.

CHANNELL, J.E.T. & KOZUR, H.W. (1997): Geology, 25: 183–186.

DIMO-LAHITTE, A., MONIE, P. & VERGELY, P. (2001): Tectonics, 20/1: 78–96.

DILEK, Y. (2003): Geological Society of America Special Papers, 373: 1–16.

HOECK, V., IONESCU, C. & KOLLER, F. (2004): In: Abstracts of the 32nd International Geological Congress, Florence, Italy, 1: 90–91.

IONESCU, C. & HOECK, V. (2004): In: Proceeding of the 5th International Symposium on Eastern Mediterranean Geology, Thessaloniki, Greece, 1: 256–259.

KARAMATA, S. & KRSTIĆ, B. (1996): In: KNEŽEVIĆ, V. & KRSTIĆ, B. (eds.): Terranes of Serbia. Belgrade: University of Belgrade, 25–40.

KARAMATA, S., OLUJIĆ, J., PROTIĆ, L., MILOVANOVIĆ, D., VUJNOVIĆ, L., POPEVIĆ, A., MEMOVIĆ, E., RADOVANOVIĆ, Z. & RESIMIĆ-ŠARIĆ, K. (2000): Academy of Sciences and Arts of the Republic of Srpska, Collections and Monographs, Department of Natural, Mathematical and Technical Sciences, 1: 131–135.

LANPHERE, M.A., COLEMAN, R.G., KARAMATA, S. & PAMIĆ, J. (1975): Earth and Planetary Science Letters, 26: 271–276.

LUGOVIĆ, B., ALTHERR, R., RACZEK, I., HOFMANN, A.W. & MAJER, V. (1991): Contributions to Mineralogy and Petrology, 106: 201–216.

NICOLAE, I. (1995): Romanian Journal of Tectonics and Regional Geology, 76: 27–39.

PAMIĆ, J., TOMLJENOVIĆ, B. & BALEN, D. (2002): Lithos, 65: 113–142.

PANĂ, D., BALINTONI, I., HEAMAN, L. & ERDMER, P. (2002): Studia Universitatis Babeş–Bolyai Cluj-Napoca, Geology, Special Issue, 1: 265–277.

ROBERTSON, A.H.F. (2002): Lithos, 65: 1–67.

RESIMIĆ-ŠARIĆ, K., KARAMATA, S., POPEVIĆ, A. & BALOGH, K. (2000): Academy of Sciences and Arts of the Republic of Srpska, Collections and Monographs, Department of Natural, Mathematical and Technical Sciences, 1: 81–85.

RUSSO-SĂNDULESCU, D., SĂNDULESCU, M., UDRESCU, C., BRATOSIN, I. & MEDEŞAN, AL. (1983): Anuarul Institutului de Geologie şi Geofizică, Bucureşti, 61: 245–252.

SACCANI, E., NICOLAE, I. & TASSINARI, R. (2001): Ofioliti, 26: 9–22.

SĂNDULESCU, M. (1984): Geotectonics of Romania. Bucureşti: Editura Tehnică, 336 p. (in Romanian)

SAVU, H. (1982): Dări de Seamă ale Institutului de Geologie şi Geofizica Bucureşti, 69/5: 57–71.

SPRAY, J.G. & RODDICK, J.C. (1980): Contributions to Mineralogy and Petrology, 72: 43–55.

RARE SULPHOSALT MINERALS IN ROMANIA

ILINCA, GH.
Department of Mineralogy, University of Bucharest, Bd. N. Bălcescu, 1, RO-701111 Bucharest, Romania
E-mail: ilinca@geo.edu.ro

Introduction

The territory of Romania contains a significant part of the Alpine–Carpathian chain and has witnessed complex geological and mineralogenetical cycles spanning from Precambrian to Neogene, with an expectedly comprehensive yield of rock forming and ore minerals. Sulphosalt minerals are constant accessories of various polymetallic ore deposits and mineralized bodies in Romania, *i.e.*: 1) deposits related to Upper Cretaceous – Paleocene magmatism in Southwestern Banat and Bihor Mts. 2) deposits related to Neogene volcanism in East Carpathians and Apuseni Mts. 3) Hercynian granites of Northern Dobrogea or Highiş Mts (Fig. 1).

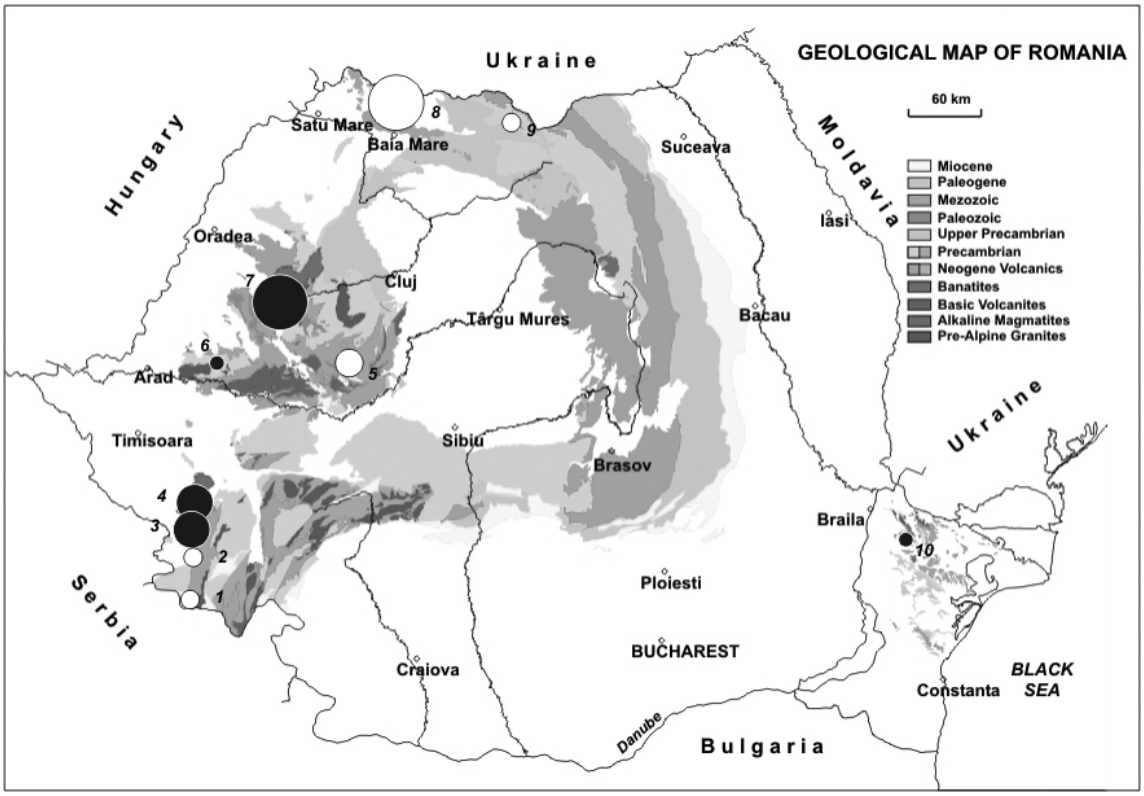

Fig. 1: Simplified geological map of Romania with the main areas of occurrence for sulphosalt minerals: (1) Moldova Nouă; (2) Sasca Montană; (3) Oravița – Ciclova; (4) Dognecea – Ocna de Fier; (5) Metaliferi Mts.; (6) Highiş Mts. (7) Băița Bihor – Valea Seaca; (8) Baia Mare; (9) Baia Borşa; (10) Pricopan – Greci. Black circles denote prevailing Bi sulphosalts; white circles, Sb(As) sulphosalts. Higher circle diameters correspond to higher frequency/diversity of sulphosalt species (base map after Geological Institute of Romania).

Many of the sulphosalt species in Romania – as mostly everywhere else – occur in minute grains or in very small quantities suggesting that they might not be of great importance in the ore forming processes. Different views might point to the fact that sulphosalt scarcity reflects very narrow genetical conditions, thus worth to be known and deciphered.

Another possible reason behind sulphosalts low esteem is the difficulty to build a long term research program, especially against today's widely accepted priorities. However, one of the main significance of sulphosalts arises from the fact that they represent the most general example of modern principles applied to mineral classification and crystal chemistry. Many of today's fundamental concepts, such as polysomatism, homology, plesiotypism, merotypism, hierarchical classification of crystal structures, the understanding of the role and constraints imposed by the atomic structure upon the chemical variability of minerals, find a good and relevant illustration in sulphosalts. Natural sulphosalts are of renowned significance for mineralogical, geological and material-science studies. Considerable interest has been raised during the last decades by this specific group of minerals, in connection with their potential benefits for modern technologies based on photovoltaic effects and superconductibility. The interest in sulphosalts as relevant materials is also driven by the lack of knowledge in the field of macroscopic physical properties, such as elastic, dielectric, Raman and infrared

behaviour, *etc*. to serve as constraints in *ab-initio* computer simulations. Detailed crystal structures, chemical variability data and physical measurements would be of highest relevance for such determinations.

Natural mineral occurrences are often singular and highly valued sources of sulphosalts for the study of crystal structures and material properties, as only a small proportion of such compounds may be obtained by synthetic methods. In spite of a considerable progress achieved by experimental mineralogy, many sulphosalts remain outside the actual possibilities of mineral synthesis. It is especially the case of sulphosalts with ordered supercells (*e.g.* ordered superstructure members of the bismuthinite-aikinite series, Bi_2S_3–$CuPbBiS_3$, involve reaction times in the order of 28-30 months, while maintaining a relatively high temperature of at least 175 °C (PRING, 1995). Another example is given by the 4th, 7th and 8th pavonite homologues, the 5th lillianite homologue as well as several fundamental phases in the cuprobismutite series (*e.g.*, paděraite), which could never be synthesized in laboratory. Crystallographic research on natural phases is often influenced by the discovery of new, less common or not yet known natural compounds. Therefore, entirely new opportunities to verify some of today's structural predictions or to initiate not yet foreseen directions in the complex study of this group can arise if new sulphosalt minerals are discovered and described.

Sulphosalt definition and features

Sulphosalts are a group of complex sulphides (rarely selenides and tellurides) with the general formula $A_xB_yC_z$ where *A* is commonly Pb, Ag, Cu and less commonly Hg, Tl, Fe, Mn, Cd, Sn^{2+}, Sn^{4+}, Na, K *etc*. *B* can be As, Sb or Bi (metalloids) with a conventional 3+ charge and a fundamental trigonal, non-planar [BS_3] coordination. *C* position is S^{2-} and or Se^{2-}, rarely Te^{2-}. Sulphosalt crystals are generally silvery grey in colour and are characterized by a fine needle-like morphology caused by a usually present 4 Å short cell axis. The extreme steric mobility of metalloids (Bi, As, Sb), the structural analogies between these elements and common sulphosalt metals (Pb, Ag, Cu) are the fundaments of an unmatched structural diversity and complexity in the mineral realm. Each sulphosalt phase has a well-defined crystal-chemical identity, requiring a specific definition and classification. While extremely numerous and diverse (Fig. 2), sulphosalt structures can be derived from just two major structural archetypes and include a limited range of chemical elements, to which most of the common indirect mineralogical determination methods fail, asking instead for complex quantitative determinations of chemical composition and crystal structure, or other parameters uniquely identifying the structural features.

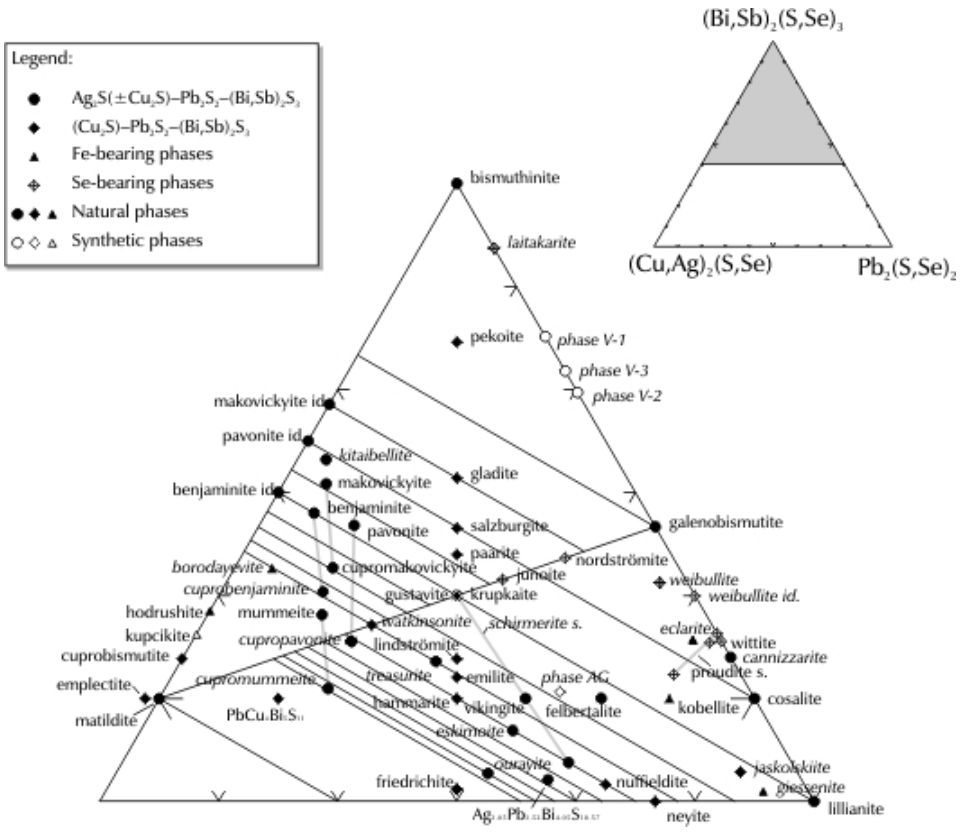

Fig. 2: Synoptic view of the upper part of the $(Bi,Sb)_2(S,Se)_3$–$(Cu,Ag)_2(S,Se)$–$Pb_2(S,Se)_2$ compositional diagram, showing several known natural and synthetic sulphosalt minerals. Phases still unknown in Romanian occurrences are in italics.

Important families of sulphosalt minerals in Romanian occurrences

Though rare, Bi-based sulphosalt minerals identified in Romanian occurrences are so diverse that to describe them in their entire complexity would be far beyond the reach of this lecture. Therefore, only the most remarkable examples will be mentioned and illustrated here.

The pavonite homologous series is represented by a family of crystal structures with two types of slabs parallel to (001): thinner slabs with single metal octahedra alternating with pairs of square pyramids [Bi(Pb)S_5], and thicker slabs composed of parallel chains of little deformed metal octahedral in a galena-like pattern. Without significant amounts of Cu, the general formula of the series is $Ag_{(N-1)/2-x}Pb_{2x}Bi_{(N+7)/2-x}S_{N+5}$, where N is the number of octahedra in one octahedral chain across thicker, 'galena-like' slabs in the structure, and x is the degree of substitution for Pb (KARUP-MØLLER & MAKOVICKY, 1979).

The co-ordination requirements of Ag and Cu, as well as near-octahedral co-ordination of Bi play a decisive role in the layout of the series, and control – by still incompletely known mechanisms – the exsolution phenomena that are typical for pavonite homologues (Fig. 3).

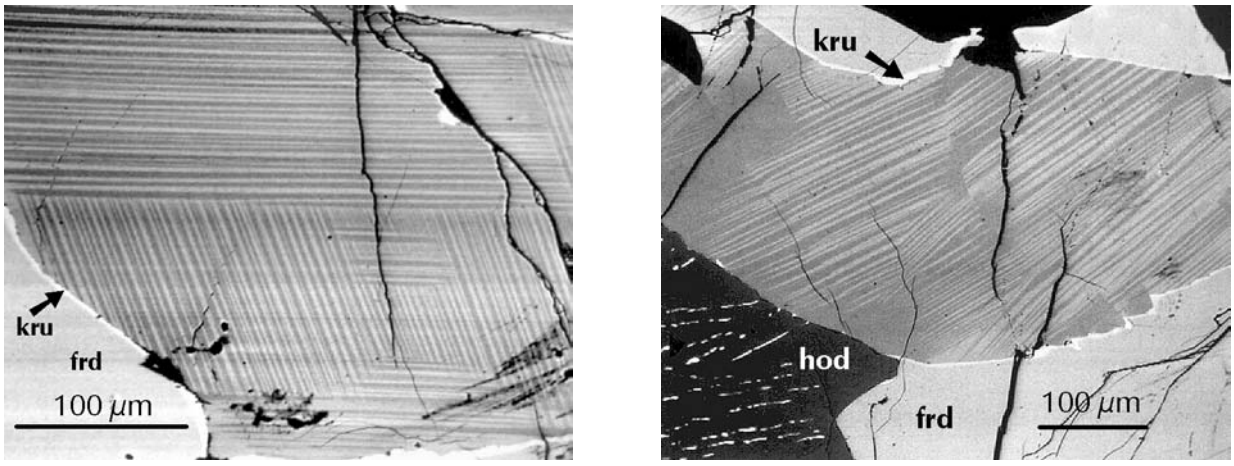

Fig. 3: Typical aspects of makovickyite–cupromakovickyite exsolutions from Băiţa Bihor; krupkaite, friedrichite and hodrushite are associated with the pavonite homologues. BSE image.

Several occurrences such as those at Băiţa Bihor, Valea Seacă, Ocna de Fier and Oravița are unique in holding an entire range of exsolved or homogeneous Cu-free and Cu-rich pavonite homologues, among which the presence of hitherto completely unknown 6th and 9th homologues and the presence of mummeite-cupromummeite pair (the 8th homologue, KARUP-MØLLER & MAKOVICKY, 1979) is assumed. Furthermore, new investigations are expected to clarify the background of the doubling of the *c* unit-cell dimension of cupropavonite (KARUP-MØLLER & MAKOVICKY, 1979), a copper-rich variety of the 5th homologue, in respect to the *c* axis of pavonite, and to observe a similar mechanism for Cu-rich 4th homologues, which are frequent in the above mentioned occurrences.

Due to their modular structure, the members of the pavonite series are also prone to developing intermediate homologues with mixed layers of N and $N + 1$ octahedra wide, already found in synthetic products such as $Cd_{2.8}Bi_{8.1}S_{15}$ (CHOE *et al.*, 1997).

The junoite-felbertalite-(neyite) series may be interpreted as an accretional homologous series, with the general formula $Cu_2Pb_{3N}Bi_8S_{3N+13}$, where junoite – $Cu_2Pb_6Bi_8(S,Se)_{16}$ (a = 26.4, b = 4.01, c = 16.6 Å, β = 126.5º, $C2/m$, Z = 2) is the N = 1 and felbertalite – $Cu_2Pb_3Bi_8S_{19}$(a = 27.6, b = 4.05, c = 20.7 Å, β = 131.3º, $C2/m$, Z = 2) is the N = 2 homologue (MAKOVICKY *et al.*, 2001). Both structures posess identical $(100)_{PbS}$ layers, which are two atomic layers thick and which are periodically sheared, giving rise to tetrahedral Cu sites. The accretion takes place in the kinked and periodically sheared $(111)_{PbS}$ layers, which are single-octahedron in junoite and double-octahedron in felbertalite.

The crystal structure of neyite – $Ag_2Cu_6Pb_{25}Bi_{26}(S,Se)_{68}$ (a = 37.5, b = 4.07, c = 43.7 Å, β = 108.8º, $C2/m$, Z = 2; MAKOVICKY *et al.*, 2001) can be described as an alternation of triple-octahedra $(111)_{PbS}$-like layers with $(100)_{PbS}$-like layers, two atomic planes thick. Both sets of layers are sheared, giving rise to tetrahedral Cu sites, and truncated by complex PbS-like layers $(001)_{ney}$, three atom planes thick. The resulting structure can be described as a supercomplex structure, built up from three different elements. Neyite does not belong to the junoite homologous series, but it relates to it by containing elements of what should correspond to the hypothetical 3th homologue of the stepped layer structure of the junoite–felbertalite homologous series. A new occurrence of neyite in association with cosalite, has recently been identified at Dognecea (ILINCA & TOPA, 2005, unpublished data).

Recent investigations revealed the presence of junoite in the skarn deposits of Băiţa Bihor and of felbertalite at Ocna de Fier and Oravița (Fig. 4). Junoite from Băiţa Bihor is among the very few occurrences departing from the Se-bearing archetype described at Tennant Creek, Australia (MUMME, 1975) and requires new crystal structure determinations. Wider knowledge on the detailed crystal chemistry

of the extremely rare felbertalite and neyite is also likely to occur from these new findings.

The same stands for *proudite* – which has been recently identified in a Se-free form – $CuPb_{7.5}Bi_{9.3}(S)_{22}$ at Ocna de Fier, Southwestern Banat, where it associates with cosalite, felbertalite and bismuthinite derivatives (Fig. 4).

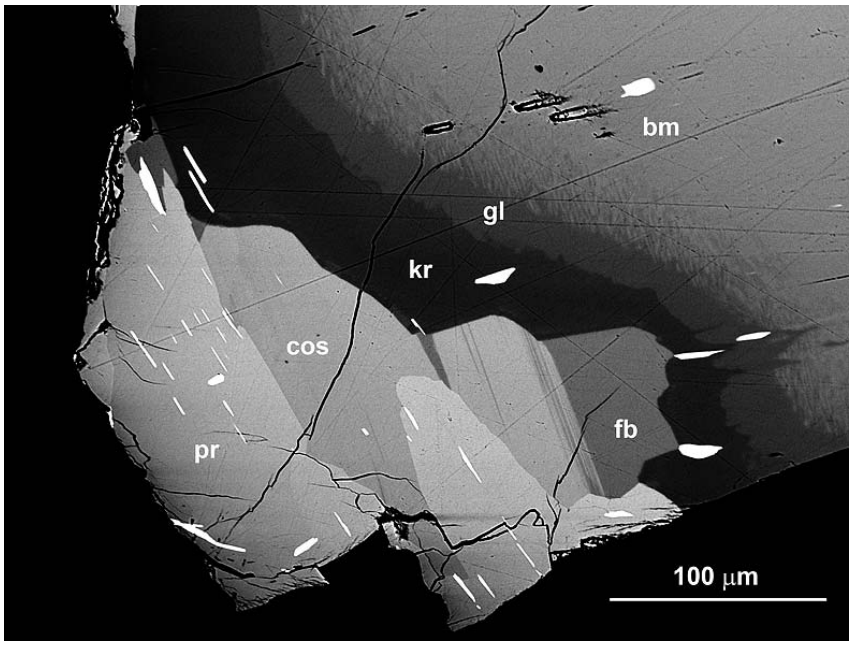

Fig. 4: Complex sulphosalt assemblage with bismuthinite (bm), gladite (gl), krupkaite (kr), proudite (pr), cosalite (cos) and felbertalite (fb) – Ocna de Fier, Southwestern Banat. White laths are Bi (sulpho-) tellurides (BSE image).

Some rare occurrences such as the one at Ciclova, potentially contain at least two new sulphosalt minerals with chemical compositions plotting in the felbertalite-nordströmite region: phase A: $\sim Cu_{0.6}Ag_{0.3}Pb_{3.1}Bi_{5.7}S_{12.3}$ and phase B: $\sim Cu_{0.4}Ag_{0.8}Pb_{3.4}Bi_{5.3}S_{11.9}$ (Fig. 5) and for which, crystal structure determinations are ongoing. Phase B displays a relic character due to widespread replacement by wittite and bismuthinite derivatives. Due to elevated Ag contents, phase B might be a false felbertalite plot in a combined Cu + Ag compositional diagram such as the one in Fig. 2.

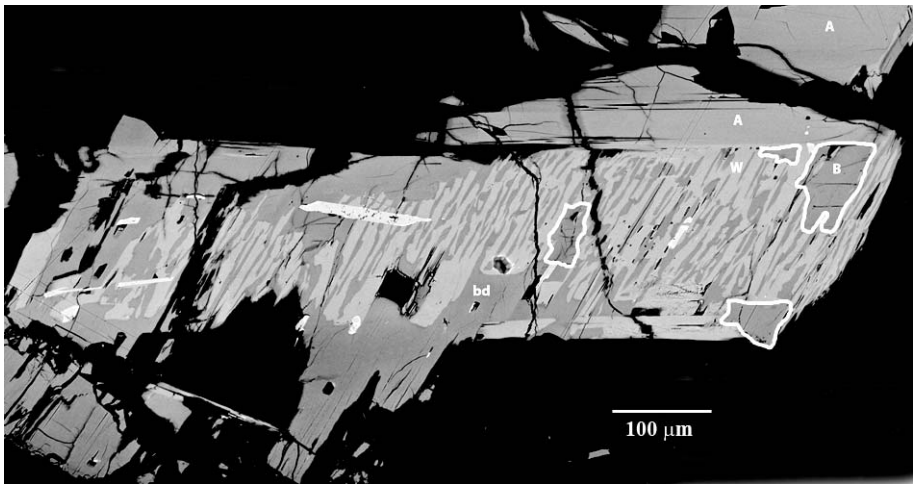

Fig. 5: BSE imaging of Bi-sulphosalt assemblage from Ciclova, Southwestern Banat: unknown phases A and B, wittite (W) and bismuthinite derivatives (bd). White needles are Bi tellurides.

All members of *the cuprobismutite family – i.e.*, cuprobismutite, hodrushite, paděraite and the recently discovered kupčíkite are represented in Romanian occurrences. Such episodes are confined to ore-deposits related to contact-metamorphic aureoles of Upper Cretaceous–Palaeocene calcalkaline igneous rocks in the so-called Banatitic Belt.

Structural affinities of cuprobismutite members often reflects in coherent intergrowths of two or three different phases, such as hodrushite + kupčíkite ± paděraite (Fig. 6). A similar case of intergrowths between cuprobismutite and paděraite from Ocna de Fier has recently been discussed by CIOBANU *et al.* (2004). Typical assemblages include bismuthinite derivatives, makovickyite-cupromakovickyite, emplectite and various Bi tellurides.

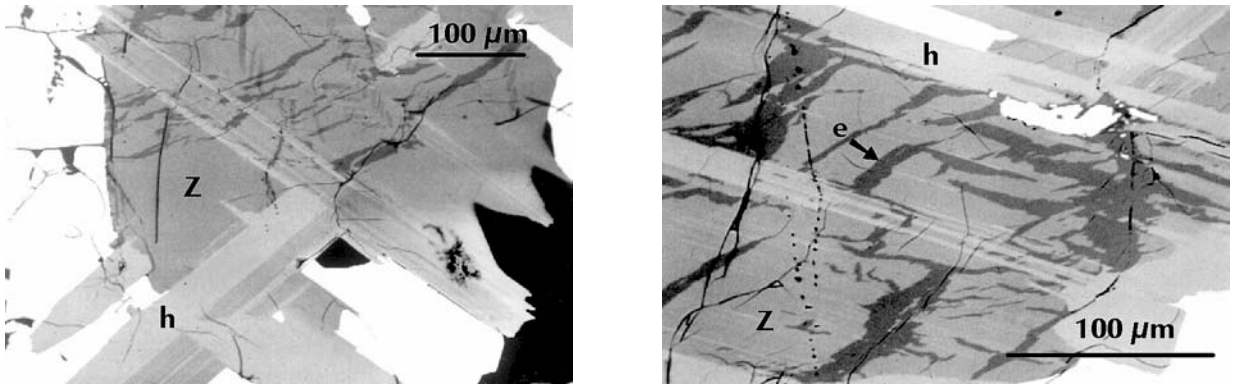

Fig. 6: Parallel intergrowths between hodrushite (h) and kupčíkite (Z) at Băiţa Bihor. Kupčíkite is preferentially altered by emplectite (e) BSE image.

Finally, not all sulphosalts may be considered rare, yet many of the more common species reveal very peculiar aspects of their crystal chemistry. It is the case of *the bismuthinite–aikinite series* (Bi_2S_3–$CuPbBiS_3$), a discrete family of sub- and supercell structures which seemed a closed case some ten years ago, but to which three more 4-fold and 5-fold superstructure members were added: salzburgite $Cu_{1.6}Pb_{1.6}Bi_{6.4}S_{12}$, paarite $Cu_{1.7}Pb_{1.7}Bi_{6.3}S_{12}$ and emilite $Cu_{10.7}Pb_{10.7}Bi_{21.3}S_{48}$ (BALIĆ-ZUNIĆ *et al.*, 2002; MAKOVICKY *et al.*, 2001; TOPA *et al.*, 2005). Compositional ranges pointing to these three phases have already been identified in several occurrences from Romania, but they will be in need of detailed crystal structure determinations.

Cosalite – ideally $Pb_2Bi_2S_5$ – is another example of a rather common sulphosalt species but with a complicated history in what concerns substitutional mechanisms involving Ag and Cu, *e.g.* $2Pb \Leftrightarrow Bi(+Sb) + Ag$; $Bi(+Sb) \Leftrightarrow Pb + Cu$; $Pb + \square \Leftrightarrow Me^{+} + Me^{+}$; $Pb + \square \Leftrightarrow Cu^{2+}$ *etc*. Significant amounts of chemical and structural data are necessary to identify the relevant trends for such replacement schemes.

Acknowledgements

The author wishes to thank Dr. DAN TOPA from the University of Salzburg for the kindly provided support and mineralogical data, and Professor EMIL MAKOVICKY from the University of Copenhagen for the entire long-term support and contribution to the topic discussed.

References

BALIĆ-ZUNIĆ, T., TOPA, D. & MAKOVICKY, E. (2002): Canadian Mineralogist, 40: 239–245.

CHOE, W., LEE, S., O'CONNEL, P. & COVEY, A. (1997): Chemistry of Materials, 1997 (2): 2025–2030.

CIOBANU, C. L., PRING, A. & COOK, N. J. (2004): Mineralogical Magazine, 68: 279–300.

KARUP-MØLLER, S. & MAKOVICKY, E. (1979): Bulletin de Minéralogie, 102: 351–367.

KARUP-MØLLER, S. & MAKOVICKY, E. (1992): Neues Jahrbuch für Mineralogie, Monatshefte, (12): 555–576.

MAKOVICKY, E. (1989): Neues Jahrbuch für Mineralogie, Abhandlungen, 160: 269–297.

MAKOVICKY, E., BALIĆ-ZUNIĆ, T. & TOPA, D. (2001): 39: 1365–1376.

MAKOVICKY, E., TOPA, D. & BALIĆ-ZUNIĆ, T. (2001): Canadian Mineralogist, 39: 1377–1382.

MUMME, W.G. (1975): American Mineralogist, 60: 548–558.

PRING, A. (1995): American Mineralogist, 80: 1166–1173.

MAKOVICKY, E., TOPA, D. & BALIĆ-ZUNIĆ, T. (2001): Canadian Mineralogist, 39: 1377–1382.

TOPA, D., MAKOVICKY, E. & BALIĆ-ZUNIĆ, T. (2005): Canadian Mineralogist, 43: 907–917.

A NEW OCCURRENCE OF MANGANILVAITE $CaFe^{2+}Fe^{3+}(Mn^{2+}, Fe^{2+})[Si_2O_7]O(OH)$ AT DOGNECEA, SOUTHWESTERN BANAT, ROMANIA: CHEMICAL COMPOSITION, CRYSTAL STRUCTURE AND CATION ORDERING

ILINCA GH.[1], VIZITIU, A.[1], TOPA, D.[2] & VLAD, Ş.[3]
[1] Department of Mineralogy, University of Bucharest, Bd. N. Bălcescu, 1, RO-701111 Bucharest, Romania
E-mail: ilinca@geo.edu.ro
[2] Department of Material Sciences, University of Salzburg, Hellbrunnerstrasse 34/III, A-5020 Salzburg, Austria
[3] Ecological University of Bucharest, Franceza str., 3, Bucharest, Romania

Samples of ilvaite systematically exceeding 0.5 *apfu* Mn (in formula normalized on the basis of 6 cations) and suggesting the presence of the recently discovered mineral manganilvaite (ZOTOV *et al.*, 2005; BONEV *et al.*, 2005) were identified in the skarn deposit at Dognecea, where they occur in association with Mn-hedenbergite and magnetite. A number of 14 EDS chemical analyses of such ilvaites resulted in the following ranges of variation: (in weight percents; numbers in parentheses read as average values and standard deviations, respectively): **Si**: 13.39–14.09 (13.92; 0.15), **Al**: 0.00–0.27 (0.09; 0.11), **Fe**: 32.88–34.53 (34.62; 0.64), **Mn**: 7.30–9.17 (7.85; 0.54), **Mg**: 0.00–0.26 (0.07; 0.10), **Ca**: 9.86–10.64 (10.26; 0.22). Atomic proportions of Fe^{2+} and Fe^{3+} for a chemical formula unit normalized for 6 cations, were calculated as $Fe^{2+} = 2 - Mn^{2+}$ and $Fe^{3+} = Fe_{total} - Fe^{2+}$. The variation domains of Fe^{2+}, Fe^{3+} and Mn^{2+} atomic proportions were the following: 1.34–1.48 (average 1.44; standard deviation 0.04), 0.98–1.04 (1.01; 0.021) and 0.52–0.66 (0.56; 0.04), respectively. Other varieties of Mn-poorer ilvaites were identified, too.

Manganilvaite from Dognecea is a $P2_1/a$ polymorph (a = 13.014 Å, b = 8.846 Å, c = 5.848 Å and β = 90.34°) with significant ordering of Fe^{2+} and Fe^{3+} among *Me*11 and *Me*12 structural sites. The single crystal structure determination of manganilvaite – based on 1509 unique reflections, was refined down to a final R = 5.41% (with single generic metals – Fe or Mn – in *Me*11, *Me*12 and *Me*2 positions). The crystal structure data allowed the calculation of interatomic and per-polyhedra average distances for all relevant cation-oxygen pairs and the evaluation of Fe^{2+} and $Fe3^{+}$ occupancies in *Me*11 and *Me*12 structural sites. Statistical Fe^{x+} occupancies were calculated on the basis of two classic atomic radii models, *i.e.* GHOSE (1966) – (G) and SHANNON (1976) – (S). Thus, *Me*11 structural site is 53% (G) or 84% (S) occupied by Fe^{2+} (normalized values for *Me*11 + *Me*12 = 100%). Fe^{3+} occupancy in *Me*11 and Fe^{2+} occupancy in *Me*12 site is complementary to these values. The corresponding ordering parameter (TAKEUCHI *et al*., 1983) was 0.34 (G) or 0.47 (S). Same calculations concerned the *Me*2 structural site and allowed indirect evaluation of Mn^{2+} occupancy *vs*. complementary Fe^{2+}. Calculation of Mn occupancy in *Me*2 based on a simple linear variation of *Me*2–O Shannon distances between 2.18 Å (Fe^{2+}–O) and 2.23 Å (Mn–O), resulted in 42% Mn^{2+} whereas the empirical model of Carrozzini (1994) yielded 52% Mn^{2+}. Similar discrepancies between the Shannon and Carrozzini models may be described in the case of the type manganilvaite from Ossikovo (BONEV *et al.*, 2005). The refinement of the structure with split *Me*2 position (Mn and Fe) resulted in a slightly lower R = 5.33%. Attempts to refine the structure with Mn in Ca, *Me*11 or *Me*12 position have failed, suggesting that Mn is confined to the *Me*2 position.

The experimental β value is slightly discrepant with regard to the ones calculated on the basis of correlated ordering parameter and degree of monoclinicity (TAKEUCHI *et al.*, 1983 (T); FINGER & HAZEN, 1987 (FH)): 90.16° (T) and 90.27° (FH).

Local paragenetical relations and various published correlations between the ordering parameter and the temperature of formation, suggest that Mn-ilvaite from Dognecea represents a reaction product of 6 hed + 4 mgt + 3 $H_2O \rightarrow$ 6 ilvaite + ½ O_2, formed at temperatures not exceeding 300 °C, and in conditions of relatively low fO_2.

References

BONEV, I.K., VASSILEVA, R.D., ZOTOV, N. & KOUZMANOV, K. (2005): Canadian Mineralogist, 43: 1027–1042.

CARROZZINI, B. (1994): European Journal of Mineralogy, 6: 465–479.

FINGER, L.W. & HAZEN, R.M. (1987). Zeitschrift für Kristallographie, 179: 415–430.

GHOSE, S. (1969): In: WEDEPOHL, K. H. (ed.): Handbook of Geochemistry, Berlin: Springer-Verlag, II/3, 26-A, 1–14.

SHANNON, R.D. (1976): Acta Crystallographica, A32: 751–767.

TAKEUCHI, Y., HAGA, N. & BUNNO, M. (1983): Zeitschrift für Kristallographie, 163: 267–283.

ZOTOV N., KOCKELMAN W., JACOBSEN S.D., MITOV I., PANEVA D., VASSILEVA R.D. & BONEV I.K. (2005): Canadian Mineralogist, 43: 1043–1053.

MINERALOGICAL, PETROGRAPHIC AND GEOLOGICAL STUDIES ON ROMAN BRICKS AND TILES FROM *ALBURNUS MAIOR* AND *APULUM* (DACIA PROVINCE): POSSIBLE RAW MATERIALS SOURCES

IONESCU, C.[1], GHERGARI, L.[1] & ŢENTEA, O.[2]
[1] Department of Mineralogy, Babeş-Bolyai University, 1 Kogălniceanu Str., RO-400084 Cluj-Napoca, Romania
E-mail: corinai@bioge.ubbcluj.ro
[2] Romanian National History Museum, 12 Calea Victoriei, RO-030026 Bucharest, Romania

A high number of Roman ceramic tegular material *i.e.* bricks and tiles, from the beginning of the IInd century AD were found at Roşia Montană (*Alburnus Maior*) and Alba Iulia (*Apulum*), in Romania. A large part of these are marked with the stamp of the famous Legion XIII Gemina, which played an important role in defending the Apuseni Mts. gold-mining area.

Twelve samples from the Roşia Montană archaeological site have been compared, from a mineralogical-petrographical-geological point of view, with ten samples of tegular material belonging to same legion and found at *Apulum*. For comparison, material belonging to the same chronological segment only, was studied. Consequently, *Apulum* samples marked with similar types of stamps as those from the *Alburnus Maior* were selected. The main aim of the investigation was the search for the provenance area for both, the raw clays and the temper sources. The ceramics consists mainly of a matrix with crystalline and/or amorphous fabric, showing different degrees of sintering and vitrification. In the matrix variable amounts of magmatic, metamorphic and sedimentary lithoclasts, various crystalloclasts (quartz, feldspar, mica), and rare ceramoclasts and bioclasts are present. Regarding the grain size, the ceramics is mainly lutitic-silticarenitic, with a contribution of arenaceous-sized grains exceeding 15% and reflecting the coarse category for all samples. Quartzites, granites-granodiorites, basalts, andesites/basaltic andesites, gneisses and limestones are ubiquitous lithoclasts.

Microscopical observations on the matrix as well as the X-ray diffraction indicate the use of polymictic clays, consisting mainly of illite, kaolinite ± smectite ± calcite ± micas as raw materials. The clays seem to be similar for both, the Rosia Montana and the Alba Iulia, artefacts.

The thermal changes of primary minerals as noticed in thin sections are represented mainly by the fissuring of quartz, the decomposition of calcite, the occurrence of contraction holes around some lithoclasts, the change of the anisotropy of clay minerals, the forming of glass, gehlenite, wollastonite and hematite. Additionally, the XRD show the disappearance of some lines belonging to clay minerals and the modification of calcite lines. Based on the above-mentioned thermal alterations, compared with our experimental data and references (RICCARDI *et al*., 1999; CULTRONE *et al.,* 2001; ANTONELLI *et al*., 2002; *etc*.), the firing temperatures were inferred and the ceramic artefacts were classified in three categories: a) type I ceramics, fired at lowest temperature (800-850^{o}C); b) type II ceramics, fired at 850-900^{o}C and c) type III ceramics, fired at 900-950^{o}C. In the Alba Iulia site the ceramics of type III is prevalent, followed by type II ceramics. The Rosia Montana ceramics is mainly of type II and subordinately of type I. Nevertheless, from mineralogical-petrographical point of view, both ceramics (*Apulum* and *Alburnus Maior*) are very similar.

Based on the mineral composition of the matrix (illite, kaolinite ± smectite ± calcite + micas), we presume that clays with an according composition, outcropping west and north-west of Alba Iulia were used as raw materials.

The mineralogical and petrographical composition of the crystalloclasts and lithoclasts respectively, in the ceramics from both Rosia Montana and Alba Iulia sites is similar. Granites and granodiorites are like those crossed by the Aries river, north of Alba Iulia, basalts, basaltic andesites, radiolarites are surely originated from the Mesozoic ophiolitic zone outcropping westwards of Alba Iulia, while limestones outcrop also westwards of Alba Iulia, together with the ophiolites. These lithoclasts are also found in the alluvial sediments of the Mures River downstream the confluence with the Ampoiu River. Thus, we presume that the temper was most likely mined from the right bank of the Mures River, south-east of Alba Iulia. Even today this location provides quartz sands, used for bricks and tiles manufacture.

This study was financially supported by the Romanian Ministry of Education and Research (Grant 1762/2005).

References

ANTONELLI, F., CANCELLIERE, S. & LAZZARINI, L. (2002): Journal of Cultural Heritage, 3: 59–64.

CULTRONE, G., RODRIGUEZ-NAVARRO, C., SEBASTIAN, E., CAZALLA, O. & DE LA TORRE, M.J. (2001): European Journal of Mineralogy, 13: 621–634.

RICCARDI, M.P., MESSIGA, B. & DUMINUCO, P. (1999): Applied Clay Science, 15: 393–409.

GLAUCONITE AND CELADONITE IN THE ALTERED BASALTIC ROCKS FROM THE DELENI-6042 DEEP WELL (TRANSYLVANIAN DEPRESSION, ROMANIA)

IONESCU, C.[1], HOECK, V.[2] & POP, D.[1]
[1] Department of Mineralogy, Babeş-Bolyai University, 1, Kogălniceanu Str., RO-400084 Cluj-Napoca, Romania
E-mail: corinai@bioge.ubbcluj.ro
[2] Salzburg University, 34, Hellbrunner Str., A-5020 Salzburg, Austria

The Deleni-6042 deep well was drilled in the northern part of a major gas-bearing structure, in the Transylvanian Depression (Romania). After penetrating Cenozoic, Upper Cretaceous and Upper Jurassic sediments, the drill crossed, between 4700 and the final depth of 5062 m, a thick pile of basalts, basaltic andesites and andesites, most likely of Jurassic age. The previous mineralogical, petrographical and geochemical studies (HOECK & IONESCU, 2003; IONESCU & HOECK, 2004) showed the calcalkaline-SSZ features of these volcanics. Geochemically, three groups of rocks were distinguished: A) the lowermost group, with low Cr, Ni and Zr as well as low alkalies; B) the middle group, with very high Cr and Ni and low Zr and alkalies and C) the uppermost group, with low Cr and Ni and high Zr and alkalies.

Some of the rocks are rich in alteration products, e.g. the sample Del-10 collected from the basaltic andesites in a depth of 4850 m. Geochemically it belongs to the uppermost level of the volcanic sequence (C). Macroscopically, the sample consists of black-greenish massive basaltic rock containing greenish veins and nests. Microscopically, basaltic andesite shows a porphyritic, sometimes glomeroporphyritic texture, with zoned plagioclase and rare augite phenocrysts in an intersertal groundmass. A wide range of secondary minerals formed at low-TP conditions were noticed by IONESCU *et al*. (2003) and IONESCU & HOECK (2004), among which are glauconite, smectite (Fe-saponite), Fe-clinochlore, calcite, Fe oxides, and chalcedony. Based on microscopical observations and microprobe analyses, two generations of glauconite forming aggregates of platelets or fibres, were noticed. Glauconite I has a yellowish-green colour (1N) and low birefringence (+N) while glauconite II has an intense bluish-green colour (1N), and higher birefringence (+N). Glauconite I occurs mainly as aggregates of platelets with rosette texture, filling in vesicles, irregular voids or veins while glauconite II occurs mainly as fibres filling in vesicles, forming thin rims around augite phenocrysts, or replacing partly or totally, augite. Glauconite II substitutes also the former volcanic glass in the groundmass. Chemically, glauconite I has lower Mg and Si and higher Fe content while glauconite II has higher Mg and Si and lower Fe content. The following succession was observed: glauconite I, followed by Fe-saponite, then glauconite II and finally a Fe-clinochlore appeared.

In this study we present more details on these glauconite I and II. From microprobe analyses, the crystal chemical formulas based on a mica-like structure with a total charge balance of 11 oxygen atoms were calculated. For celadonite, Fe^{2+} to Fe^{3+} ratio was calculated based on ideal dioctahedral site occupancy of 2. In some cases, in particular for glauconite, the total amount of Fe was assigned to Fe^{3+}, by these procedures. According to the IMA criteria (RIEDER *et al.,* 1998), our minerals classify as ***glauconite*** (the previous glauconite I, yellowish-green) and ***celadonite***, respectively (the previous glauconite II, bluish-green), with the calculated formulas listed below:

$(K_{0.8}Na_{0.01}Ca_{0.04})(Fe^{3+}_{1.31}Al_{0.28}Mg_{0.4})(Si_{3.58}Al_{0.42})_4O_{10}(OH)_2$ for glauconite,

$K_{0.94}(Fe^{3+}_{0.72}Al_{0.42}Mg_{0.6}Fe^{2+}_{0.24})(Si_{3.9}Al_{0.1})_4O_{10}(OH)_2$ for celadonite.

This study confirms the presence of glauconite (first reported as glauconite I by IONESCU *et al*., 2003 and IONESCU & HOECK, 2004) and provides the first record of celadonite (glauconite II in IONESCU *et al*., 2003 and IONESCU & HOECK, 2004) in the upper level of the volcanic sequence in the Deleni-6042 deep well (Transylvanian Depression, Romania). The occurrence of these minerals proves the alteration processes of basaltic andesite in a marine environment.

Acknowledgments are due to Dr. D. Topa (Salzburg University) for microprobe analyses and to Dr. T. Weiszburg and E. Tóth (Eötvös Loránd University, Budapest) for suggestions regarding glauconite-celadonite.

References

HOECK, V. & IONESCU, C. (2003): Acta Mineralogica-Petrographica, Abstract Ser., 1: 45.

IONESCU, C. & HOECK, V. (2004): In: Proceedings of the 5th International Symposium on Eastern Mediterranean Geology, Thessaloniki, Greece, 256–259.

IONESCU, C., HOECK, V. & TOPA, D. (2003): Acta Mineralogica-Petrographica, Abstract Ser., 1: 47.

RIEDER, M., CAVAZZINI, G., D'YAKONOV, Y.S., FRANK-KAMENETSKII, V.A., GOTTARDI, G., GUGGENHEIM, S., KOVAL, P.V., MÜLLER, G., NEIVA, A.M.R., RADOSLOVICH, E.W., ROBERT, J.-L., SASSI, F.P., TAKEDA, H., WEISS, Z. & WONES, D.R. (1998): Canadian Mineralogist, 36: 905–912.

METASOMATIC-HYDROTHERMAL PROCESSES ALONG THE CONTACT ZONE OF LOWER CRETACEOUS MAGMATIC SILLS INTRUDED INTO LOWER JURASSIC COAL BEDS AT PÉCS-VASAS, MECSEK MTS., HUNGARY

JÁGER, V.
Department of Mineralogy, Herman Ottó Museum, Kossuth u. 13, H-3525 Miskolc, Hungary
E-mail: jagerviktor@yahoo.co.uk

In the Mecsek Mts. Lower Cretaceous magmatic rock of ankaramite-alkali basalt series intruded in Lower Jurassic paralic coal seams. The coking effects and the fissure networks produced by these magmatics in the coal deposits and their influence on hydrocarbon migration and methane explosions in the coal mines has already been discussed in several papers, but the hydrothermal events caused by these magmatic sills have been barely mentioned yet.

The magmatic sills generally intruded into the coal beds, on the whole concordantly with the coal seams.

A few of the magmatic sills reach 6-7 meter in thickness. The sills bear conspicuous macroscopic features, *i.e.* a network of cooling cracks parallel to the contacts with the coal beds; another network of shorter cracks, perpendicularly to the previous crack system; and directly along the contact a coke zone (up to 1.5 m in thickness) dissected by hexagonal, columnar joints. The change of colour of the sill from dark green through paler tints to whitish and the decrease of size and quantity of the phenocrysts from the centre of the sill towards the contacts are also obvious. The magmatic sills frequently contain cavities within 30-cm distance from the contact; they are often flattened according to the flow direction. Some cavities reach 4-5 cm in diameter. They may contain pyrite, siderite, calcite, quartz, barite and dickite. The largest quartz crystals in the cavities reach 2.5 cm. The crack network of the sills is filled with minerals. These veinlets consist of calcite, quartz, chalcedony, barite, pyrite, and rarely sphalerite crystals up to a few mm in size.

Free-standing calcite, quartz and barite crystals in the veins may reach about 1 cm. It is conspicuous, that the quartz veinlets occur in the sill only within 0.7–1.5-m distance from the contact, depending on the thickness of the sill (within 0.7 m for a 4-meter thick sill and within 1.5 m for a 6.5-meter thick one). In some sills brecciated claystone and coal xenoliths have been observed; in their surroundings there are calcite veins containing euhedral quartz crystals of 1-2 cm length. It is to be noted that on some places euhedral quartz or smoky quartz crystals of about 1-cm length can be found in the fissures of the country rocks (siltstone and sandstone) within 1-2 m distance from the contact.

The origin of hydrothermal minerals found in a 4-meter wide sill that intruded in a coal bed was studied using optical microscopy and SEM-EDS. In the sample, collected from the interior of the sill ***1.7 m from the lower contact***, there are euhedral, 1-2 mm long, sector zoned pyroxene showing violet pleochroism, with a Ti content increasing towards the edges. This pyroxene is rich in Ca and Fe, in some crystals the amount of Cr is also considerable. Moreover, chromian spinel inclusions up to 5 μm are common. Ni-Co-(Fe) sulfide inclusions of a few μm in size have also been found. Ilmenite and rutil inclusions (50–80 μm) are also common. In many cases pyroxene has been calcitized and argillized along the cracks. Fresh kaersutite phenocrysts also occur. Plagioclase shows a labradorite–bytownite composition. The amount of analcime in the rock is considerable. Opaque minerals are ilmenite, titanomagnetite, and pyrite. Some pyrite grains contain galena, barite and Fe-rich sphalerite inclusions up to a few μm. The texture of the rock is microholocrystalline.

1.3 m from the contact only small parts of pyroxene are fresh; it is mainly altered to calcite, clay minerals and iron oxides. Calcite occurs in the matrix, analcime has not been observed. In the rock calcite veins are getting more and more frequent.

90 cm from the contact pyroxene is totally altered to calcite, opal, lussatite, chalcedony, quartz, clay minerals and partly iron oxides. The outline of the pyroxene was preserved, forming a pseudomorphous texture. Calcite and quartz varieties formed due to the alteration of pyroxene fill in crevices and coalescent cavities. Veinlets consisting of rhombohedral, free-grown calcite, chalcedony, free-grown quartz and barite are remarkable. The plagioclase is calcitized more strongly than in the middle of the vein.

50 cm from the contact pyroxene is totally altered to calcite.

At about ***30 cm from the contact*** even the remains of altered phenocrystals are barely visible. The rock consists of calcite, clay minerals, quartz, iron oxides and pyrite. Its texture is microcrystalline, due to the faster cooling. At 30 cm from the contact the mineral-filled cavities are getting more and more frequently. Pyritization is also intensive.

Directly at the contact the magmatic rock is altered to clay minerals and iron oxide. In calcite veinlets found in the aleurolite 2-m from the lower contact of the magmatic sill there are euhedral quartz crystals, 0.5 cm in length.

A rough scenario of mineral formation can be summarised as follows. The intrusion of the magmatic sills suddenly elevated the pressure of aqueous vapour in the country rock. Released volatiles penetrated into the magma (having originally a lower vapour pressure) and formed first gas bubbles, which later dissolved. Volatiles reacted with the minerals crystallizing from the magma. At about 90 cm from the contact silica was released from the altered pyroxene and precipitated as quartz in cavities and veinlets in the sill. CO_2 derived from the coal beds reacted with Ca released from the altered pyroxene and plagioclase to form calcite. In the middle of the sill barite and sphalerite are found as microscopic inclusions in pyrite, but in the veinlets near to the contact they already reach some mm (sphalerite) or 1 cm in size (barite). This fact suggests Ba and Zn mobilization and migration from the country rock into the sill driven by the hydrothermal processes.

MARMAROSH DIAMONDS – THE TYPICAL ASSOCIATION WITH THE ORGANIC MATTER IN THE OUTER CARPATHIANS

JARMOŁOWICZ-SZULC, K.[1], KARWOWSKI, Ł.[2] & DUDOK, I. V.[3]
[1] Polish Geological Institute, Rakowiecka 4, 00-975 Warsaw, Poland
E-mail: katarzyna.jarmolowicz-szulc@pgi.gov.pl
[2] Department of Geochemistry, Mineralogy and Petrology, University of Silesia, Będzińska 60, 41-200 Sosnowiec, Poland
[3] Institute of Geology and Geochemistry of Combustible Minerals, Academy of Sciences of Ukraine, Naukova 3a, 79053 L'viv, Ukraine

The Marmarosh diamonds (MD) – a special type of the quartz, locally called *dragomites* – occur in the Outer Carpathians over a widespread area in a distinct paragenesis with different hydrocarbonic compounds. Since their description by TOKARSKI (1905), the MD have been a study object for about a century aiming at explanation of the phenomena of mineral formation and characteristics (*e.g.* VOZNYAK *et al*., 1973; KOZŁOWSKI *et al*., 1996). In Polish and Ukrainian territories, the following areas have been defined as examples of MD occurrence: the Mszana Dolna (Poland) tectonic window – KARWOWSKI & DORDA (1986); HURAI *et al*. (2002), the Rabe region (Bieszczady Mts., Poland) – JARMOŁOWICZ-SZULC & DUDOK (2005), the Stavne village vicinity (Ukraine) – DUDOK & JARMOŁOWICZ-SZULC (2000).

Despite their above described occurrence, the MD have in general a very characteristic euhedral crystal habit, transparency and a perfect reflection (KARWOWSKI & DORDA, 1986). There is a combination of rhombohedra $(10\bar{1}1)$ and $(01\bar{1}1)$, rare trigonal pyramid $(11\bar{2}1)$ and hexagonal prism $(10\bar{1}0)$. In the studied samples, that last one is often short or totally reduced.

The observed MD are present in the fissures, either as crystals in quartz veins or in the Carpathian fractures filled additionally with other minerals as calcite (at least two generations), traces of ore mineralization (*e.g.* pyrite) and the organic matter. The presence of primary or of secondary hydrocarbon inclusions is a characteristic phenomenon of the MD. Those primary ones observed in three sample areas, may be divided into three phase groups of state, being of homogeneous or heterogeneous nature. The solid inclusions comprise different bitumens, while the liquid inclusions are filled with different non-mixing fluids. Gas inclusions contain methane with some admixtures of heavier hydrocarbons, nitrogen and occasionally carbon dioxide. The heterogenic inclusions contain different types of the filling, *e.g.* gas and liquid hydrocarbon and the aqueous solution; gas and heavy hydrocarbon and the aqueous solution and solid bitumens *etc.* Heavy bitumens are rare in quartz. When present, they are responsible for the black colour of the crystals. Such feature was observed in the Rabe region together with a relatively long crystal form, *i.e.* with a well-developed hexagonal prism. The Mszana Dolna area is full of quartz crystallized directly on the fissure walls, with calcite veinlets in the neighbourhood, tectonically disturbed. Such quartz is observed eastwards, too, in the tectonically engaged places. In other localities, individual crystals occur in "pockets" with black organic matter. For the vein formations of the Eastern Carpathians, the presence of anthraxolite is shown (DUDOK *et al*., 2002).

Based on the studies conducted *pT* conditions of the mineral formation may be stated as: high pressure values in the Mszana region (0.75–2 kbar, compare: HURAI *et al*., 2002), lower in the Rabe vicinity (0.9–1.7 kbar, JARMOŁOWICZ-SZULC & DUDOK, 2005) and the highest near Stavne (2.4–2.7 kbar, DUDOK & JARMOŁOWICZ-SZULC, 2000). Temperatures fall into a wide interval, while local differences enable a wide regional discussion of the formation history.

References

DUDOK, I. V. & JARMOŁOWICZ-SZULC, K. (2000): Geological Quarterly, 44: 415–423.

DUDOK, I.V., KOTARBA, M. & JARMOŁOWICZ-SZULC, K. (2002): Geologiya i Geokhimiya Goryuchikh Kopalin: 76-87.

HURAI, V., KIHLE, J., KOTULOVA, J., MARKO, F. & ŚWIERCZEWSKA, A. (2002): Applied Geochemistry, 17: 1259–1271.

JARMOŁOWICZ -SZULC, K. & DUDOK, I. V. (2005): Geological Quarterly, 49: 291–304.

KARWOWSKI, Ł. & DORDA, J. (1986): Mineralogia Polonica, 17: 3–12.

KOZŁOWSKI**,** A., METZ, P. & MŁYNARCZYK, M. (1996): Jahrestagung der Deutschen Mineralogischen Gesellschaft, Kiel, 9–12 September 1996. Berichte der Deutschen Mineralogischen Gesellschaft – Nachtrag von Kurzreferaten.

TOKARSKI, J. (1905): Kosmos, 30: 443–460.

VOZNYAK, D. K., GRYCIK, V.V., KVASNYTSYA, V. N. & GALABURDA, Y. A. (1973): Dopovidi Akademii Nauk URSR, 12: 1050–1062.

MANGANESE MINERALS FROM THE OXIDATION ZONE OF BANSKÁ ŠTIAVNICA DEPOSIT

JELEŇ, S.[1], HÁBER, M.[1], ANDRÁŠ, P.[1] & STANKOVIČ, J.[2]
[1] Geological Institute, Slovak Academy of Sciences, Severná 5, 97401 Banská Bystrica, Slovakia
E-mail: jelen@savbb.sk
[2] CLEOM, Faculty of Natural Sciences, Comenius University, Mlynská dolina G, Bratislava, Slovakia

The interesting and varied manganese and iron mineral association was described within the southern subsurface parts of the Terézia vein, which represent probably the oxidation zone of the Banská Štiavnica deposit. Besides the manganese oxide – todorokite, cryptomelane and pyrolusite have also been identified. The presence of vernadite, feroxyhyte and woodruffite is also assumed but these minerals have not been determined undoubtedly. Aggregates of these minerals are closely connected with the central cavities of the vein, where they fill up empty area among quartz crystals, but more often they form coatings on mineral surfaces, which suggest their formation in oxidizing conditions supported by bacteria activity (HÁBER *et al.*, 2003).

Within the primary vein filling sphalerite, galena, chalcopyrite, pyrite, tetrahedrite–tennantite, acanthite, polybasite–pearceite, gold–electrum, silver and hematite are present in substantial amounts. Pyrrhotite, marcasite, bornite, Cu-Ag-S mineral phases, chalcocite, gersdorffite, magnetite, ilmenite and rutile are present only as accessory minerals. With regard to non-metallic and secondary minerals, quartz, carbonates (calcite, dolomite, ankerite, siderite, kutnohorite, cerussite, smithsonite, witherite), rhodonite, anglesite, covellite, chlorites, clinozoisite, epidote, barite, gypsum, clay minerals (kaolinite, illite, illite/smectite) and hydroxides of iron are present (HÁBER *et al.*, 2002). The association of manganese and iron oxides and hydroxides represent the relatively youngest constituents of the vein fillings. Bright silver-grey, euhedral, tabular pyrolusite crystals form 1-2 mm thick crusts on the quartz surface. Pyrolusite crystals occur on the rims of globular aggregates composed of Mn and Fe minerals. Cryptomelane usually fills interstices in the quartz aggregates in the form of black masses.

The chemical composition of pyrolusite and cryptomelane was investigated using a CAMECA SX 100 electron microprobe. EDS spectra showed that pyrolusite contained Mn (60.67–61.53 wt%) and O. In cryptomelane K (3.10–3.82 wt%) and also Na, Zn, Ca, Mg and Fe contents were determined besides Mn (56.03–60.05 wt%) and O. The empirical formula of cryptomelane is as follows: $(Na_{0.10}K_{0.72}Ca_{0.02}Zn_{0.05})_{0.91}Mn_{8.03}O_{16}$.

X-ray study of pyrolusite and of cryptomelane was realised using a DRON-2 diffractometer and an RKG-86 Debye-Scherrer camera (Fe radiation, diameter of the sample 0.3 mm). Strongest lines observed on the Debye-Scherrer film (pyrolusite – 3.109 (10), 2.386 (9), 2.101 (4), 1.618 (7), 1.552 (3), 1.426 (1), cryptomelane – 6.96 (8), 4.81 (6), 3.109 (9), 2.39 (10), 1.54 (5)) and on the diffractogram (pyrolusite – 3.113 (100), 2.401 (15), 2.111 (4), 1.620 (27.5), 1.557 (19.5), 1.433 (1.5)) agree with the characteristic reflections of the cryptomelane and pyrolusite standards (MIKHEEV, 1957). X-ray study of the analysed homogenous grains of supposed vernadite and feroxyhyte samples was inconclusive because some characteristic reflections necessary for unambiguous identification have been missing. Probably insufficiently recrystallized amorphous phases, resp. X-ray amorphous phases of aggregates were investigated; the assumption that the samples contain probably vernadite and feroxyhyte is supported by the electron microscopic study (using JEOL JSM-840) and by the chemical composition of the grains in question.

We suppose, that within the oxidation zone of the upper part of Terézia vein, a stromatolitic texture with higher content of Mn minerals has been formed, by gradual growth of altered spongy soil tissues. Similarly to normal stromatolites, after they became gradually mineralised, mainly by Mn hydroxides. As the presence of unmineralized basidia and idiomorphic rhombohedral crystals of up to now unidentified Ca-Mg carbonates have been found in the studied samples, we suppose that this process has been going on up to the present.

Todorokite formations similar to those described from Terézia vein at Banská Štiavnica had been found by BOSTON *et al.* (2001) in New Mexico, USA. They described sinter coatings on walls and hanging-walls from Hidden Cave, Lechuguilla and Spider Caves. By means of SEM they found that the peculiar forms were built by microorganisms, which are composed of, besides other minerals, mixture of todorokite, buserite and amorphous Mn oxides ("filamentous manganese snow").

References

BOSTON, P.J., SPILDE, M.N., NORTHUP, D.E., MELIM, L.A., SOROKA, D.S., KLEINA, L.G., LAVOIE, K.H., HOSE, L.D., MALLORY, L.M., DAHM, C.N., CROSSEY, L.J. & SCHELBLE, R.T. (2001): Astrobiology, 1 (1): 25–55.

HÁBER, M., JELEŇ, S., KOVALENKER, V.A., GORSHKOV, A.A., SIVTSOV, A.V. & SHKOLNIK, E.I (2002): Mineralogie Českého masivu a Západních Karpat. Olomouc, 31–36.

HÁBER, M., JELEŇ, S., SHKOLNIK, E.I., GORSHKOV, A.A. & ZHEGALLO, E.A. (2003): Acta Mineralogica-Petrographica (Szeged), Abstract Ser. 1: 41.

MIKHEEV, V.I. (1957): Rentgenometricheskiy opredelitel' mineralov. Moskva: Gosgeoltechizdat, 868 p.

Zn-BEARING CINNABAR FROM RABE NEAR BALIGRÓD (BIESZCZADY MTS., OUTER CARPATIANS, SE POLAND)

KARWOWSKI, Ł. & SZEŁĘG, E.
Faculty of Earth Sciences, University of Silesia, Będzińska 60, 41-200 Sosnowiec, Poland
E-mail: lkarwows@wnoz.us.edu.pl, szeleg@wnoz.us.edu.pl

Presence of cinnabar associated with As sulphides from Rabe near Baligród was described by KARWOWSKI & SZEŁĘG (2005). This As-Hg mineralization is epigenetic and is connected with dislocated zones within sedimentary rocks (sandstones, shales, conglomerates) of the Bystre thrust-sheet (Fore Dukla unit, Silesian nappe) (ŚLĄCZKA, 1958; RYBAK, 2000). Realgar and orpiment are the main As minerals (OSTROWICKI, 1958; GAWEŁ, 1970). Cinnabar is represented by two types differing in optical and chemical properties. The first type is pure HgS, the second type contains Fe as impurity up to 0.01 *apfu* and shows lower reflectance than the first one. Cinnabar occurs together with realgar, orpiment, As-bearing pyrite, carbonates (dolomite–ankerite–siderite series), kaolinite and automorphic quartz. Chalcopyrite inclusions within cinnabar have been observed. Cinnabar crystallized before realgar.

TOMKINS *et al.* (2004), in accordance with OSADCHII (1990) and POWELL & PATTISON (1997), described sphalerite–cinnabar solid solution at temperature above 200 °C and at pressure of 1 bar. Two separate phases: Hg-rich sphalerite and cinnabar (in the $Zn_{0.80}Hg_{0.20}S$–HgS range) coexist below 200 °C. LEONARD *et al.* (1978) described a new mineral – polhemusite. Its composition is within the $Hg_{0.10}Zn_{0.92}S_{0.99}$ to $Hg_{0.22}Zn_{0.83}S_{0.95}$ range.

In this paper we report the co-occurrence of pure cinnabar together with Zn-bearing cinnabar represented by sector-zoned crystals (Fig. 1) and isolated exsolutions. Sector-zoned crystals occur outside the pure cinnabar aggregates. Dark sectors on Fig. 2 contain up to 0.12 *apfu* of Zn. Iron and silver (trace) are evenly distributed. Investigated phases are high-Zn varieties of cinnabar.

Isolated small exsolutions of Zn-bearing cinnabar (up to 5 μm) occur within pure cinnabar. The authors observed a few grains, in which Zn predominated over Hg, *e.g.* $(Zn_{0.52}Hg_{0.39}Fe_{0.09})S$. These phases are anisotropic and probably are high-Hg varieties of a mineral close to polhemusite. Pure sphalerite has not been observed. Probably, the structure of cinnabar trapped all Zn from mineralizing fluids precluding sphalerite crystallization.

References

GAWEŁ, A. (1970): Mineralogia Polonica, 1: 7–16.
KARWOWSKI, Ł. & SZEŁĘG, E. (2005): Mineralogical Society of Poland – Special Papers, 25: 318–322.
LEONARD, B.F., DESBOROUGH, G.A. & MEAD, C.W. (1978): American Mineralogist, 63: 1153–1161.
OSADCHII, E.G. (1990): Neues Jahrbuch Mineralogie. Monatshefte, (1): 13–34.
OSTROWICKI, B. (1958): Kwartalnik Geologiczny, 2: 644–653.
POWELL, W.G. & PATTISON, D.R.M. (1997): Economic Geology, 92: 569–577.
RYBAK, B. (2000): Przegląd Geologiczny, 48: 1023–1029.
ŚLĄCZKA, A. (1958): Kwartalnik Geologiczny, 2: 637–643.
TOMKINS, A.G., PATTISON, D.R.M. & ZALESKI, E. (2004): Economic Geology, 99: 1063–1084.

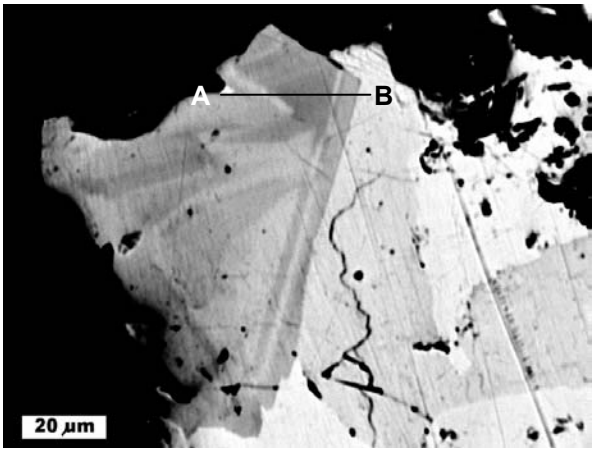

Fig. 1: BSE image of Zn-bearing cinnabar (left) and pure cinnabar (right). A–B: line scan.

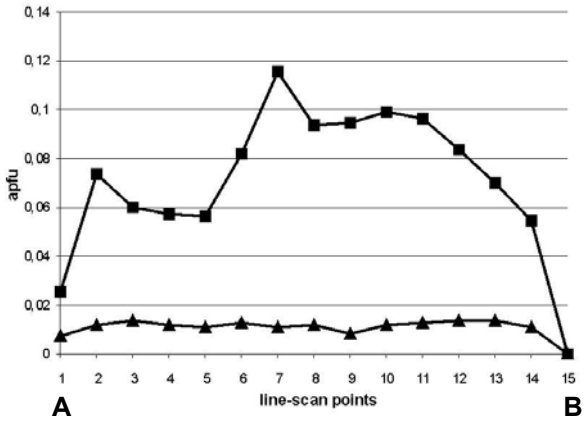

Fig. 2: Variability of Zn (-■-) and Fe (-▲-) within Zn-bearing cinnabar. A–B: line scan.

MINERALOGY AND ORIGIN OF GEODES IN THE BALATONFELVIDÉK SANDSTONE FORMATION AT CSOPAK VILLAGE, BALATON HIGHLAND, HUNGARY

KISS, G. & MOLNÁR, F.
Department of Mineralogy, Eötvös Loránd University, Pázmány Péter sétány 1/C, H-1117 Budapest, Hungary
E-mail: gabriella-kiss@chello.hu

The Balatonfelvidék Sandstone Formation – in which geodes can be found – is a continental, siliciclastic flood-plain sediment of uppermost Permian age. Locally it contains carbonate knots as remnants of palaeosoil carbonates formed in a swamp environment (MAJOROS, 1983). The sandstone is covered by the lower Triassic Werfen Group, which is a lagoonal and/or shelf carbonate sediment

At some localities, the sandstone locally contains large amount of geodes with up to 5-cm diameter (Fig. 1). Along the wall of a typical geode opal-CT forms millimetre thick encrustation. Towards the centre of geodes coarse grained, subhedral to euhedral, short prismatic quartz crystals ("Cumberland" habit) can be found. They contain large amounts (up to approx. 20-30 mass %) of inclusions of euhedral to anhedral anhydrite crystals. Geode centres are usually hollow; tabular barite crystals grown up on the surface of quartz can be found in these spaces. Barite crystals have sometimes a light blue colour, and have elevated (several wt%) Sr content. Main forms of barite crystals are *c*{100} and *m*{110}. Faces of *d*{102} are less developed on some crystals, which otherwise have well developed *o*{011} faces. Encrusting late stage calcite fills up the centre of some of the geodes.

Fluid inclusion (Fig. 2) petrography of quartz revealed extreme differences among the phase proportion of primary inclusions. This indicates inhomogeneous fluid inclusion entrapment from a parent fluid with heterogeneous phase composition. Because of this, no inevitable conclusion can be drawn in connection with the temperature of the formation on the basis of fluid inclusion microthermometric studies. Considering salinities of fluid inclusions, two fluid types were recognised: the first one is characterised by a concentration of 2,07–1,73 NaCl equ. wt%, and the second one is characterised by a concentration of 1,05–0,35 NaCl equ. wt%. Microthermometric behaviour of some inclusions suggests carbonic/organic gas content of fluids.

The geodes are evidently epigenetic formations in the sandstone and probably were formed at the time of deposition of the Lower Triassic cover. Mineralization of geodes could have formed in the mixing zone of two types of fluids. The first type of fluids descended from the Triassic cover and, because of the characteristics of that depositional environment, it contained Ca^{2+}, Sr^{2+} and SO_4^{2-}. The second type was an ascending, probably higher temperature fluid, which contained Ba^{2+} and H_3SiO_4 from alteration of rock forming feldspars in the deeper zones of the sandstone and gas from decaying organic material. In the mixing area, at first the upwelling fluid dissolved carbonate knots in the sandstone and thus prepared the space for geodes. Cooling of those fluids by mixing with the descending solutions resulted in oversaturation in silica due to drop of temperature and that is why opal-CT formed at the first stage of mineralization. Quartz started to precipitate by decreasing of silica saturation. Because of their retrograde solubility, anhydrite and barite had precipitated by warming up of descending fluids in the mixing zone together with silica minerals.

Reference

MAJOROS, GY. (1983): Acta Geologica Hungarica, 26: 7–20.

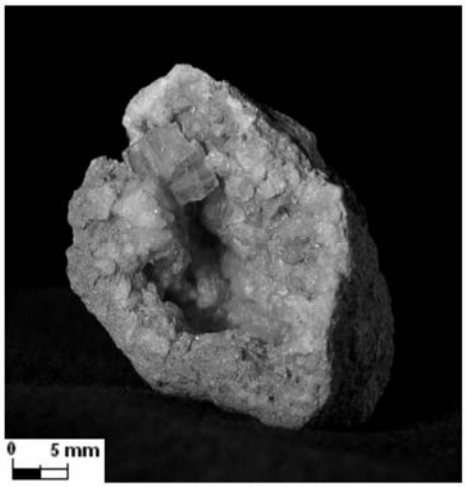

Fig. 1. (left): A geode with tabular barite crystal. Encrusting calcite can also be seen.

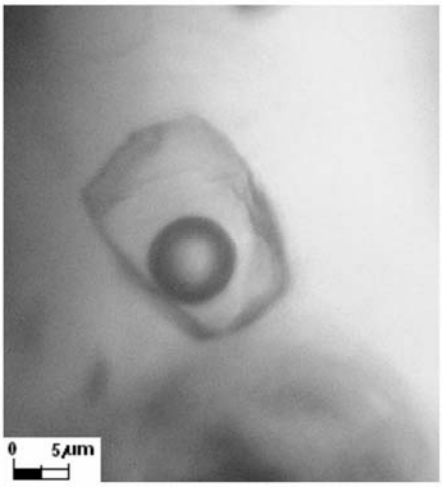

Fig. 2. (right): Fluid inclusions are usually 15-45 µm in size. This is a little one, with a concentration of 0.4 NaCl equ. wt%.

THE TECTONIC SETTING OF THE PLUTONIC SEQUENCE IN SOUTHERN ALBANIAN OPHIOLITES

KOLLER, F.[1], HOECK, V.[2], MEISEL, T.[3], IONESCU, C.[4] & ONUZI, K.[5]
[1] Department of Geological Sciences, University of Vienna, Geozentrum, Althanstr. 14, A-1090 Vienna, Austria
E-mail: friedrich.koller@univie.ac.at
[2] Department of Geography, Geology and Mineralogy, University of Salzburg, Hellbrunnerstr. 34, A-5020 Salzburg, Austria
[3] Institute of General and Analytical Chemistry, University of Leoben, A- 8700 Leoben, Austria
[4] Department of Geology, Babeş-Bolyai University, 1 Kogălniceanu Str., RO-400084 Cluj-Napoca, Romania
[5] Institute of Geological Research, Blloku Vasil Shanto, Tirana, Albania

The Albanian (Mirdita) Ophiolites are part of a large NNW–SSE striking ophiolite zone, which comprises the Dinaric Ophiolites as well as some Greek ophiolites such as Pindos, Vourinos or Othris. Their Jurassic age is constrained by palaeontological evidence of the sediments on top of the ophiolites, by the age of the metamorphic soles and by the age determinations of the intrusive plagiogranite (BORTOLOTTI *et al*., 2004; DILEK *et al.*, 2005 and references herein). The origin of the Albanian ophiolites is essential to restore the continent/ocean distribution in the Jurassic in the Eastern Mediterranean realm and the possible sites of the subduction zones and related thrusts. The environment of formation of these ophiolites and the mode of their emplacement is still controversial.

The Mirdita zone is commonly divided into two ophiolite belts, an eastern one and a western one (e.g. SHALLO *et al*., 1990). The western belt of the Southern Albanian ophiolites consists of six major (Voskopoja, Rehove, Morava, Devolli, Vallamara, Shpati) and two smaller (Luniku and Stravaj) ophiolite massifs. Each massif has a distinct sequence of mantle tectonites, ultramafic cumulates, cumulate gabbros, troctolites and isotropic gabbros. The western belt was supposed to consist of predominantly MOR-type ophiolites with lherzolites, troctolites, gabbros and MOR-type basalts (HOECK *et al*., 2002). A volcanic section together with volcanogenic sediments is restricted to the massifs of Voskopoja and Rehove as well as to the small massifs of Luniku and Stravaj.

The eastern belt is characterized by harzburgites, wehrlites, gabbronorites, clinopyroxene gabbros, plagiogranites and volcanics. The latter show a wide range of SSZ compositions from basalts to andesites, dacites and rhyolites (SHALLO, 1994; BORTOLOTTI *et al.*, 1996; ROBERTSON & SHALLO, 2000; BORTOLOTTI *et al*., 2004).

Here we present evidence that at least in southern Albania the SSZ influence in the western belt is not restricted to the volcanic suite but is as well recorded in the ultramafic tectonites, ultramafic and mafic cumulates as in gabbros. Based on the close spatial and temporal relationship of MOR and SSZ magmas and cumulates, a backarc origin for the Albanian ophiolites is discussed.

The whole-rock geochemistry and mineral chemistry suggest a mid-ocean ridge environment for the origin of cumulates and gabbros from Voskopoja, Rehove and Morava, with only a minor SSZ contribution. The Shpati and the small Luniku massifs show MOR and SSZ signatures in their plutonic sequence. Cumulates and gabbros from Devolli and Vallamara formed in a SSZ environment. The predominance of MOR-generated crustal rocks and the relatively minor occurrence of SSZ-generated plutonics together with the volcanogenic sediments in Voskopoja and Rehove indicate a backarc basin origin of the western belt ophiolites and a westward-dipping subduction zone.

References

BORTOLOTTI, V., KODRA, A., MARRONI, M., MUSTAFA, F., PANDOLFI, L., PRINCIPI, G. & SACCANI, E. (1996): Ofioliti, 21(1): 3–20.

BORTOLOTTI, V., CHIARI, M., MARCUCCI, M., MARRONI, M., PANDOLFI, L. & PRINCIPI, G. (2004): Ofioliti, 29(1): 19–35.

DILEK, Y., SHALLO, M. & FURNES, H. (2005): International Geology Review, 47: 147–176.

HOECK, V., KOLLER, F., MEISEL, T., ONUZI, K. & KNERINGER, E. (2002): Lithos, 65: 143–164.

ROBERTSON, A. H. F. & SHALLO, M. (2000): Tectonophysics, 316: 197–254.

SHALLO, M. (1994): Ofioliti, 19(1): 57–75.

SHALLO, M., KODRA, A. & GJATA, K. (1990): In MALPAS, J., MOORES, E., PANAYIOTOU, A. & XENOPHONTOS, C. (eds.): Ophiolites, Oceanic Crustal Analogues. Proceedings of the Symposium "Troodos 1987". Nicosia: Cyprus Geological Survey Dept., 265–269.

METAMORPHIC EVOLUTION OF THE EASTERN ALPS

KOLLER, F.[1], SCHUSTER, R.[2], HOECK, V.[3], HOINKES, G.[4] & BOUSQUET, R.[5]
[1] Department of Geological Sciences, University of Vienna, Geozentrum, Althanstr. 14, A-1090 Vienna, Austria
E-mail: friedrich.koller@univie.ac.at
[2] Geological Survey, Rasumofskygasse, A-1030 Vienna, Austria
[3] Department of Geography, Geology and Mineralogy, University of Salzburg, Hellbrunnerstr. 34, A-5020 Salzburg, Austria
[4] University of Graz, 2 Universitätsplatz, A-8010 Graz, Austria
[5] University of Basel, 30 Bernoulli Str., CH-4036 Basel, Switzerland

The Eastern Alps are the product of two orogenies, a Cretaceous orogeny followed by a Cenozoic one (FROITZHEIM *et al.,* 1996). The former is related to the closure of an embayment of the Neotethys ocean into Apulia (Meliata Ocean), the latter is due to the closure of the Alpine Tethys oceans between Apulia and Europe. The result of the orogenic movement is a complex nappe stack, which is built up from north to south and from bottom to the top by the following units (Plate 1 in SCHMID *et al.*, 2004): The proximal parts of the Jurassic to Cretaceous European margin built up the northern Alpine foreland and the Helvetic nappes, whereas the distal margin is represented by the Subpenninic nappes. The Penninic nappes comprise the Piemont-Ligurian and Valais Ocean (Alpine Tethys) and the Briançonnais Terrain. Apulia consists of the northern Austroalpine nappes and the Southern Alpine unit (STAMPFLI & MOSAR, 1999). Remnants of the Neotethys embayment occur as slices within the eastern part of the Austroalpine nappe stack. Both orogenic events are accompanied by regional metamorphism of variable extent and P-T conditions. The Cretaceous (Eo-Alpine) metamorphism affects mainly the Austroalpine Nappes, the Penninic domain by the Cenozoic metamorphism, some units of the Lower Austroalpine Nappes show signs of both events.

The distribution of the metamorphic facies zones in the Eastern Alps is mainly controlled by the northwards transport of the Austroalpine nappes. They show a Cretaceous metamorphism and are thrusted over the Penninic domains with Tertiary metamorphism. The latter are exposed in the Eastern Alps only as tectonic windows.

The **eo-Alpine (Cretaceous) metamorphic event** is widespread within and restricted to the Austroalpine unit. It is related to the continental collision following the closure of an embayment of the Tethys Ocean during late Jurassic to Cretaceous times. Recent investigations indicate that the northern part of the Austroalpine unit forms the tectonic lower plate. The southern parts and the north-eastern margin of the Southalpine unit acted as the tectonic upper plate during the continental collision following the disappearance of the oceanic embayment (SCHMID *et al*., 2004). The peak of the eo-Alpine metamorphic event was reached at about 100 Ma, the youngest cooling ages are recorded at 65 Ma (THÖNI, 1999). The eo-Alpine metamorphism starts at the base of the lower plate with greenschist facies and increases structurally upwards the nappe piles until eclogite facies is reached. It decreases again in the uppermost nappes to sub greenschist facies. The whole section represents a transported metamorphism. An overprint of the Variscan crystalline of the lower plate, prior to the eo-Alpine metamorphic event, controlled by a thermal Permian event is widespread.

The **Tertiary Alpine metamorphic event** is due to the closure of the Jurassic to early Cenozoic Briançonnais and Valais oceans (Alpine Tethys). According to WAGREICH (2001) the re-arrangement of the Penninic-Austroalpine border zone from a passive to an active continental margin starts at about 120 Ma. From that time on the oceanic lithosphere and slices from the northern margin of the Austroalpine unit (Lower Austroalpine units) were subducted towards the south below (Upper) Austroalpine units. The Tertiary event reaches blueschist facies conditions in some Mesozoic parts of Penninic windows and some units of the Lower Austroalpine (Tarntal nappe). Eclogite facies conditions followed by a blueschist event occur only in a narrow zone of the Tauern Window. The thermal peak ranges from greenschist to amphibolite facies, the latter was only reached in the central part of the Tauern Window. After the thermal peak at about 30 Ma (BLANKENBURG *et al.*, 1989) uplift and cooling is recorded by K-Ar and Ar-Ar ages on white micas and fission track ages on zircon and apatite (GRUNDMANN & MORTEANI, 1985; FÜGENSCHUH *et al*., 1998). In the lower nappes of the Lower Austroalpine units the Tertiary Alpine metamorphism overprints the Cretaceous metamorphic event.

References

BLANKENBURG, F. v., VILLA, I.M., BAUR, H., MORTEANI, G. & STEIGER, R.H. (1989): Contributions to Mineralogy and Petrology, 101: 1–11.

FROITZHEIM, N., SCHMID, S.M. & FREY, M. (1996): Eclogae Geologicae Helvetiae, 89(1): 81.

FÜGENSCHUH, B., SEWARD, D. & MANCKTELOW, N. (1998): Terra Nova, 9: 213–217.

GRUNDMANN, G. & MORTEANI, G. (1985): Jahrbuch der Geologischen Bundesanstalt Wien, 128: 197–216.

SCHMID, S.M., FÜGENSCHUH, B., KISSLING, E. & SCHUSTER, R. (2004): Eclogae Geologicae Helvetiae, 97: 93–117.

STAMPFLI, G.M. & MOSAR, J. (1999): Memorie di Scienze Geologiche, 51(1): 141–154.

THÖNI, M. (1999): Schweizerische Mineralogische und Petrographische Mitteilungen, 79: 209–230.

WAGREICH, M. (2001): Terra Nova, 13: 401–406.

SULFIDE INCLUSIONS IN ULTRAMAFIC XENOLITHS FROM TUVA (SOUTH SIBERIA)

KONC, Z.[1], HIDAS, K.[1], SZABÓ, CS.[1] & SHARYGIN, V.[2]
[1] Lithosphere Fluid Research Lab, Department of Petrology and Geochemistry, Eötvös University, Pázmány Péter sétány 1/C, H-1117 Budapest, Hungary
E-mail: zoltan.konc@geology.elte.hu
[2] Institute of Mineralogy and Petrography, Siberian Branch of the Russian Academy of Science, Koptyuga pr., 3, Novosibirsk, Russia

In this work we present detailed study on petrographic and geochemical features of sulfide inclusions occurring in spinel peridotite and spinel pyroxenite xenoliths from Sangilen Plateau, Tuva (South Siberia/North Mongolia). The xenoliths outcropped in Late Ordovician alkali basalts, $^{39}Ar/^{40}Ar$ ages ranging between 448-441 Ma (VOLKOVA *et al.,* 2004). The spinel peridotites are mainly protogranular, but in some cases equigranular texture types are also found (MERCIER & NICOLAS, 1975). The peridotites are olivine- and orthopyroxene-rich lherzolites and harzburgites. The pyroxenite suites are orthopyroxene-rich spinel websterites and orthopyroxenites. Their texture is mainly igneous according to their fractional crystallization related origin.

Sulfide inclusions are found in the peridotite and pyroxenite series in several textural appearances. The great majority of sulfides is interstitial (type-i), however some were found enclosed (type-e) in orthopyroxene, clinopyroxene and olivine (Fig. 1a & 1b). The shape of both type-i and type-e sulfide inclusions are rounded or irregular. Their size ranges from 100 to 150 μm (type-i), whereas type-e is generally smaller (50-100 μm) (Fig. 1a & 1b). Furthermore, small spherical blebs or inclusions along healed fractures (5-20 μm) and grain boundaries (5-10 μm) were also found, addressed as type-f sulfides.

Type-i, type-e and type-f sulfide inclusions consist of chalcopyrite, pentlandite and/or pyrrhotite/monosulfide solid solution (MSS) (Fig. 1a & 1b).

The major element chemical composition and textural appearance of sulfide inclusions suggests that type-e is clearly primary inclusions, however type-i have identical composition and texture and therefore also assumed to be primary ones. The type-f sulfides are clearly secondary inclusions. Primary inclusions were trapped during the crystallization of rock-forming minerals, whereas secondary inclusions are thought to be subsequent remnants of primary inclusions.

The main aim of this study is to compare the chemical composition and textural appearance of sulfide inclusions in order to gain more information on deep lithospheric processes beneath the studied area.

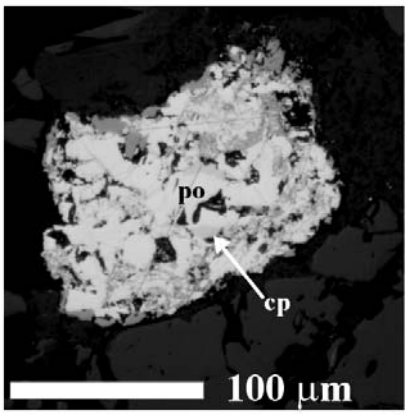

Fig.:1a: interstitial (type-i) sulfide inclusion (cp: chalcopyrite, po: pyrrhotite)

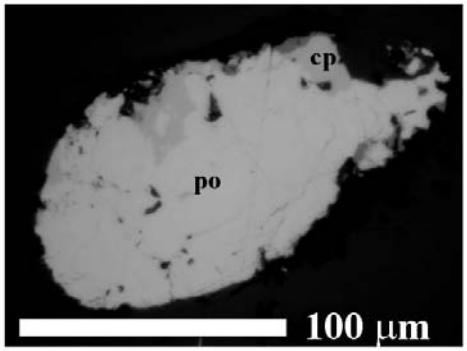

Fig.:1b: enclosed (type-e) sulfide inclusion (cp: chalcopyrite, po: pyrrhotite)

References

MERCIER, J-C. C. & NICOLAS, A. (1975): Journal of Petrology, 16: 454–487.

VOLKOVA, N., EGOROVA, V., IZOKH, A. & SHELEPAEV, R. (2004): 32nd International Geological Congress, Florence, Abstract Volume, 1154.

TWINNED PHILLIPSITE CRYSTALS IN THE BASALTS OF THE TÁTIKA GROUP, BALATON HIGHLAND, HUNGARY

KÓNYA, P.
Geological Institute of Hungary, Stefánia út 14, H-1143 Budapest, Hungary
E-mail: kope@mafi.hu

We studied twinned phillipsite crystals from cavities of young alkaline basalts of the western part of the Bakony–Balaton Highlands Volcanic Field (BBHVF), Hungary. This mineralisation is characterised by zeolites, carbonates and smectites.

Pliocene volcanic rocks are found on the northern part of the Keszthely Mts. These rocks are separated from the main volcanic zone of the Balaton Highland and form a distinctive cluster. The volcanic rocks in this area form a north-west to south-east trending zone. The immediate pre-volcanic rocks are Neogene siliciclastic siltstones, sandstones, silt and sand. Pyroclastic rocks crop out in large volumes only at the Uzsa locality, and in smaller volumes on Tátika Hill. The other localities show only basanite. The mountains are a shallow subsurface sill and dyke complex (MARTIN & NÉMETH, 2004). The ages of the lava flows are among the youngest of the Pliocene intraplate volcanic rocks in the western Pannonian Basin and range between 3,4 to 2,7 My (BALOGH *et al.*, 1986).

Phillipsite forms pseudo-orthorhombic twinned prismatic crystals, commonly elongated along the *a*-axis. Blocky, equant crystals and radiating aggregates are common. Some of the twins imitate a tetragonal prism.

Phillipsite always forms complex penetration twins. Untwinned phillipsite crystals have not been found. The complex interpenetration twinning of phillipsite was classified by LACROIX (1897) to include the Morvenite twin, Marburg twin, Perier twin and Stempel twin according to the dominant habits.

The first studies on phillipsite from Hungarian localities go back to the first decades of the 20th century. Twinned phillipsite crystals were first described by LIFFA (1914) from the Badacsony Hill at Badacsonytomaj. Later complex phillipsite twins were identified by MAURITZ (1929, 1931, 1955) and ERDÉLYI (1941) from Hermántó Hill at Zalaszántó, Uzsa quarry at Lesenceistvánd, Kovácsi Hill at Vindornyaszőlős, Prága Hill at Bazsi and Sarvaly Hill at Sümeg but they have never been classified into the groups of LACROIX.

In this work we identified by binocular microscopy some types of phillipsite twins (Marburg, Perier and Stempel twins).

References

BALOGH, K., ÁRVA-SÓS, E., PÉCSKAY, Z. & RAVASZ-BARANYAI, L. (1986): Acta Mineralogica–Petrographica (Szeged), 28: 75–94.

ERDÉLYI, J. (1941): Földtani Értesítő, 6: 60–82.

LACROIX, A. (1897): Minéralogie de la France et de ses colonies. Vol. II. Paris: Librairie polytechnique.

LIFFA, A. (1914): Földtani Közlöny, 44: 80–87.

MARTIN, U. & NÉMETH, K. (2004): Geologica Hungarica, series Geologica, 26: 133–152.

MAURITZ, B. (1929): Mathematikai és Természettudományi Értesítő, 46: 657–662.

MAURITZ, B. (1931): Neues Jahrbuch für Mineralogie, Beilage Bd. 64A: 477–494.

MAURITZ, B. (1955): Acta Mineralogica–Petrographica (Szeged), 8: 34–36.

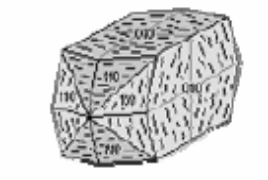

Marburg twin

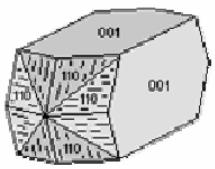

Perier twin

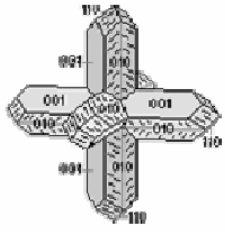

Stempel twin

NEW TYPE OF CORDIERITE ASSEMBLAGES FROM THE SLANSKÉ VRCHY MTS., EASTERN SLOVAKIA

KOŠUTH, M.
Dept. of Geology & Mineralogy, Institute of Geosciences, Faculty B.E.R.G., Technical University, Košice, Slovakia
E-mail: Marian.Kosuth@tuke.sk

Rock quarries along the Slanské Vrchy Mts. volcanic range (Eastern Slovakia) are well known for the occurrences of xenoliths/enclaves. Apart from them, new type of hornfelse-like rocks with cordierite high-alumina mineralization was found here. Although a sample supposed to be a sekaninaite-bearing xenolith had been found even earlier – first in the Vechec quarry (ĎUĎA, 1977), last years' research has brought findings of similar samples from 4 other quarries and repeatedly in Vechec. The distribution of localities suggests similar conditions in the deep levels beneath the volcanic massif, which is necessary to produce such uniform assemblages. Homogeneous black to dark-blue enclaves from all of the occurrences (Fintice, Borovník, Brestov, Vechec and Vyšná Kamenica) are very similar to each other due to their compact glassy-like to fine-grained fabric and its mineral composition, too. Mineral grains are subhedral to anhedral, poorly distinct in thin sections, so the mineral composition was first examined by XRD analyses, and then the individual minerals were investigated by EMPA. Although the cordierite diffraction pattern resembles to that of amphibole, cordierite was clearly detected as a main phase in samples from Fintice and Borovník; in enclaves from Brestov, Vechec and Kamenica plagioclase prevailed. Fine-grained polymineralic aggregates also consist of associated Fe-rich spinel / Ti-rich magnetite and/or K-feldspar, orthopyroxene (En), biotite, ilmenite, with zircon and apatite as accessories. The composition is not uniform, enclaves from Fintice and Vechec contain andalusite, too; in exceptional cases quartz (Borovník), tridymite and corundum (Vechec) were also detected.

Bulk rock composition of the enclaves ranges from 44.7 to 49.9% SiO_2 (except for a more acidic sample from Borovník: 54.7% SiO_2), Al_2O_3 ranges from 19.9 to 30.5% – in the most dry sample from Vechec. Reported samples are not hydrated – vibrational IR-spectra show only the traces of absorbed molecular H_2O. Cordierite series electron microprobe data reflect some differences among five localities: usually more magnesian (up to 9.8–10.3 wt% MgO, correspondingly to 6.1–6.7 wt% FeO, Borovník) to most ferrous sekaninaite from Fintice (5.9–6.1 wt% MgO, with 12.0–12.6 wt% FeO). Each locality represents only a slight variability with respect to Mg/Fe ratio. Average X_{Fe} calculated for separate locality are: Fintice X_{Fe}= 0.53; Borovník X_{Fe}= 0.26; Brestov X_{Fe}= 0.36; Vechec and Vyšná Kamenica X_{Fe} = 0.37. Intra-grain zoning was analyzed only in larger grains from the Vechec quarry, but decreasing Mg content from the core to rim, followed by increasing Fe was observed in all grains. Na contents of cordierite from all 5 localities range up to 0.25 wt% Na_2O, whereas K contents is higher, suggesting a metamorphic origin.

Cordierite is predominantly a product of metamorphism, but here it is found captured in andesite. It formed presumably by assimilation of argillaceous rocks. Intruded hot calc-alkaline magma can induce immediate metamorphic impact on crust metapelites (found frequently as xenoliths) or even high-alumina melt formation. We suppose that the observed cordierite enclaves may represent anatectic products of pelitic rocks around the contact aureole of the magmatic chamber. Such preposition supports the result of thin section investigation with observed plagioclase phenocrysts coming from andesite. The presence of mineral inclusions in cordierites and associated frequent Fe-rich spinel / Ti-rich magnetite could be a part of precursor assemblage of low Ti. Present concentration of ilmenite and Ti-rich magnetites in the mineral assemblage of enclaves is interpreted as the proof of long-lasting exposure of the protolith in the magma chamber level.

The equigranular fabric with minimum apparent porosity of the enclaves found in andesites has some similarities to dense cordierite ceramics, utilized as thermal shocks-resistant material. Artificial cordierite is usually produced by crystallisation at high temperature through amorphous glassy and intermediate silicate phases with spinel. The addition of boron, water and/or other catalyst fluids promotes its formation by attaining lower energy background (SUMI *et al.*, 1999). Natural enclaves described here have some similarities with artificial cordierite ceramics (SHU *et al.*, 2000). Relatively sharp bands of IR spectra, with splitting of broad bands between 500–400 cm^{-1} suggest intermediate to fully ordered low cordierite internal structure and reflect gradual cooling before uprising. The Cl contents in cordierite from Fintice (up to 0.037 wt%) and Vechec (0.045 wt%) along with minimum CO_2, could be relics of channel fluids, decreasing the temperature of melt. A part of the chlorine (with boron eventually) could be originated from the Neogene salt-bearing sediments, deposited in the Karpatian age.

This article was created with significant 1/ 0208/03 VEGA grant support.

References

GOTTESMANN, B. & FÖRSTER, H.-J. (2004): European Journal of Mineralogy, 16: 483–491.

SHU, C., MINGXIA, X. & TAN, J. (2002): Material Research Bulletin, 37: 1333–1340.

SUMI, K., KOBAYASHI, Y. & KATO, E. (1999): Journal of the American Ceramic Society, 82: 783–868.

MORDENITE IN OPHIOLITES FROM THE METALIFERI MTS., ROMANIA

KRISTÁLY, F. & SZAKÁLL, S.
Department of Mineralogy and Petrology, University of Miskolc, H-3515 Miskolc-Egyetemváros, Hungary
E-mail: askkf@gold.uni-miskolc.hu

Mordenite is a common zeolite, with sedimentary (by diagenesis in volcanic tuffs) or hydrothermal origin. Mordenite is usually found in radial aggregates of acicular or fibrous crystals. Mordenite of hydrothermal origin is a frequent member in hydrothermal mineral assemblages of ophiolites, or ocean-floor type metamorphosed rocks.

Today's known fibrous zeolites of the Metaliferi Mts. are natrolite (?) (SZAKÁLL, 2002) and mesolite (BEDELEAN, 1971; SZAKÁLL, 2002); mordenite has not been mentioned to date. The two studied occurrences of mordenite in the ophiolite type rocks of Metaliferi Mts are at Săliştioara (an abandoned basalt quarry, sample S1) and in the Bodii valley at Techereu (TB1 sample).

At Săliştioara mordenite appears as fine fibrous aggregates filling amygdales of the altered basalt, up to 5 mm in diameter. The amygdales are white to pale rose and reddish, due to the hematite inclusions that are usually associated with reddish clinoptilolite.

At Techereu mordenite appears as white, fibrous aggregates. The aggregates are nested in the calcite veins filling in the voids between heulandite crystals. In contrast with the Săliştioara occurrence, in this case the colour of mordenite does not vary, but heulandite crystals show a white to reddish colour zoning.

The presence of mordenite was confirmed by X-ray powder diffraction (Table 1).

Five chemical analyses (Table 2) were carried out with EPMA (by Giovanna Vezzalini, at the University of Modena, Italy). H_2O could not be determined due to the paucity of available material. The results are similar to those published by PASSAGLIA (1975). The analyzed samples are Ca-Na dominant, with a low content of K and light variation of exchangeable cations.

Samples of the investigated mordenite are deposited in the mineral collection of the Herman Ottó Museum (Miskolc, Hungary).

References

BEDELEAN, I. (1971): Zeoliții din Munții Apuseni. Doctoral theses, Manuscript. Babeş–Bolyai University, Cluj-Napoca.

PASSAGLIA, E. (1975): Contributions to Mineralogy and Petrology, 50, 65–70.

SZAKÁLL, S. (ed., with the contributions of UDUBAŞA, G., ĎUĎA, R., SZAKÁLL, S., KVASNYTSYA, V., KOSZOWSKA, E. & NOVÁK, M.) (2002): Minerals of the Carpathians. Prague: Granit.

Table 1: Strongest reflections of mordenite observed on the XRPD pattern of the samples.

TB1		S1		ICDD 29-1257		
d (Å)	*I* (%)	*d* (Å)	*I* (%)	*d* (Å)	*I* (%)	*hkl*
8.809	23.9	8.924	100	9.060	100	200
3.968	2.8	3.967	41	4.000	70	150
3.490	0.3	3.465	24	3.480	45	202
3.374	2.7	3.375	39	3.390	35	350
3.267	0.2	3.199	35	3.220	40	511

Table 2: Chemical composition of the samples (EPMA).

S1						
FeO	K_2O	CaO	Na_2O	SiO_2	Al_2O_3	Sum
0.45	1.17	3.77	2.74	68.52	13.09	89.81
0.20	0.93	3.78	2.69	68.72	13.50	90.05
0.30	0.58	4.05	2.59	69.16	13.35	90.21
0.57	0.67	5.02	2.17	66.93	14.22	90.55
0.42	0.59	4.20	2.42	68.40	13.42	90.56

HEAVY METALS IMPACT ON PLANTS AT MINING AND RECOVERY DUMPS OF POLYMETALLIC WASTE ORE MATERIAL IN THE SURROUNDINGS OF THE NEOVOLCANITES OF THE ŠTIAVNICKÉ VRCHY MTS. AREA

KRIŽÁNI, I., ANDRÁŠ, P. & JELEŇ, S.
Geological Institute, Slovak Academy of Sciences, Severná 5, 97401 Banská Bystrica, Slovakia
E-mail: andras@savbb.sk

The most expressive manifestations of exploitation activities in mining regions are rests of mining dumps, which represent dumping grounds of disintegrated rocks, fine-milled ores and chemical matters used during the dressing activities. Until now these dumping grounds were perceived only as *"memorials to the industry"* or as anthropogenic relief-creating elements. Surroundings of Banská Štiavnica is a very good model area in this respect. All this region was affected by mining activity even during Antiquity (maybe even during Primeval Age).

Vegetation at dumps of various age was investigated. The oldest dumps from 14th to 16th centuries, worked as meadows, are covered by grass, which consists of species resistant against heavy metals: *Alnus glutinosa*, *Acetosella vulgaris*, *Luzula campestris*, *Arrhenatherum elatius*, *Avenella flexuosa*, *Leucanthemum vulgare*, *Dianthus carthusianorum*. Roveň dump from 18th and 19th centuries is predominantly planted by trees *Pinus nigra*, *Pinus sylvestris* and more rarely by *Picea abies*. On the youngest dumps (Wolf and Michal**)** *Betula pendula*, *Alnus glutinosa*, *Salix caprea* and some other plants subsist.

The following evolutionary vegetation stages were recorded on dumps and soils influenced by heavy metal pollution: on dump areas with fine-grained substrate: *Tussilago farfara*, *Agrostis tenuis* and *Artemisia vulgaris*, *Daucus carota* and *Tanacetum vulgare*, while on places where more humus is available, we can find the next species: *Avenella flexuosa, Nardus stricta*, and mainly species from the surroundings: *Arrhenatherum elatius*, *Veronica chamaedrys*, *Phleum pratense* and *Festuca rubra*. The Fe, Mn, Cu, Zn, Pb, Cd, As and Hg contents in their dry tissues are presented in Table 1.

Percolating acid waters intensively damage and destroy the whole biotope, contaminate underground waters by Zn, Cu, Cd, Fe, Bi, Mn. The result of biological-chemical processes is the biological transformation of the original sulphides as well as of the alumosilicates. The comparison of heavy metal concentrations in *Acetosella vulgaris* from the old dumps and in *Tussilago farfara* from the youngest dumps show that the plants are contaminated by heavy metals and that the contents in *Acetosella vulgaris* are much higher than in *Tussilago farfara*. Both species are resistant to heavy metal pollution and are able adapt themselves to the strongly contaminated soils. According to BANÁSOVÁ *et al.* (1998) the plants can resist the toxic effect of heavy metals by two ways: 1) they prevent heavy metal incorporation to the tissues ("*exclusion mechanism*"), *e.g. Aldus glutinosa* or 2) they convert the metal within their cells to a less toxic form ("*tolerance mechanism*").

Reference

BANÁSOVÁ, V., DANÁKOVÁ, A. & KRIŽÁNI, I. (1998): Bulletin Slovenskej botanickej spoločnosti, 20: 166–171.

Table 1: Average contents (mg · kg^{-1}) of selected heavy metals in dry tissues of *Tussilago farfara (Tf)* and *Acetosella vulgaris (Av)*

	Tussilago farfara				*Acetosella vulgaris*	
Element	dump Roveň	dump Lintich	dump of the Michal adit	dump of the Nová shaft	dump Roveň	dumps Wolf
Fe	169.00	344.00	644.00	280.00	173.00	634.00
Mn	32.50	125.00	57.00	75.00	325.00	1 230.00
Cu	13.00	15.00	11.00	20.00	5.00	22.00
Zn	48.50	190.00	261.00	98.00	353.00	323.00
Pb	13.50	24.00	37.00	21.00	6.00	47.70
Cd	1.00	tr.	6.00	3.00	tr.	1.30
As	0.41	0.44	0.43	0.45	0.49	0.45
Hg	0.02	0.04	0.04	0.03	0.05	0.06

THE NATURAL Cu_5FeS_4–$Cu_{6.0}Fe_{0.5}S_4$–$Cu_7Fe_{0.3}S_4$–$Cu_9Fe_{0.5}Pb_{0.4}S_6$–Cu_2S SYSTEM, LUBIN COPPER DEPOSITS, POLAND

KUCHA, H. & WDOWIN, M.
Faculty of Geology, Geophisics and Environmental Protection, AGH University of Science and Technology, Al. Mickiewicza 30, Krakow, Poland
E-mail: wdowin@uci.agh.edu.pl

Sulphide-calcite veins cutting black shale in Kupferschiefer deposits, Poland, contain Cu-Fe-Pb-S minerals showing unusual stoichiometry:

1) $Cu_9Pb_{0.5}Fe_{0.4}S_6$ forms isometric crystals intergrown with chalcocite, bornite, galena, "half" bornite, digenite and sphalerite. In reflected light $Cu_9Pb_{0.5}Fe_{0.4}S_6$ shows optical similarity to betekhtinite $Cu_{10}Fe_{0.6}Pb_{0.3}S_6$ (SCHÜLLER & WOHLMANN, 1955). The mineral contains (wt%, average of 8 microprobe measurements): S 21.36, Fe 2.40, Cu 62.87 and Pb 12.59. The Pb content is twice as high as that of betekhtinite. The mineral is pale cream, has weak bireflectance in air visible only at crystal boundaries changing from white-cream to pale cream, its reflectance at 550 nm is 30.40% in air, 15.75% in oil, so it is 2% lower than that of betekhtinite.
Preliminary interpretation of XRD and electron diffraction data suggests that the mineral is either monoclinic $a_0 = 7.30$, $b_0 = 8.70$, $c_0 = 7.86$ and $\beta = 97°$ or triclinic $a_0 = 7.50$, $b_0 = 9.05$, $c_0 = 8.06$, $\alpha = 88°$, $\beta = 97°$, $\gamma = 89°$. The mineral discussed differs from betekhtinite by:

a) twice higher Pb content and consequently by its chemical formula,
b) isometric crystal habit,
c) XRD pattern and single crystal electron diffraction patterns.

2) "Half" bornite $Cu_6Fe_{0.5}S_4$ occurs in the same mineral assemblage as $Cu_9Pb_{0.5}Fe_{0.4}S_6$. It occurs as intermediate mineral between chalcocite and bornite or chalcocite and $Cu_9Pb_{0.5}Fe_{0.4}S_6$. Preliminary electron diffraction patterns suggest domain structure for "half" bornite. Basic diffraction spots are split into 3 or 6 nodes suggesting the existence of 3 similar unit cells with left and right twisted symmetry. The angle of twist is ±3°. Reflectivity of "half" bornite at 550 nm is 19.43% in air and 9.81% in oil, so it is darker than accompanying bornite, digenite and chalcocite. Reflectivity curve of "half" bornite is very different from that of bornite and is more similar to that of digenite.

3) "Quarter" bornite $Cu_7Fe_{0.3}S_4$ occurs as inclusions in chalcocite. Its reflectivity at 550 nm is 24.78% in air and 11.30% in oil, so it is distinctly lighter than bornite and digenite but darker than chalcocite. The dispersion reflectivity curve of "quarter" bornite is similar to that of chalcocite.

Electron diffraction patterns of the mineral are indexable according to the chalcocite cell although all basic diffraction spots are split into extra two modes accompanying basic chalcocite diffraction spots.

References

ANTHONY, J., BIDEAUX, R., BLADH, K. & NICHOLS, M. (1990): Handbook of Mineralogy. Vol. 1. Elements, Sulfides, Sulfosalts. Mineral Data Publishing Inc., Tucson.

SCHÜLLER, A. & WOHLMANN, E. (1955): Geologie, 4: 535–555.

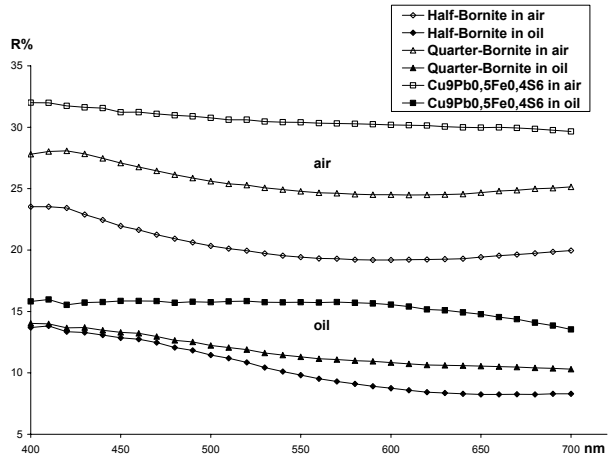

Fig. 1: Reflectivity curves of the minerals studied in air and oil.

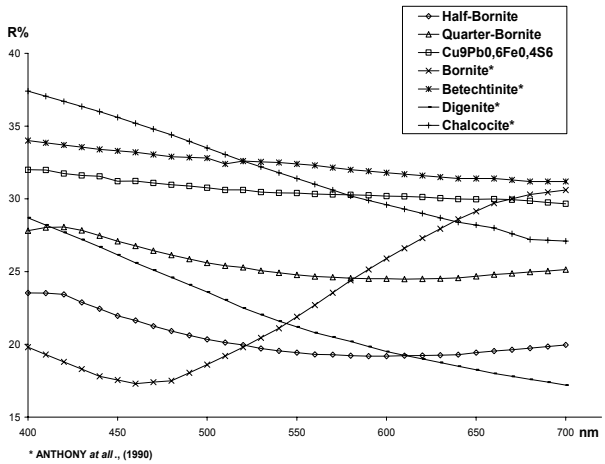

Fig. 2: Reflectivity curves of the minerals studied in air compared to bornite, betekhtinite, digenite and chalcocite standards.

NATIVE COPPER OF THE UKRAINIAN CARPATHIANS AND ADJACENT AREAS

KVASNYTSYA, I.
Geological Faculty of Taras Shevchenko Kyiv National University, Vasyl'kivs'ka Street 90, 03022 Kyiv, Ukraine
E-mail: irenek@bigmir.net

Native copper is a rare mineral of the Ukrainian Carpathians and a widespread mineral of their adjacent areas, especially in the Volyn' region (LAZARENKO *et al*., 1960; LAZARENKO *et al*., 1962; LAZARENKO *et al*., 1963; KHRUSHCHOV *et al*., 1977; SHCHERBAK *(ed.)*, 1990). In the Ukrainian Carpathians copper is known as mineral of oxidation zones in some ore deposits and occurrences as well as in Cu-bearing sandstones and also in the alluvium of Carpathian rivers. In the Volyn' region copper occurs in many localities of Cu-bearing basalts, tuffs, volcanic breccia, and sandstones. Short description of native copper from these occurrences is given in Table 1.

References

LAZARENKO, E.K., GABINET, M.P. & SLIVKO, E.P. (1962): Mineralogy of sedimentary formations of the Precarpathians. L'viv: L'viv State University, 482 p. (in Ukrainian).

LAZARENKO, E.K., LAZARENKO, E.A., BARYSHNIKOV, E.K. & MALYGINA, O.A. (1963): Mineralogy of the Trans-Carpathians. L'vov: L'vov State University: 614 p. (in Russian).

LAZARENKO, E.K., MATKOVSKY, O.I., VINAR, O.N., SHASHKINA, V.P. & GNATIV G.M. (1960): Mineralogy of igneous complexes of the Western Volynia. L'viv: L'viv State University, 509 p. (in Ukrainian).

KHRUSHCHOV, D.P., NECHAEV, YU.A., KARDASH, V.T. AND GALIY, S.A. (1977): Copper ores of strata bound type in deposits paragenetically connected with evaporites of the Ukraine, Kiev: IGPHM, 47 p. (in Russian).

SHCHERBAK, N.P. (ed.) (1990): Minerals of the Ukrainian Carpathians. Native elements, tellurides and sulphides, Kiev: Naukova dumka, 150 p. (in Russian).

Table 1: Characteristics of native copper of the Ukrainian Carpathians and adjacent areas.

Region, area, district	Rocks, ores, their ages	Mineral associations	Distribution, form and size of copper	Composition of copper
Trans-Carpathians: Beregove poly-metallic deposit	Zone of oxidation of sulphide ores in Neogene rhyolite tuffs	Sphalerite, galena, cerussite	Rare mineral. Very tine and thin films on sphalerite crystals	99.1–99.3% Cu, traces of Ag and Sb
Ukrainian Carpathians: Marmarosh crystalline massif, the Rakhiv district	Pyritiferous-polymetallic ores in Riphean-Paleozoic metamorphic rocks of Bily Potik and Dilovets' suites	Sphalerite, galena, pyrite, chalcopyrite, pyrrhotine, quartz, calcite	Rare mineral. Small isometric grains, sometimes up to 2–3 mm.	99.0% Cu, traces of Fe, Ag, Sb and V
Ukrainian Carpathians: Marmarosh crystalline massif, the basin of Bily Cheremosh and Chorny Cheremosh rivers	Modern alluvial sediments	Cuprite, chalcocite, hematite, sphalerite, galena, cinnabar, malachite	Rare mineral. Small table like grains, sometimes up to 5–7 mm	99.0% Cu, traces of Fe and Ag
Precarpathians: the basin of Bystrytsya Nadvirna and Prut rivers (Nadvirna and Delyatyn district)	Neogene cupriferous sandstones and clays of Nyzhny Stebnyk suite	Pyrite, chalcocite, cuprite, covellite, tenorite, chalcopyrite, malachite, azurite, hydroxides of iron	Rare mineral. Very small films and table like grains, 0.01–0.1 mm in size	98.9–99.3% Cu, traces of Fe and Ag
Northern-western part of the Volyn'–Podillya plate: Volyn' region	Vendian volcanic and volcano-sedimentary rocks (basalts, their lava and tuff breccias, tuffs, quartz veins, sandstones)	Quartz, chalcedony, calcite, chlorite, analcime, zeolites, chalcocite, cuprite, chalcopyrite, native Ag, native Fe, malachite, azurite	Widespread mineral. Xenomorphic grains, hypidiomorphic and idiomorphic crystals, from 0.1 to 140 mm in size	99.5% Cu, up to 1.04% Fe, up to 0.37% Ag, traces of Au

NATIVE GOLD OF THE UKRAINIAN CARPATHIANS

KVASNYTSYA, V.
Institute of Geochemistry, Mineralogy and Ore Formation of NAS Ukraine, Palladin av. 34, 03680 Kyiv-142, Ukraine
E-mail: vmkvas@i.com.ua

Native gold is a widespread mineral on the territory of the Ukrainian Carpathians. Many gold localities are known in various structural-facial zones of the Carpathian Folds and Transcarpathian inner and the Precarpathian outer depressions (Table 1). In the Transcarpathians gold is related to Neogene volcanites while in the Carpathians to Proterozoic–Paleozoic metamorphosed rocks. Placer gold has been also found in Quaternary sediments (in alluvium of Bily Cheremosh, Chorny Cheremosh, Turya Remeta and Lyuchka rivers) of the following areas: Chyvchyny, Verkhovyna, Perechyn and Yabluniv.

In Ukrainian Carpathians, like in the other regions of the world, with the transition of late deep-seated and medium-deep-seated mineralizations to younger shallower ones, gold's fineness became lower, its heterogeneity higher; the composition and concentration of its admixtures changes; the proportion of idiomorphic crystals increases and their morphology becomes more complex; equidimensional crystals are replaced by modified ones; the role of dendrites and complex twin crystals increase. Minerals of gold also vary between electrum, Au-rich silver ("küstelite"), Hg- and Cu-rich gold.

Table. 1: The characteristic features of native gold of the Ukrainian Carpathians

Area	Deposit, occurrence, structural-geological setting	Mineral association	Size of grains, mm	Morphology	Limits of fineness (frequent values)	Minor impurities, 0.0*n*–0.*n* %
Beregove	*Muzhieve deposit:* Quartz-sulphide veins and stockworks in Neogene acidic volcano-sedimentary rocks	Quartz, galena, sphalerite, pyrite, alunite, barite, adularia, chalcopyrite, arsenopyrite, tetrahedrite, hematite	0.1–1.0, rarely up to 10	Dendrites, polyhedrons, xenomorphic and hypidiomorphic grains	500–880 (600, 650, 720, 760)	Fe, Cu, Zn, Pb, As, Sb, Te, Hg
Rakhiv	*Saulyak deposit*: Quartz and quartz-carbonate veins and veined-patched bodies in metamorphosed quartz-carbonate and quartz-mica-chlorite rocks	Quartz, pyrite, pyrrhotite, chalcopyrite, galena, sphalerite, hessite, altaite, carbonates	0.1–0.5, rarely up to 3	Xenomorphic and hypidiomorphic grains, rarely polyhedrons	750–930 (830, 860, 910)	Fe, Pb, As, Hg
	Bily Potik occurrence: Quartz veins and veined-patched bodies in slaty quartzites	Quartz, pyrite, arsenopyrite, hematite, goethite, lepidocrocite	0.1–0.5, up to 3	Xenomorphic and hypidiomorphic grains, rarely polyhedrons	780–950 (880, 890, 900, 910)	Fe, Cu, Pb, As, Sb, Hg
Chyvchyny	*Marmarosh zone:* Cretaceous conglomerates	Quartz, pyrite	0.1–0.8, up to 3	Xenomorphic and hypidiomorphic grains, slightly rounded	840–995 (930, 950)	Pb, Sb, Hg
Nyzhni Vorota	Paleogene flysch	Quartz, pyrite	0.1–0.5, up to 1	Xenomorphic and hypidiomorphic grains, slightly rounded	790–960 (910)	Cu, Pb, As
Yabluniv	Miocene conglomerates	Quartz	0.1–0.5, up to 2.5	Xenomorphic and hypidiomorphic grains, slightly rounded	920–980	Cu, Pb

MINERALOGICAL AND GEOCHEMICAL STUDY OF MINE TAILINGS MATERIAL FROM THE ANTIMONY DEPOSIT PEZINOK – KOLÁRSKY VRCH (SLOVAKIA)

LALINSKÁ, B.[1], CHOVAN, M.[1] & MILOVSKÁ, S.[2]
[1] Department of Mineralogy and Petrology, Comenius University, Mlynská dolina G, 842 15 Bratislava, Slovakia
E-mail: lalinska@fns.uniba.sk
[2] Slovak Academy of Sciences, Banská Bystrica, Slovakia

Weathering and dissolution processes in the environment of mine tailings mobilize toxic elements such as arsenic and antimony, which represent dangerous contaminants for the ground and surface water around. Therefore we are trying to make a complex study about the tailings material, its mineralogy, stadium of weathering, water quality etc.

The aim of this work was to study the chemical composition of ochres and alteration rims of ore minerals from the oxidation zone, and we also made a few batch tests using contaminated water from the impoundment and Fe^0 as a reactive medium for arsenic and antimony removal.

Concentrations of Fe, As, Sb, Ca, Mg, $(SO)_4^{2-}$ and Zn in ochres were determined in solution after leaching in 5M HCl by AAS method. Content of $(SO)_4^{2-}$ was relatively low, in the most of the samples did not reach the detection limit. Four samples showed values in interval of 7.43–258.25 mg/kg. Concentration of arsenic was relatively high 0.81–51.39 g/kg, as well as antimony 0.33–53.97 g/kg. Fe content varied from 154.95 g/kg to 763.16 g/kg.

Ore minerals from tailings were studied in polarized light and by electron microprobe. The most abundant ore minerals are arsenopyrite and pyrite. Both minerals are characteristic by alteration rims in oxidation zone, average content of As_2O_5 in the rims of arsenopyrite is 25.92 wt%, Sb_2O_5 7.73 wt%. The content of this oxides are lower in the pyrite alteration rims, 2.13 wt% in case of As_2O_5 and 6.17 wt% in case of Sb_2O_5. Berthierit is rare, but the average contents of As_2O_5 (10.5 wt%) and Sb_2O_5 (27.54 wt%) in the alteration rims are high. There is nearly no stibnite in the oxidation zone of tailings, so we assume that the most of stibnite grains have already been oxidized– the content of Sb_2O_5 in Sb oxides varies from 21 wt% to nearly 100 wt%.

Recently we have done 2 pilot experiments using Fe for As and Sb removal from contaminated water. The water was collected from the drills in both tailings. We have used laboratory Fe (content of Fe 99.98 %, Lambda) and also some steel manufacturing by-products. Both procedures were successful in As and Sb removal. The best results were reached by using of laboratory iron (Fig. 1–4).

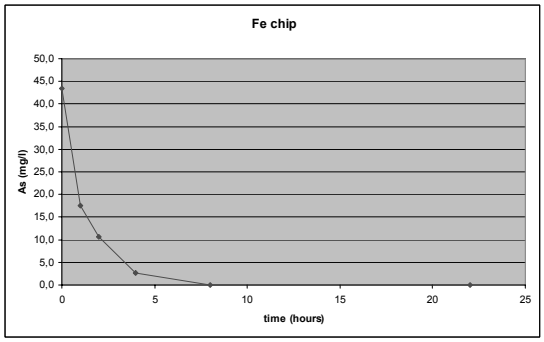

Fig. 1: Kinetic of As removal by Fe chip (Lambda).

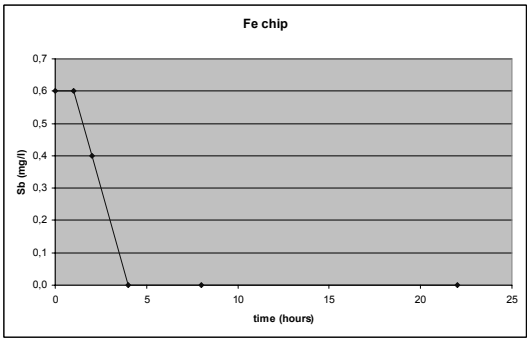

Fig. 2: Kinetic of Sb removal by Fe chip (Lambda).

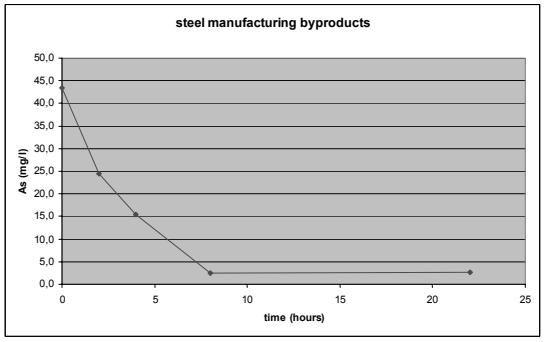

Fig. 3: Kinetic of As removal using Fe by-products.

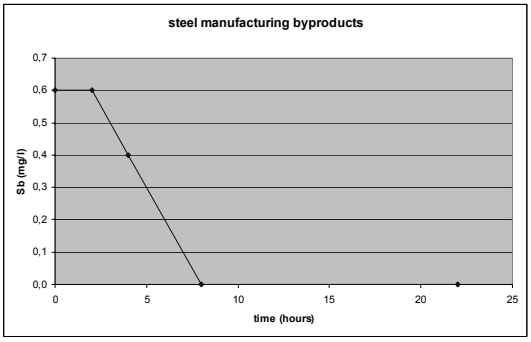

Fig. 4: Kinetic of Sb removal using Fe by-products.

INFLUENCE OF MINERAL COMPONENTS ON GEOCHEMISTRY OF HEAVY METALS IN SEDIMENTS OF THE WILGA RIVER

ŁOJAN, E. & KUCHA, H.
Faculty of Geology, Geophysics and Environmental Protection, AGH-University of Science and Technology, Al. Mickiewicza 30, Krakow, Poland
E-mail: lojan@agh.edu.pl

The Wilga River is a tributary of the Vistula River. It flows into the Vistula River as the largest and the most polluted tributary in the Krakow area. Investigations of bottom sediments of the Wilga River were made on samples collected at the last of 1.5-km section of the river between the Rydlówka Street and the Vistula River.

The collected samples were divided into light (clays, quartz) and heavy fractions (iron oxide, oxysulphides, authigenic sulphides). Chemical analyses of samples were made with atomic absorption spectrometry (AAS) for Cr, Ni, Cu, Zn, Cd, Pb. Heavy fraction is enriched in (ppm): Zn 210–26839, Cu 95–13858, Pb 225–17939 & Cd 3–310. From the other hand the concentration of Cr and Ni is much higher in the light fraction (Cr up to 43, Ni up to 20 mg/kg).

Investigations with a field emission scanning electron microscope (FEMES) showed the presence of clay minerals intercalated with hydrated iron oxides and oxysulphides (Figs. 1, 2). The presence of covellite, chalcopyrite and pyrite in the heavy fraction was also confirmed.

Results obtained show, that the mineral composition of the investigated fluvial sediments is the basic factor controlling the distribution of heavy elements in fluvial bottom sediments in the Wilga River. The main heavy metal sorbents are hydrated iron oxides, iron oxysulphides and less clay minerals.

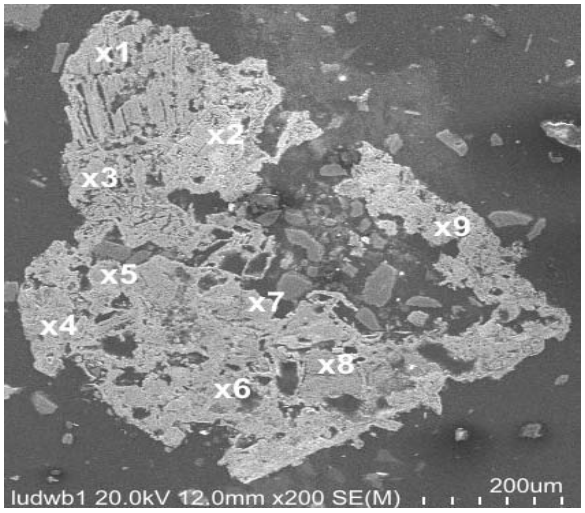

Fig. 1: SEM picture of syntaxial intergrowths of clay minerals (illite) with covellite and hydrated Fe oxides (1 & 3: pseudomorph of goethite after Cu-sulphide?, 2: goethite, 4 & 5: Fe oxysulphide with Pb, 6: Fe oxysulphide with Cu, 7 & 8: goethite, 9: Fe-oxysulphide with Pb).

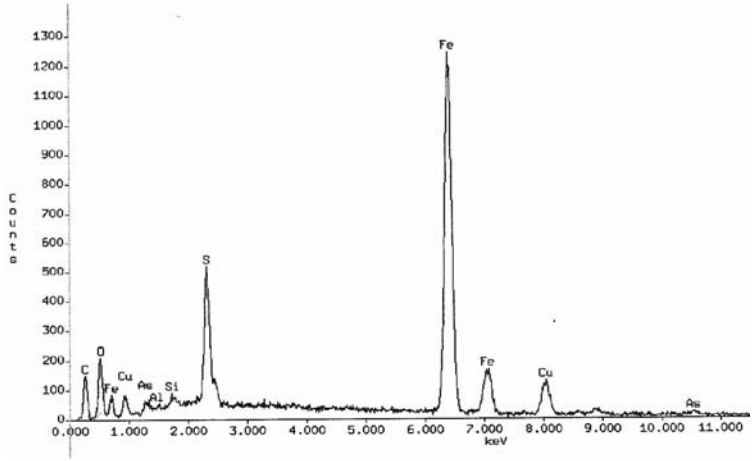

Fig. 2: Emission spectrum of Fe oxysulphide showing significant amounts of Cu and O, and important admixture of As.

TEPHROSTRATIGRAPHY IN THE CARPATHIAN–PANNONIAN BASIN: MINERAL CHEMICAL CONSTRAINTS

LUKÁCS, R.
Department of Petrology and Geochemistry, Eötvös Loránd University, Pázmány P. sétány 1/C, H-1117 Budapest, Hungary
E-mail: reka.lukacs@geology.elte.hu

Neogene volcanism in the Carpathian–Pannonian Region started with repeated explosive eruptions of silicic magmas. Volcanic products cover large areas, although presently most of them are overlain by Late Miocene to Quaternary sediments. This volcanism occurred during a long time interval, from 21 Ma to 13.5 Ma, and therefore these pyroclastic deposits have great stratigraphic importance. The Bükkalja Volcanic Field provides a good study area for tephrostratigraphy, because several units of the silicic volcanism can be found here on the surface. Our study showed that the geochemical data are the most effective correlation criteria to distinguish the main volcanic units, particularly the major and trace element data of the main mineral phases and the glass shards (HARANGI *et al*., 2005). Then, we can extend our results to other areas, such as drilling cores to correlate the scattered occurrences of the ignimbrite units and define marker horizons for the Neogene stratigraphy.

Based on the results obtained from the Bükkalja study, we attempt to correlate and distinguish pyroclastic units in three boreholes drilled in 1986 east of the Bükk Mts. (Miskolc-7, Miskolc-8 and Nyékládháza-1). These three boreholes contain continues drilling core sequence and therefore have great significance. Some of the pyroclastic units are divided by sedimentary formations, but they consist also of thick volcanic suite with fairly similar physical volcanological features. We sampled all the macroscopically defined units and then determined the mineralogical content and the chemical composition of the phenocrysts. In addition, 4 samples had been analysed by K/Ar radiometric method. Although these radiometric age data gave overlapping result, they fit in the age period of the pyroclastic rocks of the Bükkalja area. In contrast to the geochronological method, we could successfully use the geochemical data to distinguish different volcanic units. The most significant discriminating tools are the Mg, Ti, Al and Fe contents of biotites and anorthite contents of plagioclases. In addition, slight differences can also be observed in the major element composition of glass shards. These data enabled to distinguish at least three major volcanic units, which can be partly correlated with the pyroclastic units cropping out in the Bükkalja Volcanic Field. These results have significance in the further tephrostratigraphic studies in the Carpathian–Pannonian Region.

Reference

HARANGI, SZ., MASON, P.R.D. & LUKÁCS, R. (2005): Journal of Volcanology and Geothermal Research, 143: 237–257.

MINERALOGICAL STUDY OF HYDROTHERMAL VEIN Pb-Zn DEPOSIT POD BABOU (MALÉ KARPATY MTS., SLOVAKIA)

LUPTÁKOVÁ, J.[1], CHOVAN, M.[2] & ANDRÁŠ, P.[1]
[1] Geological Institute, Slovak Academy of Sciences, Severná 5, SK-974 01 Banská Bystrica, Slovakia
E-mail: luptak@savbb.sk
[2] Department of Mineralogy and Petrology, Faculty of Natural Sciences, Comenius University, Mlynská dolina G, SK-842 15 Bratislava, Slovakia

The deposit Pod Babou is situated 2.5 km SE of Pernek in the Malé Karpaty Mts. Hydrothermal ore veins are hosted by metamorphic rocks – gneisses, less phyllites of Palaeozoic age, that belong to Limbach formation (PUTIŠ *et al.*, 2004) and make up the envelope of the Bratislava granitoid massif.

Deposit comprises two main veins – the upper and the lower one, which were exploited at the end of 19th century (CAMBEL, 1959). Nowadays adits are inaccessible and only dump material is available. This small-scale deposit is interesting only from mineralogical and metallogenetical point of view and has no economic importance.

Mineralization originated during four mineralizing events. The first, **quartz-arsenopyrite (Q-Asp) stage** consists of black quartz, arsenopyrite and pyrite. Arsenopyrite has increased Sb (up to 1.6 wt%) and rarely also Bi (up to 0.5 wt%) contents. Arsenopyrite grains show zonality under the BSE caused by variable contents of As a S. Contents of As in pyrite vary between 0.1 and 0.9 wt%. Minerals of the first stage are cataclased and enclosed in minerals of younger **Pb-Zn stage**. The most abundant ore mineral of this stage is sphalerite. It is also the oldest mineral of this stage, together with quartz and pyrite. Sphalerite is brown coloured, with Fe and Cd contents of 3.4 wt% and 0.2 wt%, respectively. Later minerals of Pb-Zn stage fill the space between grains of sphalerite and quartz. This association is comprised of galena, boulangerite, bournonite, tetrahedrite, stephanite, chalcopyrite, marcasite and also pyrite, sphalerite and quartz. The most abundant features observed under reflected polarized light are intergrowths of galena with tetrahedrite, bournonite, and sphalerite or with boulangerite and bournonite. Other minerals are quite scarce. Tetrahedrite is rich in Ag. Its composition gradually proceeds from argentian tetrahedrite (9.6 wt% Ag) to freibergite (30.7 wt% Ag). It is also enriched in Fe (up to 5.7 wt%). Another Ag mineral is stephanite, which is present only in small amount. However, Ag contents in galena associating with Ag-bearing minerals do not exceed 0.04 wt%. Contents of microelements in boulangerite and bournonite are only about 0.0*X* wt% except for Bi content, which reaches 0.3 wt%.

Q-Asp and Pb-Zn stages are common for both main veins. The latest stage is different. In the case of lower vein it is the carbonate stage, and in the case of upper vein it is the barite stage. There is no evidence about the relative age of these two stages. No relationship was observed during the fieldwork.

Carbonate stage is comprised of little amount of quartz, older fine-grained dolomite occurring in the vein boundaries and younger coarse-grained calcite filling vein centre.

Barite stage consists of white fine-grained barite that encloses fragments of older mineral associations. Content of SrO in barite varies from 0.1 to 1.6 wt%. Content of other elements is negligible.

This study provides new compositional data on Pod Babou Pb-Zn deposit. Moreover, previously unreported mineral species – boulangerite, tetrahedrite–freibergite, stephanite and dolomite – are described.

Acknowledgments

This work was supported by Slovak Scientific Agency VEGA grant Nr: 1/1027/04.

References

CAMBEL, B. (1959): Acta Geologica et Geographica Universitatis Comenianae, 3: 338.

PUTIŠ, M., HRDLIČKA, M. & UHER, P. (2004): Mineralia Slovaca, 36: 183–194.

CROSS-CHECKING OF AERIAL IMAGES AND RESULTS OF LOCAL SAMPLING OF GYÖNGYÖSOROSZI FLOTATION TAILING IMPOUNDMENT, NORTH-EASTERN HUNGARY

MÁDAI, V.
Department of Mineralogy and Petrology, University of Miskolc, H-3515 Miskolc-Egyetemváros, Hungary
E-mail: askcesar@gold.uni-miskolc.hu

Pyrite-containing ore mining wastes may seriously damage their surrounding environment. The phenomenon is the so-called Acid Rock Drainage (ARD) or Acid Mine Drainage (AMD). Oxidation of iron sulphides produces low pH-solutions and Fe(III) ions. The process is extremely complex, and heavily influenced by vital functions of sulphide oxidizing bacteria. Products of the oxidation among others are gypsum, jarosite, goethite, hematite, and lepidocrocite. Using hyperspectral or multispectral remote sensing methods, anomalies of these secondary mineral phases can be plotted (VIJDEA *et al.*, 2004).

In this study hyperspectral aerial photography of the flotation tailing impoundment (KARDEVÁN *et al.*, 2003) and results of local sampling were cross-checked. In the aerial picture, goethite and jarosite anomalies could be seen. In my local sampling programme nearly 100 samples were gathered from the surface of the tailing impoundment covering the whole area. Samples were analyzed by an HZG-3 powder diffractometer and a MOM Derivatograph C equipment.

The thickness of the vegetation, the roughness of the surface and the presence of mineral component enrichments may influence the quality of the reflected beam, which determines the detectable mineral phases in the aerial picture.

Samples, collected from any part of the tailing impoundment, were rich in jarosite. Nevertheless, on the aerial photography, jarosite anomaly on the surface of the older and heavily oxidized parts of the tailing impoundment covered by richer vegetation cannot be seen. The samples, collected from these areas, were rich in jarosite as well, but other mineral component enrichment could not be detected which should cover the reflected beam component of the jarosite in the near infra red and visible range of the spectrum. Surface roughness was the same all over the impoundment. The differences between the results of the two methods might be explained by the high sensitivity of the hyperspectral method to the thickness of the vegetation.

It might be concluded, that the results obtained by the two methods are comparable only on the non-vegetated areas. Data of remote sensing give valuable information about the mineral phases, but detailed and accurate sampling on the spot is indispensable.

References

KARDEVÁN, P., VEKERDY, Z., RÓTH, L. SOMMER, S., KEMPER, TH., JORDÁN, GY., TAMÁS J., PECHMANN, I., KOVÁCS, E., HARGITAI, H., LÁSZLÓ, F. (2003): In: HABERMEYER, M., MÜLLE, A., & HOLZWARTH, S. (eds.): Proceedings of the 3rd EARSeL workshop on imaging spectroscopy, Herrsching, Germany, 13–16 May 2003, 324–332.

VIJDEA, A., SOMMER, S. & MEHL, W. (2004): PECOMINES, Inventory, Regulations and Environmental Impact of Toxic Mining Wastes in Pre-Accession Countries, A Report of the JRC Enlargement Project. 4–32.

THE STRUCTURE AND AGEING OF As-RICH FERRIHYDRITE FROM PEZINOK, SLOVAKIA

MAJZLAN, J.[1], CHOVAN, M.[2], LALINSKÁ, B.[2], MILOVSKÁ, S.[3] & JURKOVIČ, Ľ.[4]
[1] Institute of Mineralogy and Geochemistry, Albert-Ludwig University, Albertstraße 23b, 79104 Freiburg, Germany
E-mail: Juraj.Majzlan@minpet.uni-freiburg.de
[2] Department of Mineralogy and Petrology, Comenius University, Mlynská dolina G, 842 15 Bratislava, Slovakia
[3] Geological Institute, Slovak Academy of Sciences, Banská Bystrica, Slovakia
[4] Department of Geochemistry, Comenius University, Mlynská dolina G, 842 15 Bratislava, Slovakia

Arsenic is permanently attracting significant attention from the viewpoint of its negative influence on the human health, transport through the trophic chain, and consequently its biogeochemical cycle. It has been classified as one of the priority pollutants, contested in its toxicity only by few other elements. In this work, we have been investigating the formation process, the structure, and ageing of As-rich ferrihydrite from the Pezinok deposit. At this site, As-ferrihydrite serves as a transport medium for As contamination.

The abandoned Sb deposit Pezinok lies in the in Malé Karpaty Mts in western Slovakia. The deposit is located in carbonaceous and actinolite schists and amphibolites and contained abundant stibnite and smaller amounts of other Sb minerals. In addition to the Sb minerals, pyrite and arsenopyrite were also common. The mineralization occurred as quartz-carbonate lenses, veinlets, nests, and impregnations in the host rocks. The ores were milled and Sb minerals were collected by flotation. The waste was then deposited in two large tailing impoundments.

The fine-grained waste is currently slowly weathering and releasing the toxic elements into the surrounding soils and streams. The principal weathering product is As-rich ferrihydrite, a mineral almost amorphous to X-rays. Because of the lack of long-range order, techniques other than X-ray diffraction (XRD) had to be used to describe this mineral.

Using X-ray absorption near-edge structure (XANES) spectroscopy, we have determined that all probed elements (Fe, As, S) are present in their highest oxidation states. Thus, the material escaping from the impoundments is already fully oxidized, and no further changes in its oxidation state should be expected.

Extended X-ray absorption fine-structure (EXAFS) spectroscopy gave valuable evidence about the structure of As-ferrihydrite. EXAFS spectra at the Fe K edge have shown that the particles in the studied material are extremely depolymerized. The octahedra $Fe(O,OH,OH_2)_6$ are connected almost exclusively by edges, forming short polyhedral chains. EXAFS spectra at the As K edge indicate that the AsO_4 tetrahedra are attached to the iron oxide particles in a binuclear-bidentate fashion. Our results agree well with previous conclusions of WAYCHUNAS *et al*. (1993), obtained on a chemically similar synthetic material.

Selected samples were kept at 60 ºC in a wet state for a period of almost 4 months and the changes in the samples were monitored by XRD, leaching and chemical analysis of the leachates, and EXAFS spectroscopy. Essentially no changes were observed in the XRD patterns. On the other hand, leaching the samples with 0.5 M $NaHCO_3$ solution showed that the amount of extractable Fe decreased and the amount of extractable As increased as a function of ageing time. Therefore, the samples are indeed changing, but these changes cannot be detected by XRD. Fe EXAFS spectra have documented clearly an increase in the number of Fe neighbours in the second coordination shell. In other words, the small particles polymerize during ageing and probably evolve toward a goethite-like structure. The polymerization and recrystallization of the Fe oxide particles is accompanied by the release of As.

The results presented here have important consequences for the remediation effort at this and other sites. As-ferrihydrite is an excellent medium for capturing As, but an unfavourable choice for the long-term storage of this toxic element. When As-ferrihydrite ages, it releases the arsenic back into the solution. Thus, care must be taken when the As-ferrihydrite is disposed.

Reference

WAYCHUNAS, G.A., REA, B.A., FULLER, C.C. & DAVIS, J.A. (1993): Geochimica et Cosmochimica Acta, 57: 2251–2269.

MINERALOGICAL DATA ON THE BAT GUANO DEPOSIT FROM POLOVRAGI CAVE (CĂPĂȚÂNII MOUNTAINS, ROMANIA)

MARINCEA, Ş.[1], DUMITRAŞ, D.-G.[1], DIACONU, G.[2] & BILAL, E.[3]
[1] Geological Institute of Romania, Bucharest, Romania
E-mail: marincea@igr.ro
[2] "Emil Racoviță" Institute of Speleology, Bucharest, Romania
[3] École Nationale Supérieure des Mines, Saint Etienne, France

Recent investigations in one of the most famous caves from the South Carpathians (Romania), namely the Polovragi Cave in Căpățânii Mountains, prompted to the identification of a quite representative fossil bat guano deposit, whose mineralogy was so far ignored. The cave is located on the left slope of Olteț Valley, at about 2 km upstream from the Polovragi Monastery and 200 m upstream from the end of the Olteț Gorges. The cave, which is one of the longest in Romania (having more than 9 km in length), is developed in massive limestones of Upper Jurassic – Neocomian age. The cave is typically dry, the mean temperature being of about 8°C, with small variations over the seasons. This favors the presence of an active bat colony, located mainly in the initial portion of the cave and particularly in the so-called "Bat Gallery". Patches of slightly indurate guano cover the floor of this gallery. The present study aims to give some preliminary mineralogical data on the main mineral species in the deposit, issued from their examination by scanning electron microscopy (SEM), inductively-coupled plasma - atomic emission spectrometry (ICP-AES) and X-ray powder diffraction (XRD).

Restricted to the guano patches, the mineral association includes hydroxylapatite, brushite, taranakite, low quartz, illite (the $2M_1$ polytype), amorphous iron sesquioxides and calcite. The unit-cell parameters of selected specimens of these mineral species, refined by least-squares from X-ray powder data (Cu K_α, λ = 1.54056 Å) are given in the following Table:

Mineral	System, S.G.	Sample	*a* (Å)	*b* (Å)	*c* (Å)	$\beta^{(\circ)}$	*n*	*N*
hydroxylapatite	*H*, $P6_3/m$	PP 3 B	9.426(3)	-	6.879(3)	-	4	38
hydroxylapatite	*H*, $P6_3/m$	PP 4 A	9.405(3)	-	6.867(3)	-	10	41
brushite	*M*, *Ia*	PP 1 A	5.797(2)	15.163(7)	6.228(3)	116.28(2)	7	70
taranakite	*R*, $R\bar{3}c$	PP 1 A	8.690(3)	-	94.90(5)	-	3	88
quartz	*R*, $P3_121$	PP 2 B	4.909(1)	-	5.398(2)	-	4	20
illite $2M1$	*M*, *C*2/*c*	PP 1 B	5.215(8)	8.974(6)	19.98(2)	94.27(9)	6	20
calcite	*R*, $R\bar{3}c$	PP 4 A	4.9843(9)	-	17.037(6)	-	4	26

S.G.: space group; *n*: number of refining cycles; *N*: number of reflections used for refinement in the 2θ range 16–88° for hydroxylapatite, 5–90° for brushite, 5–66° for taranakite and 10–90° for quartz and calcite.

Hydroxylapatite occurs in the lower part of the guano pile, at the direct contact with the carbonate floor. The mineral forms white-yellow or orange crusts composed by fine platy crystals of up to 20-µm diameter and 1 µm in thickness, randomly disposed or forming post-colloidal, rosette-like aggregates. The mineral has typically a reduced crystallinity: the indices of crystallinity, calculated using the method proposed by SIMPSON (1964) are, for the two samples in the Table, 0.211 and 0.167, respectively. A ICP-AES analysis of a carefully handpicked separate, recalculated at 100 % after deduction of water in order to assess the charge balance, gave (in wt%): K_2O = 0.04, Na_2O = 0.02, CaO = 54.96, MnO = 0.08, MgO = 0.05, FeO = 0.41, P_2O_5 = 42.28, SO_3 = 0.23, H_2O = 1.93. This composition, normalized on the basis of 6 (P + S) and 26 (O,OH) per formula unit (*pfu*), leads to the chemical-structural formula: $[K_{0.009}Na_{0.006}Ca_{9.824}Mn_{0.011}Mg_{0.012}Fe^{2+}_{0.057}](P_{5.971}S_{0.029})O_{23.852}(OH)_{2.148}$.

Brushite forms millimeter-sized snow white coatings on hydroxylapatite or small (up to 5 mm in diameter) nodules in the guano mass. The SEM study showed that the brushite aggregates are composed of finely bladed crystals, flattened on (010) and elongated toward a direction that may be [101] or [102]. Individual crystals are up to 0.1 µm thick, 7 µm wide and 15 µm long. The ICP-AES analysis of the sample PP 1 A yielded (in wt%): Na_2O = 0.01, CaO = 32.48, MnO = 0.03, MgO = 0.02, FeO = 0.03, P_2O_5 = 40.08, SO_3 = 1.32, H_2O (as calculated for the charge balance) = 26.03. This composition, normalized on the basis of 1 (P+S) and 4 (O) in the anhydrous part of the compound, leads to the chemical-structural formula:
$[Na_{0.001}Ca_{0.996}Mn_{0.001}Mg_{0.001}Fe^{2+}_{0.001}](HPO_4)_{0.972}(SO_4)_{0.028} \cdot 2H_2O$.

Taranakite occurs as dull white crusts or small veins of chalky appearance composed by clusters of crystals whose SEM examination shows roughly hexagonal forms. The individual crystals are up to 15 µm across and 1 µm thick. The mineral is typically associated with $2M_1$ illite and low (alpha) quartz. The cell parameters in the Table are indicative for a variety with low ammonium content.

Reference

SIMPSON, D.R. (1964): American Mineralogist, 49: 363–376.

CERAMIC RAW MATERIALS FROM THE GILĂU MTS. (ROMANIA)

MARIS, C.[1], GHERGARI, L.[2] & IONESCU, C.[2]
[1] S.C. Cominex S.A. Cluj-Napoca, Romania
E-mail: emc_cristina@yahoo.com
[2] Department of Mineralogy, Babeş-Bolyai University, 1 Kogălniceanu Str., RO-400084 Cluj-Napoca, Romania

Three well-known deposits from the Gilău Mts. (North Apuseni Mts., Romania), *e.g.* pegmatitic granite from Bedeci (source of feldspar and quartz), pegmatites from Muntele Rece (source for feldspar) and quartzites from Mănăstireni (source for quartz) are presented. They are used as raw materials for obtaining high quality household porcelain. The Bedeci raw material represents the Muntele Mare granite (composed from quartz, plagioclase, orthoclase, muscovite and biotite), intensely affected by late metasomatic processes which formed albite, microcline and generated pegmatitic granite. The pegmatite bodies from the Muntele Rece area are constituted from feldspars and quartz in various ratios so that three different petrographic types could be identified: orthoclase, plagioclase and orthoclase-plagioclase pegmatites. The Mănăstireni quartzite bodies, almost monomineralic in composition, have a hydrothermal origin related to the Muntele Mare granite.

The sequence of the processing phases used for the above-mentioned raw materials, are as follow: crushing and grinding, sieving and micas flotation, weak-field magnetic separation, feldspars flotation, drying, strong-field magnetic separation, final grinding. Several sorts of concentrates intended to be used for producing ceramics, tiles, electroceramics, glass, binders, glazes, enamels, ceramic pigments represent the results of these technological phases. Among them, the so-called *feldspar FC* concentrate is outstanding due to its chemical, mineralogical and technological characteristics. It is produced by processing a single raw material, *i.e.* the Bedeci pegmatitic granite, containing both feldspar and quartz. Granulometrically, this concentrate presents a bimodal distribution of the grains with two maxima, at 5 μm and 11 μm respectively; 80% of the particles have diameters below 63 μm. The chemical composition of the *feldspar FC* concentrate is: 78.1% SiO_2, 12.23% Al_2O_3, 0.26% Fe_2O_3, 0.5% MgO, 1.5% CaO, 3.8% Na_2O, 3.3% K_2O, and 1.02% LOI. The XRD patterns show the presence of quartz (40%), plagioclase, *i.e.* albite and oligoclase (39%), potassium feldspar, *i.e.* microcline (17%), and muscovite (4%).

Several recipes for producing household porcelain were tested, including domestic and imported raw materials, by firing at 1360 °C. The study shows that the porcelain made from recipe A (kaolinite + *feldspar FC* concentrate) compared with the porcelain obtained from recipe B (kaolinite + imported feldspar + domestic sands) has superior characteristics. Microscopically, the A-type porcelain is composed from 87-89% vitreous-microcrystalline matrix and 11-13% clasts of quartz, rare biotite and other minerals. The firing minerals are represented mainly by mullite, rare cristobalite and spinel. The amount of glass is over 50%, mullite reaches up to 39-40%, while quartz represents 9%. The B-type porcelain contains less glass (45-50%) and mullite (37%), and more quartz (10%). Additionally, the experimental data shows that A-type porcelain has the same characteristics, even fired at lower temperature, *i.e.* 1260 °C instead of 1360 °C.

ADA TEPE AND NEIGHBOURING GOLD PROSPECTS: SEDIMENTARY-HOSTED, EPITHERMAL DEPOSITS AND OCCURRENCES IN THE EASTERN RHODOPES, BULGARIA

MÁRTON, I.[1], MORITZ, R.[1], MARCHEV, P.[2], BONEV, N.[3], HASSON, S.[4] & VENNEMANN, T.[5]
[1] Section des Sciences de la Terre, University of Geneva, Geneva, Switzerland
E-mail: Istvan.Marton@terre.unige.ch
[2] Geological Institute, Bulgarian Academy of Sciences, Sofia, Bulgaria
[3] Department of Geology and Paleontology, Sofia University "St. Kliment Ohridski", Sofia, Bulgaria
[4] Balkan Mineral and Mining AD, Krumovgrad, Bulgaria
[5] Faculté des Géosciences et de l'Environnement, University of Lausanne, Lausanne, Switzerland

The epithermal gold mineralization with a low-sulfidation character at Ada Tepe and surrounding prospects are dominantly hosted by syn-detachment sedimentary rocks of Maastrichtian-Paleocene age. The associated dominant structure is a low angle normal fault, named Tokachka detachment fault, which is a major lithological and structural contact between the metamorphic basement and the Maastrichtian-Paleocene sedimentary rocks (BONEV *et al.*, 2005). These newly discovered deposits are economically significant and open up new exploration possibilities in this part of the Tethyan Metallogenic Belt. There is presently the potential open pit mining at the Ada Tepe deposit with high grade ore (5.2 Mt @ 5.0 g/t Au), with a total of 835000 ounces of gold indicated by Balkan Mineral and Mining (Dundee Precious Metals Inc., Report on Feasibility Study, 2005). Another prospect at Rosino has been developed up to the feasibility level with a 6.07 Mt of ore but at a lower grade (2.3 g/t Au) estimated by Cambridge Mineral Resources Plc. (Press Release, 2005).

The Ada Tepe deposit is located along the northern part of the N-NE-oriented Kessebir-Kardamos dome, which is a prominent geological feature in the Eastern Rhodopes. Geologic structures around the Ada Tepe deposit and adjacent prospects can generally be modelled by domino-style rotational normal faulting in the upper plate above the detachment fault. The importance of structural and lithological controls is reflected by the geometry of the ore bodies. They include: (a) strongly faulted rocks of the highly permeable Shavar Formation that offered a favorable channel-way for fluid circulation generating open space filling bonanza type mineralization in veins with a general E-W direction; (b) in contrast, the deformed metamorphic rocks with a ductile fabric and the cataclastic deformed detachment zone were the loci for focused fluid flow, toward lower pressure areas, where a massive, tabular ore body, named the "Wall" was formed immediately above the detachment fault. These zones consist of strongly altered rocks, replaced by silica minerals, adularia, sericite, pyrite and carbonate minerals. They formed through total replacement of the original metamorphic minerals included as clasts in conglomerates, and are associated with relict quartz and muscovite.

The ore mineralogy is simple, and consists of electrum (~75% Au), subordinate pyrite (more abundant in Surnak) and traces of galena and tellurides. The gangue is comprised of chalcedony, fine-grained quartz-adularia intergrowths and carbonates displaying typical colloform banded textures. Bladed texture is also abundant with quartz pseudomorphs replacing platy calcite (MARCHEV *et al.*, 2004). Evolution of the intensity of silica alteration can be observed in many places, starting with an initial network of small quartz veins along fractures, followed by either a total silica replacement of the host rock or leaching of the host rock, resulting in extreme cases of leaching, in a network of small quartz veins with no host rock left between them.

On the basis of the alteration mineralogy and textural relationships, it is possible that gold may have been deposited as a consequence of different physical-chemical processes in the various prospects. The abundant bladed quartz pseudomorphs replacing platy calcite suggest boiling in different prospects, including at Ada Tepe, Kuklitsa and Kupel. However, in cases of other prospects, such as Surnak, Kremenitz and Skalak, boiling textures are scarce to absent, and intense fluid-rock interaction may be responsible for gold mineralization, possibly due to pH and Eh variations of the gold-transporting fluid. In two prospects, *i.e.* Ada Tepe and Surnak, areas enriched in organic carbon can be identified which correlate with high Au grades, due probably to the intense reduction locally of the hydrothermal fluids. The intensive altered, tabular silica bodies (e.g. the "Wall" zone in Ada Tepe and Kuklitza) possibly overlap with fluid mixing areas.

According to preliminary stable isotope analyses the $\delta^{18}O$ values (*vs.* V-SMOW) range from 11.2-13.5‰ in quartz samples and 9.2‰ and 10.0‰ in adularia dominated samples from the Ada Tepe deposit. Assuming a low temperature deposition of about 150-200 °C (MARCHEV *et al.*, 2004), the calculated oxygen isotopic compositions of water in equilibrium with both minerals are about 0 to 4‰. The Ada Tepe and Surnak pyrite samples have comparable $\delta^{34}S$ values (vs. CDT) between –3.7‰ and 0.2‰. The stable isotope compositions can be interpreted as typical for dominantly magmatic/metamorphic mineralizing fluids, but does not allow us to exclude a meteoric or sedimentary input, especially if we consider extensive fluid-rock interactions.

References:

BONEV, N., BURG, J.-P. & IVANOV, Z. (2005): International Journal of Earth Sciences, online edition.

MARCHEV, P., SINGER, B., JELEV, D., HASSON, H, MORITZ, R., BONEV, N. (2004): Schweizerische Mineralogische und Petrographische Mitteilungen, 84: 59–78.

MARCHEV, P., KAISER-ROHRMEIER, M., HEINRICH, C.A., OVTCHAROVA, M., VON QUADT, A. RAICHEVA, R. (2005): Ore Geology Reviews, 27: 53–89.

WEATHERING OF THE GABBRO STONES OF THE UNKNOWN SOLDIER MONUMENT (MT. AVALA, SERBIA)

MATOVIĆ, V. & VASKOVIĆ, N.
Institute of Mineralogy, Crystallography, Petrology and Geochemistry, Faculty of Mining & Geology, University of Belgrade, Đušina 7, 11 000 Belgrade, Serbia and Montenegro. E-mail: vesnamat@beotel.yu; nadavask@eunet.yu

The Unknown Soldier monument on Mt. Avala was built of Jablanica gabbro in 1934–1938 (Fig. 1). It is the work of the world famous sculptor Ivan Meštrović and represents a part of outstanding value of our cultural heritage.

The Jablanica Gabbro has high compressive strength and wear resistance. It is frost resistant with low porosity and water absorption but decay types appeared indicating the ability of the gabbro to absorb water and moisture hygroscopically and capillarily.

The results of the first mapping have shown a great variety of weathering forms (loss of stone material, discoloration/deposits, detachment of stone material and fissures/deformation), and a wide range of intensity. Damage such as break-out, discoloration, crust deposits, granular disintegration, contour scaling, flaking and biological colonization, are observed both on the exposed and sheltered stone surfaces of the monument (Fig. 2).

Fig. 1: The Unknown Soldier Monument.

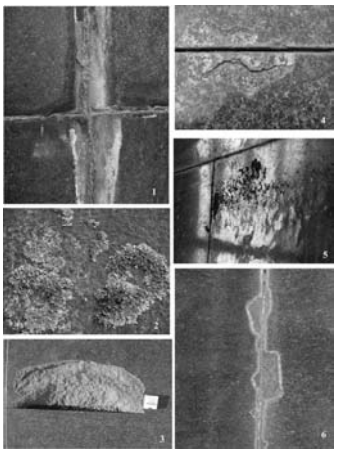

Fig. 2: Weathering forms: 1. Incrustration; 2. Lichen; 3. Contour scaling & granular disintegration; 4. Flaking; 5 Blistering and roughening; 6. Contour scaling and light-coloured crust.

Considerable amounts of severe or even very severe damage were noted on the lower and middle parts of the monument.

Most of the damage observed on the monument is superficial and caused by synchronous physical and chemical processes. They are controlled by the migration of solutions through half-filled joints and the porous stone network. These solutions originated from rainwater and condensation water, dissolved cement mortar and lead elements, they migrate through the stone under the influence of capillary tensions. They evaporate during dry periods and leach out the dissolved components in the forms of white and dark incrustations. This in turn leads to mechanical disruption (fracturing, contour scaling, granular disintegration, flaking) and to chemical transformations of the polished stone surfaces (loss in lustre and changes in colour). Exposed stone surfaces are bleached or covered by hard crusts leaked from the joints. Some of the mechanical damage is caused by freezing and thawing water. In winter, when temperatures oscillate around freezing point, at the rise of water/ice volume in the joints or stone pores, pressure on the walls increases and the stone is subjected to internal mechanical stresses. Simultaneously, captive stresses between the grains of the minerals arise from differences in their temperature coefficient of linear extension. When the ice melts, the water volume decreases and a new quantity of water is absorbed into the capillaries. During freezing, a new cycle of the same process begins and in consequence, the mechanical disruption of the stone grows repeatedly (WINKLER, 1994). The same mechanism appears in the fissures and microcracks during the freezing and melting of water and moisture.

Salt deposits (thermonatrite, trona, aphthitalite, calcite, halite, anglesite, hydrocerussite, plumbonacrite) occur on facades and in sheltered areas, especially inside of the monument. They cause very considerable very frequent damage. Where liquid water transfer is fast and porosity allows a flow that compensates for the evaporation, salts crystallize on the surface as efflorescence. In contrast, when the capillary supply does not compensate for the evaporation, the salts precipitate inside the stone, under the surface in form of subefflorescence and gabbro surfaces became rough and are affected by blistering, granular disintegration, and flaking.

Generally, the Jablanica gabbro has low vulnerability to decay mechanisms. The stone surfaces on the monument display evident signs of degradation clearly associated with local environmental conditions and factors encountered during construction. It must be stressed that the Unknown Soldier monument represents a unique structure for that period. Masons did not find a similar model in the entire world for that kind of building and had to solve many technical problems which arose during the construction. From our standpoints, it is clear for us that they made some mistakes in the final phases of work (the mode of joint filling, the binding between the foundation and the mausoleum, the mode of polishing and installation of glass doors at the entrance and exit of the mausoleum) which caused different kinds of damages.

MICROMINERALOGY OF IGNIMBRITES OF SOKYRNYTSYA ZEOLITE DEPOSIT (TRANSCARPATIANS, UKRAINE)

MELNIKOV, V. S.[1], GRECHANOVSKAYA, E. E.[1], DEMENKO, D. P.[2], KVASNYTSYA, V. N.[1] & LAZARENKO, E. E.[3]
[1] Institute of Geochemistry, Mineralogy and Ore Formation of NAS Ukraine, Palladine av. 34, Kyiv, Ukraine
E-mail: vsmel@i.com.ua
[2] Institute of Geological Sciences of NAS Ukraine, Gonchara str. 55-b, Kyiv, Ukraine
[3] Institute of Geochemistry Environment of NAS of Ukraine, Palladine av. 34-a, Kyiv, Ukraine

Ignimbrites stretching under clinoptilolite tuffs of the Sokyrnytsya deposit belong to the Teresvinskaya suite (Upper Tortonian). These ignimbrites consist of a) splinters of volcanic glass, b) magmatogenic minerals (fragments of crystals and entire, non-destructed crystals); c) newly formed minerals. In some areas felsitic texture changed into vitroclastic and crystalloclastic ones on the scale of a thin section. The shape of the glass splinters is formed by spherical surfaces of destroyed (blown up) gas bubbles. The indications of ignimbrites are as follows: a) crystals of magmatic feldspars and quartz are broken and cemented by rock of felsitic texture; b) highly deformed crystals of biotite; c) fragments of crystal are shifted and rotated in the plastic felsitic medium.

Phenocrysts of magmatic minerals are plagioclase (oligoclase–andesine #28–32 and andesine #40), quartz, sanidine and biotite. Apatite, zircon, magnetite are accessory minerals. Plagioclase, K-feldspar, quartz, cristobalite (?), mafic and opaque minerals and glass constitute microfelsitic groundmass. The main new mineral formations are adularia, albite and calcite. Muscovite, analcime and acicular zeolites occur sporadically. A cryptocrystalline bluish-green mica (polytypes $1M$ and $1M_d$) is a characteristic mineral of ignimbrites. This mica may be an alteration product of pumice inclusions.

Large idiomorphic crystals of quartz with high-temperature habit are not often observed but fragments of this quartz prevail in the rock. The later quartz forms accretions of prismatic crystals on the faces of adularia.

Idiomorphic transparent crystals of plagioclase can reach 1-2 mm in size but they occur only occasionally. Zoned crystals are rarely observed. Twins according to the albite law are predominant but crystals are often untwinned or the twins are built up by a few wide domains only. Plagioclase (oligoclase–andesine) is the main clastic material of ignimbrite.

Phenocryts of sanidine are seldom, but crystal fragments are common. In rare cases anisotropic strips similar to "tweed orthoclase" are observed.

The main femic mineral of ignimbrites is mosaic-textured biotite (0.1–2.0 mm). Small crystals are concentrated in the felsite. They are strongly deformed (curved, folded, split).

Adularia is widespread postmagmatic mineral of the welded tuffs of Sokyrnytsya deposit. It forms small (less than 0.05 mm) crystals substituting the fragments of volcanic glass. Adularia growing in the pores of the rock creates fine microdruses. Its crystal forms according to SEM studies are {110}, {001}, {–201}, {100}. Adularia crystallized on the boundary of glass and felsite and a complete substituting of glass can be observed sometimes. An interesting peculiarity of adularia from the Sokyrnytsya ignimbrite is the low degree of Si/Al-ordering in the structure ($2t_1$ = 0,58–0,62); it is comparable with the degree of Si/Al-ordering in sanidine. Calcite forms aggregates of grains, which recrystallized into large mosaic crystals.

Melt inclusions are always present in magmatic minerals (plagioclase, quartz). Every inclusion have rectilinear shape and they are oriented along crystallographic axes. Homogeneous glass inclusions prevail. Gas bubbles in glass inclusions can be observed very seldom, however the gas may be hidden among recrystallized grains. So these inclusions reflect different degree of gas saturation of magmatic melt. Inclusions in adularia have never been observed.

Formation of adularia of ignimbrites is connected to the influence of hot mineralizing solutions on rhyolite-dacite glass. The heat source was the large mass of hot ignimbrite. Vertical loading and transfer of plastic ash materials (incompletely consolidated fallen aerosol) caused opening of the gas microbubbles and saturation of the solution by CO_2. Adularia crystallized as a metastable phase immediately from volcanic glass. It is suggested that the low degree of Si/Al-ordering in the structure of adularia was inherited from the amorphous glass.

MINERALOGICAL STUDIES IN THE POLISH CARPATHIANS (PERIOD 2000-2005)

MICHALIK, M. & BUDZYŃ, B.
Institute of Geological Sciences, Jagiellonian University, Kraków, Poland
E-mail: michalik@geos.ing.uj.edu.pl

Mineralogical studies in the Polish Carpathians during last five years were focused on several topics.

1. Inner Carpathians

Reconstruction of P-T conditions of crystalline rocks formation and hydrothermal alterations were studied by J. BURDA, A. GAWĘDA, K. JACHER-ŚLIWCZYŃSKA and J. LEICHMANN.

Accessory minerals in crystalline rocks. Chemical composition and internal structure of zircon in granitoid rocks (J. BURDA), xenotime-zircon intergrowths, REE minerals in chlorite schists. Crystallization, stability and breakdown are discussed (D. DYLSKA, M. KUSIAK, M. MICHALIK, M. PASZKOWSKI, R. POPCZYK, M. STANISŁAWSKA).

Mineralogy and geochemistry of carbonate and silicate minerals of the Križna unit. Exhalative origin of Mn-bearing sequence of Toarcian carbonate/silicate deposits were studied by T. DUDEK and R. JACH. Silicate minerals and their terrigenous and diagenetic origin were investigated by M. MICHALIK and M. SKIBA.

Geochemical and isotopic studies of speleothems from the Tatra caves (origin of caves, dating of speleothems by means of the U-Th method, estimation of climatic changes based on analysis of speleothem growth frequency, and reconstruction of the type of vegetation cover during the cold and warm periods using carbon isotopic composition) were performed by M. GRADZIŃSKI and H. HERCMAN.

Heavy minerals in recent alluvia. Heavy minerals from crystalline rocks and anthropogenic components related to historical industrial activity were studied (A. KIEBAŁA, A. LADENBERGER, M. MICHALIK).

Diagenesis and uplift of the Podhale basin and underlying Mesozoic nappes. From XRD %S measurements (percent smectite in mixed-layer illite/smectite) on present surface and in boreholes, supplemented by K-Ar dating it was concluded that the Podhale basin together with the Tatra block underwent major subsidence along the Ruzbachy fault and since 18 Ma a major uplift also along this fault. Up to 6 km of erosion was inferred for the eastern part of the basin from these data. The diagenesis of the Mesozoic nappes is 90 Ma old and during Tertiary the Tatras were buried under the flysch sediments to ca. 3-4 km *(*M. KOTARBA*,* P. SUCH, J. ŚRODOŃ). These conclusions were confirmed by AFT study (A. ANCZKIEWICZ and J. ŚRODOŃ).

Weathering and soil forming processes. Mineralogy and geochemistry of the podzolization processes on granitoids (M. SKIBA), stability of accessory minerals from granitoids during podzolization (I. JERZYKOWSKA).

2. Pieniny Klippen belt

Pieniny andesites. Petrology, petrogenesis, K-Ar ages, mineralogy and related hydrothermal alterations and mineralization were studied by P. ALEKSANDROWSKI, N. BAKUN-CZUBAROW, A. BIAŁOWOLSKA, K. BIRKENMAJER, A. BOUVIER, A. LADENBERGER, M. MICHALIK, Z. PÉCSKAY, C. PIN, Ł. SKUBLICKI, W. SZELIGA, M. WARZECHA, B. ZYCH.

Sedimentology, mineralogy, geochemistry of pelitic rocks from the Pieniny unit (P. WÓJCIK-TABOL).

3. Outer Carpathians

Teschenites in the Outer Carpathian flysch (mineralogy, petrology and age determination) R. ANCZKIEWICZ, Ł. KARWOWSKI, A. LUCIŃSKA-ANCZKIEWICZ, E. STARNAWSKA, A. ŚLĄCZKA, I.M. VILLA, R. WŁODYKA, R. WRZALIK.

Clay diagenesis both in the flysch nappes (Kraków–Nowy Targ section and Kużmina borehole (M. KOTARBA, J. ŚRODOŃ) *and in the Carpathian Foredeep* (T. DUDEK, J. ŚRODOŃ). Inner nappes (Magura) were found to be more diagenetically advanced than the outer nappes (Silesian and Subsilesian). The diagenesis in the Kraków–Nowy Targ section is older than the present-day tectonic structure. The advance of diagenesis in the Kużmina profile was studied by measurements of the illite crystal size distribution.

Clay minerals were used to reconstruct thermal evolution of tectonic windows or mechanisms such as variable uplift in the Magura Nappe (A. Świerczewska).

Provenance of the crystalline clasts and clastic material of sandstones. Mineralogical, petrological, geochemical and geochronological (K-Ar method on micas, U-Pb method on zircon and CHIME on monazite) studies of gravel-size extrabasinal clasts of crystalline rocks (K. BĄK, I. BROSKA, B. BUDZYŃ, B. DZIUBIŃSKA, M. GARECKA, I. HOLICKÝ, K. JACHER-ŚLIWCZYŃSKA, P. KONEČNY, M. KUSIAK, E. MACHANIEC, T. MALATA, M. MICHALIK, M. PASZKOWSKI, Z. PÉCSKAY, P. POPRAWA, J. RUBINKIEWICZ, J. SKULICH, A. WOLSKA). Heavy minerals were studied by B. DZIUBIŃSKA, M. KUSIAK, J. LEICHMANN, N. OSZCZYPKO, M. PASZKOWSKI and D. SALATA.

Early diagenetic carbonate concretions (sideroplesites and manganospherites) were studied by B. DZIUBIŃSKA and W. NARĘBSKI.

Mineralogy of clinoptilolite-bearing rocks and sorption mechanisms on clinoptilolite from flysch rocks (sorption of heavy metals and gases) (T. BAJDA, W. FRANUS, A. MANECKI, W. MOZGAWA, T. WIESER).

Hydrothermal mineralization in flysch rocks. Cinnabar and arsenic sulphide associations (Ł. KARWOWSKI, E. SZEŁĘG), kaolinite-barite intergrowths from Rabe near Baligród (M. MICHALIK, W. WILCZYŃSKA-MICHALIK).

Secondary minerals on weathered surfaces of the flysch sandstones were studied to determine differences in concentration of air-pollution in the Carpathians (M. MICHALIK, W. WILCZYŃSKA-MICHALIK).

SECONDARY MINERALS IN THE PIENINY ANDESITES (SOUTH POLAND)

MICHALIK, M., LADENBERGER, A., SKIBA, M., WARZECHA, M. & ZYCH, B.
Institute of Geological Sciences, Jagiellonian University, 30-063 Kraków, Poland
E-mail: michalik@geos.ing.uj.edu.pl

So-called Pieniny andesites occur in form of dykes in the Pieniny klippen belt and Magura Unit sedimentary rocks. We present here results of mineralogical study of selected fresh-looking samples of andesites collected from the Malinów quarry, the Bryjarka Hill in Szczawnica and from the Wżar Hill. The studied rocks represent basaltic andesites (two samples from Wżar) and andesites (one sample from Wżar and samples from Malinów and Bryjarka) (according to TAS classification; LOI free basis). The studied samples have SiO_2 content ranging between 51.5 and 61.5 wt %. LOI value varies from 1.3 to 3.8 wt%.

Optical microscopy, X-ray diffraction and SEM-EDS methods were applied. Both powdered bulk rock samples and separated <2 μm fractions were analysed using XRD. XRD analyses were performed in air dry conditions, after saturation of the mounts with ethylene glycol and after heating at 550 °C.

Rocks studied are porphyritic with abundant phenocrysts. Phenocryst assemblage is represented by plagioclase (which predominates over mafic phenocrysts in samples from Malinów and Bryjarka), amphiboles, clinopyroxenes (present in higher amount only in samples from Wżar hill) and Fe-Ti oxides.

Plagioclase phenocrysts composition varies from oligoclase to bytovnite (almost pure albite is of secondary origin). Small differences in average plagioclase composition between samples are observed. Plagioclase phenocrysts are zoned. In some samples plagioclase phenocrysts cores are rich in glass inclusions whereas rims are inclusion-free and exhibit euhedral shape. Plagioclases are partly replaced by calcite and chlorite (commonly in samples from Malinów). Amphibole phenocrysts represent magnesian hastingsitic hornblende and magnesian hastingsite (samples from Malinów, Wżar) and ferroan pargasite, ferroan pargasitic hornblende, edenitic hornblende (Wżar) according to the classification of LEAKE (1978). Amfiboles are often altered – replaced completely or partly by chlorite, calcite, Fe-Ti oxides, titanite. Coronas composed of fine-crystalline aggregates of plagioclases, pyroxene, Fe-Ti oxide minerals are commonly developed around amphiboles. Pyroxene phenocrysts are represented by diopside (in Morimoto (1988) classification). Alterations of pyroxene result in formation of chlorite and calcite. Fe-Ti oxides phenocrysts belong to ulvöspinelo-magnestite series. Degree of mafic phenocrysts alteration is higher in samples from Bryjarka and Malinowa in comparison with samples from Wżar.

Rock groundmass contains small crystals of plagioclase and Fe-Ti oxides. K-feldspar often rich in Ba is relatively common. Groundmass of the sample from Bryjarka is almost completely composed of Ba-rich K-feldspar and quartz (probably of secondary origin); Ba-rich feldspars are present also in sample from Malinowa. Ba content in K-feldspar varies from 0.0 to 0.1 at. *pfu*. Rocks with secondary Ba-enriched K-feldspars seem to exhibit more Ba in bulk rock analysis. Calcite fills voids in one sample from Wżar. Fibrous (potassium rich) illite-like mineral as well as aggregates of Mn-Fe oxides of corn-flake morphology around mafic phenocrysts are observed in samples from Wżar.

Smaller than 2 μm fraction separated from andesite samples and studied using XRD method are composed of illite/smectite (and vermiculite/smectite?) and cristobalite (samples from Wżar), chlorite/smectite, smectite, swelling chlorite?, chlorite? (samples from Malinów), chlorite and small amount of illite/smectite (sample from Bryjarka).

Samples with more altered mafic phenocrysts are richer in secondary chlorite, chlorite/smectite and Ba-enriched K-feldspars as compared to samples with less altered mafic phenocrysts (containing illite/smectite (or vermiculite/smectite)).

Andesite samples differ in the proportions of minerals in phenocryst assemblages but the chemical composition of phenocrysts is generally similar. Rocks significantly differ in degree of mafic phenocrysts alteration and composition of secondary minerals. Differences are the result of variable conditions of secondary alteration of rocks induced by different volumes of magmatic bodies and their emplacement in rocks of different lithology and properties.

Reference

LEAKE, B. E. (1978): Mineralogical Magazine, 42: 533–569.

PRELIMINARY MINERALOGICAL ASPECTS OF SOME ZEOLITES FROM THE MUREŞ VALLEY, ROMANIA

MIRON, D.
Department of Geology, Faculty of Biology and Geology, Babeş-Bolyai University, 1 Kogălniceanu St., 400084 Cluj-Napoca, Romania
E-mail: mirondanro@yahoo.com

The paper presents the first results of a study made on some zeolites from the basaltic rocks near Vălişoara village (Hunedoara County, Romania) located on the road between Deva and Brad (Southern Apuseni Mountains).

The main rocks in this area belong to the "Ophiolitic" Complex, which is a part of the Transylvanide Group. The "ophiolites" from Vălişoara area were placed by NICOLAE (1994) in the calcalkaline series. The main rocks are basalts (basaltic andesites) in pillow-lava facies, which were exposed to a hydrothermal alteration. The basaltic rocks contain nests and fissures filled up with zeolites and other secondary minerals (chlorites, carbonates).

The zeolites identified by macroscopic and X-ray diffraction analysis are analcime, clinoptilolite (heulandite ?), stilbite and laumontite.

Reference

NICOLAE, I. (1994): In: ALCAPA II Field Guidebook "South Carpathians and Apuseni Mountains". Romanian Journal of Tectonics and Regional Geology, 75, Suppl. 2: 136–140.

YTTRIUM IN ROMANIAN PEGMATITES

MURARIU, T.
Chair of Mineralogy and Geochemistry, Department of Geology, "Al. I. Cuza" University, Carol I, No. 11, Iaşi, Romania
E-mail: titusmurariu@yahoo.com

Pegmatites have always aroused the researchers' interest by their interesting features, regarding structure, petrography, mineralogy, geochemistry, metallogenetic potential and genesis.

In the Romanian Carpathian area a large pegmatite Province (PPC) is known, consisting of several subprovinces, as follows: Preluca, Rodna, Gilău–Muntele Mare and Getică (MÂRZA, 1980). The PPC pegmatites have a granite type composition and a simple mineralogy and low rare-elements contents, which are characteristic features of the metamorphic pegmatites (HANN, 1987; MURARIU, 2001 *etc*.). The pegmatites are hosted within Precambrian metamorphic rocks, typical of amphibolite facies: paragneisses, micaschist, amphibolites, crystalline marbles, usually associated with migmatites, which belong to the mesometamorphic groups of Baia de Arieş, Rebra, Someş, Sebeş–Lotru (BALINTONI, 1986).

On the basis of mineralogical and geochemical features, pegmatites from the Carpathian Province belong to the following classes (ČERNY, 1982): (1) feldspar pegmatites; (2) mica-bearing pegmatites and (3) rare-element pegmatites, which include two types: (3a) beryl type (± columbite, tantalite, montebrasite) and (3b) albite-spodumene type (+ tantalite, columbite, beryl, cassiterite, purpurite).

Yttrium is included in the heavy rare earths subgroup (HREE) by reason of his geochemical affinity with lanthanides. The rare metal yttrium is a typical lithophile element of granites, syenites, pegmatites and carbonatites.

In the Carpathian Pegmatites Province yttrium does not form its own minerals, but occurs in the structure of rock-forming minerals and accessory minerals. The yttrium contents in the Carpathian Province are evidently increasing from the rare-elements pegmatites (albite-spodumene type), from the feldspar pegmatites, mica bearing pegmatites to garnets pegmatites and apatite pegmatites. The geochemical distribution of yttrium in the minerals of the Carpathian Province Pegmatites revealed lower contents in spodumene, quartz, feldspars, micas, tourmaline as distinct from higher values in apatite and garnets.

In Romanian pegmatites apatite and garnets (almandine–spessartine species) are the main minerals that concentrate yttrium. The presence of yttrium (1564–1950 ppm) in the apatite structure is the result of the following isomorphous substitutions: $Y^{3+} + Na^{+} = 2Ca^{2+}$; $Y^{3+} + Si^{4+} = Ca^{2+} + P^{5+}$. The isomorphous penetration of yttrium in the crystal structure of garnet depends on their content in Mn: $Y^{3+} + Al^{3+} = Mn^{2+} + Si^{4+}$. The substitution of Mn with Y in the analyzed garnets is confirmed by the character of the negative correlation: Y (ppm)/Sp + Cld (%). Based on the concentration coefficient (k) the order in which yttrium was accumulated in the minerals of the pegmatites from Carpathian Province is: apatite > garnet > biotite > tourmaline > muscovite > microcline > albite > quartz > spodumene.

References

BALINTONI, I. (1996): Geotectonica terenurilor metamorfice din România. Editure Carpatica, 176 p.

ČERNY, P. (1982): In: Granitic Pegmatites in Science and Industry. Mineralogical Association of Canada, Short Course Handbook, 8: 1–39.

HANN, H.P. (1987): Pegmatitele din Carpații Meridionali. Editura Academiei RSR, 141 p.

MÂRZA, I. (1980): Anuarul Institutului de Geologie şi Geofizică, 58: 423–431.

MURARIU, T. (2001): Geochimia pegmatitelor din Romania. Bucureşti: Editura Academiei Române, 356 p.

ENVIRONMENTAL IMPACT OF ACID MINE DRAINAGE IN THE TURȚ CREEK, SATU MARE COUNTY, ROMANIA

NAGY, I.[1], WEISZBURG, T. G.[2], FODORPATAKI, L.[3] & BARTHA, A.[4]
[1] Faculty of Biology and Geology, Babeş-Bolyai University, str. Kogălniceanu 1, Cluj-Napoca, Romania
E-mail: nagy_istvan@mailnew.com
[2] Department of Mineralogy, Eötvös Loránd University, Pázmány Péter sétány 1/C, H-1117 Budapest, Hungary
[3] Department of Experimental Biology, Faculty of Biology and Geology, Babeş-Bolyai University, str. Kogălniceanu 1, Cluj-Napoca, Romania
[4] Hungarian Geological Survey, Stefánia út 14, H-1143 Budapest, Hungary

Our goal was to investigate the mineralogical, geochemical and biological impact of acid mine drainage connected to the activity of a polymetallic ore mine. We applied different chemical and mineralogical analytical methods on special sets of samples as follows: on-site electric conductivity and pH measurements of water in several points of the Turț Creek; polarised light optical microscopy of thin sections of rocks and their (recent, brownish–yellow) encrustation collected from the creek bed; X-ray powder diffraction of rock encrustations and non-consolidated creek sediments; scanning electron microscopy combined with EDX on thin sections; Mössbauer spectroscopy of rock encrustations; inductively coupled plasma optical emission spectroscopy (ICP-OES) of water samples with special attention on 1) solved and fine-grained (below 450 nm) solid and 2) coarser (above 450 nm), but still suspended solid components of the creek water.

The biological investigations consisted of germination tests of oat seeds with polluted and non-polluted water samples collected from the creek, and control, algal toxicology test, effects on algal biodiversity, and chlorophyll fluorescence analysis with PEA fluorometer in leaflets of germinated oat seedlings (SCHREIBER *et al.*, 2000).

The Oaş Mountains represents the north-western part of the volcanic chain of the inner part of the Romanian East Carpathians. They consist of Neogene volcanic and sedimentary rocks developed – especially the volcanics – in the north-western part of the small Oaş Basin, an Eastern extreme of the Pannonian Basin. Epithermal lead and zinc ore formation was connected to the Neogene volcanic activity in the area. In the 1970s a mine was established on such an ore deposit in the valley of the Turț Creek. In 1999, as a result of some technological problems, the mine seriously polluted the by-flowing creek, and, through that creek, also the river Tur. The pollution of the creek was repeated in the summer of 2005 (in July, August and September). We sampled the area in February and in the July–September period of 2005.

The chemical and mineralogical results evidenced the presence of poorly crystallised iron oxide/sulphate phase(s), like akagenéite, ferrihydrite or schwertmannite, enriched in metals like Cu and Zn. The acid mine drainage brings into the creek excessively high amounts of solved metals (*e.g.* Cd, Zn, Cu, Pb, Fe, Ni, Sr and Co), while the low pH of the water (<3) causes extensive leaching of silicate minerals of the bottom rock and soil, resulting in a very high solved concentration of elements like Al and Si, unusual in natural waters. The soluble salts of some of these metals accumulate in aquatic micro-organisms and cause an imbalance in the ecological equilibrium of the affected aquatic habitats.

The special niche formed by acid mine drainage also represents the habitat of several bacteria and protists. We identified *Euglena mutabilis* (Ehrenberg 1838), an acidophilic protist, an indicator species (FORRAY, 2002) for environments of low pH conditions (in our case pH 2.9), high amount of total dissolved solids (TDS; in our samples: 9772 mg/l) and high electric conductivity (in our samples: 5,000–9,000 μS/cm).

As an interesting by-product of our study we found also some macroinvertebrates not described from the Turț Creek previously (*e.g.* caddisfly *Micropterna lateralis* (Stephens 1834) (Trichoptera), from an unpolluted area).

References

FORRAY, F. (2002): Studia Univ. Babeş–Bolyai, Geologia, Special Issue, 1: 189–198.

SCHREIBER, U., BILGER, W., HORMANN, H. & NEUBAUER, C. (2000): In: RAGHAVENDRA, A. S. (ed.): Photosynthesis: a comprehensive treatise. Cambridge: Cambridge University Press, 320–339.

THE HYDROTHERMAL MINERAL PARAGENESIS OF THE FERENC-HEGY CAVE (BUDA HILLS, HUNGARY)

NAGY, S. & MOLNÁR, F.
Department of Mineralogy, Eötvös Loránd University, Pázmány Péter sétány 1/C, H-1117 Budapest, Hungary
E-mail: szisa@t-online.hu

During a detailed mapping of the Ferenc-hegy Cave a hydrothermal mineral assemblage was found. The host rock of the cave is the Upper Eocene Szépvölgy Limestone Formation, but the upper parts of the cave reach the Lower Oligocene Buda Marl Formation. At one place the basal conglomerate of Eocene age can be seen under the Szépvölgy Limestone.

Mapping of the hydrothermal precipitations revealed that the veins characterized by different mineral associations are bound to different fault systems therefore they might have been formed in different times. The overall strike of calcite–barite and calcite–barite–hematite veins is N–S, barite–hematite veins have a NW–SE strike, barite–hematite–cinnabar veins have a prevailing E–W strike. In some veins a kaolinite–smectite mineral association can be found. Vein fillings are generally banded, symmetrical, or rarely brecciated; geopetal features were observed in some cavities near barite veins occurring along a siliceous zone.

Euhedral barite can be divided into two morphological groups. One of them is characterized by the main forms of {001}, {010}, {100}, {110}, and corresponds to the "Wolnyn" type of MAKLÁRI (1940). The second group is characterized by the main forms of {001}, {110}, {010}, and corresponds to that reported as "Antimonit-B" by MAKLÁRI (1940). In veins, calcite occurs with scalenohedral habit and as massive-granular precipitations. Fine-grained hematite is usually found as impregnations and disseminations along veins. Cinnabar occurs as earthy dissemination in massive barite.

Fluid inclusion studies were carried out in calcite crystals from the calcite–barite veins. Microthermometric data of fluid inclusions suggest that hydrothermal processes took place under various temperature circumstances, and during these processes, warming of fluids from 70–85 °C to 90–130 °C temperature had been taken place. While precipitation of carbonates happened at some places, the raising of the temperature supposedly caused forming of dissolution cavities in the carbonate rocks at other places, thus supported opening up of thermokarstic caves. Fluid inclusions have low salinities of 0.1–0.5 NaCl equiv. wt% suggesting to a mixed meteoric/karstic origin for the water. In conclusion, in the early period of formation of the Ferenc-hegy Cave, hydrothermal events played an important role in the development of cavities in the carbonate host rocks along fault/fracture systems.

Reference

MAKLÁRI, L. (1940): Mathematikai és Természettudományi Értesítő, 59: 643–672.

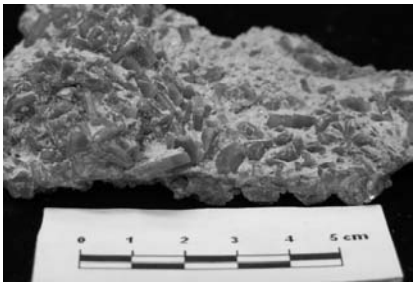

Fig. 1: Barite crystals with "wolnyn" habit from a calcite-barite-hematite vein.

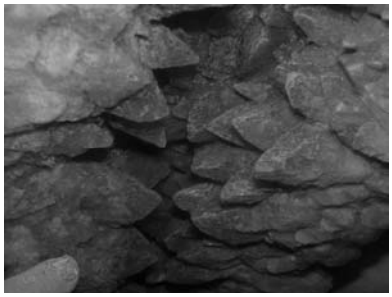

Fig. 2: Calcite crystals in calcite-barite veins.

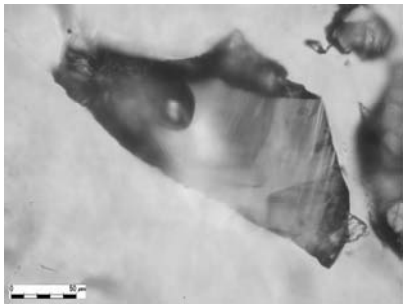

Fig. 3: Primary fluid inclusions in scalenohedral calcite.

MINERALOGICAL STUDY OF THE SÁTORKŐPUSZTA CAVE, DOROG, HUNGARY

NAGY, S., VOJNITS, A. & WEISZBURG, T. G.
Department of Mineralogy, Eötvös Loránd University, Pázmány Péter sétány 1/C, H-1117 Budapest, Hungary
E-mail: szisa@t-online.hu

The aim of our work was to give a detailed mineralogical description of the mineral precipitates of the Sátorkőpuszta Cave and to apply our results for setting up a genetic model for the cave. The Sátorkőpuszta Cave was discovered 60 years ago and has been famous for its rich gypsum encrustations. The cave opens on the SE slope of the Nagy-Strázsahegy (Nagy-Strázsa Hill) near Dorog, at a distance of only 35 km NW from Budapest.

The cave is hosted by Upper Triassic Dachstein Limestone. That formation and other, different limestone formations are characteristic for the closer and broader geological surroundings of the Nagy-Strázsa Hill. An interesting exception is the Tábla Hill, situated to the south of the hill at a short distance, built up of Eocene–Oligocene and Miocene volcanics.

The mineral precipitates of the cave were thoroughly mapped and a representative set of samples was collected (taking also the serious environmental protection regulations into account). The collected samples were studied under the stereomicroscope. X-ray powder diffraction (XRD) was applied for phase identification. Scanning electron microscopy (SEM, equipped with EDX analyser) was carried out on thin sections to reveal the textural relationship between the identified phases. Finally, dissolution experiments were carried out on the cave-hosting limestone to reveal the mineralogical composition and the amount of the insoluble residue.

According to the on-spot observations several 10 cm thick veins built up of well-crystallized calcite stand out from the walls and ceilings in the cave. These veins were obviously formed in the hosting limestone before the formation of the cave, and they were disclosed during the dissolution of the cave due to the lower solubility of the coarse calcite crystals than that of the fine calcite matter of the host rock. Iron oxide(-hydroxide) pseudomorphs after crystalline pyrite can also be found in these primary calcite veins.

The lower level of the cave is rich in mineral precipitates. Recent formation of dripstone in limited amounts can be traced in some parts of that level; however, the dominant phase covering the walls is gypsum. Gypsum forms even large columns. At the recent bottom of the cave clay-sized material, consisting mainly of kaolinite and in lesser amount quartz, blocks the access to the deeper parts.

The most interesting mineral assemblage, giving also a key to the formation of the cave, is a rhythmic precipitation of finely banded dolomite and gypsum forming a cover on the "bottom clay". Gypsum (second generation) may also fill the desiccation cracks of dolomite (Fig. 1). That texture clearly proves that dolomite was a primary precipitation (not a detrital phase) in one of the last stages of the cave formation processes. The crust-forming dolomite and gypsum on the surface of kaolinite may be considered as evaporites.

Based on the dissolution experiment the clay-sized kaolinite and quartz in the cave can partly be considered as the insoluble residue of the limestone. It should be noted, however, that the size of the cave, *i.e.* the amount of dissolved limestone in itself cannot account for the amount of kaolinite that has been accumulated on the bottom of the cave.

Based on the mineralogical results, the formation of the cave consists of at least four phases: (1) hole formation, dissolution of the limestone. During that phase calcite- and pyrite-bearing veins got disclosed, while the insoluble residue of the limestone accumulated on the floor of the cave. This stage was followed by (2) the oxidation of pyrite and the evaporitic, rhythmic precipitation of dolomite and gypsum. In the first part of stage (3), due to the retreat of water, desiccation cracks formed on the dolomite-gypsum crust, followed by the precipitation of large amounts of calcite and the second generation of gypsum (on the walls of the cave and in the desiccation cracks of dolomite). In the last stage (4), dripstones precipitated from the infiltrating water.

Further studies are planned to find out the source of kaolinite, the large amounts of sulphur necessary for the gypsum and to trace the relationship between the cave and the nearby volcanic rocks.

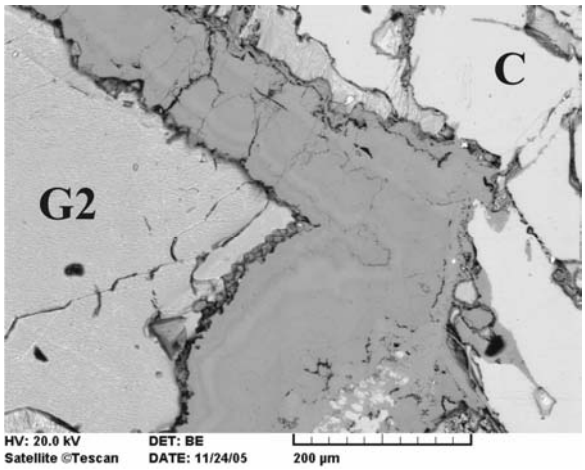

Fig. 1: Continuous bands of rhythmic precipitation of dolomite on a calcite crust (C) covering the bottom kaolinite. In the darker zones submicrometre-sized fine gypsum crystals ("gypsum generation 1") formed together with dolomite. Later a second gypsum generation (G2) of much coarser crystals filled the desiccation cracks of dolomite and the new pores (between calcite "C" and the dolomite crust) formed by the dissolution of calcite.

REMARKS ON THE GEOLOGICAL ORIGIN OF RUMANITE

NEACŞU, A.
Dept. of Mineralogy, Faculty of Geology & Geophysics, University of Bucharest, N. Bălcescu Blvd., RO-010041 Bucharest, Romania
E-mail: antonela@geo.edu.ro

Amber is a fossil resin with a disputed paleobotanical origin. Physico-chemical analysis indicated that Baltic amber (succinite) is more similar to the resin produced by family Araucariaceae. But this suggestion is not confirmed by paleobotanical research results (KOSMOWSKA-CERANOWICZ, 1999). In Romania a spectacular amber, named rumanite, has been exploited for a long time near Colţi (Buzău County). The infrared spectra of rumanite resemble those of succinite, but there are some important differences: *e.g.* rumanite has more carboxylic groups than succinite, probably because it is more oxidised than the latter. NMR studies (LAMBERT *et al.*, 1993) suggested that rumanite-like European fossil resin samples might have been weathered materials derived from an Agathis-like source. But the frequent presence of Sequoioxylon gypsaceum both in the amber-bearing formation and in the rumanite itself suggests that this conifer could have been the source of the ancient resin that has fossilized into the present-day amber occurring in the Oligocene deposits at Colţi. The botanical origin of amber may be traced back to plants belonging to Gymnosperms and Angyosperms, although the physico-chemical analysis indicate that it is not abietic acid or its derivatives but byciclic diterpen acid of the labdanum-type which is the fundamental component of amber. This means that pine cannot be regarded as an amber-producing tree. The solution could be a compromise. LARSSON (in FRAQUET, 1987) said that "the tendency is to consider it as rather a primitive type, representing an early stage in the developmental history of the Pinaceae which in their chemistry still retained archaic characteristics in common with the Araucariaceae". The precise origin may be established only when amber occurs together with the wood that produced it, and this is a very rare situation.

References

FRAQUET, H. (1987): Amber. London: Butterworths.
KOSMOWSKA-CERANOWICZ, B. (1999): Estudios del Museo de Ciencias Naturales de Álava, 14/2: 73–117.
LAMBERT, J. B. *et al.* (1993): Geoarchaeology, 8/2: 141–155.

CHEMICAL COMPOSITION OF TOURMALINE; A SIGNIFICANCE OF CRYSTAL-STRUCTURAL CONSTRAINTS

NOVÁK, M.[1] & CEMPÍREK, J.[2]
[1] Institute of Geological Sciences, Masaryk University, Kotlářská 2, 611 37 Brno, Czech Republic
E-mail: mnovak@sci.muni.cz
[2] Department of Mineralogy and Petrography, Moravian Museum, Zelný trh 6, 659 37 Brno, Czech Republic

Tourmaline is a common accessory to minor mineral in many magmatic and metamorphic rocks. General formula of tourmaline is: $XY_3Z_6T_6O_{18}(BO_3)_3V_3W$, where X = Na, Ca, □, K; Y = Mg, Fe^{2+}, Li, Al, Fe^{3+}; Z = Al, Mg, Fe^{3+}, Cr^{3+}, V^{3+}; T = Si, Al, B; B = B; V = OH, O; W = OH, F, O; chiefly heterovalent substitutions operate in the tourmaline group minerals. Tourmaline is widely used as an indicator of various processes. However, its chemical composition is controlled, besides external factors (*e.g.*, PT conditions, chemical potentials and competition with associated minerals) also by internal factors (crystal structural constraints – short-range ordering); consequently, using chemical composition of tourmaline as a strict indicator of geochemical processes might be misleading. We will focus on several examples of tourmaline from different geological and geochemical environments where short-range ordering play principal role on chemical composition of the relevant tourmaline. The following systems are discussed:

a) (Ca, F)-poor peraluminous system (*e.g.*, primitive barren pegmatites with the assemblage Qtz + Ab + Kfs + Ms + Bt + Tur; *e.g.*, NOVÁK *et al.*, 2004) with tourmaline showing $X_{Fe} < \sim 0.80$, a simple compositional trend was recognized showing increase X_{Fe} and ^{Y}Al during fractionation and tourmaline composition commonly tends to the simplified formula:

$^{X}(Na_{0.5}\square_{0.5})\ ^{Y}(Fe^{2+},Mg)_2Al\ ^{Z}Al_6\ (BO_3)_3\ ^{T}Si_6O_{18}\ ^{V}(OH)_3\ ^{W}(O_{0.5}OH_{0.5})$.

b) Ca-poor, F-rich peraluminous system (*e.g.*, Li-poor tourmaline-muscovite granite with the assemblage Qtz + Ab + Kfs + Ms + Tur; *e.g.*, NOVÁK *et al.*, 1998) with tourmaline showing high Na and low vacancy in the X-site, $X_{Fe} > \sim 0.90$ and low ^{Y}Al; tourmaline composition tends very well to the formula:

$^{X}Na\ ^{Y}Fe^{2+}_3\ ^{Z}Al_6\ (BO_3)_3\ ^{T}Si_6O_{18}\ ^{V}(OH)_3\ ^{W}F$;

or Li-rich peraluminous system (complex pegmatite with the assemblage Qtz + Ab + Elb + Ms + Lpd; *e.g.*, NOVÁK & TAYLOR, 2000) with tourmaline showing high Na and F, and tourmaline composition tends to the simplified formula:

$^{X}Na\ ^{Y}(Li,Fe^{2+},Al)_3\ ^{Z}Al_6\ (BO_3)_3\ ^{T}Si_6O_{18}\ ^{V}(OH)_3\ ^{W}F$.

c) F-poor, Fe^{3+}-rich alkaline system (metaevaporites with the assemblage Dol + Mgs + Kfs + Gp + Anh, Alto Chapare, Cochabamba, Bolivia; ŽÁČEK *et al.*, 2000) with tourmaline showing high K, very low X-site vacancy, high $^{Y}Fe^{3+}$ and very low ^{Z}Al; tourmaline composition tends to the simplified formula:

$^{X}K\ ^{Y}Fe^{3+}_3\ ^{Z}Mg_2Fe^{3+}_4\ (BO_3)_3\ ^{T}Si_6O_{18}\ ^{V}(OH)_3\ ^{W}O$.

These well-defined distinctive trends in tourmaline strongly suggest significant role of crystal-structural constraints on the tourmaline composition. In F-poor peraluminous rocks with variable X_{Fe} in tourmaline, the composition is characterized by high vacancy in the *X*-site, and significant amount of O in the *W*-site (NOVÁK *et al.*, 2004). The occupation of the *Y*-site, *Z*-site and O(1) site is controlled by short-range requirements (HAWTHORNE, 1996, 2002) and the configuration R^{2+}–R^{2+}–Al^{3+} in the *Y*-site and disorder of Mg and Al between *Y*- and *Z*-site is the most suitable; this configuration controls 0.5 *pfu* vacancy in the *X*-site and 0.5 *apfu* O in the *W*-site. In F-rich peraluminous rocks high amount of F in the *W*-site controls high Na and low vacancy in the *X*-site. The occupation of the *Y*-site is controlled by short-range requirements and the configuration with lowest charge of 3Y sites (Fe^{2+}–Fe^{2+}–Fe^{2+} in Li-poor system) or (Li–Fe^{2+}–Al in Li-rich system) in tourmaline is the most suitable; this configuration is compensated best by the low valence of *W*-site (high F) and it controls the low vacancy in the *X*-site. In F-poor, Fe^{3+}-rich alkaline system, high K in the *X*-site is controlled by high (Fe^{3+}) in the *Y*-site and especially by the network of the *Z*-site octahedra, built up by Fe^{3+} and Mg. Enlarged unit cell, due to Fe^{3+} dominant in the *Z*-site and rather small Fe^{3+} cation relative to Fe^{2+} in the *Y*-site, enables entering of large cation of K into the *X*-site; K is typically very low (commonly below the detection limit of electron microprobe) in tourmaline from K-rich peraluminous systems (*e.g.*, blocky K-feldspar unit in granitic pegmatites). Presence of O^{2-} in the *W*-site is necessary due to very high total charge of the *Y*-site.

This research was supported by the research projects MSM0021622412 to MN and MK00009486201 to JC.

References

HAWTHORNE, F.C. (1996): Canadian Mineralogist, 34: 123–132.
HAWTHORNE, F.C. (2002): Canadian Mineralogist, 40, 789–797.
NOVÁK, M. & TAYLOR, M.C. (2000): Canadian Mineralogist, 38: 1399–1408.
NOVAK, M., SELWAY, J.B. & HOUZAR, S. (1998): Journal of the Czech Geological Society, 43: 37–44.
NOVÁK, M., POVONDRA, P. & SELWAY, J.B. (2004): European Journal of Mineralogy, 16: 323–333.
ŽÁČEK, V., FRÝDA, J., PETROV, A. & HYRŠL, J. (2000): Journal of the Czech Geological Society, 45: 3–12.

BREAKDOWN OF PRIMARY COLUMBITE-TANTALITE RELATED TO ALPINE TYPE HYDROTHERMAL ALTERATION, AND REDISTRIBUTION OF ITS COMPONENTS

NOVÁK, M. & DOSBABA, M.
Institute of Geological Sciences, Masaryk University; Kotlářská 2, 611 37 Brno, Czech Republic
E-mail: mardos@sci.muni.cz

Maršíkov-Schinderhübel I pegmatite (LCT family, beryl-columbite subtype) forms symmetrically zoned dike, up to 1 m thick, cutting Sobotín Massif (amphibole gneiss). Accessory minerals assemblage includes: spessartine, beryl, gahnite, zircon and columbite-tantalite crystals (<1 cm) occurring mainly in albite unit. This primary assemblage was affected by dynamic metamorphism causing origin of rare chrysoberyl and sillimanite. Later the dike was cut by swarm of epidote rich Alpine type veinlets. This type of hydrothermal mineralization is very abundant in this region. There were observed two different textural-paragenetic assemblages containing primary columbite-tantalite replaced by later microlite, fersmite and rare betafite and tantalite. Proximal *replacement assemblage* is developed within fissure epidote (± chlorite, titanite, albite). Pseudomorphs after primary columbite-tantalite are formed mostly by fersmite > microlite; microlite, betafite and tantalite form overgrowths. Distal *fissure-filling assemblage* distributed randomly within the pegmatite is represented by microlite and fersmite developed on open microscopic fissures within primary columbite-tantalite (CERNY *et al.*, 1992). Primary oscillatory zoned columbite-tantalite and secondary tantalite exhibit Ta / (Ta + Nb) = 0.33–0.66 (0.82–0.85), Mn / (Mn + Fe) = 0.63–0.86 (0.52–0.57) and Ti < 0.19 (0.02) *apfu*; highly heterogeneous microlite is characterized by Ta / (Ta + Nb) = 0.46–0.96, Ti = 0–0.58 *apfu*, high Ca (~1.4 *apfu*), low Na (<0.23 *apfu*) and vacancy in the A-site (~0.4 pfu), highly variable F contents (0–0.63 *apfu*), rare betafite shows Ti = 0.69–0.85 *apfu*, Ta = 0.63–0.74 *apfu* and Nb = 0.50–0.56 *apfu*; slightly heterogeneous fersmite has Ta / (Ta + Nb) = 0.12–0.50 and Ti < 0.13 *apfu*. Both assemblages have minerals with similar chemical composition; they differ by presence/absence of epidote, textures (replacement *versus* fissure-filling) and more abundant Ti-rich minerals in the replacement assemblage. Chlorite thermometry yielded temperature range between 250 and 300 °C, which is in agreement with occurrences of hydrothermal systems with the assemblage epidote-chlorite (*e.g.*, 230–280°C – NOURALIEE, 2000; 220–300°C – TOMITA *et al.*, 2002). Such conditions probably correspond with the retrograde greenschist metamorphism during Palaeozoic ascent of this region.

Alteration of primary columbite-tantalite at both assemblages caused redistribution of its basic components – Nb, Ta and Ti. Nb was concentrated in fersmite, Ta in microlite and Ti in betafite (+Ti rich microlite and titanite). Coexistence of microlite and fersmite is unusual indicating its higher stability at given PTX conditions relative to pyrochlore-microlite with Ta / (Ta + Nb) matching primary columbite-tantalite precursor. Abundance of fersmite in similar assemblages may be more significant but it can be easily mistaken for pyrochlore with empirical formula $\square CaNb_2O_6\square$. Dominance of microlite and fersmite at both assemblages is a result of high activity of Ca. Higher activity of Ti and Fe resulted in origin of betafite and titanite at the proximal assemblage. Fersmite prevailing above microlite in pseudomorphs, and microlite forming overgrowths and isolated grains randomly occurring in epidote indicate higher mobility of Ta relative to Nb at conditions of lower greenschist metamorphosis. Prevailing epidote, minor chlorite, titanite and albite in Alpine veins, and textural relations in associated Nb-Ta oxides suggest that Ca, Al, most of Ti and perhaps Fe (Mg) were received from host amphibole gneiss. The relative mobility Ca > Ti > Ta > Nb is implied for these assemblages.

References

CERNY, P. NOVÁK, M. & CHAPMAN, R. (1992): Canadian Mineralogist, 30: 699–718.

NOURALIEE, J. (2000): United Nations University Reports, 15: 303–329.

TOMITA, T., OHTANI, T., SHIGEMATSU, N., TANAKA, H., FUJIMOTO, K., KOBAYASHI, Y., MIYASHITA, Y. & OMURA, K. (2002): Earth Planets Space, 54: 1095–1102.

EXPERIMENTAL ALTERATION OF VOLCANIC GLASS

OSACKÝ, M.[1], UHLÍK, P.[1] & KUCHTA, Ľ.[2]
[1] Department of Geology of Mineral Deposits, Faculty of Natural Sciences, Comenius University; 842 15 Bratislava, Slovakia
E-mail: osacky@fns.uniba.sk
[2] Department of Inorganic Chemistry, Faculty of Natural Sciences, Comenius University; 842 15 Bratislava, Slovakia

Experimental alteration of volcanic glass by variable concentrations of NaOH, NaOH + KOH, HCl was carried out at 70 °C for 25, 28, 50 days and at 150 °C, for 10 and 20 days. The products were examined by X-ray powder diffraction (XRD), infrared spectroscopy, scanning electron microscopy (SEM) and energy dispersive X-ray spectrometry (EDS). Experimental alteration was performed using an obsidian from Viničky and a perlite from Lehôtka pod Brehmi as starting materials. It was confirmed by XRD that starting perlite from Lehôtka pod Brehmi contained biotite, albite, quartz and smectite. Some of these minerals were observed by microscopic observation too. However uncrystalline glassy phase was predominated in obsidian from Viničky.

Experiments at 70 °C were carried out in closed PVC bottles with 5 g (grain size < 0.16 mm) and 2 g (grain size 10 μm) of the starting material in contact with 100 ml of 11.7 pH NaOH + KOH solution (NaOH/KOH ratio 1:1). Duration of experiments were 28 days. The experiments at 70 °C were carried out in opened bottles with 2 g (grain size 10 μm) of the starting material in contact with 20 ml of 11.7 or 7.7 pH NaOH + KOH solution (NaOH/KOH ratio 1:1) and 4.5 pH HCl solution. After transpiration of reaction solution 20 ml of distilled water was added (50 or 100 time) to volcanic glass. Duration of experiments were 25 and 50 days.

Experiments at 150 °C were conducted in teflon bottles containing 200 mg of starting material and 40 ml of 1 M NaOH or KOH solution, or 150 mg of starting material and 30 ml of 1 M NaOH or KOH solution. Each bottle was placed in an autoclave and was kept at 150 °C for 10 and 20 days.

XRD patterns of all volcanic glasses after low temperature experiments (70 °C) showed decrease of diffraction peaks of original minerals (Fig. 1a). Slight dissolution of volcanic glass was documented by elliptical micrometer-sized etch pits on the surface of volcanic glass grains. For the 150 °C experiment with 1 M NaOH solution, aggregates of phillipsite appeared initially after 10 days (Fig 1b). Analcime and albite were the most abundant reaction products using 1 M NaOH solution after 20 days (Fig 1b).

The results of experimental alteration of obsidian from Viničky in the present study fit well with diagenetic alterations of volcanic glass in the East Slovak Basin (ŠAMAJOVÁ, 1997).

Reference

ŠAMAJOVÁ, E. (1997): In: KIROV, G. N., FILIZOVA, L. & PETROV, O. (eds.) Natural Zeolites – Sofia '95, Sofia – Moscow: Pensoft Publishers, 215–226.

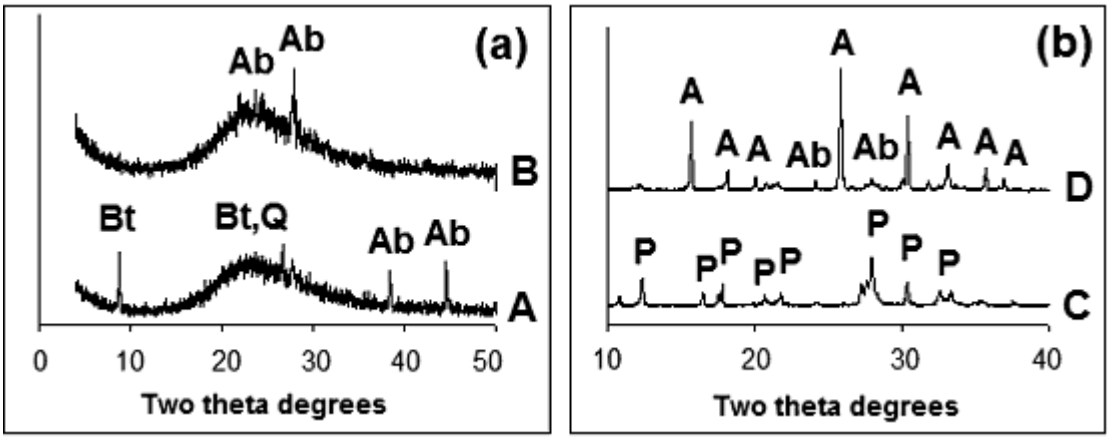

Fig. 1a: XRD pattern of the starting perlite from Lehôtka pod Brehmi (A), XRD pattern of perlite after experiment at 70 °C for 28 days in 11,7 pH NaOH + KOH solution (B). Ab = albite, Bt = biotite, Q = quartz.
Fig. 1b: XRD patterns of reaction products formed from obsidian from Viničky by reaction at 150 °C, for 10 days (C) and 20 days (D) in 1 M NaOH solution. P = phillipsite, A = analcime, Ab = albite.

STUDY OF HYDROTHERMAL VEINS WITH AXINITES FROM THE WESTERN CARPATHIANS

OZDÍN, D.[1], VOLEK, M.[2] & ŠTEVKO, M.[1]
[1] Department of Mineralogy and Petrology, Faculty of Natural Sciences, Comenius University, Mlynská dolina G, 842 15 Bratislava, Slovak Republic
E-mail: ozdin@fns.uniba.sk
[2] Karpatská 22, 90001 Modra, Slovak Republic

In the Western Carpathians two genetic types of axinite are found. Axinites occur in hydrothermal veins with characteristic Alpine-type paragenesis in metamorphic rocks (localities Limbach, Jasenie, Gretla, Čučma, Gemerská Poloma, Košice and Miskolc) or in contact zone of granitoids with sedimentary (Modra) or volcanic rocks (Vyšná Šebastová near Prešov). We studied axinite from five localities from Slovakia and one from Hungary (Miskolc) using electron microprobe and fluid inclusion study.

(1) Locality Limbach is situated in the Malé Karpaty Mts. near Bratislava and is formed by hydrothermal veins in grey-green metabasites. Hydrothermal veins contain mostly light brown ferro-axinite, albite and calcite; is acicular actinolite, quartz, pyrite, chalcopyrite etc. are rare. This ferro-axinite is the richest in magnesium in the Western Carpathians, it contains up to 2.88 wt. % (0.40 *apfu*) Mg. Homogenization temperature (Th) is in the 133–204 °C range (mean = 158 °C), ice melting temperature (Tm) is in the –2.8 to –12.9 °C range (mean = –9.18 °C). Average salinity of fluid inclusions is 12.8 NaCl equ. wt%. Average size of fluid inclusions is 18 μm.

(2) Hydrothermal veins on the locality Čučma (dump of Gabriela adit) and Čučma-Grexa (3) occur in the Early Paleozoic porphyroides in the Spišsko-gemerské rudohorie Mts. Various mineral assemblages are present at the locality Čučma. We described actinolite, quartz, dravite, chamosite, orthoclase, albite, calcite, zircon, titanite and fluorapatite. From among sulphides molybdenite, sphalerite, gersdorffite and pyrite occur. The axinite group is represented by ferro-axinite with Fe ↔ Mg substitution. This ferro-axinite contains only 0.3–0.8 *apfu* Mn. As a peculiarity of this mineralization the very rare overgrowth of two borosilicates, dravite and ferro-axinite can be mentioned.

(3) On the locality Grexa axinite occurs with magnesio-hornblende, quartz, calcite, annite, chamosite, titanite, dravite, schorl and minerals of the epidote group. The chemical composition of axinite is very variable and varies from prevalent ferro-axinite to manganaxinite. The content of Fe is in the range 0.45–0.96 *apfu*, Mg 0.06–0.39 *apfu* and Mn 0.08–0.57 *apfu*. We determined two characteristic substitution trends. In the first one Fe is replaced by Mg and in second substitution trend is Fe replaced by Mn.

(4) Dark green actinolite and dark brown axinite are the most abundant minerals in hydrothermal veins in the amphibolitic schists at the locality Gemerská Poloma (Pintiková valley). These two principal minerals are associated with andradite, quartz, calcite, fluorapatite, titanite, allanite-(Ce), zircon, cobaltite and gersdorffite. Chemical composition of axinite is variable and varies from ferro-axinite to prevalent manganaxinite (Fe 0.42–0.57 *apfu*, Mn 0.44–0.64 *apfu* and Mg 0.09–0.14 *apfu*). Zoned crystals of axinite from this locality have usually Fe-rich core (ferro-axinite) and Mn-rich rim (manganaxinite). Fluid inclusion study of manganaxinite indicates that axinite originated from highly saline fluids. Th values are 120–233 °C (mean Th 183 °C), Tm value is in the–26.1 to –13.5 °C range (mean –20.3 °C). Average of salinity of fluid inclusions is 22.2 NaCl equ. wt%. Average size of fluid inclusions is 11 μm. Th of associated quartz is in the 120–58 °C range (mean 136 °C), Tm of quartz is in the range –2.8 to –21.9 °C (mean 14 °C) and the average salinity is 18.36 NaCl equ. wt%.

(5) Axinite from the locality Košice-Bankov forms isolated grains in chloritic schists. The studied sample originated from the KV-2 borehole. According to microprobe analyses it is a homogenous ferro-axinite with major substitution Fe for Mg or Mn.

(6) Calcite–quartz–albite veins with axinite were described from Miskolc-Lillafüred by SZAKÁLL & FÖLDVÁRI (1995). These veins occur in metabasalt rocks. According to its chemical composition the mineral in question is ferro-axinite and its content of divalent cations (in *apfu*) is as follows: Fe 0.49–0.73, Mn 0.09–0.35 and Mg 0.21–0.38. Ferro-axinite from Miskolc is mostly chemically homogenous, but some crystals are zoned. The cores and the rims are enriched in Fe and Mg, respectively. On the basis of 20 wavelength dispersive microprobe analyses the relatively large scatter of the analytical values of ferro-axinite may correspond to two probable substitution trends. The first one is Fe ↔ Mg and the second is Fe ↔ Mn.

Reference

SZAKÁLL, S. & FÖLDVÁRI, M. (1995): Földtani Közlöny, 125: 433–442.

ENVIRONMENTAL RADIOCHEMISTRY AND COMPLEX ENVIRONMENTAL GEOCHEMISTRY OF YOUNG LAKE SEDIMENTS AT THE SZEGED FEHÉR-TÓ, HUNGARY

PÁL-MOLNÁR, E., BOZSÓ, G. & FRIEBERT, Z.
Department of Mineralogy, Geochemistry and Petrology, University of Szeged, P.O. Box 651, H-6701 Szeged, Hungary
E-mail: palm@geo.u-szeged.hu

Our study is focusing on the effects of natural radioactive elements of young lake sediments on living organisms. Besides we searched for the reasons for the enrichment of natural radionuclides and trace contaminants in the sediment of Szeged Fehér-tó Lake.

The Szeged Fehér-tó is well known of intensive fish breeding, and our study area was allocated on two hatcheries of the lake system. Hatcheries have got a complex environmental role, since large areas of them fall under natural protection (Kiskunság National Park), as the territory has got a major ornithological importance. Radioactive elements (members of natural radioactive series) and heavy metals in the sediment might have indirect effects on humans, as well as on birds migrating and feeding in the area.

The aim of the study was to measure the natural γ-radiation, determining the amount of natural radionuclides (^{238}U, ^{232}Th, ^{40}K), and to determine the total γ-radiation of the area. Besides, main element and trace element compositions, mineral composition and total carbon content were measured in order to determine the causes of radionuclide enrichment in the sediment.

Main and trace element contents were determined with X-ray fluorescence (XRF). Based on the results of these measurements representative samples were chosen for further X-ray diffraction (XRD) analysis. These provided the means for determining the mineral composition of sediments on the area. Results show mineralogical homogeneity. Total organic carbon content (TOC) was measured with Rock-Eval pyrolysis for representative samples of the two hatcheries.

The enrichment or the anomalies in the normal distribution of radionuclides and trace contaminants in the sediment of the lakes cannot be interpreted, unless the distribution of the medium, carrying these elements is known. XRD and TOC measurements were carried out for this reason. Based on the results, element distribution maps and correlation charts were compiled, presenting the relations between main, trace and radioactive elements. The enrichment of radioactive and contaminant elements were understood with the help of these relations.

Analyses have shown that irrespective of the methods of extraction the radionuclide concentration is 5-10 times higher than the average data for saline lakes, however concentrations higher than the natural value by an order of magnitude or more did not occur. The research proved that natural isotopes could be linked to argillic minerals, oxides with good absorption capabilities, and heavy minerals. Main and trace element contents of the lake sediments do not exceed the usual values by an order of magnitude, nevertheless the concentrations of some trace elements (As, Cr, Cu) are close to the contamination threshold, and other trace elements (Mn, Ni) appear in larger quantities, than it was previously expected.

Based on the results of our research we recommend further dosimetric and trace element analyses in the area.

LAPIDATOR PROJECT – KOCH SÁNDOR MINERAL COLLECTION, DEPARTMENT OF MINERALOGY, GEOCHEMISTRY AND PETROLOGY, UNIVERSITY OF SZEGED

PÁL-MOLNÁR, E. & JÁNOSI, T.
Department of Mineralogy, Geochemistry and Petrology, University of Szeged, P.O. Box 651, H-6701 Szeged, Hungary
E-mail: palm@geo.u-szeged.hu

The main goal of the Lapidator Project is to compile the digital archive of the Koch Sándor Mineral Collection, which is located at the Department of Mineralogy, Geochemistry and Petrology, University of Szeged. The archive would be managed by an up-to-date software, handling 2D and 3D photographs and databases on the characteristics of minerals.

As an early outcome of the project we have already set up a software, which goes well beyond the execution of ordinary database commands, and ensures the technical background for various educational, demonstrational and promotional projects.

Preliminary works have started with the planning of the general setup of the system. As a first step a Systematic Mineralogy Database was constructed on the basis of the IMA (International Mineralogical Association) accepted minerals (www.mindat.org, www.webmineral.com, www.matident.com, etc.). This contains the name, taxonomy, formula, elementary composition, physical characteristics, and photographs of the minerals. Further sub-databases were also added to the software in order to enhance the primary, systematic framework. These are: the digital Koch Sándor Mineral Database, the archive of Hungarian mineralogical publications, and the most important places of occurrences within the Carpathian Basin, supplemented with maps. The basis of the software, i.e. the Systematic Mineralogy Database, also provides a didactic guideline for the user to digest the presented knowledge. The digital Koch Sándor Mineral Database includes all the 6000 minerals of the collection, with 3D rotating images of some of the most beautiful pieces, exhibited at the department in glass-cases. With a simple search one can gather the publications of the previous decades that write about or mention a chosen mineral. Further important information can be gained by checking the places of occurrence and accessibility on maps covering the whole Carpathian Basin. Beside all of these, the software can also give a historical view on the life and work of famous scientists dealing with mineral collection.

The appearance of the software was designed to be simple and elegant at the same time. Different options can be accessed easily, while parameters referring to each other and hypertext solutions provide a web like character for the whole system. In accordance with the Hungarian user environment the software is supported by Win32 based operational systems, however current developments aim at involving Macintosh based systems too. The installed software downloads updates and changes in the database through the Internet automatically, thus the user is always faced with the latest version of the digital collection.

In all we have produced a software which is ready to be applied by people of any age, both with a professional or non-professional background and either for research or simply for studying the wonders of minerals.

"HISTORY OF MINERALS, ROCKS AND FOSSIL RESINS DISCOVERED IN THE CARPATHIAN REGION" – A NEW HANDBOOK

PAPP, G.
Department of Mineralogy and Petrology, Hungarian Natural History Museum, Pf.: 137, H-1431 Budapest, Hungary
E-mail: pappmin@ludens.elte.hu

Not only mineralogy has a long tradition in the Carpathian region but mineral species, first described from here, also have their own, sometimes a long and eventful, history. A classic example is nagyágite: first found in 1747, described at the end of the 1760s, obtained its present name in 1845 but had the first reliable structural model only in 1999. Discredited species may also have their exciting story, even if it has already been ended. Synonyms, language and spelling variants of a given mineral name are also of interest. A comprehensive review of the history of Carpathian minerals, however, had not been published earlier. To fill this gap a long-term research was begun in the 1990s. A bilingual list of valid and discredited species and names (PAPP & SZAKÁLL, 1996) and a paper containing brief case studies (PAPP, 1997) embodied preliminary results of this project. Publication of the first comprehensive topographical mineralogy of the Carpathian region (SZAKÁLL, 2002), including a geological background and some mining history, made it possible to concentrate even more on the historical aspects of the minerals of the area and to write a book that can be regarded as a kind of "historical companion" to that excellent topographical mineralogy. The first version of the book was published in Hungarian (PAPP, 2002), and now an updated, corrected and slightly rearranged English version is available (PAPP, 2004).

The book discusses the minerals (and rocks, fossil resins and hydrocarbons) that were first described from the Carpathian region (*i.e.* their type locality is in the region). Information is arranged alphabetically into 230 entries corresponding to mineral names. They include modern scientific names (terminated by -ite or -ine), outdated scientific names (like descriptive, systematic or chemical names), "popular" or "trivial" names and miners' terms and their spelling variants or misspellings, collected from international handbooks and papers.

For each entry the chemical formula and symmetry of the mineral (or an explanation of non-species or invalid species names), a reference to the first publication of the name, history of the mineral, type locality and etymological data are given. The historical part of the entries summarises the most important steps of the research history of the mineral from its discovery and reviews the subsequent changes of its status. Details of the descriptions taken from the original papers (given in PAPP, 2002) are omitted but a selection of their data (chemical analyses and basic crystallographic data) is given in tables. 592 synonyms and spelling variants are listed as cross-references and their data are appended to the relevant entry. The chapters on rocks and fossil resins contain 23 and 21 entries plus 19 and 32 cross-reference entries, respectively. The text is illustrated by 85 black and white (mainly crystallographic) drawings.

Localities mentioned in the entries are listed in a table with their co-ordinates and most of them are shown in a sketch map. Type localities are briefly described in a separate chapter containing 10 historical pictures.

Biographical data of 59 eponyms of minerals (persons, whose name was given to the species) along with 49 portraits are given in a special chapter. Further 12 portraits are included in the second page of the volume.

Detailed bibliographical data of ~1270 references cited in the text can be found in the reference list.

Advice and help was given by many colleagues of the countries of the region, among them A. Gawęda (Poland), Gh. Damian, V. Gorduza, Gh. Ilinca, D. Pop, Gh. Udubaşa (Romania), M. Chovan, R. Ďuďa, M. Orvošova, D. Ozdín (Slovakia) and V. M. Kvasnytsya (Ukraine) can be mentioned first. Some of the chapters were reviewed by F. Pertlik (minerals), F. Koller, Gy. Lelkes-Felvári, Gy. Szakmány (rocks), M. Hámor-Vidó, N. Vávra (fossil resins and hydrocarbons), J. Földessy, I. Gatter (locality descriptions). Special thanks are due to C. J. Stanley (NHM, London) for the English editing. Publication of the book was sponsored by the grant of the Ministry of Cultural Heritage and the National Cultural Fund of Hungary (2312/0348) and by the Hungarian Natural History Museum.

Further data on the book together with downloadable pages, list of corrections and additions are available at http://www.nhmus.hu/~pappmin/pg_hp_studia15_1.html.

References

PAPP, G. (1997): Acta Mineralogica-Petrographica (Szeged), 38 (Suppl.): 65–75.

PAPP, G. (2002): A Kárpát-övezetben felfedezett ásványok, kőzetek és fosszilis gyanták története. Budapest: Magyar Természettudományi Múzeum.

PAPP, G. (2004): History of minerals, rocks and fossil resins discovered in the Carpathian region. Budapest: Magyar Természettudományi Múzeum.

SZAKÁLL, S. (ed., with the contributions of UDUBAŞA, G., ĎUĎA, R., SZAKÁLL, S., KVASNYTSYA, V., KOSZOWSKA, E. & NOVÁK, M.) (2002): Minerals of the Carpathians. Prague: Granit.

SZAKÁLL, S. & PAPP, G. (1996): A Kárpát-övezetben felfedezett ásványok / Mineral species discovered in the Carpathian area. Miskolc: Herman Ottó Múzeum.

EUHEDRAL, JURASSIC DIAGENETIC OPAL-CT FROM ÚRKÚT, BAKONY MTS., HUNGARY

PEKKER, P. & WEISZBURG, T. G.
Department of Mineralogy, Eötvös Loránd University, Pázmány Péter sétány 1/C, H-1117 Budapest, Hungary
E-mail: pekker.peter@vipmail.hu

During the systematic mineralogical characterisation of the Toarcian–Dogger pelagic sedimentary "Eplény Limestone" Formation in Úrkút, Bakony Mts., Hungary, we found an alternation of softer, more clayey and harder, strongly silicified strata. We showed that this silicification was related to early diagenetic processes (PEKKER & WEISZBURG, 2006).

SiO_2 phases were identified, mainly by using separated and specially prepared (polished; broken, etched etc.) samples, by X-ray powder diffraction (XRD), by local Fourier transform infrared spectroscopy (FTIR) and by scanning electron microscopy (SEM + EDX).

Beside various forms of quartz **opal-CT "polycrystals"** were identified, forming two groups on the basis of aggregate morphology: "**spheres"** made up of micrometre-sized euhedral blades and **"pore wall coatings"** made up of similar blades, covering apparently the original pore walls of the not fully consolidated sediment.

The **spheres** made up of blades have a uniform diameter of 7–10 μm and are widespread in the original pore space. These spheres resemble both in size and morphology euhedral opal-CT crystal aggregates, described as *lepispheres* by FLÖRKE *et al.* (1975). The only, but significant, difference is that the spheres in our samples have a pronounced concentric inner structure: most cases they are built up of a core of 1–3 μm and a distinct outer shell of varying thickness. The gap between the outer surface of the core and the inner surface of the outer shell may reach up to 1–2 μm (Fig. 1). Spheres often coalesce so that within one common outer shell two or more discrete cores are present. That concentric inner structure indicates that opal-CT crystallised directly as perimorphose on the surface (outer shell) and on the inner wall (core) of spherical cavernous structures present during the early diagenesis. That observation and the strikingly uniform size distribution of the spheres suggest that the crystallisation surface was provided by living organisms like bacteria that are abundant in a wide variety of environmental conditions, including deep sea environments. Fossilised (calcified) bacteria of similar aggregate morphology were reported from a different environment (BEHR & RÖHRICHT, 2000; cyanobacteria, *e.g. Pleurocapsa*, *Gloeocapsa*). FORTIN *et al.* (1997) described silica "crust" precipitating on bacterial surfaces, too. The presence of the second aggregate morphology, the **opal-CT coating,** found on the original pore walls (Fig. 2.) support the hypothesis of a syndiagenetic opal-CT crystallisation on the surface of contemporary (Jurassic) organisms, namely bacteria, based on their size and shape.

References

BEHR, H.-J. & RÖHRICHT, C. (2000): International Journal of Earth Sciences, 89: 268–283.

FLÖRKE O. W., JONES J. B. & SEGNIT E. R. (1975): Neues Jahrbuch für Mineralogie, Monatshefte: 369–367.

FORTIN, D., FERRIS, G. F. & BEVERIDGE, T. J. (1997): In: BANFIELD, J. F. & NEALSON, K. H. (eds.): Geomicrobiology: Interactions between Microbes and Minerals. Reviews in Mineralogy, 35: 161–180.

PEKKER, P. & WEISZBURG, T. G. (2006): Földtani Közlöny, Budapest, 136: accepted.

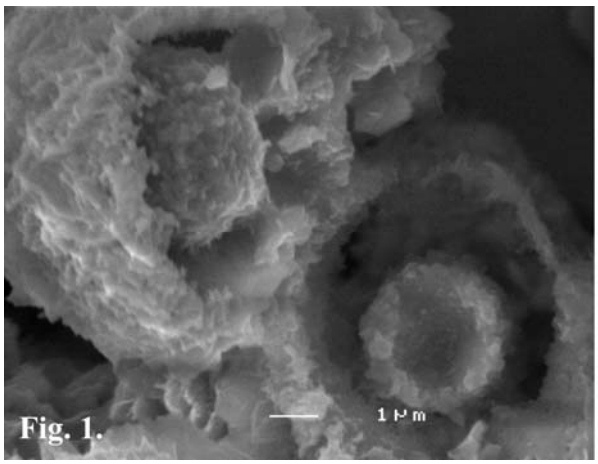

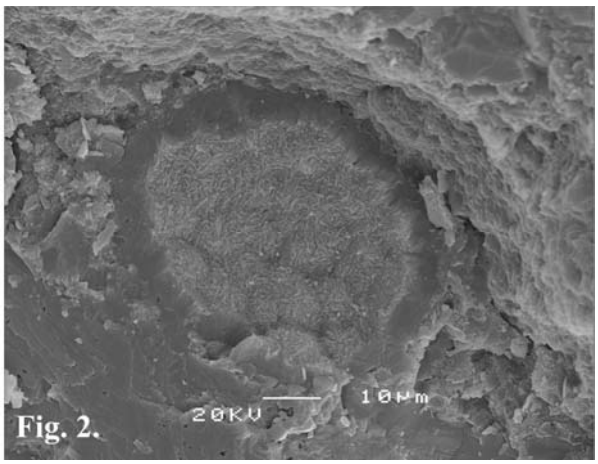

Fig. 1: Concentric spheres of blade-shaped euhedral opal-CT crystallites – perimorphs after bacteria.
Fig. 2: Coating of blade-shaped euhedral opal-CT crystallites – pore wall coating.

MINERALOGY AND FORMATION CONDITIONS OF GABBRO PEGMATITES AND OVERPRINTING HYDROTHERMAL PARAGENESES IN THE SZARVASKŐ COMPLEX, BÜKK MTS., NE-HUNGARY

PÉNTEK, A.[1], MOLNÁR, F.[1] & WATKINSON, D. H.[2]
[1] Department of Mineralogy, Eötvös Loránd University, Pázmány Péter sétány 1/C, H-1117 Budapest, Hungary
E-mail: pentekatti@hotmail.com
[2] Department of Earth Sciences, Carleton University, 1125 Colonel By Drive, Ottawa K1S 5B6, Canada

Gabbro pegmatites are common features in the Szarvaskő Ophiolite Complex, Bükk Mts., NE Hungary. Pegmatitic structures like these are less studied in ophiolitic gabbros, especially in those of the Neotethyan realm. Hence, one of the major aspects of our work (PÉNTEK, 2004) was to support the knowledge on pegmatites in ophiolite-related gabbro intrusions by analyzing their relationships to the host rock, textural variations and mineral composition. These observations were used to characterize volatile enrichment, segregation of magmatic fluids and their interaction with silicates during crystallization of the pegmatite bodies. Previous investigations (ÁRKAI, 1983; SADEK *et al.*, 1996) have shown that rocks of the SOC have suffered alteration during sea-floor hydrothermal and low-grade regional metamorphic events. Our study was also aimed to refine knowledge about these processes by combining mineralogical and fluid inclusion data.

Pegmatites of two studied localities were classified according to their shape and texture. Pegmatitic patches, pockets and narrow dykes precipitated from a locally segregated hydrous melt, while thick and felsic dykes were intruded later. Homogeneous pegmatitic pods crystallized simultaneously (Fig. 1) in contrast to zoned pods, indicating further differentiation of the hydrous melt. In pegmatites, clinopyroxene, amphibole, plagioclase, Fe-Ti oxides, biotite, quartz and apatite are the main rock-forming phases. Variation of the mineral assemblages and their chemistry in pegmatite bodies was also influenced by enrichment of volatiles and incompatible elements in the melt due to interaction with the host sedimentary rocks. During crystallization of pegmatites a fluid phase separated, as indicated by granophyric textures and fluorapatite compositions. This magmatic fluid caused deuteric alteration of the primary pegmatitic assemblage, which is manifested by the alteration of magnetite and pyroxene, accompanied by the formation of biotite and zoned amphibole (Fig. 2). This process took place under continuous cooling magmatic-submagmatic conditions.

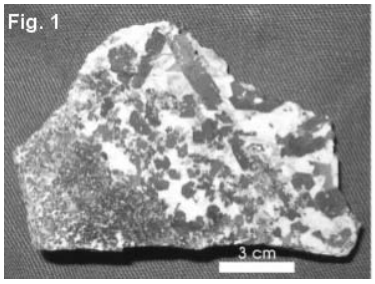

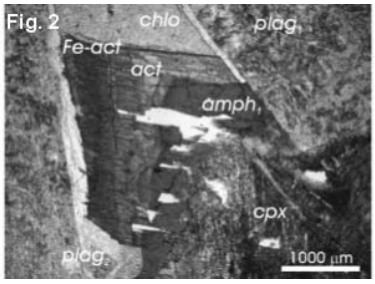

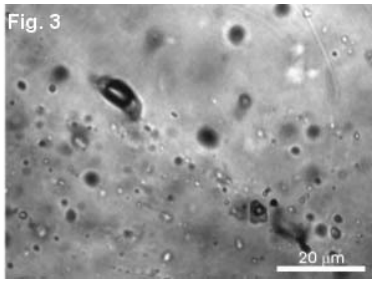

The pegmatites and the host gabbro underwent postmagmatic alteration due to sea-floor hydrothermal activity. The responsible fluids were identified in two fluid inclusion generations. Both occur secondary in pegmatitic quartz, and have salinities clustering around the mean seawater salinity (~3,2%). One of them (Fig. 3) represents a boiling aqueous system, where heterogeneous entrapment occurred around 300 °C. The other fluid exhibits constant 15-20 vol% vapour phase and an average homogenization temperature of 240 °C. Typical of this process is alteration of all primary phases and formation of actinolite, chlorite, clinozoisite and albite. Mineral assemblage, mineral- and fluid inclusion thermometry indicate a polyphase hydrothermal process between 250 and 400 °C. The Alpine regional metamorphism was accompanied by intense veining of a prehnite-chlorite-quartz-calcite-feldspar assemblage. Chlorite thermometry and isochores of primary fluid inclusions could be used to define entrapment conditions of the low grade metamorphic fluids, ranging between 270–285 °C and 1.5–2 kbars.

This work was supported by the NSF (OTKA) No.T 049633 and by the Canadian-Hungarian (CAN-2/04) and Croatian-Hungarian (HR-17/2004) Science and Technology Cooperation, both funded by the Technological and Innovation Found, Hungary.

References

ÁRKAI, P. (1983): Acta Geologica Hungarica, 26: 83–101.
PÉNTEK, A. (2004): In: Conference of Students' Scholarly Circles (TDK) Thesis, 72. (in Hungarian)
SADEK, G.D., ÁRKAI, P. & NAGY, G. (1996): Acta Mineralogica-Petrographica, 37: 99–128.

HEAVY METAL POLLUTION IN THE AREA OF CRUCEA URANIUM MINE (ROMANIA)

PETRESCU, L.[1] & BILAL, E.[2]
[1] Department of Mineralogy, University of Bucharest, 1 Nicolae Bălcescu Blvd., 010041 Bucharest, Romania
E-mail: lucpet@geo.edu.ro
[2] Département Géochimie et Procèdes de l'Environnement, École Nationale Supérieure des Mines, 158 Cours Fauriel, 42023 Saint Etienne, France

Inductively Coupled Plasma – Atomic Emission Spectroscopy and X-Ray Fluorescence Spectroscopy methods were used to evaluate the metals (ppm) from soils for the mine dumps of Crucea-Botusana uranium deposit (Bistriţa Mountains, Romania) related to exchangeable fraction and respective available for vegetation roots. Samples were collected in June 2004 from different mine dumps in the Crucea-Botusana uranium deposit, mainly from G1, G4, G5, G6, G8, G9, G1/30 and G950 mine waste galleries.

Prior to "blaming" mining activities for the contamination of the environment, one must first determine the baseline contamination due to the natural existence of the mineralization in the area. In the mineralized area, there is an increase of the uranium concentration in the soil as a result of supergene alteration of the uraniferous formations. After having calculated the means and the standard deviations for the trace elements in the soils, we were able to determine the 95% confidence limits. Thus, the values of 61.92 ppm appear to be the anomalous threshold for uranium and 43.04 ppm the background level. In the case of thorium the background level is 14.78 and the geochemical threshold is 30.30 ppm. Anomalous values for U, exceeding the geochemical threshold, were determined for the soil of the former experimental gallery, G5 gallery and for the soil from the proximity of the ore bunker. In the case of Th, we determined values above the geochemical threshold only in the soil samples taken from the G8-gallery waste dump.

The enrichment in any of such elements represents a negative factor for the environment. The pollution of the environment is, almost always, caused by a mixture of contaminants and not by one single element. This is why, in the environmental studies, we used the cumulative enrichment factor (or the contamination index) of the geological materials in order to identify the multi-element contamination, which may increment the toxicity of the metals. The contamination index (CI) is calculated according to formula:

$$CI = \frac{\sum_{N=1}^{n}\left(\frac{C_N}{B_N}\right)}{N}$$; where: C_N = total concentration of the element, expressed in ppm; B_N = background value of the concentration for the same element, expressed in ppm; N = total numbers of elements. In our case, CI varies from 1.485 to 5.02, indicating that all the mine dumps contain radioactive and heavy metals at levels that may induce toxicity in the ecosystem. The wastes that could represent a greater danger are those connected to the Ae, G8 and G1/30 galleries.

The short-term impact on the soil-to-plant system depends on the bioavailability of heavy metals. In order to select the mine dumps that could induce a short-term impact on the environment, the danger index (DI) was calculated. This one derives from CI and was calculated according to formula:

$$DI = \frac{\sum_{N=1}^{n}\left(\frac{C_{\text{exchangeable fraction}}}{C_{\text{available for vegetation roots}}}\right)}{N}$$; were: $C_{\text{exchangeable fraction}}$ = the concentration of metals determined after extraction with $MgCl_2$, expressed in ppm; $C_{\text{available for vegetation roots}}$ = the concentration of metals determined after extraction with EDTA, expressed in ppm; N = number of elements. The calculated DI has proved that none of the examined mine dumps represent a danger for the vegetation.

By comparing the contamination index with the danger index the following tendency was emphasized: CI of mine dumps G1, G1bis, G4, G5, G5bis, G6, G8, G9, Ae, G1/30 and G950 is >1, while DI is < 1. This indicates that the related dumps are contaminated, but the short-term impact on the environment is not alarming.

Based on the contamination index and danger index calculated for the mine dumps, we can conclude that Crucea-Botusana mine don't need urgent remediation.

Acknowledgments

The inorganic chemical components were determined at Département GENERIC of the École Nationale Supérieure des Mines de Saint Etienne (France) under Rhône-Alpes Region – TEMPRA Project 00825042. The authors thank Dr. Jacques Moutte and Frederic Gallice for technical assistance.

MONAZITE FROM A LOW TATRA GARNET LEUCOGRANITE: AGE, ORIGIN AND RELATION TO GARNET

PETRÍK, I.[1], KONEČNÝ, P.[2] & HOVORKA, D.[3]
[1] Geological Institute, Slovak Academy of Sciences, Dúbravská 9, 84005 Bratislava, Slovakia
E-mail: igor.petrik@savba.sk
[2] Geological Survey of the Slovak Republic, Mlynská dolina 1, 81704 Bratislava, Slovakia
[3] Faculty of Sciences, Comenius University, Mlynská dolina G, 842 15 Bratislava, Slovakia

A garnet-bearing leucogranite occurs within the complex of ortho- and paragneisses on southern slopes of the Nízke Tatry Mts. The rock is medium-grained leucogranite with 4% of biotite and up to 4% of garnet. K-feldspar (20%) is perthitic, interstitial, plagioclase (40%, An_{13-20}) forms small phenocrysts. Garnet is euhedral (0.5–3 mm) partly chloritised. Its composition is (centre–rim): $py_{20–7}$, $spess_{5–22}$, $alm_{72–67}$, $andr_{2.5–2}$, $gross_{0.5–3}$. Muscovite was found within feldspars, rarely enclosing fibrolitic sillimanite. Among accessories, monazite is the most prominent forming large subhedral crystals. It is accompanied by apatite and small needle-like zircons, and hosted by quartz, plagioclase or late muscovite.

The rock composition is peraluminous (A/CNK = 1.15) with low Rb/Sr ratio (0.33) and elevated MnO and HREE due to accumulation of garnet. Zr and LREE saturation temperatures give 740 and 809 °C, respectively (WATSON & HARRISON 1983, MONTEL 1993), the higher LREE-derived value being probably due to inherited nature of a large part of monazite.

The big monazite grains commonly show brighter cores and darker rims due to increased Y contents. The darker zones are saturated by Y as documented by small late xenotimes at monazite grain boundaries. Empirical thermometer of PYLE *et al.* (2001) yielded 650 °C for rims and 470 °C in the core probably indicating a restite character of the core, which seems to be inherited from a metamorphic protolith of the granite. The high-Y rims result from exchange reaction with garnet and are, therefore, interpreted as directly related to the granite formation. Garnet is considered a product of incongruent vapour-absent melting of biotite:

$$Bt + sill + qtz = grt + Kfs + melt$$

The present biotite may have formed by retrogression of the garnet on cooling segment of the *P*-*T* path. The assemblage bt – grt – plg – sill – H_2O gives average $T = 609 \pm 113$ °C and $P = 4.1 \pm 1.9$ kbar and 710 ± 139 °C and $P = 6.3 \pm 2.6$ kbar for various garnet rim compositions (THERMOCALC, HOLLAND & POWELL, 1998).

More than 30 grains were dated by microprobe Cameca SX-100 (KONEČNÝ *et al.* 2005) some using detailed profiling: The brighter core containing low Y yielded 352 ± 5 Ma ($n = 59$) while the rims 334 ± 6 Ma ($n = 24$). The coincidence of temperatures recorded by monazite Y-rich rims and garnet–biotite suggests that the rims date the last retrogressive event in history of the rock. Retrogression of garnet by biotite and sillimanite by muscovite requires free fluids, which could have acted also as agents between monazite and garnet.

It is concluded that the leucogranite formed 330-340 Ma ago via biotite fluid-absent melting producing peritectic garnet. Fluids evolved during cooling retrogressed parts of garnet to biotite and mobilized Y, which attacked restitic monazite. Dissolved and re-precipitated monazite rims record the lower age limit of this event. The higher limit is given by the age of restitic low Y monazite centres between 350–360 Ma.

References

HOLLAND, T.J.B. & POWELL, R. (1998): Journal of Metamorphic Geology, 16: 309–343.
KONEČNÝ, P., SIMAN, P., HOLICKÝ, I., JANÁK, M. & KOLLÁROVÁ, V. (2004): Mineralia Slovaca, 36: 225–236.
MONTEL, J-M. (1993): Chemical Geology, 110: 127–146.
PYLE J.M., SPEAR, F.S., RUDNICK, R.L. & MCDONOUGH, W.F. (2001): Journal of Petrology, 42: 2083–-2107.
WATSON, E.B. & HARRISON, T.M. (1983): Earth and Planetary Science Letters, 64: 295–304.

PRELIMINARY DATA CONCERNING THE Cu, Au, Ag DISTRIBUTION IN THE BOLCANA ORE DEPOSIT, METALIFERI MTS., ROMANIA

POPESCU, GH. C. & CIOACA, M.
Department of Mineralogy, University of Bucharest, 1, N. Bălcescu Bvd., RO-010041 Bucharest, Romania
E-mail: mihaela2012@yahoo.com

The Bolcana ore deposit is one of the 14 porphyry copper structures belonging to the Neogene metallogenesis of the Metaliferi Mts. The deposit is located on the south-western border of the Brad–Săcărâmb District, approximately 25 km NE of Deva. It constitutes a part of the Troița–Măgura metallogenetic field, with an exceptional concentration of metallic elements, presenting a copper-gold ring-zoned structure (POPESCU & NEACSU, 2005); the porphyry mineralization occupies a central position around which gold-silver and polymetallic veins have developed. The copper-gold mineralization has a spatial and genetical relationship with a subvolcanic body of Sarmatian age, formed of amphibole-bearing andesites/microdiorites. The structure exhibits a brecciated structure with intensely hydrothermally altered microveins and/or impregnations within the host rock. The main metallic minerals are pyrite, chalcopyrite, magnetite and subordinately, bornite, hematite, molybdenite, and native gold. The most abundant minerals are chalcopyrite and magnetite; subordinate amounts of pyrite and bornite occur in the central part of the ore deposit. The mineralization is superimposed on a potassic alteration zone, whereas pyrite becomes dominant towards the upper and marginal part of the intensely argillized mineralized body. The copper-gold mineralization is cross-cut by epithermal polymetallic veinlets formed of sphalerite, galena, pyrite, chalcopyrite, tetrahedrite, bournonite, marcasite, *etc.*, associated with carbonates and quartz-gold veinlets.

The ore deposit has been investigated with mining works (at five levels) and drill works spanning over 1000 m in depth. Such works have made possible to outline four cylindrical breccia columns within the Bolcana subvolcano ("breccia pipe") which were richer in mineralization (the F17, F282-F13, F21-F4 and F3 zones). Distribution of Cu, Au and Ag marks an increase of the metal content with depth, and a direct correlation between Au and Cu. Distribution maps drafted for each horizon and outlining the four mineralized columns mentioned above, show Cu contents of over 2% and Au contents of over 0.3 g/t, as well as the overlapping of Cu, Au and Ag mineralization in most situations. There are cases where copper, gold and silver occur separately, suggesting two stages of mineral genesis: one with copper and another one with gold-silver.

Reference

POPESCU, GH & NEACSU, A. (2005): In: Abstracts, Vol. 37, No. 97, GSA Annual Meeting SLC 2005, p. 516.

PHYSICOCHEMICAL CONDITIONS AND STAGES OF MINERAL FORMATION IN THE SAULYAK GOLD DEPOSIT (RAKHIV ORE DISTRICT, TRANSCARPATHIAN REGION)

POPIVNYAK, I., TSIKHON', S., OLIYNYK, T., NIKOLENKO, A., NIKOLENKO, P. & MARUSYAK, V.
Ivan Franko National University, L'viv, Ukraine
E-mail: tsikhon_s@ukr.net

The results of integrated mineralogical-genetic analysis of ores, accompanied by thermobarochemical research of inclusions in minerals as well as the investigation of thermoelectric properties of minerals-semiconductors show that within the limits of the Saulyak deposit each delineated mineral assemblage was formed during the corresponding stages of ore formation characterized by mineral fluids, different portions of which entered into the ore body after intensive tectonic movements. Every portion of fluids that entered into the ore body can be characterized by its specific chemical composition and p-T conditions and can be delineated both spatially and chronologically.

Formation of ores of the Saulyak deposit took place during five stages within the pneumatolytic–hydrothermal process of mineral formation: 1) pyrrhotite–quartz stage (475–385 °C); 2) tourmaline–quartz stage (465–385 °C); 3) pyrite–quartz stage (410–250 °C); 4) gold–polysulphide stage (335–110 °C); 5) quartz–carbonate stage (150–80 °C). The overall temperature range of mineral formation was 475–80°C; the pressure of the gold-bearing system varied from 145–105 to 90–85 MPa; bulk density of the gold-bearing carbonic aqueous fluids was 0.815–0.770 g/cm^3. Temperature ranges of formation of paragenetic associations of the productive (gold-bearing) complex are as follows: 320–240 °C: quartz–pyrite–sphalerite with gold; 335–220 °C: sphalerite–galena with gold; 220–160 °C: gold–chalcopyrite; 170–110 °C quartz–carbonate with gold; overall temperature range of the productive mineral formation is 335–90 °C; the most part of native gold was formed in the temperature range of 280–120 °C.

As for the majority of deposits of gold-bearing provinces, Saulyak deposit is also characterized by a cyclic development of hydrothermal mineral formation processes. Based on the inverse-regressive variability of the p-T conditions, the cyclic character is detected in the succession of minerals (quartz → sulphides → carbonates) within each cycle.

Gold-bearing fluids were first of all medium-temperature carbonic aqueous ones and despite the complex polycyclic character of the gold-bearing ore formation, native gold precipitated from only one kind of fluid during the gold–polysulphide stage of mineral formation.

Results of comprehensive geological-genetic, mineralogical-physical and thermobarogeochemical analyses of ores of the Saulyak deposit enabled us to make a conclusion that the natural diversity of the gold-bearing sulphide-quartz mineralization of the Saulyak deposit is the result of the development of a uniform pneumatolytic-hydrothermal sequence, with discrete stages and inverse-regressive variability of p-T conditions of thermobaro-geochemical parameters in time as well as in space.

RELATIONSHIPS BETWEEN THE PROPERTIES OF FERRIMAGNETIC NANOCRYSTALS AND BIOLOGICAL CONTROL OVER CRYSTAL GROWTH IN MAGNETOTACTIC BACTERIA

PÓSFAI, M.[1], KÓSA, I.[1], KASAMA, T.[2], CHONG, R. K. K.[3], SIMPSON, E. T.[3], FINLAYSON, A. P.[3], DUNIN-BORKOWSKI, R. E.[3], BUSECK, P. R.[4] & FRANKEL, R. B.[5]
[1] Department of Earth and Environmental Sciences, University of Veszprém, Veszprém, POB 158, Hungary
E-mail: posfaim@almos.vein.hu
[2] Frontier Research System, The Institute of Physical and Chemical Research, Japan
[3] Department of Materials Science and Metallurgy, University of Cambridge, Pembroke Street, Cambridge, UK
[4] Department of Geological Sciences, Arizona State University, Tempe, AZ, USA
[5] Department of Physics, California State University, San Luis Obispo, CA, USA

We have used several advanced transmission electron microscopy techniques to study the physical and chemical properties of intracellular ferrimagnetic magnetite (Fe_3O_4) and greigite (Fe_3S_4) crystals in magnetotactic bacteria that had been collected from lakes and streams. Our measurements provide indirect information about mechanisms of biomineralization.

The orientations and morphologies of magnetite crystals in a double magnetosome chain were identified using electron diffraction, high-resolution electron microscopy and high-angle annular dark field electron tomography. Each of the two chains is analogous to beads on a string, in which biological control appears to be stricter in setting the [111] magnetocrystalline easy axis of the crystals to be parallel to the chain axis than in constraining their orientation about this direction. We used off-axis electron holography to record magnetic induction maps from the same particles. The magnetic signal was dominated by inter-particle interactions and by the shapes of the individual crystals.

We studied the diversity of magnetosomes in bacteria collected from Lake Balaton. In stained thin sections of *cocci*, magnetite crystals appear to be anchored to the inner cell membrane. They are enveloped by stained material, which may correspond to the magnetosome membrane. The sections contain no detectable iron outside the magnetite magnetosomes.

The shapes, orientations, microstructures and magnetic properties of iron sulfide nanocrystals in magnetotactic bacteria that had been collected from salt marshes were also studied. Rod-shaped cells were found to contain multiple chains of greigite magnetosomes with random shapes and orientations. Many of the greigite crystals appeared to be only weakly magnetic, presumably because their magnetic induction direction was almost parallel to the electron beam. The disordered three-dimensional arrangement of the crystals in a multiple chain resulted in the magnetic field in the chain following a meandering path between adjacent crystals. Nevertheless, the magnetosomes were observed to collectively comprise a permanent magnetic dipole moment that is sufficient for magnetotaxis. Over a three-year period, with the sample stored in air, each greigite crystal developed an amorphous iron oxide shell and its magnetic moment decreased. When taken together, these results provide a better understanding of magnetotaxis in sulfide-producing cells, and they have implications for the interpretation of paleomagnetic signals recorded from greigite-bearing sedimentary rocks.

INTERDISCIPLINARY (MINERALOGICAL–GEOLOGICAL–ARCHAEOLOGICAL) STUDY OF THE ANCIENT POTTERY FROM PĂLATCA (TRANSYLVANIA, ROMANIA)

PRECUP, C., IONESCU, C. & GHERGARI, L.
Babeş-Bolyai University, 1 Kogălniceanu Str., RO-400084 Cluj-Napoca, Romania
E-mail: precupcar@yahoo.com

Finding the provenance of raw materials and the manufacturing conditions represents the first target of the mineralogical-petrographical-geoarchaeological studies on ancient ceramics, after the ceramics characterization and classification. Twenty eight potsherds exhumed from a Middle Bronze Age site (Wietenberg culture) located in the actual Pălatca village (east of Cluj-Napoca, Romania), were studied by polarized light microscopy in thin sections, X-ray powder diffractometry and porosity measurements.

The potsherds belong to common vessels (pots, bowls, cups, plates) having various colours, from light yellow and light red, to dark brown and dark grey. Microscopically, the ceramic body is constituted from plastic material (clayey matrix), nonplastic inclusions (fragments of rocks, crystals, potsherds) and voids (pores). The clayey matrix has crystalline and/or amorphous fabric, showing different degrees of thermal sintering and vitrification. In the matrix, variable amounts of magmatic, metamorphic and sedimentary lithoclasts, various crystalloclasts and rare ceramoclasts (potsherds) and bioclasts are present. The texture of the ceramic body is in general not oriented or loosely oriented. The granulometric measurements reveal the presence of the semifine and coarse ceramics, classified according to GHERGARI *et al.* (1999) and IONESCU & GHERGARI (2004).

The estimation of the firing temperatures between 800 °C and 900 ºC was based both on the microscopical observation and XRD data. The first revealed the melting of quartz rims, the sintering and vitrification processes, and the partial or total decomposition of fine-grained calcite. The X-ray diffraction patterns showed changes of some lines, such as the disappearance of clay minerals or mica lines, the alteration of calcite lines.

The ceramic samples have both primary (due to modelling and drying) and secondary pores (due to firing), in various amounts. The apparent porosity, expressed by the volume of the open pores, was calculated based on formula given by SHEPARD (1976) and varies from 8 up to 35%.

Microscopical data of the matrix and the X-ray diffractometry of the bulk ceramic sample indicate that most likely polymictic clays, composed from illite, kaolinite ± smectite ± calcite were used as raw material. Similar clays, of Miocene age, occur in the surroundings of the site. Quartz sands and ceramoclasts were used as tempering materials.

This study was financially supported by the Romanian Ministry of Education and Research (Grant 1762/2005).

References

GHERGARI, L., LAZAROVICI, GH., IONESCU, C. & TAMAS, T. (1999): Angvstia, 4: 1–7.

IONESCU, C. & GHERGARI, L. (2002): In: Proceedings of XVII. Congress of Carpathian-Balkan Geological Association Bratislava, September 1st–4th 2002, Geologica Carpathica, 53, Spec. Issue.

SHEPARD, A. (1976): Ceramics for the archaeologist. 7th ed. Washington: Carnegie Institution of Washington.

MINERALOGICAL AND PETROGRAPHICAL STUDY OF MIDDLE BRONZE AGE CERAMICS FROM DERŞIDA (NW TRANSYLVANIA, ROMANIA)

PRECUP, C., IONESCU, C., GHERGARI, L. & SIMON, V.
Babeş-Bolyai University, 1 Kogălniceanu Str., RO-400084 Cluj-Napoca, Romania
E-mail: precupcar@yahoo.com

Twenty two fragments selected from hundreds of pottery remnants excavated in 60s at Derşida site in the north-western part of Transylvania (Romania), were studied by polarized light microscopy, X-ray powder diffractometry, scanning electron microscopy (SEM) and thermal analyses. Archaeologically, the pottery remnants belong to the Wietenberg culture (around 1800-1300 BC), *i.e.* Middle Bronze Age. The potsherds have a brownish-grayish colour, sometimes even blackish, with a smoothed surface, frequently decorated by incision or imprinting.

Microscopically, the ceramic body is composed from a clayey matrix, in which various nonplastic inclusions (clasts) and voids occur. Granulometrically, most of the samples (77%) have coarse characteristics, while 23% belong to the semifine category. The clayey matrix is thermally sinterized and has an amorphous-crystalline fabric. The porosity, expressed by primary and secondary pores, is relatively high. The inclusions are represented by crystalloclasts (quartz, plagioclase feldspar, biotite, muscovite, calcite and rarely garnets, epidote, zircon, titanite, tourmaline, apatite), lithoclasts (various metamorphic, magmatic and sedimentary rocks), ceramoclasts (potsherds) and rare bioclasts (fossil remnants). In cross section a general chaotic orientation of the lamellar particles, rarely a slight parallel arrangement to the wall of the ceramics can be noticed.

X-ray diffraction patterns show the presence of mineral components as muscovite, biotite, chlorite, feldspar as well as the thermally-modified lines of kaolinite, illite, montmorillonite and illite/montmorillonite. The thermal analyses point to endothermic effects at 50-200 °C, due to the adsorbed-water loss, at 400 °C, due to the loss of OH^- from the clay minerals structure and the last, at 650-800 °C, due to the structural collapse of some of the clay minerals. SEM images reveal different degrees of sinterization-melting processes which had affected mainly the clayey matrix and less the clasts.

The mineralogical composition of the matrix points out the use of a reddish clay (Late Pleistocene age) occurring west of the site, as raw material. The clasts composition reflects that the ancient potters used sands from the alluvial sediments of the Crasna river, as tempering material for ceramics. Based on the microscopical observations, the modification of the X-ray diffraction lines of clay minerals, the thermal analyses and SEM, compared with reference data (*e.g.* MAGGETTI, 1982; CULTRONE *et al.*, 2001, *etc*.) we may consider that the firing temperature of the Middle Bronze Age ceramics from Derşida exceeded 600 °C (kaolinite basal line is missing) but not more than 900 °C (as calcite is still thermally unchanged).

This study was financially supported by the Romanian Ministry of Education and Research (Grant 1762/2005).

References

CULTRONE, G., RODRIGUEZ-NAVARRO, C., SEBASTIAN, E., CAZALLA, O. & DE LA TORRE, M.J. (2001): European Journal of Mineralogy, 13: 621–634.

MAGGETTI, M. (1982) in OLIN, J.S. & FRANKLIN, A.D. (eds.): Archaeological ceramics, Washington, DC: Smithsonian Institution, 121–133.

CHEMICAL COMPOSITION OF THE SULPHOSALTS FROM THE BISMUTHINITE–AIKINITE SERIES FROM THE WESTERN CARPATHIANS

PRŠEK, J. & OZDÍN, D.
Deparment of Mineralogy and Petrology, Comenius University, Mlynská dolina G, 842 15 Bratislava, Slovakia
E-mail: prsek@yahoo.com

Sulphosalts of the bismuthinite–aikinite series are mostly accessory minerals in several types of mineralizations. We studied samples of these group of sulphosalts from stibnite mineralizations (Dúbrava deposit, Klačianka occurrence) and siderite mineralizations (Vyšná Boca, Bystrá-Hviezda, Bacúch, Ľubietová-Kolba, Slovinky deposits) in the Western Carpathians, using an electron microprobe. The position of the studied phases in the bismuthinite–aikinite series was classified at the base of n_a using the formula: $n_a = 25(x + y)/2$, proposed by MAKOVICKY & MAKOVICKY (1978), where x is the number of Pb *apfu* and y is the number of Cu *apfu*. For the determination of the exact position of these phases in the system Cu_2S–PbS–$Bi(Sb)_2S_3$ the classification proposed by TOPA *et al.* (2002) was used.

These sulphosalts formed a part of complex sulphide associations usually together with tetrahedrite and many other Bi sulphosalts as lillianite homologues, pavonite homologues, nuffieldite, cosalite, galenobismutite, cuprobismutite homologues and kobellite homologues. They form small homogeneous grains, needles up to 2 cm in size, complicated intergrowths with other sulphosalts and galena, decomposition products or exsolution lamellae (especially gladite and bismuthinite). Furthermore, they often form thin veinlets up to few cm in size or aggregates in the hydrothermal veins.

We identified all the known members except the three new ones (paarite, salzburgite and emilite). Bismuthinite, gladite, krupkaite and aikinite are the most common members; the others (lindströmite, hammarite and friedrichite) are rare. Cu-rich members occur together with tetrahedrite in the older parageneses; Bi-rich members with other Bi sulphosalts are part of the younger parageneses. We followed chemical compositions of these phases, especially the degree of substitutions and the contents of microelements as Ag, Fe and Sb. The content of Ag in all the studied samples is usually very low – it reach maximally 0.1 wt%, the same as the content of Fe (up to 0.1 wt%). Sometimes, in the localities richer in Fe minerals as siderite and pyrite in the paragenesis, they could contain more Fe (up to 0.5 wt%; Slovinky, Ľubietová-Kolba or Vyšná Boca). The content of Sb in the analyses is variable and strongly depends from the type of mineralization or mineral paragenesis. The phases coming from localities without any Sb mineral (Bacúch, Čierna Lehota) have small contents of Sb (up to 0.3 wt% only in few analyses). The phases coming from localities with tetrahedrite as the only Sb mineral (Vyšná Boca) usually contain around 1 wt% Sb. Samples from localities with Sb overprint or close to the Sb mineralizations (Hviezda) are richer in Sb (up to 5 wt%). The samples richest in Sb come from the stibnite type mineralizations, where various intermediate members of the bismuthinite–stibnite solid solution series occur together with other Sb-rich sulphosalts (tintinaite, bournonite, jamesonite and chalcostibite). The most interesting phase from that paragenesis is "krupkaite with n_a around 51" from Dúbrava, where the content of Sb could reach up to 28 wt%, which corresponds to 2.11 *apfu*. The nature of the individual sulphosalt phase does not exert big influence on the content of Sb. The same content was found in coexisting gladite and bismuthinite or in other phases, but generally the highest values of Sb are shown by the members of the bismuthinite–stibnite solid solution series. The degree of Cu + Pb = Bi + vac. substitution (n_a) in the individual members is various. The n_a values in bismuthinite started approximately about 0 and gradually increased through the value 10.6 up to n_a = 14.5 (Kolba and Hviezda), exceeding the field of bismuthinite. In the field of pekoite the value started at the n_a = 16.5 and gradually increased to n_a = 32. The analyses of gladite fall into the field of n_a values from 33 up to 39.2. The analyses of krupkaite fall into the n_a interval 45.42 up to 59.23. Lindströmite, hammarite and friedrichite are very rare and their analyses fall into the known fields for these minerals. The n_a values of aikinite vary from 80.7 up to 96.8, but in the special case of the locality Slovinky, n_a of aikinite vary from 90.5 up to 108.9. These "oversubstitued" analyses with very high values of n_a are caused by increased content of Cu without adequate amount of Pb and could probably correspond to another mineral, thought all used calculations suggest that the mineral should be aikinite.

References

MAKOVICKY, E. & MAKOVICKY, M. (1978): Canadian. Mineralogist, 16: 405–409.

TOPA, D., MAKOVICKY, E. & PAAR, W. H. (2002): Canadian Mineralogist, 40: 849–869.

MINERALOGICAL STUDY OF THE FRUMOASĂ CAVE, HĂLDĂHAIA AREA, ROMANIA

PUSCAŞ, M.
Department of Mineralogy, Babeş-Bolyai University, 1 Kogălniceanu Str., RO-400084 Cluj-Napoca, Romania
E-mail: montana.puscas@gmail.com

The Frumoasa Cave is located on the south-western part of the Trascăului Mountains (within the Apuseni Mountains), in a small karst area known as Hăldăhaia, approximately 25km from the city of Alba Iulia, Alba County, Romania (Fig. 1).

From a geological point of view, this area belongs to the Southern Apuseni Mountains, and more specifically to the Bedeleu Nappe. The 700-m thick sparitic Tithonian limestone in which the cave has been carved probably represents a 'back-reef' type formation.

Although it has been long known to the locals and visited by cavers ever since 1983, this is the first paper concerning the mineralogy of the 1,168 m long cave, developed on three levels and having a single, extremely narrow entrance (VADEANU *et al*., 1985). Due to the periodic existence of a bat colony in the second level a very thin layer of bat guano covers its floor, representing an important source for phosphates in caves (HILL & FORTI, 1997).

We have collected 15 samples from two locations on the intermediary level, in the vicinity of bat colonies. The samples are fragments of speleothems and earthy masses. The X-ray diffraction analyses show that the minerals belong to five chemical groups: carbonates (calcite and aragonite), sulfates (gypsum), phosphates (fluorapatite), silicates (illite and muscovite), and oxides (quartz and minium). We consider minium (Pb_2PbO_4) to occur as a result of human activity in the cave. The source for gypsum may be represented either by the sedimentary deposits above the cave, or by the guano layers from the inside (ONAC, 2000). In the Frumoasă Cave gypsum occurs in association with quartz and calcite, along cracks in the walls. Silicates and quartz are present in the cave as allogenic minerals, their source being the sedimentary alluvia transported by the percolation waters that infiltrate from the surface and the subterraneous water courses.

As far as the phosphates are concerned, this is the first fluorapatite occurrence in the caves of the Trascăului Mountains (ONAC, 2003). In the Frumoasă Cave the phosphate forms either crusts on the floor or powdery earth masses along the cracks in the walls.

References

HILL, C. A. & FORTI, P. (1997): Cave Minerals of the World, 2nd ed., Huntsville: National Speleological Society

ONAC, B. P. (2000): Geology of carstic areas. Bucureşti: Editura Didactică şi Pedagogică. (in Romanian)

ONAC, B. P. (2003): Theoretical and Applied Karstology, 13–14: 33–38.

VADEANU, T., GYŐRFI, S. & ARDELEAN, D. (1985): Buletin Speologic Informativ, 8 (1): 27–34.

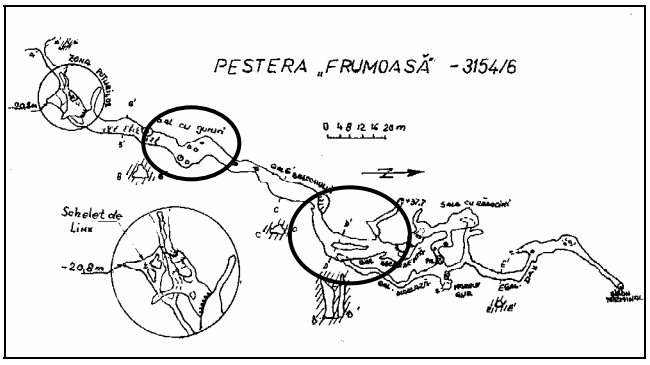

Fig. 1. Schematic map of the Frumoasă Cave.

THE PROTON: A CATION LIKE THE OTHERS IN ROCK-FORMING MINERALS

ROBERT, J.-L.
ISTO, UMR 6113, CNRS-Université d'Orléans, 45071 Orléans Cedex 2, France and IMPMC, UMR 7590, CNRS-Universités Paris VI, Paris VII, IPG, 140 rue de Lourmel, 75015 Paris, France
E-mail: jlrobert@cnrs-orleans.fr

In hydrous rock-forming minerals, the hydroxyl hydrogen and the hydroxyl oxygen are usually considered as a whole and permanent entity, *i.e.* the hydroxyl group, which acts as a monovalent anion within the structure. The reality is more complicated and more interesting, since the hydroxyl proton leads its life independently. Depending on the local charge balances, the hydroxyl group can be considered as a point charge or as dipole in which oxygen and hydrogen play a different role, since hydrogen is able to share a part of its charge with surrounding oxygens, usually the underbonded oxygens of adjacent tetrahedra.

The properties of the OH group (O–H distance and resulting O–H stretching and bending wavenumbers) closely reflect the local variations of crystal-chemical properties in the mineral structure: charge distributions, and distances. An examination of these properties allow a careful description of the crystal-chemical landscape around the proton, up to the fifth cationic neighbour in favourable cases, and a prediction of many geochemical properties of H-bearing rock-forming phases.

The main factor controlling these properties is the nature (bulk charge, electronegativity) of the first cationic neighbours. The higher the bulk charge carried by the immediately adjacent cations, the weaker the O–H bond within the hydroxyl group. Contrary to a commonly accepted idea, the orientation of the OH dipole is not the main factor controlling these properties. An example is given by the comparison between talc $Mg_3Si_4O_{10}(OH)_2$, a trioctahedral 2:1 layer silicate, with the OH dipole bonded to Mg_3 and perpendicular to (001), and pyrophyllite, $(Al_2\square)Si_4O_{10}(OH)_2$ ($\square$ stands for an octahedral vacancy), with the OH group adjacent to $Al_2\square$ and strongly tilted towards (001). The resulting OH bond strength is the same in talc and pyrophyllite, as shown by the similarity between their OH-stretching wavenumbers (3676 ± 1 cm^{-1}). As long as the local charge balance around the OH group remains constant, the bond strength within the OH group and the resulting OH-stretching wavenumber remain constant, whatever the mineral family. It is interesting to note that the trioctahedral OH group in the tetrasilicic magnesium mica $K(Mg_{2.5}\square_{0.5})Si_4O_{10}(OH)_2$, in richterite, a clinoamphibole, $(K,Na)(NaCa)Mg_5Si_8O_{22}(OH)_2$, and the inner OH-group in dravite, a tourmaline, $NaMg_3Al_6(BO_3)_3(Si_6O_{18})(OH)(OH)_3$, have the same OH-stretching wavenumber, 3735 cm^{-1}, within experimental uncertainties. In these there major silicate families, the OH group is bonded to Mg_3 and point towards an alkaline cation, in the middle of a ring of six SiO_4 tetrahedra, which can be summarised as follows: Mg_3-OH → $(6SiO_4)$-A^+ (with $A^+ = Na^+$ or K^+).

A decrease of the local charge carried by the first adjacent cations raises the O–H bond strength and consequently the OH-stretching wavenumber, up to 3755 cm^{-1}, the highest value known in any compound under room conditions, observed in tainiolite $K(Mg_2Li)Si_4O_{10}(OH)_2$. By contrast, as the bulk charge carried by the first cationic neighbours increases, for example Mg_2Al or Al_2Li, the OH-stretching wavenumber drops to values around or below 3650 cm^{-1}, indicating that a part of the proton charge is shared with surrounding oxygens. This is observed in all mineral families.

Heterovalent cationic substitutions in octahedral sites adjacent to the OH-group are generally coupled with replacements in other polyhedra, *e.g.* the tetrahedral sites, the interlayer space in layer silicates, the pseudo-cubic antiprism *M*4 site in amphiboles, the second, third, …, neighbours, must be considered.

Using selected synthetic minerals allows to determine the respective influence of all substitutions, up to the fifth cationic neighbouring sites in favourable cases, through a careful analysis of the perturbations induced on the OH group. In this way, it is possible to assign all observed OH vibrations to a peculiar environment, and then to deduce local order-disorder relations around the hydroxyl proton.

The influence of the A^+ cation can be analysed using A^+-bearing and A^+-free minerals. For example, the influence of K^+ on hydroxyl properties can be deduced from the comparison between talc [Mg_3–OH → $(6SiO_4)$] and the trioctahedral OH of the tetrasilicic Mg mica [Mg_3–OH → $(6SiO_4)$–K]. The shift induced by K^+ facing the OH group is +59 cm^{-1}. A similar value is observed in amphiboles, for example between tremolite $\square Ca_2Mg_5Si_8O_{22}(OH)_2$ and richterite $A^+(NaCa)Mg_5Si_8O_{22}(OH)_2$, and in tourmalines, Mg-foitite $\square(Mg_2Al)\ Al_6(BO_3)_3(Si_6O_{18})(OH)(OH)_3$, compared to dravite $NaMg_3Al_6(BO_3)_3(Si_6O_{18})(OH)(OH)_3$. Increasing the charge of the cation facing the hydroxyl group raises the OH-stretching wavenumber, as observed along the phlogopite $KMg_3(Si_3Al)O_{10}(OH)_2$–kinoshitalite $BaMg_3(Si_2Al_2)O_{10}(OH)_2$ join, where the K^+/Ba^{2+} substitution provokes a shift of +20 cm^{-1} in the OH-stretching wavenumber. The tilting of the OH group towards (001) in dioctahedral phases withdraws this interaction, as shown by the comparison between muscovite or paragonite $A^+(Al_2\square)(Si_3Al)O_{10}(OH)_2$, with $A^+ = K^+$ and Na^+, respectively, and phlogopite $KMg_3(Si_3Al)O_{10}(OH)_2$.

Contrary to a commonly accepted belief, the effect of the orientation of the OH group on the exchange properties of clay minerals is practically negligible, since the interlayer water molecules act as a screen between the hydroxyl proton and the compensating cation, and there is almost no interaction between them even in the case of trioctahedral smectites, like saponites. As a matter of fact, in one-layer high-charge saponites, the OH-stretching wavenumber is only 3682 cm^{-1}, *e.g.* very close to that of talc, a 2:1 layer silicate without interlayer compensating cation. Therefore, in smectites, only the charge location and the charge value have an influence on exchange properties, and the behaviours of the dioctahedral beidellites and trioctahedral saponites, both with tetrahedral charge, on one side, and of the dioctahedral montmorillonites and the trioctahedral hectorites, both with octahedral charge,

on the other side, are similar provided that the layer charge is the same.

The properties of the OH-group also allow to investigate the tetrahedral cationic distributions (mainly Si, Al), since the OH···O interactions depend on the charge balance on surrounding oxygens, *i.e.* the oxygens of tetrahedra. A careful quantitative investigation of OH-stretching band intensities for different first neighbours (octahedral), and second neighbours (tetrahedral) shows that the Si, Al distributions are generally not ordered, but follow a homogeneous charge distribution pattern, in agreement with high-resolution NMR data. Considering the influence of second cationic neighbours effects (*i.e.* tetrahedrally coordinated cations), on band positions and band intensities, leads to conclude that in many cases the extinction coefficients are constant, which allow quantitative determinations of cationic distributions around the hydroxyl proton.

The method is sensitive enough to enlight long distance effects, even for subtle substitutions like Ca^{2+}/Mg^{2+} at *M*4 sites in clinoamphiboles along the tremolite $\square Ca_2Mg_5Si_8O_{22}(OH)_2$–cummingtonite $\square Mg_7Si_8O_{22}(OH)_2$ join, or Na^+/Li^+ along the ferri-clinoferroholmquistite $\square Li_2Fe^{2+}{}_3Fe^{3+}{}_2Si_8O_{22}(OH)_2$–riebeckite $\square Na_2Fe^{2+}{}_3Fe^{3+}{}_2Si_8O_{22}(OH)_2$ series. Owing to the distances, these long-range effects are not direct. They are induced through the structure by the propagation of tiny distortions required by local charge balance requirements.

In addition to this role of privileged observer, the proton H^+ frequently plays a key role in many situations. Deprotonation in the case of in situ oxidation of a variable charge cation, *i.e.* $Fe^{2+} \rightarrow Fe^{3+}$, in biotites, hornblendes, and so, no protonation when high cation (Mn^{3+}, Ti^{4+}) are incorporated to crystal structures, in micas like norrishite $K(Mn^{3+}{}_2Li)Si_4O_{10}O_2$ and many high-Ti phlogopites, or amphiboles like ungarettiite $NaNa_2(Mn^{2+}{}_2Mn^{3+}{}_3)Si_8O_{22}O_2$, obertiite $NaNa_2(Mg_3Fe^{3+}Ti)Si_8O_{22}O_2$ and dellaventuraite $NaNa_2(MgMn^{3+}{}_2LiTi)\ Si_8O_{22}O_2$. Additional protonations are also known in hydrous minerals, for example in partially dioctahedral micas with a tetrahedrally coordinated cation, Be^{2+}, Mg^{2+}, Ni^{2+} or Co^{2+}, or in clinoamphiboles (richterites), with Li^+ replacing Ca^{2+} at the M4 site.

The approach is also very useful for identifying unusual coordinations for cations, for example $^{[4]}M^{2+}$ in micas and in amphiboles like joesmithite, $PbCa_2Mg_5(Si_6Be_2)O_{22}(OH)_2$, or $^{[4]}B^{3+}$ in high pressure olenite (a tourmaline) $NaAl_3Al_6(BO_3)_3(Si_3B_3O_{18})(OH)(OH)_3$.

The interactions of the hydroxyl proton with the neighbouring oxygens, influenced by the charge distributions and the distances, also control the possible OH^-/F^- exchange properties, whatever the fluorine activity in the environment. When the hydroxyl proton has no or little interactions with its neighbours, it acts as a point charge in the structure and the OH^-/F^- is easy. It is the case in most trioctahedral layer silicates, in all amphiboles and at the inner OH^- site of tourmalines. By contrast, if the hydroxyl proton is involved in H-bonds with surrounding oxygens, its replacement by fluorine is more energetically difficult, and becomes impossible if OH···O bonds are strong. It is why dioctahedral layer silicates do not trap much fluorine, and why outer hydroxyl groups cannot be replaced by fluorine in tourmalines.

DISCRIMINATION BETWEEN TECTONIC ENVIRONMENTS OF OBSIDIAN SAMPLES USING GEOCHEMICAL DATA

RÓZSA, P.[1], SZÖŐR, GY.[1], ELEKES, Z.[2], GRATUZE, B.[3], UZONYI, I.[2] & KISS, Á. Z.[2]
[1] Department of Mineralogy and Geology, University of Debrecen, Egyetem tér 1, H-4032 Debrecen, Hungary
E-mail: rozsap@puma.unideb.hu
[2] Institute of Nuclear Research of the Hungarian Academy of Sciences [ATOMKI], Bem tér 18/C, H-4026 Debrecen, Hungary
[3] Centre de Recherches Ernest Babelon, CNRS, Orleans, France

Geochemical analysis of obsidians is of great interest to archaeometry. From the geological point of view, the importance of elemental constituents of obsidians is that mineralogical information can hardly be obtained on volcanic glasses. The non-destructive ion beam analysis (IBA) is suitable in general to determine major, minor and trace element content; therefore, IBA methods are widely used in geoscience research (RYAN, 2004), particularly in obsidian provenance studies (see for example ELEKES *et al.*, 2000).

Obsidian samples from different localities of various geological settings (Armenia, Hungary, Iceland, Mexico, Slovakia, Turkey) were analyzed by particle induced gamma-ray emission (PIGE) technique and laser ablation-inductively coupled plasma-mass spectrometry (LA-ICP-MS). Petrographically, all samples can be regarded as rhyolite according to their position in the TAS diagram. Classifying the studied obsidian samples the R1–R2 diagram (DE LA ROCHE *et al.*, 1980), where R1 = 4Si – 11(Na + K)–2(Fe + Ti) and R2 = 6Ca + 2Mg + Al, was also applied. Although it is most useful and generally used for plutonic rocks, the scheme is sufficiently general to apply to volcanic rocks, too. Samples coming from Armenia and the Tokaj Mountains belong to rhyolites. Samples from the Lipari Islands and Turkey also fall into this group, however their points are near the boundary line separating the rhyolite and alkali rhyolite fields. However, points of the samples from Iceland and Mexico are situated in the alkali rhyolite field as a consequence of their higher sodium and iron as well as lower calcium content. Obsidians are often classified chemically according to their CaO, Al_2O_3 as well as Na_2O and K_2O contents (MACDONALD *et al.*, 1993). According to this characterization, all of the analyzed samples are subalkaline–peraluminous obsidians.

Use of discrimination diagrams to classify granites according to their tectonic setting is common in the petrologic practice. Applying the Ta–Yb and Nb–Y diagrams (PEARCE *et al*., 1984) it can be stated that samples from Hungary dominantly belonged to the field of volcanic-arc granites (VAG) as well as that of volcanic arc and syn-collisional granites (VAG + syn-COLG) as expected on the basis of their tectonic setting. Position of samples from Turkey (syn-COLG and VAG + syn-COLG, respectively) also corresponds to the expectations. Armenian obsidians are described as products of a subduction related volcanic area. Their position in the Nb-Y diagram corresponds to this fact; however, one sample can be found in the field of within-plate granites (WPG) in the Ta-Yb diagram. The sample from Lipari Islands also belongs to the WPG fields in both diagrams. On the other hand, however, these samples are close to the dividing line between WPG as well as syn-COLG and VAG fields. Both discrimination diagrams show the samples from Iceland and Mexico to belong to the WPG field. This pattern may be in connection with the alkaline character of the samples indicated by the R1–R2 diagram.

Acknowledgements
This work has been supported by the Hungarian National Science Research Foundation (OTKA) under Research Contract No. T046579.

References

DE LA ROCHE, H., LETERRIER, J., GRANDECLAUDE, P. & MARCHAL, M. (1980): Chemical Geology, 29: 183–210.

ELEKES, Z., UZONYI, I., GRATUZE, B., RÓZSA, P., KISS, Á. Z. & SZÖŐR, GY. (2000): Nuclear Instruments and Methods in Physics Research B, 161/163: 836–841.

MACDONALD, R., SMITH, R.L., & THOMAS, J. E. (1993): Chemistry of the subalkalic silicic obsidians. US Geological Survey Professional Paper, 1523. Washington: US Geological Survey.

PEARCE, J. A., HARRIS, N. B. W. & TINDLE, A. G. (1984): Journal of Petrology, 25: 956–983.

RYAN, C. G. (2004): Nuclear Instruments and Methods in Physics Research B, 219/220: 534–549.

FERRUGINOUS CONCENTRATIONS IN SANDSTONES NEAR DOBCZYCE (SILESIAN UNIT, THE WESTERN POLISH CARPATHIANS) – PRELIMINARY RESULTS

RZEPA, G., BAZARNIK, J., MUSZYŃSKI, M. & GAWEŁ, A.
Department of Mineralogy, Petrography and Geochemistry, AGH University of Science and Technology, al. Mickiewicza 30, 30-059 Krakow, Poland
E-mail: grzesio@geolog.geol.agh.edu.pl

The Istebna Beds that build the northern edge of the Dobczyce retention reservoir on the Raba River near Brzączowice (*ca*. 30 km SE of Kraków) contain layers and beds enriched in Fe compounds. They are rusty or yellowish, in some places become distinctly black. Within these iron-rich horizons, there occur characteristic, boxwork-like goethite concretions.

Mineral composition of these ferruginous concentrations with special attention to the boxwork-like concentrations, whose origin is still a matter of discussions, was investigated using transmitted light microscopy, X-ray diffractometry (XRD) and scanning electron microscopy (SEM-EDS). The authors also determined the contents of Fe and Mn; the figures cited below refer to the HCl-soluble Fe.

Five types of Fe-rich concentrations that differ in their mode of occurrence, Fe content and mineral composition have been distinguished on the basis of hand specimen features and preliminary mineralogical investigations:

1) sandstones cemented (uniformly or non-uniformly) with Fe oxyhydroxides (especially goethite), with colours from yellow to almost black, containing dozen or so wt% Fe;
2) goethite incrustations on the surfaces of sandstones, containing up to *ca*. 30 wt% Fe;
3) boxwork-like concretions proper, composed almost of pure goethite and containing up to 87 wt% Fe;
4) sulphate-oxide concentrations, that are composed of jarosite, goethite and detrital material and contain up to 53 wt% Fe. Similar concentrations with secretion-like features were described by GUCWA & WIESER (1976);
5) phosphate-oxide aggregates that are mainly composed of apatite, quartz, Fe and Mn oxides and contain up to 12 wt% Fe.

The main Fe mineral is usually cryptocrystalline goethite, but it may also form characteristic, fan-shaped aggregates of elongated crystals, lining the walls of pores and fractures. Mn oxides are present in all types of ferruginous concentrations, either dispersed or in the form of incrustations, irregular concentrations, veins and dendrites.

On the basis of these preliminary investigations, the origin of the Fe concentrations studied may be related to weathering under oxidizing conditions of primary, Fe-bearing minerals (silicates, sulphides and, possibly, carbonates) that must have been present in surrounding rocks. Goethite, the main Fe component of these aggregates, can be formed in different weathering environments characterized by a wide spectrum of physicochemical conditions (pH, Eh, foreign ions; CORNELL & SCHWERTMANN, 1996). Variations of these parameters may have controlled the forms of occurrence and the degree of crystallinity of goethite. Its presence in different forms indicates several stages and/or mechanisms of weathering, various Fe sources, etc. The boxwork-like structures resulted probably from precipitation of goethite from the solutions that penetrated cracks in sandstones and progressively replaced the primary rock with the iron oxyhydroxide (RUKHIN, 1953). In sulphate secretions goethite is probably a final product of co-existing jarosite transformation. Jarosite crystallizes from acid solutions with pH < 3 that are rich in sulphates and Fe^{3+} (DUTRIZAC & JAMBOR, 2000) and its presence strongly implies weathering of sulphides.

The investigations were supported by AGH-UST research project no. 11.11.140.158.

References

CORNELL, R. M. & SCHWERTMANN, U. (1996): The iron oxides. Structures, properties, occurrences, characterization and uses. Weinheim: VCH, 573 p.

DUTRIZAC, J. E. & JAMBOR, J. L. (2000): In: ALPERS, C. N., JAMBOR, J. L. & NORDSTROM, D. K. (eds.) Sulfate minerals – crystallography, geochemistry and environmental significance. Reviews in Mineralogy & Geochemistry, 40: 405–452.

GUCWA, I. & WIESER, T. (1976): Rocznik Polskiego Towarzystwa Geologicznego, 46: 197–215 (in Polish).

RUKHIN, L. B. (1953): Osnovy litologii. Moskwa: Gostoptekhizdat, 671 p. (in Russian).

TELKIBÁNYA FIELD TRAINING PARK – POTENTIAL FIELD PROGRAMS IN MINERALOGY, PETROGRAPHY AND GEOCHEMISTRY

SERESNÉ HARTAI, É., FÖLDESSY, J. & ZELENKA, T.
Department of Geology and Mineral Resources, University of Miskolc, H-3515 Miskolc-Egyetemváros, Hungary
E-mail: foldshe@gold.uni-miskolc.hu

The Telkibánya mining area is located in the northern part of the Tokaj Mountains. It is one of the most important mining places in Hungary, a medieval industrial and cultural heritage, which has never been protected before and we don't know exactly its real extent and actual condition.

The area is a part of the Miocene volcanic arc stretching from Tokaj in the south to Prešov in the north and called Tokaj Mts. (southern part) and Slanské vrchy Mts. (northern part). The thickness of the volcanic mass is nearly 3000 m. There is a caldera structure between Telkibánya and Hollóháza, with intrusions of andesitic bodies, which underwent strong K-metasomatism. In the subvolcanic bodies epithermal LS-type gold-silver mineralization occurs. During the mineralization 14 veins were formed. The veins are 40-80 cm in width and a few km in length. The vein-fillings are siliceous on the top, but they are dominated by argillic then carbonate material in the deeper sections. Ore minerals can be found in the upper 300 m of the veins.

Mining in Telkibánya goes back to prehistoric times but systematic open-pit mining started in the 12-13th century. In 1341 and 1344 royal decrees declared the status of the mining town. In the 14-15th century underground mining started. The prosperity ended by a mining catastrophe in the 16th century, which was followed by a 200 years long break in mining. The re-opening resulted in a second prosperity in the 18-19th century. In the 20th century mining was ceased, but there were explorations at deeper levels, during which drifts and drill holes were made and geophysical and geochemical data were obtained. However, the ore reserves haven't proven to be economic. The monuments of one-time mining are represented now by old adits, about 3000 pits and ruins of processing plants.

In 2005 the University of Miskolc made a study in the framework of a PHARE CBC project in co-operation with the Technical University of Košice. The following objectives were examined in the study: (a) the environmental status and impact of former mining activities, (b) research of surface and underground mining facilities and database creation, (c) safety assessment of mine facilities for future education purposes, (d) educational tools and information about geological monuments for field training centre.

As a result of the study, Telkibánya proved to be an ideal place for field training programs. It has favourable infrastructure conditions. The training centre includes several field training tools: drill core documentation, underground drift mapping, surface sampling, geophysical testing *etc*., and offers comparisons with the earlier exploration database, maps, *etc*. Beside geotechnical and structural geological examinations, different programs can be carried out in mineralogy and petrography by studying the various types of volcanic rocks, the ore mineralization and rock alteration (surface and underground). The University of Miskolc plans to co-ordinate and organize programs at different levels on the site.

HERZENBERGITE AND Sn-BEARING TINZENITE FROM THE NYF PEGMATITE IN TŘEBÍČ PLUTON, MOLDANUBICUM, CZECH REPUBLIC

ŠKODA, R. & ČOPJAKOVÁ, R.
Institute of Geological Sciences, Faculty of Science, Masaryk University, Brno, Czech Republic
E-mail: rskoda@sci.muni.cz

The most common Sn-rich minerals in the granitic pegmatites include cassiterite and wodginite, scarcely also Sn-bearing ixiolite and varlamoffite. Stokesite, brannerite, kristiansenite *etc.* are very rare Sn silicates. Minerals of the stannine–kesterite group are the most frequent Sn-bearing sulphides, whereas herzenbergite, SnS, occurs in granitic pegmatites only exceptionally: the Sollefteå pegmatite field, North Central Sweden (SMEDS, 1993) and sporadically Viitaniiemi, Finland (LAHTI, 1981). Herzenbergite and associated stokesite, varlamoffite, cassiterite and tinzenite were recently found during systematical investigation of the NYF pegmatites from Třebíč pluton, Moldanubicum, Czech Republic.

Třebíč pluton forms a large (~540 km^2), probably sheet-like body of ultrapotassic (5.2–6.5 wt% K_2O) plutonic rocks of the durbachite emplaced in medium- to high-grade metamorphic rocks. The rocks are highly magnesian (3–10.4 wt% MgO), rich in Cr, Rb, Cs, U and Th. The bulk composition of TP is characterized by metaluminous signature ASI = 0.85–0.93; radiometric dating yielded age 343±6 Ma. Durbachitic rocks are interpreted as a product of mixing of an enriched mantle magma and crustal melt. Pegmatites derived from this rock belong to the NYF family. Several morphological types in different degree of fractionation were distinguished: i) irregular segregations to nests of primitive allanite subtype, ii) lenses to dykes of the more evolved euxenite subtype and iii) the most fractionated zinnwaldite–masutomilite–elbaite pegmatite at Kracovice of the Mixed family. Pegmatites form lenses or dykes with maximal thickness of 1.5 m. Concentric asymmetrical zoning comprises from the contact inwards contact zone, locally transitional to host rock, granitic zone, graphic zone, blocky K-feldspar and small quartz core. Albite replaces blocky K-feldspar and graphic zone. Quartz, K-feldspar (locally pale green amazonite), plagioclase and Mg-rich biotite are major minerals. Tourmaline is typical minor mineral, the accessory minerals include: Y, REE, Nb, Ta, Ti oxides, titanite, ilmenite, allanite-(Ce) and Sn minerals. Primary muscovite is not present.

Sn mineralization was found at locality Klučov, which belongs to euxenite subtype. It fills tiny vugs and fractures in the strongly albitized part of graphic and block zone with common tourmaline. Based on the mineral paragenesis, two different associations were distinguished: i) herzenbergite I-II–varlamoffite–stokesite–cassiterite, ii) cassiterite–tinzenite–varlamoffite.

Cassiterite I forms anhedral to corroded grains up to 20 μm; its chemical composition show increased content of Ta, Nb and Fe by the substitution $Fe^{2+}(Ta, Nb)_2 \leftrightarrow 3Sn$. Euhedral crystals of cassiterite II reach 20 to 100 μm and chemical composition corresponds to nearly pure SnO_2. Elevated Nb, Ta and Fe content in cassiterite I suggest crystallization at higher temperature relative to cassiterite II. Two generations of herzenbergite were distinguished and they differ in texture and chemical composition. Herzenbergite I forms highly altered, lathy crystals and their aggregates, up to 2 mm in size. Small amount of Fe and Cu, both up to 0,007 apfu, enter the structure. Herzenbergite I is replaced by mixture of stokesite and varlamoffite. Herzenbergite II fills space among crystals of herzenbergite I or it occurs as grains mounted on the apical part of the decomposed herzenbergite I crystal. Its chemical composition corresponds to the ideal SnS. Herzenbergite II commonly encloses oriented cigar-shaped lamellae of varlamoffite and does not show any sign of alteration. Herzenbergite I probably crystallized from hydrothermal solutions as one of the latest minerals in small vugs or its lathy crystals intergrow with quartz. Later herzenbergite II crystallized either directly from hydrothermal solutions later than herzenbergite I, or as a phase formed at the expense of herzenbergite I. In the Scandinavian localities herzenbergite replaces cassiterite (Sollefteå) or it was found as exsolution lamellae in cassiterite (Viitaniemi). Specific conditions of herzenbergite formation (fS and fO_2) and stability cause their very scarce occurrence in the pegmatites.

Tinzenite forms anhedral crystals, up to 100 μm in size. Its chemical composition varies from nearly end-member tinzenite to Ca-rich tinzenite. Elevated content of SnO_2, up to 0.86 wt. % SnO_2, was detected. It is a first occurrence of tinzenite in the pegmatites and first evidence of incorporation of Sn into natural axinites.

References

LAHTI, S. I. (1981): Bull. Geol. Surv. Finland, 314: 1–63.
SMEDS, S. A. (1993): Mineralogical Magazine, 57: 489–494.

PRODUCTS OF PASSIVE TREATMENT OF ACID MINE DRAINAGE AND TECHNOLOGICAL WASTEWATER

ŠOTTNÍK, P.
Department of Mineral Deposits, Faculty of Natural Sciences, Comenius University, Mlynská dolina, 842 15 Bratislava, Slovakia
E-mail: sottnik@fns.uniba.sk

Outflows of acid mine drainage (AMD) represents serious danger for the environment as they cause pollution of surface and ground waters, soil degradation and changes in vegetation. They can induce chemical decomposition of other minerals, which can be the potential sources of toxic elements. Passive treatment systems (PTS) or constructed wetlands are artificial ecosystems, which simulate conditions typical of natural wetlands based on observations of natural processes. Consequently, the objective of metals treatment is often to return mobile contaminants to their stable, immobile mineral forms. Many of these minerals are formed from water solution in a sedimentary environment, and the reactions are catalysed by bacteria. Mechanisms of retention within wetlands listed in their order of importance include formation of metal sulfides, formation and precipitation of metal hydroxides and carbonates:

$H_2S + Zn^{2+} \rightarrow ZnS + 2H^+$

$Fe^{2+} + HCO_3^- \rightarrow FeCO_3 + H^+$

$3\ HS^- + 6\ FeSO_4 + 4\ CrO_4^{2-} + 13\ H_2O + OH^- \rightarrow 3S^0 + 6\ Fe(OH)_3 + 4\ Cr(OH)_3 + 6\ SO_4^{2-}$

Our first trial to use the PTS for cleaning of AMD was realised in the Šobov area, near the city of Banská Štiavnica in Slovakia. AMD outflow from waste dump has a pH about 2.5 and the content of dissolved salts is over 20 g/l. Al, Fe and SO_4 are the most common components found in AMD, which already affected over 145 000 m^2 of the site. Investigation of possible use of the PTS to treat AMD from mining waste dump in Šobov was realised in three steps. The first step involved low-volume laboratory experiments. In the second step, a bench-scale system (capacity = 120 l) was built directly on the place of the planned PTS. At the same time the third step was also carried out, in which the pilot PTS was gradually built. The pH in the system stayed always at least at 4. We obtained good results of AMD treatment. Concentrations of Fe were many times reduced in comparison with original values. The same phenomena could be observed for Cu and Al, too. A considerable fall could also be measured in SO_4^{2-} concentrations, but in this case the efficiency of the PTS is a little lower.

In the second experiment with the AMD from Smolník we concentrated on the bench-scale phase. A system with a capacity of 200 l filled with substrate composed of different proportions of limestone, manure, sawdust and hay were used. In all of the containers a tendency to progressive improvement of ability of the PTS to treat Fe, Cu, Zn and Al contamination was observed, the efficiency in the final phase of the experiment was 96–97%. On the other hand, the efficiency of the system to treat Fe and SO_4^{2-} was very low. It was caused by the very short time that was spent by the wastewater in the pilot-scale system.

In the next project we tried to remove heavy metal from technological wastewaters using an anaerobic bench-scale treatment model (50 l) at Vanchang village in Vietnam. After one-month treatment, the concentrations of Cr, Ni, Fe, Al in our experimental model were significantly reduced; Cr from 131 mg/l to 0.165 mg/l, Ni from 500 mg/l to 6.75 mg/l, Fe from 1450 mg/l to 6.8 mg/l, Al from 224 mg/l to 1 mg/l. The results showed high efficiency in the removal of heavy metals from wastewater and a prospect for expanding larger-scale treatment in Vanchang and other places.

In the last project we focused on treatment of water from a technological waste dump in Bošany (Slovakia). The biological treatment of chromium was used for reduction of Cr^{6+} to Cr^{3+}.

References

KONOPELEC, J. (2004): Passive treatment of Cr and As contaminated wastewater. Department of Mineral Deposits, Faculty of Natural Sciences, Comenius University, Bratislava. Manuscript (MSc Thesis, in Slovak), 71 p.

ŠOTTNÍK, P. (2000): Passive treatment of acid mine drainage (PhD theses). Department of Mineral Deposits, Faculty of Natural Sciences, Comenius University, Bratislava. Manuscript (PhD thesis, in Slovak), 116 p.

ŠOTTNÍK, P. & ŠUCHA, V. (2000). Experiences with an in-situ and passive treatment of heavy metal polluted water – a possibility also for the Nam Dinh region? In: Book of Abstracts, International Workshop on Environmental Protection, Community Health for Sustainable Development of Craft-settlements in Nam Dinh, 26–27 October 2000, Nam Dinh, Vietnam.

WILDEMAN, T. R. & UPDEGRAFF, D. M. (1997): In: MACALADY, D. L. (ed.): Perspectives in environmental chemistry. Oxford: Oxford University Press, 473-495.

HYDROTHERMAL ASSOCIATION OF ZEOLITES FROM COPĂCENI, CLUJ COUNTY, ROMANIA

STREMTAN, C.
Department of Mineralogy, Babeş-Bolyai University, 1 Kogălniceanu Str., RO-400084 Cluj-Napoca, Romania
E-mail: cstremtan@bioge.ubbcluj.ro

In the eastern part of the Apuseni Mts. (Romania), Mesozoic island arc volcanics *e.g.* basaltic pillow-lavas, massive basaltic lava flows and basaltic breccias occur, as part of the Bedeleu Nappe (BALINTONI & IANCU, 1986). They are partly covered by Oxfordian-Tithonian radiolarites and limestones, and Badenian clastic sediments. In the Copăceni area, in an old quarry, nowadays abandoned, a succession of basalt flows, with basaltic breccias on top, contain veins and voids filled with a hydrothermal mineral association composed mainly of carbonates (calcite), silica (both micro- and macro crystallized), clay minerals and zeolites.

Here we present new mineralogical and chemical data on the zeolite association, which completes the data obtained previously by KRISTÁLY *et al.* (2003). Twelve samples were analyzed by polarized light microscopy, X-ray powder diffraction, X-ray single-crystal diffraction and electron microprobe.

Six different species of zeolites were identified: stilbite, heulandite, analcime, chabazite-Ca, barrerite and mordenite.

Stilbite is the most abundant zeolite in the Copăceni association and it was identified in 9 of the 12 analyzed samples. Some stilbite crystals show an intergrowth with another zeolite, richer in Na_2O, i.e. barrerite.

Heulandite is the second zeolite in terms of abundance (6 out of 12 analyzed samples) and is associated mostly with chabazite-Ca, calcite, quartz and microcrystalline quartz. The single-crystal diffraction pattern of the C10_4 sample proves a lower value for the β angle (113.2°± 0.3°), which does not fit the references data (MORTIMER & PEARCE, 1981). It is possible to have here a new structure, as the chemistry of the sample shows no peculiarities (Table 1).

Analcime occurs together with calcite and clay minerals and was identified by both X-ray diffractometry and the Na/(Na + Ca) = 0.4 relation. The Na/(Na + Ca) = 0.6 value points on the possible presence of another zeolite, wairakite.

Barrerite, the most "exotic" species found in Copăceni, was studied by X-ray powder and single-crystal diffraction. The last two zeolites, chabazite-Ca and mordenite are associated always with calcite and clay minerals.

References

BALINTONI, I. & IANCU, V. (1986): Dări de Seamă ale Şedinţelor Institutul de Geologie şi Geofizică, 5. Tectonică şi geologie regională, 70–71: 45–56.

KRISTÁLY, F., STREMTAN, C., TÓTH, A. (2003): Acta Mineralogica Petrographica (Szeged), Abstract Ser. 1: 56.

MORTIMER, J. & PEARCE, J. (1981): American Mineralogist, 66: 309–314

Table 1: Major elements composition of two heulandite single crystals (electron microprobe).

Sample	SiO_2 %	Al_2O_3 %	MgO %	Na_2O %	CaO %	K_2O %	$FeO_{(tot)}$ %	Total %
C10_2	63.39	11.76	0.12	0.4	4.77	0.97	0.27	81.68
C10_4	63.63	12.28	0.15	0.43	5.2	1.04	0.36	83.09

WEATHERING OF SMECTITE AT KOPERNICA DEPOSIT

STRÍČEK, I., ŠUCHA, V. & UHLÍK, P.
Department of Geology of Mineral Deposits, Comenius University; Mlynska dolina, 84215 Bratislava, Slovakia
E-mail: stricek@fns.uniba.sk

Kopernica bentonite deposit is situated in the south-western margin of the Kremnické vrchy Mountains in the Western Carpathians. Deposit origin was probably influenced by two main processes – diagenetic and autohydrothermal alteration of rhyolite products.

Mineral composition of Kopernica bentonite was studied by XRD, FTIR and chemical analyses. There is a variation of smectite content and presence of other minerals like quartz, feldspars, biotite, kaolinite and a cristobalite. Dominant mineral phase is Al-Mg montmorillonite.

Weathering profile developed on the top surface of Kopernica bentonite under Central European temperate conditions was studied and compared with similar profile studied by ŠUCHA *et al.* (2001) on the Jelšový Potok deposit. Weathering of montmorillonite at the Jelšový Potok deposit resulted in the decrease of cation exchange capacity (CEC), total surface area (TSA) and in the thickness of the smectite crystals. The process was interpreted as montmorillonite partial dissolution and precipitation of amorphous SiO_2. At the Kopernica deposit we could see very similar trend but the range of weathering processes was not so intensive (Table 1). Results from sample Kop 5 do not agree with the mentioned trend due to the increased amount of cristobalite.

Reference

ŠUCHA, V., ŚRODOŃ, J., CLAUER, N., ELSASS, F., EBERL, D.D., KRAUS, I. & MADEJOVÁ, J. (2001): Clay Minerals, 36: 403–419.

Table 1: Depth of sampling from the soil surface, pH of water suspensions of the bulk samples, total organic carbon (TOC) contents of the bulk samples, total surface area (TSA), average thickness of the smectite crystals, and cation exchange capacity (CEC).

Sample	Depth (cm)	pH	TOC (%)	TSA (m^2/g)	Thickness (nm)	CEC (mEq/100g)
Kop 1	0–20	5.63	10.955	-	7.02	44.41
Kop 2	80–100	4.43	0.25	719.33	8.81	90.64
Kop 3	120–160	4.81	0.175	944.8	9.16	89.18
Kop 4	200–220	4.82	0.125	1009.97	9.83	89.54
Kop 5	300–350	5.04	0.11	893.49	9.15	63.7

SOME GEOCHEMICAL FEATURES OF METASOMATIC TOURMALINE RELATED TO PEGMATITES FROM ROMANIA

STUMBEA, D.
Department of Geology-Geochemistry, University "Al. I. Cuza", 20A Carol I Bvd., Iasi, Romania
E-mail: dstumbea@yahoo.com

The present paper deals with a geochemical comparison between the tourmaline hosted by metasomatic veins, crossing some pegmatite bodies from Romania and the so-called proto-pegmatitic tourmaline. In Romania, pegmatite bodies occur as veins and lenses in the medium-grade metamorphic terranes (micaschists, gneisses, migmatites etc.) of Southern, Western and Eastern Carpathians; generally, they have a simple mineralogy as follows: quartz, feldspars, muscovite as principal minerals, biotite, garnets and tourmaline as subordinate minerals. Pegmatites show a granite-like chemical composition; genetically, it seems that the pegmatites formed by both metamorphic differentiation and anatectic processes (MÂRZA, 1980; MURARIU, 2001; STUMBEA, 2001).

The study we carried out is based on electron microprobe analysis (major elements) performed on a CAMECA SX 50-Link Systems device; the analysis focused on the rim as well as on the core of tourmaline grains.

In terms of the variation of major elements from core toward the grain rim, a decrease of SiO_2, FeO and Na_2O and an increase of Fe_2O_3 and MgO has been found in metasomatic tourmaline; as for proto-pegmatitic tourmaline, the chemical composition of zoned grains showed a decrease of Al_2O_3 and FeO and an increase of Fe_2O_3, MgO and Na_2O amounts from core toward the grain rim.

The analyses performed on tourmaline grains show also some differences between the chemical features of metasomatic tourmaline cores/rims and those of proto-pegmatite core/rims. Thus, the core of metasomatic tourmaline has higher amounts of SiO_2 (36.60%), TiO_2 (0.60%), FeO (9.00%), MnO (0.40%), MgO (4.50%) and Na_2O (2.70%) than the core of proto-pegmatite tourmaline (35.30% SiO_2; 0.28% TiO_2; 8.40% FeO; 0.10% MnO; 2.80% MgO and 1.80% Na_2O). On the contrary, the amounts of Al_2O_3 and CaO are lower in the core of metasomatic tourmaline (33% Al_2O_3 and 0,10% CaO) as compared to the amounts of the same oxides in the core of tourmaline from proto-pegmatites (35.4% Al_2O_3 and 0.25% CaO).

The variation of chemical composition is almost similar when focusing on the rims of tourmaline grains, which proves that the distribution of major elements between the core and the rims of zoned tourmaline is the same, no matter the genesis of tourmaline is.

The mineralogical composition of tourmaline grains (mol%) reveals the presence of schorl, dravite, uvite, tsilaisite, ferridravite and alkali-deficient tourmaline end members. In terms of the mineralogical composition of cores *vs.* rims, both metasomatic and proto-pegmatitic tourmaline show higher amounts of schorl (58.7 mol%) and tsilaisite (1.2 mol%) end members and lower amounts of dravite (5.9 mol%), ferridravite (8.2 mol%) and uvite (4.3 mol%) in cores, than in the rim of grain. On the other hand, the core and the rim of metasomatic tourmaline contain lower amounts of schorl (52% in core, 45% in rim), ferridravite (7% in core, 8% in rim) and uvite (2% in core, 1% in rim) as compared to the core of proto-pegmatitic tourmaline.

Structural formulas of tourmalines reveal a smaller deficit in *X* sites (about 0.15 *pfu*) as well as in *Y* sites (about 0.16 *pfu*) than the proto-pegmatitic tourmaline (about 0.25 *pfu* in *X* sites and about 0.21 *pfu* in *Y* sites).

The present study revealed also three type of chemical substitution: Tschermak substitution – $(Mg, Mn, Fe^{2+})^Y + Si^T = Al^Y + Al^T$, alumino-buergerite substitution – $(Mg, Mn, Fe^{2+})^Y + OH^- = Al^Y + O^{2-}$ and alkali-deficient substitution – $Na^X + Mg^Y = Al^Y + \square^X$.

Starting from Ca : Fe_{tot} : Mg and Al : Fe_{tot} : Mg ratio, both metasomatic and proto-pegmatitic tourmalines belong to the group of tourmaline from Li-poor granitoids and their associated pegmatites/aplites.

References

MÂRZA, I. (1980): Anuarul Institutului de Geologie şi Geofizică, 57: 423–432.

MURARIU, T. (2001): Geochimia pegmatitelor din Romania (Geochemistry of pegmatites from Romania) (In Romanian). Bucureşti: Editura Academiei Române, 356 p.

STUMBEA, D. (2001): Geochimia pegmatitelor din sudul Gilăului (Geochemistry of pegmatites from Gilău (Apuseni Mts.) (In Romanian). Iaşi: Editura Universitatii "Al. I. Cuza", 267 p.

NEW DATA ABOUT THE MINERALS OF THE COPPER ORE DEPOSIT AT BĂLAN (EAST CARPATHIANS) AND OF LIMESTONE XENOLITHS FROM BASALT AT RACOŞU DE JOS (PERŞANI MTS.), ROMANIA

SZAKÁLL, S.[1], ALMÁSI, E.[2], KÖLLŐ, A.[2], SAJÓ, I.[3] & VEZZALINI, G.[4]
[1] Department of Mineralogy and Petrology, University of Miskolc, H-3515 Miskolc-Egyetemváros, Hungary
E-mail: askszs@gold.uni-miskolc.hu
[2] Department of Geology-Mineralogy, Babeş-Bolyai University, Kogălniceanu str. 1, RO-400084 Cluj-Napoca, Romania
[3] Chemical Research Centre, Hungarian Academy of Sciences, Pusztaszeri út 59-67, H-1025 Budapest, Hungary
[4] Dipartimento di Scienze della Terra, Università di Modena e Reggio Emilia, via S. Eufemia 19, I-41100 Modena, Italy

Rare secondary sulphates, carbonate-cyanotrichite, slavíkite, fibroferrite from the open pit of the Bălan copper ore deposit

The Bălan copper ore deposit is hosted in the epimetamorphic Tulgheş series. Primary sulphides are dominant pyrite and chalcopyrite, accompanied by sphalerite, galena, tetrahedrite and arsenopyrite. There is an extensive oxidation zone in near-surface position. Common secondary minerals include goethite, malachite, azurite, native copper; cuprite and covelline are rare (POPESCU, 1974; DAVID, 1983).

Our investigations were carried out on some secondary mineral parageneses formed in different levels of the Ferenc Ferdinánd open pit. All the minerals mentioned were identified by optical, XRD, SEM/EDS and ICP-MS methods. These minerals can be divided into two main groups according to the dominant cation, *i.e.* copper-bearing minerals (formed mainly from chalcopyrite) and iron-bearing ones (formed from pyrite). The main copper-bearing secondary minerals are chalcanthite, malachite, azurite and brochantite. As a rarity we identified carbonate-cyanotrichite, forming pale blue sprays, up to 1 mm size, in close association with colourless to blue glass-like allophane encrustation. The main iron- (and/or magnesium-) bearing secondary sulphates are halotrichite, pickeringite, fibroferrite and slavíkite. Halotrichite and pickeringite are found as white to pale yellowish, fine fibrous, hair-like efflorescences, sometimes as globular aggregates. Fibroferrite forms white to pale grey encrustations, which consist of a dense intergrowth of fine fibres. Slavíkite appears as yellowish green to pale green porous crusts, consisting of, hexagonal tabular crystals, 10-20 μm in size. Carbonate-cyanotrichite, slavíkite and fibroferrite are the first occurrence reported from Romania.

Levyne-Ca and ettringite in limestone xenoliths from basalt at Racoşu de Jos

According to radiometric age determinations the basalt area at Racoşu de Jos is one of the youngest in Europe. The locality is famous for upper mantle-derived xenoliths consisting mainly of olivine and pyroxene (DOWNES *et al.*, 1995). Quartz xenoliths and contact metamorphic minerals that has been formed at the contact of the xenoliths and the enclosing basalt were also described from here (MĂLDĂRESCU *et al.*, 1982).

In the last years we found rare limestone-derived xenoliths, in which the dominating minerals were Ca silicates. We examined these xenoliths by optical, XRD, SEM/EDS and EPMA techniques. They contain high temperature silicate minerals of contact metamorphic origin, mainly gehlenite, diopside and augite. Garnets (andradite–grossular), magnetite, ilmenite, chlorapatite, titanite, and some sulphides appear in smaller amounts.

In the cavities and fissures of the limestone xenoliths a low temperature paragenesis of hydrothermal origin occurs. This association contains mainly hydrous Ca silicates, among them zeolites, such as levyne and chabazite. Levyne forms white, hexagonal, tabular crystals up to 0.5 mm in size. According to EPMA results it is levyne-Ca. The other interesting late-stage mineral is ettringite. It occurs in white needles, some μm across and up to 0.5 mm in length, with hexagonal cross-section or forms fibrous aggregates, in close association with levyne-Ca. Ettringite crystals can be hexagonal prismatic to bladed. Ettringite was identified by XRD and SEM/EDS examinations. The three strongest XRD lines are [d (Å) (I_{rel})]: 9.72 (100), 5.61 (76), 3.87 (31). EDS analyses sometimes show chemical compositions close to thaumasite suggesting an ettringite–thaumasite solid solution in these crystals. A few white, globular aggregates up to 0.5 mm, composed of okenite, accompany earlier mentioned minerals. The last precipitations are calcite and smectite. Levyne-Ca and ettringite are the first occurrence reported from Romania.

References

DAVID, I. (1983): Studiul petrografic şi litografic al metamorfitelor din perimetrul Bălan extindere Nord cu privire specială asupra mineralizaţiilor de sulfuri polimetalice. University Theses, Manuscript, Babeş–Bolyai University, Cluj-Napoca.

DOWNES, H., SEGHEDI, I., SZAKÁCS, A., DOBOSI, G., JAMES, D.E., VASELLI, O., RIGBY, I.J., REX, D. & PÉCSKAY, Z. (1995): Lithos, 35: 65–81.

JASMUND, K. & HENTSCHEL, G. (1964): Beiträge zur Mineralogie und Petrographie, 10: 296–314.

MĂLDĂRESCU, I., ŞECLĂMAN, M., ATANASIU, M. & BĂDESCU, D. (1982): Analele Universitaţii Bucuresti, Geologie, 33: 21–26.

POPESCU, GH. C. (1974): Studiul formaţiunilor cristaline cu sulfuri metalice din zona Bălan. Studiu de sinteză. Bucureşti: Ministeriul Minelor, Petrolului şi Geologia.

OCCURRENCE OF COWLESITE IN ANDESITE AT PILISSZENTLÁSZLÓ, PILIS MTS., HUNGARY

SZAKÁLL, S.,[1] FEHÉR, B.[2] & VEZZALINI, G.[3]
[1] Department of Mineralogy and Petrology, University of Miskolc, H-3515 Miskolc-Egyetemváros, Hungary
E-mail: askszs@gold.uni-miskolc.hu
[2] Department of Mineralogy, Herman Ottó Museum, Kossuth u. 13, H-3525 Miskolc, Hungary
[3] Dipartimento di Scienze della Terra, Università di Modena, via S. Eufemia 19, I-41100 Modena, Italy

Cowlesite was first described by WISE & TSCHERNICH (1975) from seven different localities from the U.S.A. All known occurrences are in basic lavas. VEZZALINI *et al. (*1992) mentioned some localities of cowlesite in basalt from Northern Ireland. It was unknown in the Carpathian region to date.

There are a few zeolite occurrences in cavities and fissures of andesite in the Pilis Mts. (NNW from Budapest). Usual zeolite associations in this territory include stilbite, chabazite and heulandite. However, near Pilisszentlászló (in the Pálbükk quarry) white, soft, spherical aggregates have very rarely been found in the cavities of the rocks. They consist of very thin radiating plates with pearly lustre. The diameter of the spherules reaches up to 0.5 mm. These spherules are cowlesite according to XRD patterns and electron-microprobe analyses. Cowlesite is often covered by thin smectite (saponite?) and/or goethite films. In the cavities some relatively high temperature rock-forming minerals occur in the form of well-developed, but tiny crystals (*e.g.* plagioclase, amphibole, apatite, magnetite, hematite, and rarely cheralite–monazite). These earlier formed minerals are followed by cowlesite, chabazite, smectites, goethite, hematite and calcite.

Cowlesite is a zeolite with unknown structure. Complete single crystal X-ray study has not been performed so far because cowlesite crystals are always very small (up to 0.1 mm in width) and thin (up to 2 μm). According to X-ray powder data and very faint precession photographs, cowlesite is orthorhombic; this symmetry corresponds to the results of the optical studies (GOTTARDI & GALLI, 1985).

Because of the very limited quantity of available material from the cowlesite from Pilisszentlászló, experimental XRPD pattern was obtained by a 114.6 mm Gandolfi camera using CoK_α radiation. Observed reflections on the X-ray film are [*d* in Å (intensity, *hkl*)]: 15.15 (vs, 010), 12.44 (w, 001), 8.46 (w, 101), 7.64 (vw, 020), 5.68 (w, 121), 4.16 (vw, 202), 3.80 (w, 040), 3.45 (vw, 141), 3.27 (vw, 321), 3.12 (w, 004), 3.06 (vw, 050), 2.953 (vw, 051), 2.826 (w, 043), and 2.225 (vw, 352). Unit cell data calculated from the powder pattern are a = 11.46(6) Å, b = 15.19(3) Å, c = 12.45(3) Å, V = 2166(12) Å^3.

Electron-microprobe analyses (sample G145) were carried out in the wavelength-dispersive mode. The results are very close to those published earlier (WISE & TSCHERNICH, 1975; VEZZALINI *et al.,* 1992). The data (Table 1) correspond to a composition close to the stoichiometric formula for cowlesite ($CaAl_2Si_3O_{10} \cdot 6H_2O$) and indicate a relatively narrow compositional range. H_2O could not be directly determined due to the paucity of the sample.

References

GOTTARDI, G. & GALLI, E. (1985): Natural zeolites. Berlin: Springer-Verlag.

VEZZALINI, G., ARTIOLI, G., QUARTIERI, S. & FOY, H. (1992): Mineralogical Magazine, 56: 575–579.

WISE, W.S. & TSCHERNICH, R.W. (1975): American Mineralogist, 60: 951–956.

Table 1: Chemical composition (in wt%) according to electron-microprobe analyses and corresponding structural formulae for cowlesite from Pilisszentlászló (H_2O was calculated from difference)

No.	BaO	FeO	SrO	K_2O	CaO	SiO_2	Na_2O	MgO	Al_2O_3	Total
1	0.00	0.00	0.05	0.02	11.95	40.99	0.69	0.10	21.67	75.47
2	0.04	0.02	0.00	0.02	11.15	39.33	0.65	0.09	20.25	71.55
3	0.05	0.07	0.08	0.09	11.85	41.24	0.92	0.15	22.36	76.81
4	0.01	0.10	0.01	0.08	11.40	43.59	0.99	0.13	24.77	81.08
5	0.00	0.06	0.06	0.04	12.17	41.21	0.82	0.14	22.47	76.97
6	0.00	0.07	0.01	0.08	11.21	40.21	0.76	0.10	19.88	72.32
7	0.00	0.05	0.00	0.08	11.41	46.04	0.94	0.12	25.24	83.88

1) $(Ca_{0.96}Na_{0.10}Mg_{0.01})_{\Sigma=1.07}[Al_{1.91}Si_{3.06}O_{10}] \cdot 6.11H_2O$
2) $(Ca_{0.94}Na_{0.10}Mg_{0.01})_{\Sigma=1.05}[Al_{1.88}Si_{3.09}O_{10}] \cdot 7.45H_2O$
3) $(Ca_{0.93}Na_{0.13}Mg_{0.02}K_{0.01})_{\Sigma=1.09}[Al_{1.94}Si_{3.03}O_{10}] \cdot 5.68H_2O$
4) $(Ca_{0.85}Na_{0.13}Mg_{0.01}Fe_{0.01}K_{0.01})_{\Sigma=1.01}[Al_{2.02}Si_{3.02}O_{10}] \cdot 4.37H_2O$
5) $(Ca_{0.96}Na_{0.12}Mg_{0.02})_{\Sigma=1.10}[Al_{1.94}Si_{3.02}O_{10}] \cdot 5.63H_2O$
6) $(Ca_{0.93}Na_{0.11}Mg_{0.01}K_{0.01})_{\Sigma=1.06}[Al_{1.82}Si_{3.13}O_{10}] \cdot 7.19H_2O$
7) $(Ca_{0.81}Na_{0.12}Mg_{0.01}K_{0.01})_{\Sigma=0.95}[Al_{1.98}Si_{3.07}O_{10}] \cdot 3.58H_2O$

POSTMAGMATIC ALACRANITE (?) FROM THE CIOMADU AREA, SOUTH HARGHITA, ROMANIA

SZAKÁLL, S.[1], PAPUCS, A.[2], JÁNOSI, CS.[3], KRISTÁLY, F.[1] & PÁL-MOLNÁR, E.[2]
[1] Department of Mineralogy and Petrology, University of Miskolc, H-3515 Miskolc-Egyetemváros, Hungary
E-mail: askszs@gold.uni-miskolc.hu
[2] Department of Mineralogy, Geochemistry and Petrology, University of Szeged, P.O. Box 651, H-6701 Szeged, Hungary
[3] Csík County Nature and Conservation Society, Szív str. 3/14, RO-530225 Miercurea Ciuc, Romania

Alacranite, As_8S_9, monoclinic with space group $P2/c$, was first described by POPOVA *et al.* (1986) from the Uzon caldera (Kamchatka, Russian Federation). The mineral occurs with realgar and uzonite as flattened and prismatic grains up to 0.5 mm across, serving as cement in sandy gravel. Alacranite and other arsenic minerals are recent products of solfataras and hot springs in the central part of the Uzon caldera.

The structure of alacranite consists of an ordered sequence of As_4S_4 and As_4S_5 cage-like molecules, with a molecular packing closely resembling that found in the β-As_4S_4 phase (BONAZZI *et al*., 2003a). The unnamed natural β-As_4S_4 phase was first described by CLARK (1970) from Alacrán mine, Chile, as a high-temperature phase (stable in the As-S system at temperatures above 256 °C), whereas realgar is the low-temperature (α-) form of As_4S_4. Alacranite was named by POPOVA *et al.* (1986) for the similarities of the XRD pattern of the samples from the Uzon caldera to those from Alacrán mine. New chemical and crystallographic data (BONAZZI *et al.,* 2003b) suggest the existence of a continuous series between natural β-As_4S_4 and alacranite. It is now evident that minerals with chemical composition ranging continuously from As_8S_8 to As_8S_9 can crystallize.

Arsenic mineralizations in the surroundings of Ciomadu area

The first reference to arsenic mineralization in the area was published by HAUER (1860). He described realgar, sulfur and aragonite from the Hankó Valley at Covasna (~30 km E from Sfântu Gheorghe). Since then another occurrence have been discovered at Bodoc, Covasna County (~10 km NNE from Sfântu Gheorghe); during drilling of a mineral water well a drill core with calcite and orpiment was found. In 2001, during the reconstruction works of the "Nyírfürdő" spa at Lăzăreşti, Harghita County (~40 km NNE from Sfântu Gheorghe) some realgar-like minerals were found. The locality at Lăzăreşti is situated 5 km N from the Ciomadu volcanic area on the contact of the Pleistocene deposits of the Ciuc Basin and the Ciuc Mountains. The latter belongs to the Carpathian flysch (sandstone) area. At the "Nyírfürdő" spa a great number of mineral water springs and mofettes (openings emitting CO_2) can be found.

Arsenic minerals can be found as cement in the sand of the upper part of the flysch. The sand (consisting mainly of detrital quartz and muscovite) is originated from the weathered Cretaceous flysch (sandstone). Here alacranite occurs together with realgar as flattened or prismatic grains up to 0.3 mm across. Alacranite is orange, with a yellow-orange streak, greasy to adamantine lustre; it is very brittle with a conchoidal fracture. The strongest reflections on the X-ray powder pattern of Lăzăreşti specimens are, *d* in Å (int.) [in square brackets: data of POPOVA *et al.* (1986)]: 5.869 (62), [5.91 (90)], 5.063 (20), [5.11 (80)], 3.273 (58), [3.291 (50)], 3.080 (50), [3.064 (100)], 2.937 (70), [2.950 (90)].

According to our examinations we might have $As_8S_{(9-x)}$ crystals with a wide range of the x value. The powder patterns of the crystals with different x values resemble each other very nearly and it is not easy to index correctly the reflection in order to obtain reliable unit cell dimension. Single crystal diffractometry will be the best way to obtain unit cell dimensions in the future.

The available data suggest that this occurrence were formed by similar processes as that in the Uzon caldera, *i.e.* it may be related to the late volcanism of the Harghita Mts., the last known active volcanoes in the region being those in the Ciomadu area. Arsenic minerals were formed by low-temperature solfataras and springs.

References

BONAZZI, P., BINDI, L., POPOVA, V., PRATESI, G. & MENCHETTI, S. (2003a): American Mineralogist, 88: 1796–1800.

BONAZZI, P., BINDI, L., OLMI, F. & MENCHETTI, S. (2003b): European Journal of Mineralogy, 15: 283–288.

CLARK, A. H. (1970): American Mineralogist, 55: 1338–1344.

HAUER, F. von (1860): Jahrbuch der k. k. geologischen Reichsanstalt, 11: 85–86. (in German)

POPOVA, V. I., POPOV, V. A., CLARK, A. H., POLYAKOV, V. A. & BORISOVSKII, S. E. (1986): Zapiski Vsesoyuznogo Mineralogicheskogo Obshchestva, 115: 360–368. (in Russian)

SALT MINERALS IN EFFLORESCENCES ON SOIL SURFACE OF HUNGARY

SZENDREI, G.[1], TÓTH, T.[2], SZAKÁLL, S.[3], KOVÁCS-PÁLFFY, P.[4] & SAJÓ, I.[5]
[1] Department of Mineralogy and Petrology, Hungarian Natural History Museum, Ludovika tér 2, H-1083 Budapest, Hungary
E-mail: szendrei@miner.nhmus.hu
[2] Research Institute for Soil Science and Agrochemistry, Hungarian Academy of Sciences, Herman Ottó út 15, Budapest, Hungary
[3] Department of Mineralogy and Petrology, University of Miskolc, H-3515 Miskolc-Egyetemváros, Hungary
[4] Geological Institute of Hungary, Stefánia út 14, H-1143 Budapest, Hungary
[5] Chemical Research Centre, Hungarian Academy of Sciences, Pusztaszeri út 59-67, H-1025 Budapest, Hungary

The study of salt efflorescences in various environments contributes to the knowledge of salt accumulations, their processes and factors of formation.

Quite a number of occurrences are known all over the world, but very few places are described in Europe (GUMUZZIO *et al*., 1982; GUMUZZIO & CASAS, 1988; VIZCAYNO *et al*., 1995). Samples of salt efflorescences north of the Mediterranean region have not been systematically collected in Europe.

Salt-affected soils cover large area (~7%) in Hungary, mainly in the Great Hungarian Plain. Accumulations of salts are due to the sodium dominated shallow-depth groundwater.

In the years 1998–2005, 176 promising sites for occurrences of salt efflorescences were visited, out of which salt minerals on soil surfaces were found at 39 sites.

Soils were described and sampled by the Hungarian standard methods for soils survey (SZABOLCS, 1966). Soil routine, chemical and mineralogical analyses were done according to Hungarian standard methods (BUZÁS 1988, 1993). To determine salt minerals XRDA and SEM-EDXRA were used.

In the past (before 1998) 107 spots (at 65 villages) were listed (data compiled from earlier publications) and in the 19th and early 20th century salts could be found in a great extent and in large amounts. In consequence of dropping groundwater level the extent of salt efflorescences was reduced in time. Occurrences were much more frequent in the regions of Danube–Tisza interfluve and Nyírség in the past than today. Concerning the anion compositions of salts, sodium carbonate and carbonate-chloride associations were very common in the past.

Our studies showed that sodium-bearing minerals were dominant, magnesium sulphates occurred only once. Mixed-cation salts (burkeite, bloedite) were very rare. In the salt efflorescences, sodium chloride (halite), sodium sulphate (mirabilite and thenardite) as well as sodium carbonate minerals (nahcolite, natron, thermonatrite and trona) were determined. These represent the first descriptions of burkeite and nahcolite in Hungary. In the salt mineral associations, sulphate, sulphate-chloride, carbonate-sulphate-chloride mineral associations are common. Sodium carbonate mineral associations have also been found, which are very rare associations all over the world.

Salt minerals were found on the surface of soils like Solonchak, Hyposalic Fluvisol (appr. WRB), Salic Solonetz (appr. WRB), Mollic Solonetz (appr. WRB) and other soils *e.g.* Salic Fluvisol (appr. WRB). Efflorescences were found only on soils where the average ECe-values of surface horizons were above 4.8 dSm^{-1}. The anion composition of 1:10 water extracts of soil surface horizons was plotted on the CO_3–SO_4–Cl triangle. The plots were very close to the plot of the dominant anions of the minerals of the salt efflorescences.

Salt efflorescences were found on bare spots and only in a few plant associations, mainly *Puccinellietum limosae* and *Camphorosmetum annuae*. Groundwater level was generally close to the surface (80–250 cm in soils examined by opening a pit). Groundwater chemistry was also correlated with the dominant anion of the salt efflorescences but the relation was not so strict as compared to the case of the 1:10 water extracts of the soil surface horizons.

As a conclusion, salt efflorescence in Hungary varied in time and space. Relationships could be determined between salt minerals in efflorescences and soil type, soil properties as well as environmental parameters like vegetation, and level and chemistry of groundwater.

References

BUZÁS, I. (ed.) (1988): Talaj- és agrokémiai vizsgálati módszerkönyv, 2. (Methods of soil and agrochemical analysis, 2). Budapest: Mezőgazdasági Kiadó, 243 p.

BUZÁS, I. (ed.) (1993): Talaj- és agrokémiai vizsgálati módszerkönyv, 1. (Methods of soil and agrochemical methods, 1). Budapest: INDA 4231 Kiadó, 357 p.

GUMUZZIO, J. & CASAS, J. (1988): Cahiers ORSTOM. Série Pedologie, 24: 215–226.

GUMUZZIO, J., BATLLE, J. & CASAS, J. (1982): Geoderma, 28: 39–51.

SZABOLCS, I. (ed.) (1966): A genetikus üzemi talajtérképezés módszerkönyve. (Handbook for large scale, genetic soil mapping, in Hungarian). Budapest: Országos Mezőgazdasági Minőségvizsgáló Intézet, 351 p.

VIZCAYNO, C., GARCIA-GONZALES, M. T., GUTIERREZ, M. & RODRIGUEZ, R. (1995): Geoderma, 68: 193–210.

FACIES ARCHITECTURE AND PETROLOGY OF A BADENIAN SHALLOW SUBVOLCANIC RHYOLITE BODY, MULATÓ HILL AT LŐRINCI, MÁTRA MTS. (HUNGARY)

SZEPESI, J., KOZÁK, M. & PAPP, I.
Department of Mineralogy and Geology, University of Debrecen, Egyetem tér 1, H-4010 Debrecen, Hungary
E-mail: szepesij@delfin.unideb.hu

The 207-m high rhyolite body of the Mulató Hill is the last elevation at the gradually decreasing southwestern side of the Mátra Mountains. Acidic volcanic rocks appear very rarely in the essentially andesitic stratovolcanic sequence of the Mátra Mountains. The uniqueness of the hill has been attracting scientists since the early period of Hungarian petrography in the 19th century (SZTERÉNYI, 1881; MAURITZ, 1909). The stratigraphic setting was made clear by the geological mapping of the Mátra Mountains after the 2nd World War. The Mulató Hill rhyolite belongs to the Gyöngyössolymos Rhyolite Formation but its age is younger (14.83±0.5 Ma) than that of the rocks in the denominative outcrop at Gyöngyössolymos (15.9±0.5 Ma).

The rhyolite rock is quarried in a still operating, multi-level quarry, which exposes nearly the whole sequence of the sill-like body in 250 m length and in 35 m thickness. The melt came from a shallow and small magma chamber; the acidic character was caused by near-surface differentiation and contamination processes. The positions and dimensions of the facies zones verify the shallow subvolcanic character contrary to the formerly proposed subareal lava flow origin (VARGA *et al*., 1975). The rock facies was influenced by unequal distribution of volatile content, features of moving and cooling of the body and postvolcanic effects. In 2005 the mining exposed the lower brecciated border zone and made clear the emplacement conditions. The partly degassed melt penetrated into andesitic agglomerate-hyaloclastite rocks with very small extrusion rate. The margins cooled very quickly and the continuous extrusion broke the solidifying lower zone, but the upper side was unbroken. The slow moving of the melt on a gentle slope caused laminar shearing, which subsided and joined the vesicles (up to dm) and promoted gas migration to the higher levels. The accumulation of the gas content at the top of the body resulted in a vesicular rock type. Highly vesicular and compact bands alternate in the samples as a result of the large viscosity.

In the central zone there is a red, vesicular, fluidal rhyolite with columnar joints becoming thin-bedded towards the outer areas. The most characteristic facies is a black globular rhyolite (vitrophyre) with 1.5-2 m thickness, formed at the volatile-poor, quickly cooling margins. Brownish-black coloured globular structures (5-8 mm in diameter) with yellowish grey centre are scattered in the black, glassy matrix. Their distribution is variable, if their proportion is high enough and the globules touch each other, the spherical form became deformed and seems to be angular. Under microscope the matrix and the spheres consist of the same material; the spheres probably formed by quick devitrification during uneven cooling. The postvolcanic alterations caused kaolinization, fading of the rocks, depending on the primary porosity rate. Along the joints of the rock, clayey, limonitic coatings have been formed.

On the basis of the geochemical data, the rocks belong to the high-K part of the calc-alkaline series. The Mulató Hill rhyolite has a sanidine microlitic-trachytic texture type, unique among Hungarian acid lavas. The phenocrystal content is generally low, there are acidic plagioclase feldspars in the limonitic groundmass. High amount of sanidine microlites is due to lower viscosity and slow ascending rate in the vent. Mafic component is opacitic biotite. The red colour is caused by hematite and limonite patches in the groundmass.

References

MAURITZ, B. (1909): Mathematikai és Természettudományi Közlemények, 30: 133–244.

SZTERÉNYI, H. (1881): Földtani Közlöny, 12: 31–81.

VARGA, GY., CSILLAGNÉ TEPLÁNSZKY, E. & FÉLEGYHÁZI, ZS. (1975): A Mátra hegység földtana. (MÁFI Évkönyve, 56.) Budapest: MÁFI.

ORIGIN OF SEDIMENTS TRANSPORTED FROM DIFFERENT DIRECTIONS INTO THE LAKE PANNON DURING THE LATE NEOGENE, BASED ON MINERALOGICAL COMPOSITION OF SANDS AND SANDSTONES IN THE HUNGARIAN PLAIN

THAMÓ-BOZSÓ, E.[1], JUHÁSZ, GY.[1] & Ó. KOVÁCS, L.[2]
[1] Geological Institute of Hungary, Stefánia út 14., H-1143 Budapest, Hungary
E-mail: bozso@mafi.hu
[2] Hungarian Geological Survey, Stefánia út 14., H-1143 Budapest, Hungary

Sedimentological as well as seismic and sequence stratigraphic studies proved that the main sediment input came from NW and NE, subordinately from SE directions into the Lake Pannon in the area of the Hungarian Plain during the Late Miocene–Pliocene (Pannonian *s.l.*). Sediments were carried along by large fluvial and deltaic systems. To trace the origin of sediments transported from different directions we studied the available heavy mineral data of 868 sand and sandstone samples from 53 boreholes, using also statistical methods. During the interpretation the studied samples were identified in terms of depositional facies and depositional cycles, as well as lithostratigraphic units.

Tendencies in the mineralogical composition

Different kinds of tendencies were recognized which have different backgrounds. The average amount of chlorite gradually increases from fluvial sands through delta and basin-slope sediments to the deep-basinal turbidite sandstones, as opposed to garnet, pyroxenes and amphiboles, the frequency of which gradually decreases with water depth as well as with distance from the source area. These tendencies were caused by the selective sorting of minerals during transport and sedimentation, and the changing of source rocks. The maturity of the studied sands and sandstones mostly depends on the distance from their source areas. There are characteristic vertical changes in the mineralogical composition of the sedimentary succession. These changes are connected to depositional cycles rather than vertical facies changes. The closer the source area the stronger the changes are. The most considerable changes are connected to tectonically controlled 3rd order sequence boundaries, especially in those cases when they mean considerable hiatus. In the NE area, close to the sediment source, even the 4th order cycles bare well visible changes of the mineralogical composition.

Mineralogical composition of sediments derived from different directions

Sands, which came from NE into the Hungarian Plain, deposited as chlorite-rich turbidite, basin-slope and delta sediments, while on the marginal areas the basin-slope, delta and fluvial sands are immature and they have high biotite, amphibole, magnetite, garnet and pyroxene contents. Sediments that came from NW and were deposited in the delta front and delta plain environments on the Danube–Tisza interfluve, have chlorite, garnet and/or epidote-rich compositions, and there are fluvial sands with a high garnet content, too. Far from the source areas they became chlorite-rich sands, and were deposited as turbidite and basin slope sediments. Delta and fluvial sands in the Jászság subbasin, originating from NW and N directions, have chlorite, garnet, biotite, and sporadically magnetite-rich compositions. Sediments, transported from SE into the south-eastern part of the Hungarian Plain are subordinate. Here the basin slope sands are characterised by pyroxene-amphibole-garnet-chlorite compositions, the delta sediments are rich in chlorite, and the fluvial sands have varying compositions, with dominating amphibole, epidote, garnet, chlorite or magnetite.

Origin of sediments

Based on the results of cluster and discriminant analyses, we could deduce transport directions far from the source areas; e.g. sands coming from NW reached the middle and southern parts of the Hungarian Plain. The results of correlation analysis indicate the selective sorting and the origin of some minerals, too (garnets are dominantly from metamorphic rocks, pyroxenes and amphiboles from magmatic or volcanic rocks). The occurrence of source rock indicator minerals shows that detritus of low grade metamorphic rocks of the Carpathians and/or recycling the older sedimentary rocks, first of all flysch sediments of the surrounding areas, spread almost in the whole study area. Minerals that originated from medium and high grade metamorphic rocks are most abundant in the sediments of the fluvial sands of the Jászság subbasin and the Danube–Tisza interfluve. They derived from NW, from the Western Carpathians, Alps and Bohemian Massif. The sedimentary rocks on the SE and E parts of the Hungarian Plain with varying compositions and subordinate metamorphic mineral contents came from the Apuseni Mountains. Minerals from the Inner Carpathian volcanites are most frequent in the North-Transtisza region, but occur in the southern part of the Transtisza region, too.

This research was funded by the Hungarian National Scientific Research Fund (OTKA T-035168).

OPTICALLY STIMULATED LUMINESCENCE DATING OF QUARTZ FROM LATE-QUATERNARY SEDIMENTS IN HUNGARY

THAMÓ-BOZSÓ, E., NÁDOR, A., MAGYARI, Á. & BABINSZKI, E.
Geological Institute of Hungary, Stefánia út 14, H-1143 Budapest, Hungary
E-mail: bozso@mafi.hu

Optically stimulated luminescence (OSL) dating

It is a rapidly developing technique, which provides absolute chronologies for Late Quaternary clastic sedimentary rocks. OSL dating of quartz from sandy fraction can be applied up to an age of 100-200 ka. The basis of OSL dating is that OSL traps (defects in the crystal lattice) become empty due to sunlight exposure. After burial, grains are exposed to low-level ionizing radiation, which is produced by the decay of naturally occurring radioactive isotopes of K, U, Th of the surrounding sediments, and minor cosmic radiation. During this exposure to ionizing radiation, free charge carriers (electrons and holes) are produced, and some of them are trapped at defects in the crystal lattice. The total amount of charge in the OSL traps is proportional to the value and duration of the radiation, so it increases with burial time. Trapped charges are released from OSL traps when the mineral is exposed to light. Recombination of electrons released from traps and holes results luminescence, which is a very small light flux. The brightness of the luminescence signal reflects the amount of charge trapped, and hence the irradiation dose the sample received since burial (equivalent dose). After sampling and special sample preparation in dark conditions, measuring the natural luminescence signal of the sample, and the luminescence signals in response to different artificial radioactive doses, samples are excited by exposure to light, the equivalent dose (Gy) in the sample can be calculated. Measuring the value of radiation from surrounding sediments and water content of the sample, and calculating the value of cosmic radiation gives the natural dose rate (Gy/ka or Gy/a), which dose reached the sample during a year or ka. Equivalent dose (Gy) / dose rate (Gy/a) gives the age (a) of the sample.

Sampling and sample preparation

The studied samples were taken from fluvial and eolian sands and silts on the Hungarian Plain and Transdanubian Hills. They were collected in opaque PVC tubes from outcrops and boreholes. The sample preparation was performed in subdued red light. Quartz was extracted from grain size fraction of 80–200 μm using H_2O_2 to remove organic material, 10% HCl to dissolve carbonates, SPT for density separation, 40% HF for 60 minutes to remove feldspars and the outer ~10 μm layer from the quartz grains, which has absorbed a dose from alpha radiation. The clean quartz grains were mounted as monolayer on stainless steel discs (aliquots).

OSL measurements and age calculation

OSL measurements were made in the Geological Institute of Hungary, using Risø TL/OSL automatic reader with a calibrated $^{90}Sr/^{90}Y$ beta source. After checking the luminescence purity of the quartz extracts by infra-red stimulation, blue LEDs were used for the optical stimulation of quartz. A single-aliquot regenerative-dose (SAR) protocol was used to estimate equivalent doses. In this procedure the equivalent dose is determined on a single aliquot by making repeated measurements of its OSL signal intensity, all light-sensitive trapped charge is removed during OSL measurements, and the data are automatically corrected. Preheat plateau tests, dose recovery tests, dose-response growth curves and thermal transfer tests were measured too. Equivalent doses (D_e) are based on between 18-23 aliquots per sample. The dose rates were calculated on the basis of high-resolution gamma spectrometry measurements of the surrounding sediments performed in the laboratory of Eötvös Loránd Geophysical Institute.

Results

On the Hungarian Plain OSL ages of the studied 25 sand samples from the upper 2–8 m of fluvial units vary between 10–47 ka. In this area the OSL age data were used to reconstruct the evolution of Late Quaternary river network complemented with heavy mineral analysis and interpretation of aerial photographs. We have two very young samples from recent flood deposits of the Tisza and Körös rivers.

The studied 12 fluvial and eolian sand and silt samples from the Transdanubian Hills are 11 to 42 ka old in from a depth 1,5-7 m. These age data provide the chronostratigraphic framework for timing neotectonic movements in this area.

This research was supported by the Hungarian National Research Fund (OTKA T 046307 and T 037593).

NEW MINERALS: SPECIMENS FOR COLLECTORS AND MUSEUMS OR SUPPLIERS OF NEW FINDINGS IN CRYSTAL CHEMISTRY

TILLMANNS, E.
Institut für Mineralogie und Kristallographie der Universität Wien, Geozentrum, Althanstr. 14, A-1090 Wien, Austria
E-mail: ekkehart.tillmanns@univie.ac.at

A number of new minerals which display so far unknown crystal chemical features have been described by the author and his colleagues. Minerals are presented in microphotographs and crystal structure drawings with respect to the special features in crystal chemistry. Selected minerals from the Eifel area, Germany, are almarudite, $K(\square, Na)_2(Mg, Fe, Mn)_2(Be, Al)_3[Si_{12}O_{19}]$, and rondorfite, $Ca_8Mg[SiO_4]_4Cl_2$, (MIHAJLOVIĆ *et al.*, 2004), batiferrite, $Ba[Ti_2Fe_{10}]O_{19}$, (LENGAUER *et al.*, 2001), batisite, (Ba, K)(K, Na)Na(Ti, Fe, Nb, Zr)Si_4O_{14}, (SCHMAHL & TILLMANNS, 1987), bellbergite, $(K, Ba, Sr)_2Sr_2Ca_2$ $(Ca, Na)_4Al_{18}Si_{18}O_{72} \cdot 30H_2O$, (RÜDINGER *et al.*, 1993), brenkite, $Ca_2F_2(CO_3)$, (LEUFER & TILLMANNS, 1980), hannebachite, $CaSO_3 \cdot 1/2H_2O$, (HENTSCHEL *et al.*, 1985), liebauite, $Ca_3Cu_5Si_9O_{26}$, (ZÖLLER & TILLMANNS, 1992), and the zeolite minerals tschörtnerite, $Ca_4(K, Ca, Sr, Ba)_3Cu_3(OH)_8$ $[Si_{12}Al_{12}O_{48}] \cdot 20H_2O$, (EFFENBERGER *et al.*, 1998) and willhendersonite, $KCaAl_3Si_3O_{12} \cdot 5H_2O$, (TILLMANNS *et al.*, 1984). Minerals from the Odenwald and Spessart areas, Germany, are cornubite, $Cu_5(AsO_4)_2(OH)_4$, (TILLMANNS *et al.*, 1985), hentschelite, $CuFe_2(PO_4)_2(OH)_2$ and reichenbachite, $Cu_5(PO_4)_2(OH)_4$, (SIEBER *et al.*, 1987), and sailaufite, $(Ca, Na, \square)_2Mn_3O_2(AsO_4)_2$ $(CO_3) \cdot 3H_2O$, (WILDNER *et al.*, 2003), while tillmannsite, $(Ag_3Hg)(As,V)O_4$ has first been described from the copper mines of Roua, Departement Alpes-Maritimes (France) (SARP *et al.*, 2003).

References

EFFENBERGER, H., GIESTER, G., KRAUSE, W. & BERNHARDT, H.-J. (1998): American Mineralogist, 83: 607–617.

HENTSCHEL, G., TILLMANNS, E. & HOFMEISTER, W. (1985): Neues Jahrbuch für Mineralogie, Monatshefte, (6): 241–250.

LENGAUER, C.L., TILLMANNS, E. & HENTSCHEL, G. (2001): Mineralogy and Petrology, 71: 1–19.

LEUFER, U. & TILLMANNS, E. (1980): Tschermaks Mineralogische und Petrographische Mitteilungen, 27: 261–266.

MIHAJLOVIĆ, T., LENGAUER, C.L., NTAFLOS, T., KOLITSCH, U. & TILLMANNS, E. (2004): Neues Jahrbuch für Mineralogie, Abhandlungen, 179: 265–294.

RÜDINGER, B., TILLMANNS, E. & HENTSCHEL, G. (1993): Mineralogy and Petrology, 48: 147–152.

SARP, H., PUSHCHAROVSKY, D.Y., MACLEAN, E.J., TEAT, S.J. & ZUBKOVA, N.V. (2003): European Journal of Mineralogy, 15: 177–180.

SCHMAHL, W.W. & TILLMANNS, E. (1987): Neues Jahrbuch für Mineralogie, Monatshefte, (3): 107–118.

SIEBER, N.H.W., TILLMANNS, E. & MEDENBACH, O. (1987): American Mineralogist, 72: 404–408.

TILLMANNS, E. FISCHER, R:X: & BAUR, W.H. (1984): Neues Jahrbuch für Mineralogie, Monatshefte, (12): 547–558.

TILLMANNS, E., HOFMEISTER, W. & PETITJEAN, K. (1985): Bulletin of the Geological Society of Finland, 57: 119–127.

WILDNER, M., TILLMANNS, E., ANDRUT, M. & LORENZ, J. (2003): European Journal of Mineralogy, 15: 555–564.

ZÖLLER, M. & TILLMANNS, E. (1992): Zeitschrift für Kristallographie, 200: 115–126.

CRITICAL EVALUATION OF THE ANALYTICAL DATA ON DIOCTAHEDRAL IRON-RICH MICAS AND RELATED MINERAL PHASES PUBLISHED IN THE LITERATURE

TÓTH, E.[1], WEISZBURG, T. G.[1] & POP, D.[2]
[1] Department of Mineralogy, Eötvös Loránd University, Pázmány Péter sétány 1/C, H-1117 Budapest, Hungary
E-mail: zsike@abyss.elte.hu
[2] Mineralogical Museum, Babeş-Bolyai University, Kogălniceanu St. 1, Cluj-Napoca, Romania

From many respects, it is hard to obtain high-quality chemical data of iron-rich dioctahedral micas (the true mica celadonite and the interlayer-deficient mica glauconite) and the related phases (*e.g.* "Fe-illite", "skolite"). Firstly, the sample is often inhomogeneous: the less evolved glauconitic grains regularly contain inclusions of quartz, feldspar, apatite *etc.* and may be stained with iron oxy-hydroxides, while celadonite, primarily a hydrothermal alteration product of basalt, often forms only thin encrustations and is readily mixed with other clay minerals or zeolites. This high grade of inhomogeneity could still be avoided by the application of electron probe microanalysis, however, these minerals contain a considerable amount of iron in both valence states, and for the determination of the Fe^{3+} / Fe^{2+} ratio either Mössbauer spectroscopy or wet chemistry is needed.

Studying the crystal chemical space occupied by these minerals, we set up a database including all the full chemical data accessible in the earth science literature. At the moment, the database contains more than 630 records, allowing us to draw some conclusions on the quality of these data.

We found that many authors neglect publishing the measured data (oxide wt %) and give only the calculated formula (atomic coefficients). These formulae often prove erroneous from a crystal chemical point of view, and, without the original data, it is impossible to trace back where the mistake was made. Several tens of analyses were discredited (suspecting either mixed material or analytical error) on structural constraints like Si > 4.0 *apfu* (formula calculated for 11 O), octahedral occupancy > 2.5 (official limit for dioctahedral layer silicates), interlayer occupancy > 1.0 *etc*.

Only half of the remaining data, approx. 300 analyses, contained measured FeO–Fe_2O_3 values with the proportion of Fe^{2+} being in the range 0–40%. For those analyses lacking these values, the authors adopted one of the following processes: they considered the total amount of iron as Fe^{3+}, or they calculated the formula for perfect dioctahedrality (*i.e.* octahedral occupancy = 2.00), even in such nomenclature-inspiring papers like LI *et al.* (1997). From these 300 "complete" analyses we found that the octahedral occupancy has an approximately normal distribution, with the maximum near 1.99–2.01 for phases containing K = 0.85–1.00 *apfu* and 2.01–2.03 for K = 0.6–0.85 *apfu* (values are in the range 1.95–2.10). We expect that in our data set the less evolved – pale green, more smectite-like – grains are underrepresented.

For showing the effect of the occupancy *vs*. iron valence state calculations, as an example, a well-known celadonite (E' of BUCKLEY *et al.*, 1978) with given FeO–Fe_2O_3 concentrations was selected. With increasing octahedral occupancy (oct. occ.), the interlayer charge remained relatively constant, however, the amount of divalent iron increased dramatically: from 6% (oct. occ. = 1.95) to 46% (oct. occ. = 2.05). More important, the nomenclature-related (RIEDER *et al.*, 1998) discriminant value $^{VI}Al / (^{VI}Al + ^{VI}Fe^{3+})$ changed from 0.32 to 0.51, crossing the border between Fe-rich and Al-rich members. Inversely, if the amount of Fe^{2+} is estimated to be higher, the octahedral occupancy increases. It comes from two facts: (1) due to the lower amount of oxygens (each Fe^{3+} is accompanied by 1.5 O, while each Fe^{2+} by only 1 O), a higher normalisation factor is needed for the 11 O-based formula, thus the amount of each component increases; (2) as the amount of Si increases, it forces part of the tetrahedral Al into the octahedral layer. The relationship between the amount of Fe^{2+} and the octahedral occupancy is linear.

Plotting the formulae into the IMA nomenclature diagram (RIEDER *et al.*, 1998), we found that several, from a crystal chemical point of view acceptable, formulae plot outside the diagonal border of the celadonite and glauconite boxes due to imperfect (≠ 2.00) dioctahedrality. From this respect, plotting into the IMA diagram should be handled with care.

The authors wish to express their gratitude to the European Commission's Research Infrastructure Action via the SYNTHESYS Project and especially Terry Williams (NHM) for the access to the library of the Natural History Museum (London).

References

BUCKLEY, H.A., BEVAN, J.C., BROWN, K.M., JOHNSON, L.R. & FARMER, V.C. (1978): Mineralogical Magazine, 42:373–382.

LI, G., PEACOR, D.R., COOMBS, D.S. & KAWACHI, Y. (1997): American Mineralogist, 82: 503–511.

RIEDER, M., CAVAZZINI, G., D'YAKONOV, Y., FRANK-KAMENETSKII, V.A., GOTTARDI, G., GUGGENHEIM, S., KOVAL, P.V., MÜLLER, G., NEIVA, A.M.R., RADOSLOVICH, E.W., ROBERT, J.-L., SASSI, F.P., TAKEDA, H., WEISS, Z. & WONES, D.R. (1998): Canadian Mineralogist, 36: 905–912.

PRELIMINARY DATA ON THE DIAGENESIS OF CRETACEOUS DINOSAUR BONES FROM THE BAKONY MTS., HUNGARY

TUBA, GY.[1], KISS, P.[1], PÓSFAI, M.[2] & MINDSZENTY, A.[3]
[1] Department of Mineralogy, Eötvös Loránd University, Pázmány Péter sétány 1/C, H-1117 Budapest, Hungary
E-mail: gyorgyi83@monornet.hu
[2] Department of Earth and Environmental Sciences, University of Veszprém, POB 158, H-8201 Veszprém, Hungary
[3] Department of Applied and Environmental Geology, Eötvös Loránd University, Pázmány Péter sétány 1/C, H-1117 Budapest, Hungary

Mineralogical and geochemical study of Late Cretaceous Dinosaur bones (femur and rib fragments) from the alluvial Csehbánya Formation (Iharkút, Hungary) were performed by the combination of several analytical techniques (polarised light microscopy, XPD, SEM + EDX, TEM + EDS, INAA). It was demonstrated that, regardless of their age, recrystallisation of bone apatite in the studied specimens was negligible. The original bone structure is almost perfectly preserved. The very fine-grained apatite phase of the studied bones was essentially hydroxylapatite, containing a detectable amount (20–320 μg/g) of U. The size distribution of the apatite crystallites is bimodal: there are isometric crystals 10–40 nm in width and length and larger, oblong-shaped crystals up to 300 nm in length. Their orange stain comes from the presence of 1.17% bone-organic matter (collagen). Early diagenetic pyrite filling the *Haversian channels* and the tiny little *lacunae* in between the osteons shows, that mineralisation in a sulphur-rich environment must be postulated for the early stages of diagenesis. The last cement phase is sparry calcite, filling all the remaining pores.

To check the reasons for the extraordinarily slight diagenetic change, also the vitrinite reflectance of finely dispersed organic matter from the enclosing alluvial sediments was measured. These data gave a maximum burial depth of 600 to 900 m, equivalent to temperatures less than about 80 to 90 degrees Celsius for the bone-bearing beds.

Our observations raised two important questions:

(1) What was the reason for the observed intensity of pyritisation in this supposedly freshwater alluvial environment? Was it perhaps a flat extensive delta plain of a low-gradient river, where marine pore water incursions could be expected already during early diagenesis?

(2) What was the reason for the apparent „freeze-in" of the recrystallisation process of the bone apatite, resulting in the persistence of the small crystal size and in the obviously very slight chemical alteration of the apatite crystallites, as compared to other fossil dinosaur bones (ZOCCO & SCHWARTZ, 1994; HUBERT *et al.,* 1996; PERSON *et al.,* 1996; SAMOILOV *et al.,* 2001; KOLODNY *et al.,* 1996)? Was it the anomalous burial and/or thermal history of the Mesozoic Iharkút block, or rather the efficient sealing of the bones from continued circulation of diagenetic fluids either by the enclosing fine-grained overbank sediments or by early cementation?

Further studies on similar fossil bones from other localities may help to answer these questions.

References

HUBERT, J. F., PANISH, P. T., CURE, D. J. & PROSTAK K. S. (1996): Journal of Sedimentary Research, 66: 531–547.

KOLODNY, Y., LUZ, B., SANDER, M. & CLEMENS, W. A. (1996): Palaeogeography, Palaeoclimatology, Palaeoecology, 126: 161–171.

PERSON, A., BOCHERENS, H., MARIOTTI A. & RENARD, M. (1996): Palaeogeography, Palaeoclimatology, Palaeoecology, 126: 135–149.

SAMOILOV, V. S., BENJAMINI, CH. & SMIRNOVA, E. V. (2001): Sedimentary Geology, 143: 15–39.

ZOCCO, T. & SCHWARTZ, H. L. (1994): Palaeontology, 37: 493–503.

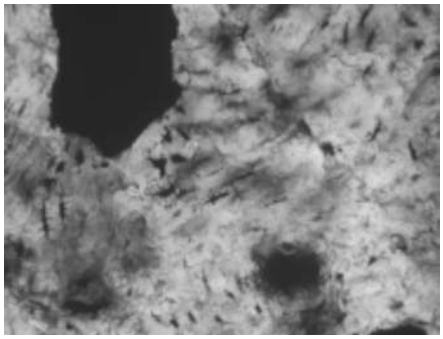

Fig. 1: An osteon identified in thin section made of a Nodosauridae rib. The boundaries of the Haversian system, the Haversian channel and the lacunae show up clearly. (Thin section perpendicular to the longitudinal axis of the rib-bone; transmitted light, crossed nicols.)

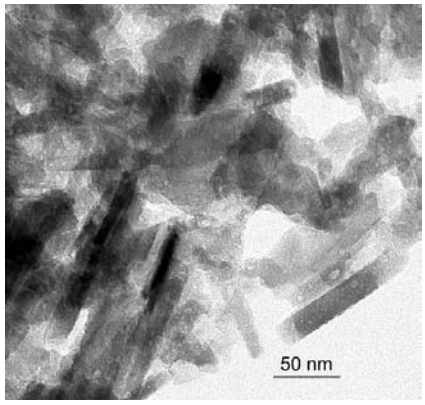

Fig. 2: Elongated apatite crystals.

NANOMETRIC INCLUSIONS IN MINERALS. AN EPMA, TEM/SAED AND MÖSSBAUER (NGR) APPROACH

UDUBAŞA, G.[1], CONSTANTINESCU, S.[2], POPESCU-POGRION, N.[2] & UDUBAŞA, S. S.[3]
[1] Geological Survey of Romania – IGR, 1 Caransebeş Str., 012271 Bucharest, Romania
E-mail: udubasa@geo.edu.ro
[2] National Institute of Material Physics, Atomiştilor 105bis, 76900 Bucharest-Măgurele, PO Box: MG-7, Romania
[3] Faculty of Geology & Geophysics, University of Bucharest, 1 Nicolae Bălcescu Blvd., 010041 Bucharest, Romania

A large number of mineral species (some 4-500 of about 4,000 known today) commonly occur as inclusions in other minerals and their identification needs as a rule more sophisticated equipment. Mineral species, which are known to occur only as inclusions are called **micro-minerals**, *i.e.* micrometer-sized bodies, such as mackinawite in pentlandite or in polyphase chalcopyrite-dominated inclusions in sphalerite. Careful microscopic investigation is commonly sufficient for identification, provided the optical properties are different as compared to the host minerals. Further examples: ulvöspinel in magnetite, sometimes valleriite in pentlandite, isocubanite (the former "chalcopyrrhotite") in chalcopyrite inclusions in sphalerite *etc*.

There are also cases when the microscope cannot help further in establishing the true nature of sub-micrometer inclusions. In such cases EPMA should be used coupled with microdiffraction devices. Examples can be given of numerous mineral species or compound found in the arsenopyrite from the Costesti gold ores, South Carpatians, Romania. Only by using EPMA sub-micrometer sized gold, a schreibersite-like phase (with Fe > Ni), greenockite and several Bi-containing phases have been determined (see UDUBAŞA, 2004, for details). Such inclusions could be called "**infra-minerals**".

A third level of inclusions can be traced at nano-size, *i.e.* microscopically impossible to be seen and hardly difficult to be hit. In such cases TEM/SAED seems to be the only way to recover the nano-world of minerals ("**nano-minerals**"). Two examples can by here given: (1) Discovery of wüstite and pyroxferroite as nanoinclusions in manganoan fayalite at Răzoare, Preluca Mts., Romania (CONSTANTINESCU *et al.*, 2004). These two minerals mark a very early, high PT mineral association during the metamorphic evolution of the rock pile. (2) Identification of nanometer-sized inclusions or "precipitates" of gold in or on arsenopyrite, pyrite and chalcopyrite from some shear-zone related ores in metamorphic rocks of the South Carpathians (for further details see UDUBAŞA S. S. *et al.*, 2006, abstract in this volume). The first level is represented by optically visible gold inclusions (most frequently seen in arsenopyrite). The second level has been established by extensive use of EPMA: around gold inclusions in arsenopyrite there were measured decreasing gold contents in apparently homogeneous parts of arsenopyrite monocrystals (UDUBAŞA & TOPA, 1995; UDUBAŞA, 2004). This is the so-called invisible gold in sulphides. The third level of gold occurrence is only possibly to visualize by using TEM/SAED techniques. In addition to gold, a further "nano-mineral" in pyrite from the Costeşti gold ores is the rare Ag-Au sulphide, uytenbogaardtite.

Note: The financial support of the Romanian Ministry of Education and Research in the frame of a research grant (4-209/2004-2006, and that is acknowledged) enabled a close cooperation between mineralogists and physicists and thus the discovery of the "nano-minerals" in sulphides.

References

CONSTANTINESCU, S., POPESCU-POGRION, N., UDUBAŞA, G., HARTOPANU, P. & REDFERN, S.T. (2004): Romanian Journal of Physics, 49: 631–640.

UDUBAŞA, G. & TOPA, D. (1995): Romanian Journal of Mineralogy, 77, Suppl. 1: 47–48.

UDUBAŞA, S. S. (2004): Metalogeneza auriferă asociată zonelor de forfecare din Munţii Căpăţânii. (Gold metallogenesis associated with the shear zones in the Căpăţânii Mts. In Romanian.). PhD thesis, Manuscript, Archives of the University of Bucharest, Romania, 182 p.

UDUBAŞA, S. S., CONSTANTINESCU, S., POPESCU-POGRION, N., GRECU, N. M. & UDUBAŞA, G. (2006): Acta Mineralogica–Petrographica, Abstract Ser. 5 (this volume): 123.

MÖSSBAUER (NGR), XRD, TEM/SAED AND ESR INVESTIGATIONS ON SOME SULPHIDES FROM COSTEŞTI, VALEA LUI STAN AND JIDOŞTIȚA GOLD ORES (SOUTHERN CARPATHIANS, ROMANIA)

UDUBAŞA, S. S.[1], CONSTANTINESCU, S.[2], POPESCU-POGRION, N.[2], GRECU, N. M.[2] & UDUBAŞA, G.[3]
[1] Department of Mineralogy, University of Bucharest, 1 Nicolae Bălcescu Blvd., RO-010041 Bucharest, Romania
E-mail: udubasa@geo.edu.ro
[2] National Institute of Material Physics, Atomiştilor 105bis,RO- 76900 Bucharest-Măgurele, PO Box: MG-7, Romania
[3] Geological Survey of Romania – IGR, 1 Caransebeş Str., RO-012271 Bucharest, Romania

In the metamorphic rocks of the Getic Realm in the Southern Carpathians (Romania) there are several shear-zone related gold ores/mineralizations, *i.e. Valea lui Stan*, near Brezoi and *Costeşti*, near Horezu, both in Vâlcea county, and *Jidoştiţa*, near Drobeta-Turnu Severin, in Mehedinţi county. Although quite similar, these occurrences show some peculiarities as concerns the main elements and the related protores, as summarized by UDUBAŞA (2004). Gold is commonly associated with, or included in, arsenopyrite, pyrite, chalcopyrite and sometimes quartz. "Invisible" gold has been identified in arsenopyrite by using EPMA, showing gradual decrease of concentration around optically visible gold inclusions.

In the frame of a research project (CERES C4-209/2004) the investigations have been continued by using extensive XRD, Mössbauer and TEM/SAED techniques, in co-operation with physicists. Powdered samples have been investigated at room temperature by using all the techniques.

^{57}Fe Mössbauer spectra of arsenopyrite have been registered and analyzed. Spectral parameters revealed that the dominant FeAsS phase represent 74%, 70% and 47% for the sample from Costeşti, Valea lui Stan and Jidoştiţa, respectively. The accompanying phases were identified in all the investigated samples. (Co, Fe)AsS and traces of $FeAs_2$ (~4%) have been found in the sample from Valea lui Stan. Pyrite and a larger quantity of loellingite (~28%) have been found in the sample of Jidoştiţa. In all the phases the Mössbauer spectra show an octahedral oxygen arrangement and a fractional ionic valence (~+2) low spin. The Mössbauer spectra of chalcopyrite and pyrrhotite exhibit the magnetic ordering and coexistence of the main phase with pyrite and/or marcasite.

Preliminary XRD analysis of arsenopyrite evidenced quartz as accompanying phase for all the investigated samples and cupride of gold (Cu_3Au) for the Valea lui Stan and Jidoştiţa ores. Cupride of gold was also recognized in the XRD spectra of chalcopyrite at Costeşti.

Hyperfine interactions of isolated Mn^{2+} were observed by ESR technique. Spectral parameters suggest Ca carbonate as host matrix. A more significant signal of manganese ion in calcite (axial symmetry) is observed in chalcopyrite. Also two distinct signals of Fe^{3+} probe (g_{ef} = 2.0 corresponding to the orthorhombic symmetry and g_{ef} = 3.78, only for the Valea lui Stan sample) were evidenced in the spectra).

SAED analyses carried out on powdery samples have shown nanometric "precipitates" of Au or an (Au, Ag) alloy on arsenopyrite grain surfaces, showing a great diversity of morphologies, *i.e.* from isolated gold nanoparticles, some tens of nanometers in size, up to "coral-like" aggregates. Such nanograins or aggregates have also been identified (although more rarely) on pyrrhotite and chalcopyrite. This is the third mode of occurrence of gold in/on sulphides, called "nano-minerals" by UDUBAŞA G. *et al.* (2006).

Moreover, in addition to metallic gold, further gold-bearing minerals have been identified, *i.e.* uytenbogaardtite, Ag_3AuS_2, closely associated with pyrrhotite at Costeşti, and auricupride, Cu_3Au, associated with arsenopyrite at Valea lui Stan and Jidoştiţa. During the investigations, some other new minerals for these ores have also been identified: cobaltite, CoAsS, in arsenopyrite samples from Valea lui Stan and Jidoştiţa and in sphalerite samples from Jidoştiţa, as well as loellingite, $FeAs_2$, in sphalerite samples from Jidoştiţa, maghemite in sphalerite samples from Jidoştiţa, moganite (monoclinic SiO_2) in arsenopyrite samples from Costeşti and Jidoştiţa, and CuO in chalcopyrite samples from Valea lui Stan.

Acknowledgements

The financial support of the Ministry of Education and Research of Romania through the research grant CERES C4-209/2004-2006 is gratefully acknowledged.

References

UDUBAŞA, S. S. (2004): Metalogeneza auriferă asociată zonelor de forfecare din Munţii Căpăţânii. (Gold metallogenesis associated with the shear zones in the Căpăţânii Mts. In Romanian.). PhD thesis, Manuscript, Archives of the University of Bucharest, Romania, 182 p.

UDUBAŞA, G., CONSTANTINESCU, S., POPESCU-POGRION, N. & UDUBAŞA, S. S. (2006): Acta Mineralogica–Petrographica, Abstract Ser. 5 (this volume): 122.

SAPPHIRE-BEARING SYENITE XENOLITH FROM GORTVA, CEROVÁ MOUNTAINS, SLOVAKIA

UHER, P.[1], GREGÁŇOVÁ, G.[2] & SZAKÁLL, S.[3]
[1] Department of Mineral Deposits, Comenius University, Mlynská dolina G, 842 15 Bratislava, Slovakia
E-mail: puher@fns.uniba.sk
[2] Department of Mineralogy and Petrology, Comenius University, Mlynská dolina G, 842 15 Bratislava, Slovakia
[3] Department of Mineralogy and Petrology, University of Miskolc, H-3515 Miskolc-Egyetemváros, Hungary

A blue corundum (sapphire) crystal, 7 mm large, in basalt from Hajnáčka maar near Fiľakovo, Cerová Mts., southern Slovakia, was first described by SZÁDECZKY (1899); the locality was re-discovered during extended paleontological research (UHER *et al.*, 1999). Numerous blue or pale violet sapphire crystals, 1–5 mm in size, were separated from Pliocene sand filling of the Hajnáčka maar together with other heavy-mineral assemblage (spinel, magnetite, magnesiochromite, ilmenite, titanite, forsterite, zircon, almandine, allanite, augite, diopside, enstatite, pargasite, kaersutite) and plagioclase with $Ab_{69–74}An_{18–25}Or_{06–08}$ composition (UHER *et al.*, 1999; GREGÁŇOVÁ, 2002). Locally, sapphire contains inclusions of zircon, monazite-(Ce), spinel, pyrrhotite (?) and an Y-U-Th-Nb-Ta phase (euxenite-(Y)?). Recently, 9 and 7 mm large, blue sapphire crystals were discovered in sands. However, all these recent finds of sapphire were described from secondary alluvial deposits and the primary rock of Hajnáčka sapphire was unknown up to now. On the basis of geological settings and rare corundum occurrence in syenitic xenoliths from Pinciná maar, 23 km NW of Hajnáčka (HURAI *et al.*, 1998), analogous syenites were assumed as the most probable parental rock for Hajnáčka sapphire (UHER *et al.*, 1999).

Fortunately, a photography of blue sapphire in host-rock from Gortva near Hajnáčka, to be found in the Herman Ottó Museum, Miskolc (inv. No. 14035), appeared in the *Minerals of the Carpathians* monograph (SZAKÁLL *ed.*, 2002) and studied now in detail by EMPA. Sapphire forms 2–4 mm crystals in white coarse-grained syenitic host rock. The whole described syenite forms a several cm large xenolith in black alkali basalt with pyroxene phenocrysts and feldspar-rich groundmass with ilmenite and titanian magnetite. Alkali feldspar of oligoclase composition ($Ab_{63–67}An_{24}Or_{10–13}$) is the dominant mineral of the syenite. Fibrolitic sillimanite forms a 0.1–0.4-mm thick contact zone between sapphire and feldspar. Fillimanite probably formed as a product of later, post-magmatic contact re-equilibration between corundum and feldspar, possibly during the thermal event connected with trapping of the syenite xenolith by the hot basalt lava. Leucite occurs as subhedral crystals (0.1–0.5 mm in size) in association with feldspar, pyroxene and Ti-rich magnetite. Pyroxene forms 0.02 to 0.15-mm long columnar crystals of augite to diopside composition ($Wollastonite_{47–51}$ $Clinoenstatite_{34–43}$ $Clinoferrosilite_{09–18}$). Feldspar composition in leucite- and pyroxene-rich areas changes to Na,K-rich, anorthoclase or sanidine-like member ($Ab_{51–59}An_{02–07}Or_{34–46}$), enriched in Ba (0.5–1.3 wt% BaO). Locally, *ca*. 1 mm large irregular zone of monomineralic analcime forms a matrix for pyroxene and leucite. Analcime formed as an *in situ* replacement product by solid-state ion exchange from leucite (X-type analcime; LINE *et al.*, 1995).

The studied sapphire and other minerals solidified from a felsic melt, probably in the lower crust and later they have been transported to the surface in syenite xenoliths or xenocrysts by alkali basalt lava. Analogous felsic syenitic xenoliths from the Pinciná maar, Slovakia crystallized under a pressure around 6 kbar (*ca*. 22 km of lithostatic load) and liquidus temperature of inclusion melts at 1080 °C (HURAIOVÁ *et al.*, 1996). Similar models for corundum origin from lower crustal felsic magma and their later uplift as xenoliths or xenocrysts in alkali basalt are widely accepted also for large sapphire occurrences in Thailand and Australia (*e.g.* COENRAADS *et al.*, 1995, SUTHERLAND *et al.*, 1998).

References

COENRAADS, R. R., VICHIT, P. & SUTHERLAND, F. L. (1995): Mineralogical Magazine, 59: 465–479.

GREGÁŇOVÁ, M. (2002): <Title>. PhD. Thesis, Manuscript, Comenius University, Bratislava, 75 p.

HURAI, V., SIMON, K., WIECHERT, U., HOEFS, J., KONEČNÝ, P., HURAIOVÁ, M., PIRONON, J. & LIPKA, J. (1998): Contributions to Mineralogy and Petrology, 133: 12–29.

HURAIOVÁ, M., KONEČNÝ, P. KONEČNÝ, V., SIMON, K. & HURAI, V. (1996): European Journal of Mineralogy, 8: 901–916.

LINE, C. M. B., PUTNIS, A., PUTNIS, C. & GIAMPAOLO, C. (1995): American Mineralogist, 80: 268–279.

SUTHERLAND, F. L., HOSKIN, P. W. O., FANNING, C. M. & COENRAADS, R. R. (1998): Contributions to Mineralogy and Petrology, 133, 356–372.

SZÁDECZKY, GY. (1899): Földtani Közlöny, 29: 240–252.

SZAKÁLL, S. (ed., with the contributions of UDUBAŞA, G., ĎUĎA, R., SZAKÁLL, S., KVASNYTSYA, V., KOSZOWSKA, E. & NOVÁK, M.) (2002): Minerals of the Carpathians. Prague: Granit.

UHER, P., SABOL, M., KONEČNÝ, P., GREGÁŇOVÁ, M., TÁBORSKÝ, Z. & PUŠKELOVÁ, Ľ. (1999): Slovak Geological Magazine, 5: 273–280.

COMPOSITIONAL VARIATIONS OF PEGMATITE Nb-Ta MINERAL ASSEMBLAGE FROM THE LIMBACH AREA, MALÉ KARPATY MTS., SLOVAKIA

UHER, P.[1], ŽITŇAN, P.[2] & OZDÍN, D.[2]
[1] Department of Mineral Deposits, Comenius University; Mlynská dolina G, 842 15 Bratislava, Slovakia
E-mail: puher@fns.uniba.sk
[2] Department of Mineralogy and Petrology, Comenius University; Mlynská dolina G, 842 15 Bratislava, Slovakia

A varied association of Nb-Ta oxide minerals was discovered during heavy-mineral prospecting in Limbach brook, NW of Pezinok, SW Slovakia. Besides of common heavy minerals (garnet, staurolite, zircon, apatite, monazite-(Ce), ilmenite, magnetite, gold), members of the columbite–tantalite (Ct) group, ferrotapiolite, Sn-rich ixiolite, Ta-rich rutile and microlite to uranmicrolite were identified together with uraninite and Hf-rich zircon (11-15 wt% HfO_2, 0.11-0.14 Hf apfu). The textural and compositional relations as well as local geological setting indicate a granitic pegmatite origin of the heavy mineral Nb-Ta assemblage. The surrounding rocks are Hercynian leucogranites of the Bratislava Massif (the Staré Mesto body) and Lower Paleozoic micaschists to paragneisses. Numerous pegmatite veins cut both the parental granites as well as the metapelites-metapsammites.

Minerals of the Ct group are the most widespread Nb-Ta phases. Five basic textural and compositional types of Ct minerals could be distinguished:

(Ct1) Large crystals (up to 4 mm) with regular fine to coarse oscillatory zoning, locally unzoned or with diffuse zonality. They belong to ferrocolumbite, rarely ferrotantalite, manganocolumbite and manganotantalite with broad compositional variations: (atomic ratio:) Mn/(Mn + Fe) = 0.17–0.52 and Ta/(Ta + Nb) = 0.19–0.70.

(Ct2) Irregular patchy intergrowths of ferrocolumbite – ferrotantalite with Ta-rich rutile (*ca.* 1 mm in size); Mn/(Mn + Fe) = 0.19–0.27 and Ta/(Ta + Nb) = 0.49–0.57. Ct shows increased Ti and W contents (up to 2.3 wt% TiO_2 and 0.7 wt% WO_3).

(Ct3) Irregular patchy intergrowths of ferrotantalite–manganotantalite with ferrotapiolite (*ca.* 0.6 mm in size); Mn/(Mn + Fe) = 0.34–0.66 and Ta/(Ta + Nb) = 0.65–0.81.

(Ct4) Irregular bended zones of ferrocolumbite (up to 0.3 mm long) with fine oscillatory zoning which replace Ct1. The zoning is caused by Nb-Ta variation with increasing of Ta/Nb ratio; Mn/(Mn + Fe) = 0.16–0.19 and Ta/(Ta + Nb) = 0.16–0.34.

(Ct5) Irregular patchy zones of ferrocolumbite to ferrotantalite (0.2–0.9 mm) along cracks and rims of Ct1; Mn/(Mn + Fe) = 0.43–0.49 and Ta/(Ta + Nb) = 0.24–0.61.

The Ct1 belongs to primary magmatic minerals, whereas Ct2 and Ct3 are probably products of sub-solidus (?) recrystallization of primary phases and textural patterns of Ct4 and Ct5 indicate late- to post-magmatic replacement of Ct1. Compositional evolution of Ct is complex without unambiguous fractionation trend.

Ferrotapiolite forms anhedral intergrowths in Ct3 or inclusions in Ct1, 60 to 100 μm in size; Mn/(Mn + Fe) = 0.05–0.07, Ta/(Ta + Nb) = 0.87–0.93. Rarely, a Sn-rich ixiolite-like phase with Mn/(Mn + Fe) = 0.40 and Ta/(Ta + Nb) = 0.81 and 9.4 wt% SnO_2 occurs as 110 μm irregular inclusion in Ct1. Ta-rich rutile (strüverite) shows relatively uniform compositions with Mn/(Mn + Fe) = 0.01–0.03 and Ta/(Ta + Nb) = 0.80–0.84. Rare microlite to uranmicrolite forms anhedral, 5–15 μm thick overgrowth on uraninite in partly recrystallized part of Ct1; Ta/(Ta + Nb) = 0.82–0.94, U = 16–47 atom % of *A* site.

The above mentioned Nb-Ta association from Limbach area with variable but relatively high Ta/Nb and Mn/Fe ratios indicates a moderate fractionation level, typical for the rare-element class of granitic pegmatites of LCT family, probably beryl-columbite subtype (*sensu* ČERNÝ, 1991). Such pegmatites with beryl, columbite–tantalite, Hf-rich zircon, gahnite and almandine–spessartine are typical of the surrounding Bratislava S-type granitic massif (UHER *et al.*, 1994, UHER & ČERNÝ, 1998).

References

ČERNÝ, P. (1991): Geoscience Canada, 18: 29–41.
UHER, P. & ČERNÝ, P. (1998): Geologica Carpathica, 49: 261–270.
UHER, P., ČERNÝ, P., NOVÁK, M. & SIMAN, P. (1994): Mineralia Slovaca, 26: 157–164.

EVALUATION OF POWDER XRD DATA USING THE MUDMASTER AND ROCKJOCK COMPUTER PROGRAMS

UHLÍK, P.[1] & EBERL, D. D.[2]
[1] Dept. of Geology of Mineral Deposits, Comenius University, Mlynská dolina G, 842 15 Bratislava, Slovakia
E-mail: uhlik@fns.uniba.sk
[2] U.S. Geological Survey, 3215 Marine Street, Boulder, Colorado, USA, 80303-1066

Powder X-ray diffraction (XRD) analysis is a fundamental mineralogical method. In addition to qualitative identification of mineral phases, XRD is able to provide other important data. The presented contribution will focus on crystallite size distribution determinations and on quantitative analyses.

Size distributions for crystallites can be measured by XRD because the widths of the XRD peaks broaden as crystallite size decreases. The MudMaster program, written by EBERL *et al.* (1996), calculates crystallite thickness distributions (CTD) according to the Bertaut-Warren-Averbach theory (DRITS *et al.,* 1998). The BWA technique has been applied to measure CTD of kaolin minerals (ŠUCHA *et al,* 1999), to explore crystal growth mechanisms for illite and smectite (ŚRODOŃ *et al*., 2000; MYSTKOWSKI *et al*., 2000), to study diagenetic evolution of crystallite thickness distributions of illitic material (KOTARBA & ŚRODOŃ, 2000), to study weathering processes that affected smectite and illite/smectite (ŠUCHA *et al*., 2001), to measure fundamental illite particle thicknesses and to study crystallite-size changes of pyrophyllite during grinding, among other applications. From MudMaster analyses one is able to distinguish various geological processes. For example, thickness distributions of smectites show clear differences between primary bentonites and secondary, redeposited bentonites, because transport of primary bentonites decreases the mean thickness of smectite crystals. Weathering intensity is also revealed by measurement of kaolinite thickness distributions. Long and intense weathering produces thicker kaolinite crystallites than does less intensive weathering.

Accurate quantitative mineral analysis is important in many scientific and applied studies. ŚRODOŃ *et al*. (2001) described reproducible and accurate calculation of the mineral contents of rock by XRD when using an internal standard. EBERL (2003) wrote the RockJock program based on this previous work. The program fits the sum of stored XRD patterns of standard, pure minerals (the calculated pattern) to the measured pattern by varying the fraction of each standard pattern, by using the Solver function in Microsoft Excel to minimize the degree of fit parameter between the calculated and measured pattern. One of the advantages of the program is that it contains more than 90 standards that can be used with XRD data from most diffractometers. The list of standards contains common and less common minerals as well representatives of organic and volcanic matter. The program was used to determine of the quantitative mineralogical composition of clastic sedimentary rocks, bentonites, and alginates with good results.

Both programs, MudMaster and RockJock, are relatively easy to use. The latest versions of this software can be obtained by anonymous ftp from the Internet address: ftp://brrcrftp.cr.usgs.gov/pub/ddeberl/.

References

DRITS, V.A., EBERL, D.D. & ŚRODOŃ, J. (1998): Clays and Clay Minerals, 46: 461–475.

EBERL, D.D. (2003): U.S. Geological Survey, Open-File Report: OF 03-78, 40 p.

EBERL, D.D., DRITS, V., ŚRODOŃ, J. & NÜESCH R. (1996): U.S. Geological Survey, Open-File Report: 96-171, 46 p.

KOTARBA M. & ŚRODOŃ J. (2000): Clay Minerals, 35: 383–391.

MYSTKOWSKI, K., ŚRODOŃ, J. & ELSASS, F. (2000): Clay Minerals, 35: 545–557.

ŚRODOŃ, J., DRITS, V., McCARTY, D.K., HSIEH, J.C.C. & EBERL, D.D. (2001): Clays and Clay Minerals, 49: 514–528.

ŚRODOŃ, J., EBERL, D.D. & DRITS, V. (2000): Clays and Clay Minerals, 48: 446–458.

ŠUCHA, V., KRAUS, I., ŠAMAJOVÁ, E. & PUŠKELOVÁ, L. (1999): Periodico di Mineralogia, 68: 81–92.

ŠUCHA, V., ŚRODOŃ, J., CLAUER, N., ELSASS, F., EBERL, D. D., KRAUS, I. & MADEJOVA, J. (2001): Clay Minerals, 36: 403–419.

SUPERDENSE CO_2 INCLUSIONS IN CRETACEOUS QUARTZ-STIBNITE VEINS OF THE GEMERIC UNIT, WESTERN CARPATHIANS, SLOVAKIA

URBAN, M.[1], KONEČNÝ, P.[2] & THOMAS, R.[3]
[1] Department of Mineralogy and Petrology, Comenius University, 842 15 Bratislava, Slovakia
E-mail: urbanm@fns.uniba.sk
[2] Geological Survey of Slovakia, 817 04 Bratislava, Slovakia
[3] GeoforschungsZentrum Potsdam, 14473 Potsdam, Germany

Variscan basement of the Gemeric unit of the Western Carpathians contains more than 1 000 hydrothermal veins (GRECULA *et al.*, 1995), which have been for centuries one of the most important resources of iron and base metals, particularly copper, quicksilver and antimony. The majority of these veins has been exploited since prehistoric times. Siderite and quartz-sulphide veins are arranged parallel to the regional metamorphic cleavage of the low-grade Palaeozoic basement, and/or within mylonite shear zones. Origin of the siderite and stibnite veins has been widely discussed for many years. Detailed fluid inclusion and mineralogical studies have been recently carried out with the aim to elucidate more exactly the origin and age of the ore-forming fluids of the Gemeric unit.

CO_2 inclusions with density up to 1,197 kg.m^{-3} occur in quartz-stibnite veins in the southern part of the Gemeric unit. It is the first known occurrence of the superdense CO_2 in hydrothermal veins and low-grade crustal environments. Inclusions with high density of CO_2 (D > 1,100 kg.m^{-3}) were described from high-pressure/high-temperature low crust and upper mantle environments. Archean garnet granulites from the South Indian craton contain CO_2 inclusions with highest density (1,174 kg.m^{-3}) recorded in crustal rocks up to present (SANTOSH & TSUNOGAE, 2003). Higher densities, up to 1,210 kg.m^{-3}, were described only from upper mantle pyroxenites from Salt Lake Crater, Hawaii (FREZZOTTI *et al.*, 1992). Inclusions of pure superdense CO_2 homogenize by melting of CO_2-solid in CO_2-liquid at temperatures greater than −56.6°C, and metastable total homogenization by CO_2-vapour disappearance can be seen at T < −56.6°C.

In the Gemeric hydrothermal veins superdense CO_2 inclusions are often accompanied by monophase CO_2 inclusions with variable density and also by two-phase aqueous and three-phase CO_2-rich aqueous inclusions with high salinity (23–32 wt% NaCl eq.). Variable phase ratios in the inclusions indicate entrapment of a heterogeneous fluid, consisting of CO_2-rich and aqueous phases. Raman microanalysis of the monophase CO_2 inclusions corroborated CO_2 as dominant gas species accompanied by small amounts of nitrogen (<7.3 mol%) and methane (< 2.5 mol%). Trapping PT conditions have been derived from coeval monophase CO_2 and two-phase aqueous inclusions. The superdense CO_2 phase exsolved from an aqueous bulk fluid at temperatures of 183–237 °C and pressures between 1.6 and 3.5 kbar, possibly up to 4.5 kbar. The wide range of fluid pressures indicates a periodical opening of the vein system due to a crack-seal mechanism, when fluid pressure varies between hydrostatic and lithostatic pressures. The calculated fluid pressures are equivalent to depths between 15 and 18 km.

Low thermal gradients (12–13 °C.km^{-1}) and the CO_2–CH_4–N_2 fluid composition rule out a genetic link of the hydrothermal veins with the subjacent Permian granites and indicate an external, either metamorphogenic (oxidation of siderite, dedolomitization) or lower crustal/mantle, source of the ore-forming fluids. According to microprobe dating of hydrothermal monazite from the quartz-tourmaline assemblage, the quartz-stibnite veins formed during early Cretaceous (~ 120 Ma) thrusting of the Gemeric unit over the adjacent Veporic unit, and rejuvenization of the veins occurred during late Cretaceous (~ 76 Ma) transpressional shearing. The 15- to 18-km depth of burial estimated from the fluid inclusion trapping PT parameters indicates an 8- to 11-km thick Upper Palaeozoic–Jurassic accretionary complex overlying the Gemeric basement and its Permo-Triassic autochthonous cover.

Acknowledgements

Financial support was provided by the Ministry of Environment and the Geological Survey of Slovakia project no. 0503, with the contributions from the VEGA grant 1/1027/04.

References

FREZZOTTI, M.L., BURKE, E.A.J., DE VIVO, B., STEFANINI, B. & VILLA, I. M. (1992): European Journal of Mineralogy, 4: 1137–1153.

GRECULA, P., ABONYI, A., ABONYIOVÁ, M., ANTAŠ, J., BARTALSKÝ, B., BARTALSKÝ, J., DIANIŠKA, I., DRNZÍK, E., ĎUĎA, R., GARGULÁK, M., GAZDAČKO, L'., HUDÁČEK, J., KOBULSKÝ, J., LÖRINCZ, L., MACKO, J., NÁVESŇÁK, D., NÉMETH, Z., NOVOTNÝ, L., RADVANEC, M., ROJKOVIČ, I., ROZLOŽNÍK, L., ROZLOŽNÍK, O., VARČEK, C. & ZLOCHA, J (1995): Mineral deposits of the Slovak Ore Mountains, Vol. 1. Bratislava: Geocomplex (Mineralia Slovaca Monograph), 834 p.

SANTOSH, M. & TSUNOGAE, T. (2003): Journal of Geology, 11: 1–16.

MODELLING IR ABSORPTION FOR Si–O STRETCHING VIBRATIONS OF 2:1 LAYER SILICATES BASED ON BOND VALENCE CALCULATIONS

VÁCZI, T., TÓTH, E. & WEISZBURG, T. G.
Department of Mineralogy, Eötvös Loránd University, Pázmány Péter sétány 1/C, H-1117 Budapest, Hungary
E-mail: thomas@ludens.elte.hu

A simple bond valence model was set up in order to aid the decomposition of Si–O vibrations in the infrared spectra of 2:1 layer silicates. Most of these infrared spectra do not show a single absorption band but rather show a more or less complex distribution of absorption wavelengths and intensities. The decomposition can be quite ambiguous as there can be a high number of different cation environments present. Our assumption in the model was that bulk chemical composition is a sum of different local compositions without any ordering constraints. This is of smaller importance for ordered structures (there are few different local arrangements) but a high degree of disorder means there is a distribution of many possible local arrangements, each contributing to the IR absorption spectrum. The present model tries to give a method for the decomposition of the tetrahedral Si–O stretching region at around 1000 cm^{-1} in the infrared spectrum.

In this model the Si–O bonds in one "central" SiO_4 tetrahedron of a *T* sheet is modelled. All possible first-cation environments, including interlayer (*IL*) and octahedral (*O*) ones, were taken into account and their contributions to the central Si–O bonds were calculated. One oxygen in each tetrahedron is bonded to the *O* sheet and is called apical, while the other three are shared with three neighbouring tetrahedra in the *T* sheet and are called basal oxygens. To cover all 2:1 layer silicates vacancies were allowed in *IL* and *O* positions. All cations were represented by their formal charge.

The bond valences for each silicon–basal oxygen bond were calculated using the first tetrahedral neighbour and two *IL* cations (the latter in 12-fold coordination). Tetrahedral neighbour cations included Si^{4+} and Al^{3+}, while only single charges (i.e., monovalent cations such as K^+, Na^+) were considered in *IL* positions. The cation environments in the modelled neighbourhood ranged from 3Si to 3Al and 0K to 3K, giving 32 possible configurations.

The bond valence for the apical oxygen was derived from all possible arrangements of divalent cations (M^{2+}), trivalent cations (M^{3+}) and vacancies for 3 octahedral positions, not excluding highly unlikely associations such as 3 trivalent cations or 3 vacancies as well. The orientation of the *O* arrangements relative to the tetrahedral sheet was ignored as only a single (apical) oxygen bridges the *O* sheet to the central tetrahedron. This setup gave 10 octahedral arrangements for each *T–IL* combination, thus a total of 320 neighbourhood configurations of a single SiO_4 tetrahedron are evaluated in the model.

Each Si–O bond valence is calculated independently from the other three using the relevant neighbouring cations' contributions. The resulting four bond valence values (3 basal and 1 apical) are then scaled to give a sum of 4 to match the charge of the central Si.

To represent chemical composition, each of the 320 configurations was assigned a weight factor calculated from the relative occupancies of cations in each of the three types of cation positions (*IL*, *T*, *O*). Relative occupancy (RO) is the ratio of the number of the given cation p.f.u. and the number of hosting cation positions per 22 negative charges. The sum of the relative occupancies of all cations and vacancies in a given type of cation position is by definition always 1. The weight factors are then calculated by multiplying appropriate relative occupancies for any given configuration. This is done 320 times, giving a distribution of probabilities of occurrence for 320 sets of four bond valence values.

The four Si–O bonds in each of the 320 configurations give 216 unique bond valence values. The weight factors associated with each bond valence value are summed up and plotted as bond valence–probability diagrams. In this paper we present calculated plots for several ideal and realistic layer silicate compositions ranging from talc and pyrophyllite through smectites to dioctahedral and trioctahedral micas. The diagrams are qualitatively compared with experimental IR spectra of minerals of equivalent compositions, based on the assumption that bond valences are related to bond lengths and therefore to IR absorption bands. The model gives promising results for phases with low *IL* occupancy. For high *IL* occupancies some further refinement is needed.

COMPARISON OF THE MAIN PERIODS OF KAOLINITE FORMATION IN SLOVAKIA AND HUNGARY

VICZIÁN, I.
Geological Institute of Hungary, Stefánia út 14, H-1143 Budapest, Hungary
E-mail: viczian@mafi.hu

The ages of kaolinite-rich sediments in Slovakia and Hungary are compared. Data on Slovakia are taken from the book of KRAUS (1989); Hungarian data were summarised by the author (VICZIÁN, 1987, 1995 and more recent results).

In Slovakia evidences for kaolin formation do not exist in the time span when simultaneously the formation of bauxites is supposed. In Hungary Upper Cretaceous and Eocene kaolinitic bauxites and kaolin-rich sediments of the Ajka Coal Formation are known.

There are Lutetian and Priabonian kaolinitic sediments in the Hornonitrianska kotlina Basin. In Hungary the counterpart is the Middle to Upper Eocene Kosd Formation, which extends from the Balaton area to the Bükk Mts. in the North Hungarian Range.

In the South Slovakian depression, in the basal part of Tertiary (Kiscellian to Eggenburgian), the main clay mineral is kaolinite. Hungarian examples are mentioned from the Paleogene Basin (borehole Balassagyarmat-5, Felsőpetény fire clay deposit), Keszthely Mts., Zagyva Graben, Salgótarján Formation in the Sajó Basin and Lower Miocene of Mecsek area (borehole Gálosfa-1).

In the Badenian to Pontian period the climate was suitable, yet when compared with Oligocene, less favourable, for kaolinite formation in both countries. In Slovakia Badenian, Sarmatian and Pannonian weathering crusts were formed on the top of the volcanic rocks, in Hungary no such crusts or only few examples of them were preserved (perhaps the Szegi kaolin deposit in the Tokaj Mts.). There are special kaolinite-rich deposits formed by intense destruction of crystalline and volcanic rocks in the Pontian in Slovakia, the Poltár Formation in the Lučenec Basin and in the Subvihorlat area in the east. In the Pliocene kaolinitic weathering crusts developed on the surface of basalts in the area around Lučenec. Such deposits in Hungary are either missing or less well studied.

There are kaolinite-rich red clay deposits of Pliocene to Lower Quaternary age on karstic surfaces in north-eastern Hungary and in the Villány Mts., as well as in the southern Slovak Karst.

References

KRAUS, I. (1989): Kaolíny a kaolinitové íly Západných Karpát (Kaolins and kaolinite clays of the West Carpathians). Západné Karpaty, Séria Mineralógia, Petrografia, Geochémia, Metalogenéza 13. Bratislava: Geologický Ústav Dionýza Štúra, 287 p.

VICZIÁN, I. (1987): Agyagásványok Magyarország üledékes kőzeteiben (Clay minerals in sedimentary rocks of Hungary). Akadémiai doktori értekezés (D. Sc. Thesis). Manuscript, Budapest: Hungarian Academy of Sciences. 205 + 139 p.

VICZIÁN, I. (1995): Romanian Journal of Mineralogy, 77: 35–44.

MINERAL CHEMISTRY OF THE PLEISTOCENE CIOMADUL VOLCANIC ROCKS, EAST CARPATHIANS

VINKLER, A. P.[1], HARANGI, SZ.[2], NTAFLOS, T.[3] & SZAKÁCS, S.[4]
[1] Department of Mineralogy, Babeş-Bolyai University, Kogălniceanu, 1, Cluj-Napoca, Romania
E-mail: vapaula@freemail.hu
[2] Department of Petrology and Geochemistry, Eötvös Loránd University, Pázmány Péter sétány 1/C, H-1117 Budapest, Hungary
[3] Institute of Earth Sciences, University of Vienna, Althanstrasse 14, Vienna, Austria
[4] Department of Environmental Sciences, Sapientia Hungarian University of Transylvania, Deva 10, Cluj-Napoca, Romania

The Ciomadul volcano is the site of the latest volcanic eruption occurred in the Carpathian–Pannonian region. The dacitic lava dome complex of the Ciomadul volcano is situated at the southern edge of the South Harghita Mountain, which belongs to the Călimani-Gurghiu-Harghita Neogene volcanic chain. The activity of the volcano began ca. 1 Ma and continued at 600-500 ka with a lava dome building phase. After about 200 kyr quiescence, two subplinian explosive eruptions occurred inside the lava dome complex through the Mohos and the younger St. Anna craters. The St. Anna eruption took place 10-30 ka. In order to constrain the possible renewal of the volcanism it is important to understand the magmagenesis of the last activities.

The bulk composition of the lava dome rocks and pumices shows a striking similarity and a fairly restricted range. They are classifies as high-K dacites. Chemical composition of the mineral phases provides information on the condition of the crystallization and possible open system processes. The main mineral phases of these rocks are amphibole, plagioclase and biotite. Some of the lava dome rocks contain also clinopyroxene phenocrysts and quartz xenocrysts. The most common accessory minerals are the apatite and sphene.

The amphiboles are mainly magnesiohornblende and magnesiohastingsite. They show wide compositional variation in Al_2O_3 ranging from 6 wt% to 14 wt%. The Al content correlates with the Ti and the total alkali concentration. These features are consistent with crystallization of various pressure and temperature. Formation of amphibole started at relatively high pressure, presumably at lower crustal levels. The high pressure crystallization is supported also by the composition of the clinopyroxene phenocrysts. A peculiar feature of the Ciomadul rocks is the occurrence of high MgO minerals such as olivine, orthopyroxene and clinopyroxene in the core of amphibole phenocrysts. These minerals could be either xenocrysts deriving directly from the upper mantle or can represent early formed mineral assemblage from a primitive mafic magma. The textural feature clearly indicates a change in the crystallization processes toward an increase of water content of the magma.

The high-MgO minerals clearly suggest the role of mafic mantle-derived magmas in the genesis of the Ciomadul rocks. Since these features are common both in the lava dome rocks and the subsequent explosive volcanic products, we infer a long-lived reservoir beneath the Ciomadul volcano. The volcanic eruptions might be triggered by episodic arrival of fresh primitive mafic magmas into this plumbing system. This could have an important implication for possible future eruption.

FLUORINE-BEARING GARNETS FROM THE TESCHENITE SILL IN THE POLISH WESTERN CARPATHIANS

WŁODYKA, R. & KARWOWSKI, Ł
Department of Geochemistry and Petrology, University of Silesia, ul. Będzińska 60, 41-200 Sosnowiec, Poland
E-mail: rwlodyka@wnoz.us.edu.pl

The occurrence of fluorian calcic garnets is rather rare. They have been reported from metacarbonates, metasomatically altered alkaline igneous rocks and contact-metamorphosed basalts (MANNING & BIRD, 1990). In Polish Western Carpathians fluorine-bearing garnets were found in metasomatically altered nepheline syenites belonging to the teschenite-picrite association. Moreover, such garnets were described from nepheline syenites of the Shonkin Sag laccolith (NASK & WILKINSON, 1970) and Magnet Cove (FLOR & ROSS, 1989). A classic area of teschenites and related rocks is restricted only to the western part of the Outer Carpathians and extends in the NE direction for over 100 km from Hranice in Moravia, Czech Republic, to Cieszyn and Bielsko-Biała in Poland. The main products of the Cretaceous volcanic activity are shallow, subsurface sills with thickness varying from a few centimeters to 40 meters.

In this magmatic province the nepheline syenite occurs only as small irregular bodies with sharp boundaries in the upper parts of the teschenite sills or as veins cross-cutting the upper or lower chilled margins. In syenite, the alkali feldspars ($Or_{70–48}Ab_{28–48}An_{2–4}$) are Ba- and Sr-rich up to 6 wt% BaO and 3 wt% SrO, respectively. Nepheline ($Qz_{4–32}Ne_{80–62}Ks_{16–6}$) and feldspars constitute about 80 vol% of the rock. The mafic phase are represented by clinopyroxene (hedenbergite–aegirine), amphibole (kaersutite–ferro-kaersutite–hastingsite) and dark mica (lepidomelane). The two-step process of primary feldspars metasomatism led to formation of an adularia–albite paragenesis which is replaced by the following zeolites: analcime, natrolite, mesolite, thomsonite, heulandite, harmotome and ferrierite.

Within metasomatically altered syenite veins from Puńców sill, secondary F-bearing hydrogarnet was identified. They form small (up to 0.4 mm in length), irregular grains with anomalous birefringence among altered alkali feldspars. They contain up to 3.48 wt% fluorine substituted in the structure, equivalent to a 6.9 mol% substitution of fluorine for oxygen. Normalization of the microprobe analysis to 5 (X + Y) atoms yields the following formula: $(Ca_{2.968}Mg_{0.006}Mn_{0.020}Na_{0.018})_{3.012}$ $(Fe^{3+}_{0.225}Al_{1.731}Ti^{4+}_{0.022})_{2.004}$ $Si_{2.359}$ $(O_{9.474}F_{0.800}OH_{1.726})_{12.000}$, where OH was calculated by valence balance. Low analytical totals (94–97 wt%) suggest significant quantities of water molecule within the investigated garnet structure. This was confirmed by Raman spectroscopy (Fig. 1). The hydrogarnets presented are composed of 1.2 to 24.6% andradite, 57.7 to 76.5% grossular, 9.3 to 19.20 % hydrogrossular and 2.2 to 6.9 % fluorgrossular. Thus, the main variation is connected with the Al_2O_3/Fe_2O_3 ratio. According to existing nomenclature (RINALDI & PASSAGLIA, 1984), two names, hibschite and katoite were distinguished within calcic hydrogarnet group (hibschite with Gr ≥ 50 % and katoite for Gr < 50 %). From above results that the proper name for garnet investigated is hibschite, where $OH^–$ and also $F^–$ may enter the garnet structure at the Si position according to the scheme: $[SiO_4]^{4–} \leftrightarrow [(OH,F)_4]^{4–}$.

References

FLOR, M.J.K. & ROSS, M. (1989). American Mineralogist, 74: 113–131.

MANNING, C.E. & BIRD, D.K. (1990). American Mineralogist, 75: 859–873.

NASK, W.P. & WILKINSON J.F.G. (1970). Contributions to Mineralogy and Petrology, 25: 241–269.

PASSAGLIA, E. & RINALDI, R. (1984). Bulletin de Minéralogie, 107: 605–618.

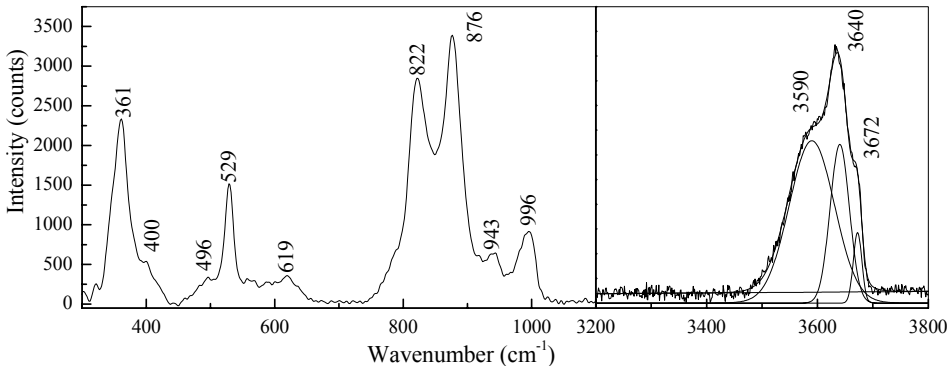

Fig. 1: Unpolarized Raman spectra of F-bearing garnet from the teschenite sill.

PRELIMINARY STUDY OF THE ORE MINERALS OF THE "AVRAM IANCU" Co-Ni-U ORE DEPOSIT, BIHOR MTS., ROMANIA

ZAJZON, N.[1], BŰDI, N.[1], SZAKÁLL, S.[1] & MÁTYÁSI, S.[2]
[1] Department of Mineralogy and Petrology, University of Miskolc, H-3515 Miskolc-Egyetemváros, Hungary
E-mail: nzajzon@gold.uni-miskolc.hu
[2] Geo Prospect Ltd., str. 13 Septembrie no. 30/1, RO-415600 Ştei, Romania

The "Avram Iancu" ore deposit is located on the southern part of the Bihor Mts., *ca*. 2.5-km southward from the Bihor (or Cucurbăta) Peak (1848.5 m). This is a Co-Ni-U type deposit with sulfide ± polymetallic associations. The deposit was explored on different levels on both sides of the uppermost reaches of Arieşul Mic River during the 1950s with Soviet contribution. Our samples from the dump could be correlated with the 1118 m-level of Gallery XI, on the left side of Arieşul Mic.

The ore deposit is found in the retrometamorphic series of the Biharia Nappe. This series consists of two formations. The lower one is built up by chlorite-albite schists, amphibolites and gneisses. The upper formation is a tuffitic carbonate rock, which is the host rock of the ore. It consists of porphyroblastic (albite-) chlorite schists, amphibolites, crystalline limestones and dolomites. The whole series was altered by hydrothermal fluids of Laramian magmatites. The "Avram Iancu" ore deposit has a layered structure, parallel to the foliation of the host rock, but dykes can also be found subordinately. The ores can be classified into three types: a U-Co-Ni, a chalcopyrite-pyrite-magnetite, and a Pb-Zn-Cu type.

X-ray powder diffraction (XRD) and energy-dispersive microprobe measurements were carried out on a dominantly Ni-bearing, and on a dominantly Co-bearing sample from the U-Co-Ni type ore. The following minerals were found: nickeline, skutterudite, cobaltite, gersdorffite, annabergite, erythrite, pyrite, chalcopyrite, galena, rutile, brannerite, uraninite, quartz, zircon, clinochlore, talc, albite, illite (10 Å clay mineral), dolomite or ankerite and a (Ca, Fe, Co) arsenate. This is the first report of brannerite (UTi_2O_6) from the locality. It forms minute (*ca*. 10 μm), isometric inclusions in cobaltite. Uraninite was found in quartz.

According to textural observations, ore formation started with nickeline, the most Ni-rich phase and continued gradually by the formation of more and more Co-rich phases. In the next stage an As-rich gersdorffite–nickel-skutterudite-like phase formed. This was followed by the formation of cobaltite together with skutterudite. Cobaltite is a Ni-bearing, As-rich variety, with a small amount of Fe. The skutterudite appears as 20 μm inclusions in a zone of an euhedral cobaltite crystal.

Annabergite and erythrite are the main alteration phases identified by XRD. Annabergite was found in veins, which cut both the gersdorffite–cobaltite ore and the quartz gangue. Near to some of the cracks of cobaltite a secondary (Ca, Fe, Co) arsenate was found as alteration product.

Silicate minerals of the Ni-rich sample included quartz, talc, chlorite accompanied by dolomite or ankerite. The Co-rich sample contained quartz, chlorite, talc, albite and illite (10 Å clay mineral). A few euhedral rutile inclusions (max. 300 μm in length) can be found in the quartz. A zircon crystal has also been found as 20 μm, euhedral inclusion in cobaltite.

Further investigations are planned for the identification of the uncertain phases.

AUTHOR INDEX

Almási, B. 3
Almási, E. 112
András, P. 4, 5, 52, 61, 68
Babič, D. 18
Babinszki, E. 6, 118
Bajnóczi, B. 7
Bálintová, T. 8
Bartha, A. 80
Batki, A. 9
Bazarnik, J. 10, 105
Benkó, Zs. 11
Beqiraj, A. 12
Beqiraj (Goga), E. 13
Berbeleac, I. 14
Bidló, A. 35, 36
Bilal, E. 71, 93
Blagojević-Babič, S. 18
Bonev, N. 73
Bousquet, R. 56
Bozsó, G. 88
Broska, I. 19
Bűdi, N. 132
Budzyń, B. 76
Buseck, P. R. 97
Cempírek, J. 20, 84
Chong, R. K. K. 97
Chovan, M. 5, 65, 68, 70
Cioaca, M. 95
Ciobanu, C. L. 22
Constantinescu, S. 122, 123
Cook, N. J. 22
Čopjaková, R. 107
Cora, I. 21
Csámer, Á. 3
Czímerová, A. 24
Damian, F. 22
Damian, Gh. 22
Datsyuk, Yu. 23
Demenko, D. P. 75
Derkowski, A. 24
Diaconu, G. 27, 71
Dódony, I. 25, 26
Dosbaba, M. 85
Dudok, I. V. 51
Dumitraş, D.-G. 27, 71
Dunin-Borkowski, R. E. 97
Eberl, D. D. 126
Elekes, Z. 104
Farkas, J. 3
Fehér, B. 113
Ferraris, G. 28
Finlayson, A. P. 97
Fodorpataki, L. 80
Földessy, J. 106
Fourman, V. 23
Frankel, R. B. 97
Franus, M. 29
Franus, W. 24
Friebert, Z. 88
Gaab, A. 19
Gál, B. 30
Gasharova, B. 35
Gaweł, A. 105
Ghergari, L. 31, 48, 72, 98, 99
Gorea, M. 32
Gratuze, B. 104
Grechanovskaya, E. E. 75
Grecu, N. M. 123
Gregáňová, G. 124
Gregor, M. 33
Grovu, P. 34
Gucsik, A. 35, 36
Háber, M. 52
Harangi, Sz. 130
Hasson, S. 73
Havancsák, I. 37
Heil, B. 35, 36
Hidas, K. 57
Hîrtopanu, P. 38
Hoeck, V. 39, 49, 55, 56
Hoinkes, G. 56
Horváth, E. 7
Hovorka, D. 94
Ilinca, Gh. 42, 47
Ionescu, C. 31, 39, 48, 49, 55, 72, 98, 99
Jáger, V. 50
Jánosi, Cs. 114
Jánosi, T. 89
Jarmołowicz-Szulc, K. 51
Jeleň, S. 52, 61
Jozja, N. 13
Jude, R. 14
Juhász, Gy. 117
Jurkovič, Ľ. 70
Karwowski, Ł. 51, 53, 131
Kasama, T. 97
Kiss, Á. Z. 104
Kiss, G. 54
Kiss, L. F. 6
Kiss, P. 121
Koller, F. 39, 55, 56
Köllő, A. 112
Konc, Z. 57
Konečný, P. 94, 127
Kónya, P. 58
Kósa, I. 97
Košuth, M. 59
Kovács, G. 35, 36
Kovács-Pálffy, P. 115
Kozák, M. 116
Kristály, F. 32, 60, 114
Križáni, I. 4, 61
Kubiš, M. 19
Kucha, H. 62, 66
Kuchta, Ľ. 86
Kvasnytsya, I. 63
Kvasnytsya, V. 64, 75
Ladenberger, A. 77
Lalinská, B. 65, 70
Lazar, C. 31
Lazarenko, E. E. 75
Łojan, E. 66

Lovas, Gy. A. 26
Lukács, R. 67
Luptáková, J. 5, 68
Mádai, V. 69
Magyari, Á. 118
Majzlan, J. 70
Marchev, P. 73
Marincea, Ş. 27, 71
Maris, C. 72
Márton, E. 6
Márton, I. 73
Márton, P. 6
Marusyak, V. 96
Masi, U. 12
Matović, V. 74
Mátyási, S. 132
Meisel, T. 55
Melnikov, V. S. 75
Michalik, M. 76, 77
Milovská, S. 65, 70
Mindszenty, A. 121
Miron, D. 78
Molnár, F. 11, 30, 54, 81, 92
Moritz, R. 73
Moutte, J. 27
Muller, F. 13
Murariu, T. 79
Muszyński, M. 105
Nádor, A. 118
Nagy, I. 80
Nagy, S. 81, 82
Neacşu, A. 83
Nikolenko, A. 96
Nikolenko, P. 96
Ninagawa, K. 36
Nishido, H. 36
Novák, M. 20, 84, 85
Ntaflos, T. 130
Nuţu, M. L. 14
Ó. Kovács, L. 117
Okumura, T. 36
Oliynyk, T. 96
Onuzi, K. 55
Osacký, M. 86
Ozdín, D. 8, 87, 100, 125
Pál-Molnár, E. 9, 88, 89, 114
Papp, G. 90
Papp, I. 116
Papucs, A. 114
Patocskai, Z. 35, 36
Pécskay, Z. 11
Pekker, P. 91
Péntek, A. 92
Petrescu, L. 93
Petrík, I. 94
Pop, D. 49, 120
Popescu, Gh. C. 95
Popescu-Pogrion, N. 122, 123
Popivnyak, I. 96
Poros, Zs. 30
Pósfai, M. 97, 121
Precup, C. 98, 99
Pršek, J. 100
Puscaş, M. 101
Robert, J.-L. 102
Rózsa, P. 3, 104
Rzepa, G. 105
Sajó, I. 112, 115
Schuster, R. 56
Seresné Hartai, É. 106
Sharygin, V. 57
Simon, V. 99
Simpson, E. T. 97
Skiba, M. 77
Škoda, R. 107
Šottník, P. 108
Stankovič, J. 52
Števko, M. 87
Stremtan, C. 109
Stríček, I. 110
Stumbea, D. 111
Šucha, V. 110
Szabó, Cs. 37, 57
Szakács, S. 130
Szakáll, S. 60, 112, 113, 114, 115, 124, 132
Szełęg, E. 53
Szendrei, G. 115
Szepesi, J. 116
Szöőr, Gy. 104
Ţentea, O. 48
Thamó-Bozsó, E. 117, 118
Thomas, R. 127
Tillmanns, E. 119
Topa, D. 47
Török, K. 37
Tóth, E. 21, 120, 128
Tóth, T. 115
Touray, J. C. 13
Tsikhon', S. 96
Tuba, Gy. 121
Udubaşa, G. 122, 123
Udubaşa, S. S. 14, 122, 123
Uher, P. 124, 125
Uhlík, P. 86, 110, 126
Urban, M. 127
Uzonyi, I. 104
Váczi, T. 128
Vasković, N. 18, 74
Vennemann, T. 73
Vezzalini, G. 112, 113
Viczián, I. 129
Vinkler, A. P. 130
Vizitiu, A. 47
Vlad, Ş. 47
Vojnits, A. 82
Volek, M. 87
Vrteľ, A. 33
Waniak-Nowicka, H. 24
Warzecha, M. 77
Watkinson, D. H. 92
Wdowin, M. 62
Weiszburg, T. G. 21, 80, 82, 91, 120, 128
Włodyka, R. 131
Zajzon, N. 21, 32, 132
Zelenka, T. 106
Žitňan, P. 125
Zych, B. 77